NASA CR-73106
(Part I)

ANALYSIS AND DESIGN OF SUPERSONIC WING-BODY COMBINATIONS, INCLUDING FLOW PROPERTIES IN THE NEAR FIELD

PART I - THEORY AND APPLICATION

By F.A. Woodward,
E.N. Tinoco, and
J.W. Larsen

D6-15044-1
August 1967

Prepared under Contract No. NAS 2-3719 by

The Boeing Company
Commercial Airplane Division
P.O. Box 707
Renton, Washington

for
AMES RESEARCH CENTER
NATIONAL AERONAUTICS AND SPACE ADMINISTRATION

CONTENTS

LIST OF FIGURES

LIST OF FIGURES (Continued)

ANALYSIS AND DESIGN OF SUPERSONIC WING-BODY COMBINATIONS, INCLUDING FLOW PROPERTIES IN THE NEAR FIELD

PART I — THEORY AND APPLICATION

By F.A. Woodward, E.N. Tinoco, and J.W. Larsen
The Boeing Company

1. SUMMARY

This report presents a numerical method for the analysis of wing-body combinations and the flow fields around them, and for the design of optimum wing camber surfaces in the presence of a body.

The method is based on the linearized theory of supersonic flow. The wing and body are represented by a large number of singularities located in the plane of the wing, on the surface of the body, and along the body axis. The velocity components induced by these singularities at selected control points define a matrix of aerodynamic influence coefficients. The aerodynamic matrix is used to calculate the pressure distribution on the wing and body for given boundary conditions, or to determine the wing camber surface corresponding to a given aerodynamic loading. Additional operations may be performed on the matrix to determine the wing camber surface required to minimize the drag of the wing-body combination under given constraints of lift and pitching moment. Once the strengths of the singularities are known, flow field velocities may be calculated from which streamlines and flow directions can be determined.

The method has been programmed for a digital computer. A special effort has been made to minimize the number of geometrical inputs required in the program by including a geometry definition section and a geometry paneling section as integral parts. A description of the program, including a flow chart and the input formats required for specific problems, is included in this report.

Application of the method to a wide variety of examples has shown good correlation with both theory and experiment. In particular, detailed pressure and force comparisons were made on a wind-tunnel model tested at Mach 1.8. The program also was used to predict the drag reduction achievable through optimizing the wing camber surface on this model.

2. INTRODUCTION

There are several current methods (references 1 through 4) for calculating the camber surface of minimum drag for an isolated wing at a given lift coefficient in supersonic flow. However, none of these allows for the effect a wing-mounted body may have in modifying the optimum wing camber surface. This report presents a new method, based on the linearized theory of supersonic flow, for calculating the optimum camber surface of a wing in the presence of a body. In this method, the boundary condition of tangential flow is satisfied simultaneously on both wing and body, eliminating iteration procedures formerly needed to solve such problems. The improved method has important applications in the design of supersonic aircraft.

This method was developed primarily to optimize camber surfaces for a wing in the presence of a body. However, because it is formulated in terms of aerodynamic influence coefficients, it can be used to solve a wide variety of equally important problems in supersonic flow. For example, it may be used to determine the pressures and forces acting on wings, bodies, or wing-body configurations of given shape or to design a wing having a given pressure distribution in the presence of a body. The bodies may have regular or irregular cross sections, camber, and incidence. The effect of wing thickness may also be included. In addition, the pressure coefficients, velocity components, and streamlines in the field may be calculated. In all these problems, the accuracy of the results ultimately depends on the number of surface boundary points at which the flow equations are satisfied.

The aerodynamic methods described in this report are felt to be significant contributions to the linearized theory of supersonic flow. Although a similar approach has been worked out by H. Carlson and W. Middleton of the NASA Langley Research Center (reference 5), their theory was restricted entirely to the analysis of isolated planar wings. Particularly significant are the theoretical development of the nonplanar, constant-pressure elemental solution to the linearized wave equation and its application to the analysis of supersonic wing-body interference problems.

This volume (Part I) explains the aerodynamic theory underlying the computer program, shows the agreement between the results and other theories, validates the method by comparison with experimental data, and presents sample

cases of design optimization and flow field visualization. It is also a self-sufficient guide for program usage. The second volume (Part II, reference 6) gives the details of the digital computer program. Subroutine descriptions, several sample problems, and a program listing make up the bulk of Part II.

Part I is a revision and extension of reference 7, which was prepared under contract to the NASA Ames Research Center. The changes include higher-order singularity distributions for improving the wing and body thickness solutions and a technique for calculating the pressures, velocity components, and streamlines in the surrounding flow field.

A further theoretical extension of this work is presented in reference 8, which is a modification of the linear theory to include higher-order effects of the local flow. This extension is limited to the wing-alone case.

Much credit is due Dr. Tse Sun Chow, a mathematics research specialist at Boeing, for the integration and checking of the many functions used in the vortex-singularity representation of the method. The aerodynamic work was done by members of the Aerodynamics Research Unit, and the programming and checkout by members of the Technical Support Section; both organizations are part of The Boeing Company's Commercial Airplane Division.

3. LIST OF SYMBOLS

$a_{(\,)}$	Aerodynamic influence coefficient
a	Panel inclination
[A]	Matrix of aerodynamic influence coefficients
$A_{(\,)}$	Panel area
A	Aspect ratio
$b_{(\,)}$	Normalized panel edge slope
b	Wingspan
[B]	Matrix of velocity components
$c_{(\,)}$	Normal velocity component
c	Wing chord
C	Aerodynamic coefficient
D	Pressure drag
$D_{(\,)}$	Downwash function
F	Normal force
$F_{(\,)}$	Auxiliary function
$H_{(\,)}$	Unit step function
J	Number of circumferential points on body
k	Line source strength
K	Number of line singularities in body
ℓ	Partial body length along which line singularity strength varies
L	Lift
L	Body length
m	Panel edge slope
M	Mach number
M	Pitching moment
n	Unit normal vector
$n_{(\,)}$	Normal velocity component
N	Number of panels
p	Pressure
$p_{(\,)}$	Strengths of vortex singularities
$P_{(\,)}$	Pressure function
P	Arbitrary point
q	Dynamic pressure

r	Radial distance
r	Body radius
R	Fraction of panel chord defining control point location
$S_{(\ )}$	Sidewash function
S	Surface area
S_B	Body cross-sectional area
s	Streamline arc length
T	Strength of line singularities
u	Nondimensional perturbation velocity in x direction
U	Free-stream velocity
v	Nondimensional perturbation velocity in y direction
w	Nondimensional perturbation velocity in z direction
x, y, z	Transformed axis system
X, Y, Z	Definition axis system
z_c	Camber line ordinate

Greek

α	Angle of attack
$\alpha_{(\ )}$	Panel inclination (see p. 49)
β	$\sqrt{M^2 - 1}$
γ	Ratio of specific heats for air (1.40)
δ	Delta function
Δ	Difference (e.g., Δp, $\Delta\theta$)
θ	Angular coordinate
θ	Panel inclination (see p. 49)
λ	Lagrange multiplier
Λ	Leading-edge slope
ν	Conormal vector
ξ_1	x-βr Mach line coordinate
π	3.14159
ρ	Density of air
ρ	Body radial distance
σ	Volterra's function
τ	Domain of dependence
φ	Velocity potential

ξ, η, ζ	Integration variables in Cartesian system
Ω	Arbitrary potential function

Subscripts

a	Axial component
A	Referred to body axis
B	Body
c	Cross component
CP	Center of pressure
D	Referred to definition coordinate system
D1	Doublet — linearly varying strength
D2	Doublet — quadratically varying strength
D	Drag
F	Fin
i	Influenced panel number
j	Influencing panel number
k	Line singularity number
k	Corner point number
L	Lift
L	Lower surface
M	Moment
n	Influenced field point
N	Normal component
p	Pressure
r	Radial component
R	Reduced
R	Wing root
S1	Source — linearly varying strength
S2	Source — quadratically varying strength
T	Wing thickness singularity
U	Upper surface
V	Vortex
W	Wing
x, y, z	Referred to Cartesian coordinates
x, y, z	Partial derivative

θ	Tangential component
∞	Free-stream condition

Superscripts

$( )'$	Referred to primed system of coordinates
$( )''$	Referred to double-primed system of coordinates
$\bar{( )}$	Fixed point or value
$\vec{( )}$	Vector

4. AERODYNAMIC THEORY

4.1 Description of Method

Aerodynamic influence coefficients are used to calculate the pressures, forces, and moments on arbitrary wing-body combinations at supersonic speeds and to predict the optimum camber surface of the wing in the presence of the body. In this method, the wing and body are represented by a large number of singularities located in the plane of the wing, on the surface of the body, and along the body axis. In addition, the velocity components, pressures and streamlines in the field may be calculated once the singularity strengths are known. It is assumed that the flow perturbations due to this system of singularities are small enough so that the equations governing the flow can be linearized without introducing significant errors into the analysis.

The basic solution is reached in the following manner. The three components of velocity induced by each elementary singularity are calculated at specified surface control points. Particularly required is the velocity component that is both normal to the body axis and in a plane that is parallel to the body axis and perpendicular to the surface through each control point. The magnitude of this normal velocity component induced at control point i by the j^{th} singularity of unit strength is referred to as the aerodynamic influence coefficient a_{ij}. Thus, the resultant normal velocity at point i is given by the sum of the products of the aerodynamic influence coefficients with their respective singularity strengths.

This resultant normal component of velocity is used to satisfy the surface-slope boundary conditions at each control point, and the resulting system of linear equations is solved for the unknown singularity strengths. The matrix of the coefficients of this system of equations is known as the matrix of aerodynamic influence coefficients, or aerodynamic matrix. It plays an important part in the following analysis.

In practice, the singularity strengths required to satisfy the given boundary conditions are not determined in a single step. The boundary conditions corresponding to wing thickness, body thickness, and body camber and incidence are separated, and the strengths of the specific singularities used to satisfy them are determined independently. In the final stage of the calculation, these separate solutions are combined by linear superposition. Any residual

interference effects, together with the wing camber and incidence boundary conditions, are satisfied by surface distributions of singularities on the wing and body.

To speed the calculation of the aerodynamic influence coefficients, the wing and body are subdivided into small panels, as shown in figure 1. Each panel has one or more singularities associated with it, depending on how the panel boundary conditions are specified. For example, the wing is represented by a maximum of 110 panels located in the wing reference plane. Two types of singularities are specified for each panel. First, a surface distribution of vorticity corresponding to a unit pressure difference across the panel simulates the lifting effects of camber, twist, and incidence; secondly, a surface distribution of sources simulates the effect of wing thickness. It will be shown later how the boundary conditions on the surface of the wing can be completely satisfied by these two independent types of singularities.

The effects of body thickness, or of camber and incidence, are shown by a maximum of 50 line sources and doublets distributed along the body reference axis. In addition, the surface of the body is subdivided into a maximum of 100 panels located in the region of influence of the wing-body intersection. These body panels simulate surface distributions of vorticity, as do the wing panels, and are used to cancel the interference effects of the wing on the body in this region. The boundary conditions on the body, as on the wing, are specified so that they exactly match the number of singularities used to represent the flow.

The location and geometric orientation of each elementary singularity is now defined. It remains to calculate the u, v, and w components of perturbation velocity that a unit strength of a singularity induces at each control point. This report gives formulas for these components for each of the seven types of singularities considered. The v and w components, particularly, can be combined to calculate the aerodynamic influence coefficients for each singularity, with due consideration of the relative orientations of the panels.

Once the aerodynamic matrix has been formed and solved for the unknown singularity strengths, it can be used to calculate the surface pressures, forces, and moments acting on the wing-body combination, and also the velocity components, pressures, and streamlines in the surrounding field.

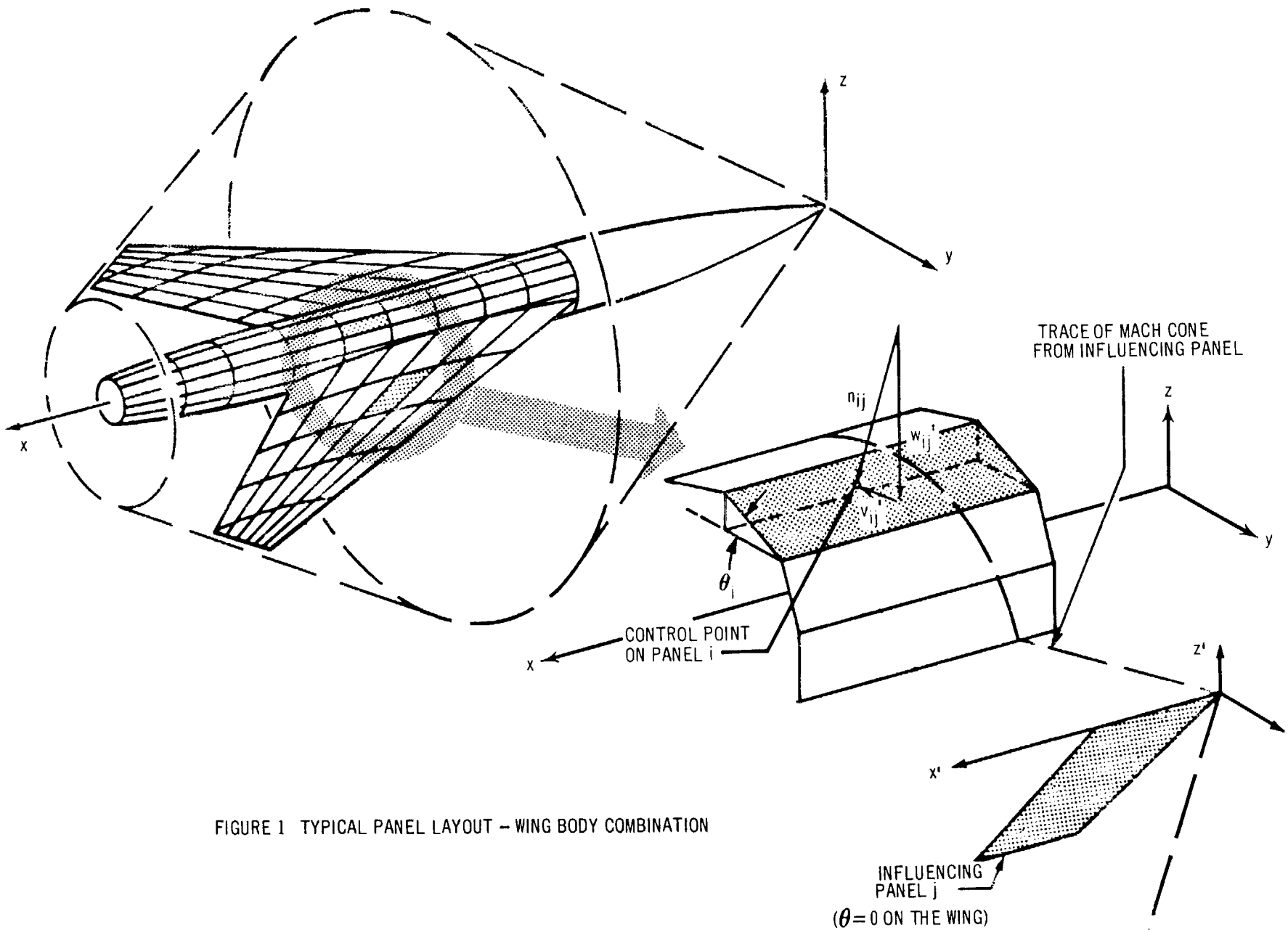

FIGURE 1 TYPICAL PANEL LAYOUT – WING BODY COMBINATION

To find the shape of the wing camber surface that will minimize drag for the wing-body combination under specified conditions of lift and pitching moment, a slightly different method is used to solve for the strengths of the singularities. In this case, an expression for the drag of the complete configuration is derived in terms of the unknown singularity strengths. Applying Lagrange multipliers to the system of equations thus formed determines the singularity strength values that will give the smallest drag for the given lift and pitching moment. These values may then be used to calculate the optimum shape of the camber surface and the corresponding pressures, forces, and moments acting on the configuration.

Calculating perturbation velocity components in the field is similar to calculating velocities on the wing-body combination. Only the singularities inside the forward-facing Mach cone from the point in question influence that point. Once the perturbation velocities are known, they can be used to calculate flow directions, pressures, and streamlines in the field.

4.2 Calculation of Velocity Components — Surface Singularities

Derivation of the generalized potential function. — The linearized differential equation for the velocity potential φ generated by a small perturbation of a steady supersonic flow is given below, where $\beta = \sqrt{M^2 - 1}$ and M is the free-stream Mach number.

$$\beta^2 \varphi_{xx} = \varphi_{yy} + \varphi_{zz} \tag{1}$$

Differential equations of identical form also govern the behavior of the three perturbation velocity components u, v, w in the flow. To extend the following analysis to include the calculation of these velocity components in addition to the potential, equation (1) will be rewritten in terms of an arbitrary variable Ω.

$$\beta^2 \Omega_{xx} = \Omega_{yy} + \Omega_{zz} \tag{2}$$

A general solution to equation (2) is given in reference 9, based on Volterra's solution of the two-dimensional wave equation. This result is repeated below and gives, in integral form, the value of Ω at any point P due to a small perturbation of the flow originating on a surface S:

$$\Omega(x, y, z) = -\frac{1}{2\pi}\frac{\partial}{\partial x}\iint_{\tau}\left(\frac{\partial \Omega}{\partial \nu} + \frac{\partial \Omega'}{\partial \nu'}\right)\sigma \, dS$$

$$+ \frac{1}{2\pi}\frac{\partial}{\partial x}\iint_{\tau}(\Omega - \Omega')\frac{\partial \sigma}{\partial \nu} \, dS \qquad (3)$$

The integrals are to be evaluated on the surface S throughout the "domain of dependence", τ, of point P(x, y, z). The unprimed variable Ω denotes the value of this variable on the same side of S as P, while the primed variable denotes its value on the opposite side of S as P. σ is the particular solution of equation (2) chosen by Volterra which vanishes, together with its derivative with respect to the conormal ν, everywhere on the surface of the Mach forecone from P. The function σ is given below:

$$\sigma = \cosh^{-1}\frac{x - \xi}{\beta\sqrt{(y - \eta)^2 + (z - \zeta)^2}} \qquad (4)$$

It should be noted that σ is the indefinite integral of the fundamental solution of equation (2) representing a supersonic source in three dimensions.

The conormal to a surface S is defined to be a vector, the three components of which are related to the components of the normal vector n to the surface as follows:

$$\nu_1 = -\beta^2 n_1, \qquad \nu_2 = n_2, \qquad \nu_3 = n_3 \qquad (5)$$

ν' is defined to be a vector having the opposite direction to ν on S.

In the following analysis, the surface S is chosen to lie in an inclined plane passing through the y axis. The equation of this plane is $\zeta = a\xi$. The sketch on the following page illustrates the conormal associated with this plane. Note that the conormal to the Mach wave originating from the leading edge of the surface S lies in the plane of that Mach wave.

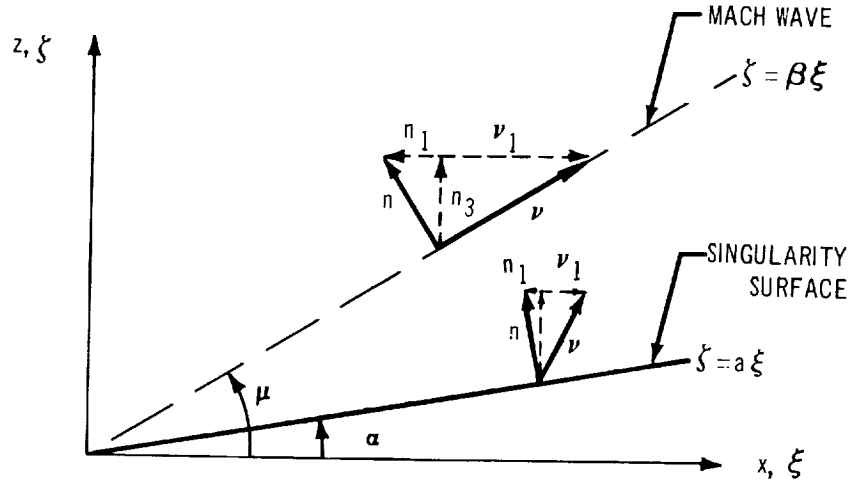

In this example,

$$\frac{\partial \sigma}{\partial \nu} = \nu_1 \frac{\partial \sigma}{\partial \xi} + \nu_3 \frac{\partial \sigma}{\partial \zeta} = -\beta^2 n_1 \frac{\partial \sigma}{\partial \xi} + n_3 \frac{\partial \sigma}{\partial \zeta} \qquad (6)$$

Now

$$n_1 = -\sin \alpha = -\frac{a}{\sqrt{1 + a^2}}$$

$$n_3 = \cos \alpha = \frac{1}{\sqrt{1 + a^2}}$$

Therefore

$$\frac{\partial \sigma}{\partial \nu} = \frac{\beta^2 a}{\sqrt{1 + a^2}} \frac{\partial \sigma}{\partial \xi} + \frac{1}{\sqrt{1 + a^2}} \frac{\partial \sigma}{\partial \zeta}$$

$$= \frac{-\beta^2 a + \dfrac{(x - \xi)(z - \zeta)}{(y - \eta)^2 + (z - \zeta)^2}}{\sqrt{1 + a^2}\ \sqrt{(x - \xi)^2 - \beta^2 (y - \eta)^2 - \beta^2 (z - \zeta)^2}}$$

(7)

Note also that an elementary area dS in the plane may be written

$$dS = d\xi\, d\eta/\cos\alpha$$
$$= \sqrt{1 + a^2}\; d\xi\, d\eta \qquad (8)$$

Consider now a semi-infinite triangular region in the plane $\zeta = a\xi$, such that the leading edge of the triangle has the projection $\eta = m\xi$ in the ξ, η plane, while the side edge lies in the ξ, ζ plane. The domain of dependence τ of the integrals in equation (3) is then the area on this oblique triangular region lying upstream of its intersection with the Mach forecone from P, OQR in figure 2. The equation of the curve QR is determined by substituting $\zeta = a\xi$ in the equation for the Mach forecone from P:

$$(x - \xi)^2 = \beta^2(y - \eta)^2 + \beta^2(z - a\xi)^2 \qquad (9)$$

Thus, for a given η, the points S and T on an elementary strip of width $d\eta$ on the surface have the coordinates $S(\xi_1, \eta, a\xi_1)$ and $T(\xi_2, \eta, a\xi_2)$

where $\xi_1 = \eta/m$

and $$\xi_2 = \frac{x - \beta^2 a z}{1 - \beta^2 a^2}\left(1 - \sqrt{1 - \frac{1 - \beta^2 a^2}{(x - \beta^2 a z)^2}\left(x^2 - \beta^2(y - \eta)^2 - \beta^2 z^2\right)}\right) \qquad (10)$$

and the point Q has the coordinates $Q(\eta_3/m, \eta_3, a\eta_3/m)$

where $$\eta_3 = \frac{m\left(x - \beta^2(m y + a z)\right)}{1 - \beta^2(a^2 + m^2)}\left(1 - \sqrt{1 - \frac{\left(1 - \beta^2(a^2 + m^2)\right)\left(x^2 - \beta^2(y^2 + z^2)\right)}{\left(x - \beta^2(m y + a z)\right)^2}}\right) \qquad (11)$$

Equation (3) may now be written:

$$\Omega(x, y, z) = -\frac{\sqrt{1 + a^2}}{2\pi}\frac{\partial}{\partial x}\int_0^{\eta_3} d\eta \int_{\xi_1}^{\xi_2}\left(\frac{\partial\Omega}{\partial\nu} + \frac{\partial\Omega'}{\partial\nu'}\right)\cosh^{-1}\frac{x - \xi}{\beta\sqrt{(y - \eta)^2 - (z - a\xi)^2}}\, d\xi$$

$$+ \frac{1}{2\pi}\frac{\partial}{\partial x}\int_0^{\eta_3} d\eta \int_{\xi_1}^{\xi_2}(\Omega - \Omega')\frac{-\beta^2 a + \dfrac{(x - \xi)(z - a\xi)}{(y - \eta)^2 - (z - a\xi)^2}}{\sqrt{(x - \xi)^2 - \beta^2(y - \eta)^2 - \beta^2(z - a\xi)^2}}\, d\xi \qquad (12)$$

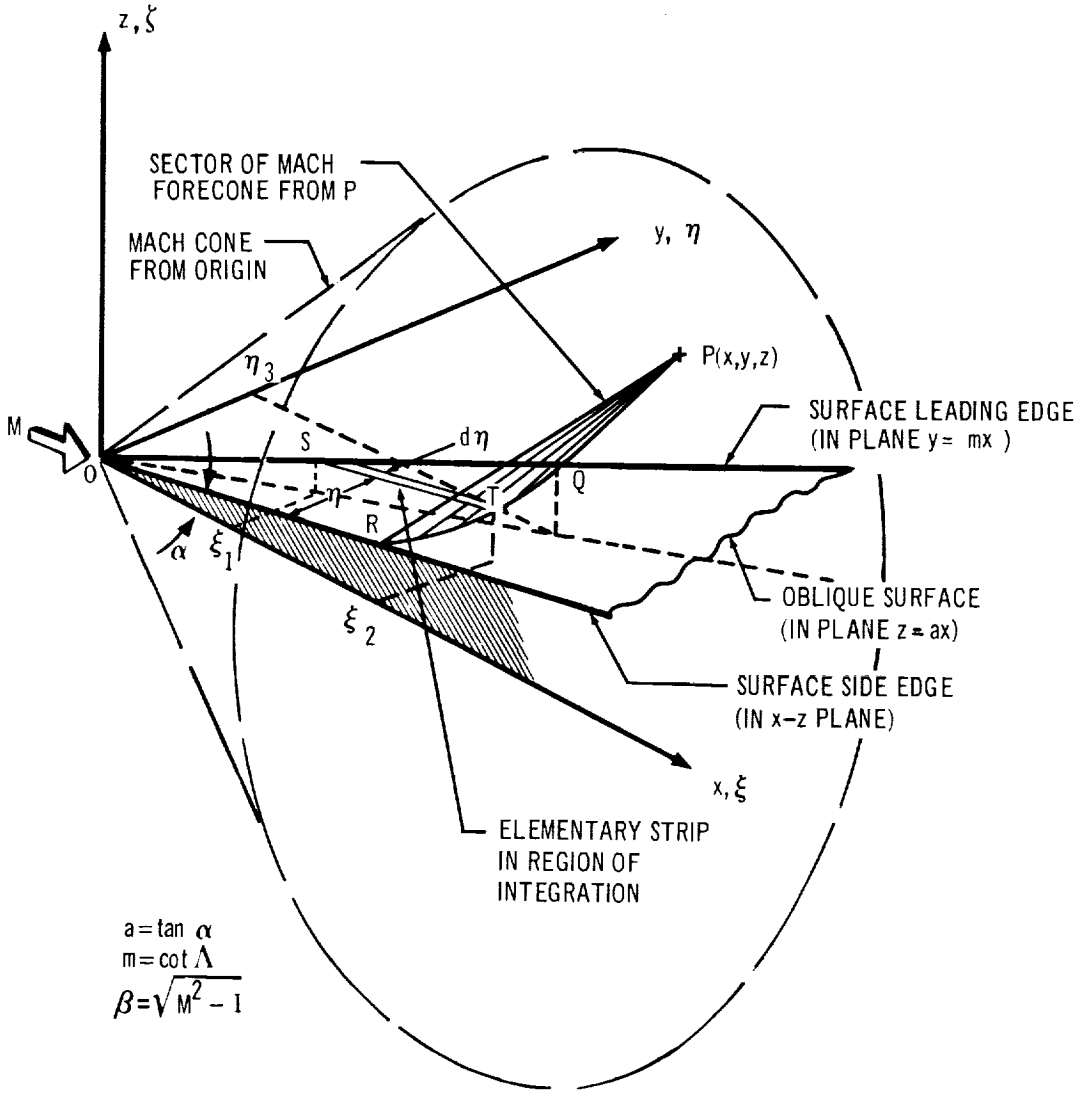

$$\xi_1 = \eta / m$$

$$\xi_2 = \frac{x - \beta^2 a z}{1 - \beta^2 a^2} \left[1 - \sqrt{1 - \frac{1 - \beta^2 a^2}{(x - \beta^2 a z)^2} (x^2 - \beta^2 (y - \eta)^2 - \beta^2 z^2)} \right]$$

$$\eta_3 = \frac{m (x - \beta^2 m y - \beta^2 a z)}{1 - \beta^2 (a^2 + m^2)} \left[1 - \sqrt{1 - \frac{\left[1 - \beta^2 (a^2 + m^2)\right]\left[x^2 - \beta^2 (y^2 + z^2)\right]}{(x - \beta^2 m y - \beta^2 a z)^2}} \right]$$

FIGURE 2 GEOMETRIC ORIENTATION OF INCLINED SINGULARITY SURFACE

The integrals in equation (12) may now be evaluated, provided the expressions $(\Omega - \Omega')$ and $(\partial\Omega/\partial\nu + \partial\Omega'/\partial\nu')$ are prescribed on S. It is most convenient to set them equal to a constant or zero. Two choices of Ω will now be described that will satisfy these conditions and yield expressions for the potential function representing either a surface distribution of sources in the ξ, η plane or a constant pressure jump across a lifting surface corresponding to a constant distribution of vorticity in the plane $\zeta = a\xi$.

Potential function for constant source distribution. — In equation (12), Ω is set equal to the perturbation velocity potential φ on the upper surface of S. The partial derivative $\partial\varphi/\partial\nu$ then represents the velocity component in the direction of the conormal to the upper surface of S. Similarly, $\partial\varphi'/\partial\nu'$ represents the velocity component of the lower surface potential function φ' in the direction of the conormal to the lower surface of S.

Now,

$$\frac{\partial\varphi}{\partial\nu} = \frac{\beta^2 a}{\sqrt{1 + a^2}} \frac{\partial\varphi}{\partial\xi} + \frac{1}{\sqrt{1 + a^2}} \frac{\partial\varphi}{\partial\zeta}$$

$$= -\frac{\beta^2 a}{\sqrt{1 + a^2}} u + \frac{1}{\sqrt{1 + a^2}} w \qquad (13)$$

Similarly,

$$\frac{\partial\varphi'}{\partial\nu'} = -\frac{\beta^2 a}{\sqrt{1 + a^2}} u' - \frac{1}{\sqrt{1 + a^2}} w' \qquad (14)$$

The sketch on the following page illustrates the geometrical orientation of these velocity components.

It can be seen that if φ' has the same sign as φ, a discontinuity in the ν component of velocity will appear in the flow on the surface $\zeta = a\xi$ which in turn implies surface discontinuities in the u and w velocity components. In fact, if $\varphi' = \varphi$, then $u' = -u$, $w' = -w$ on the surface.

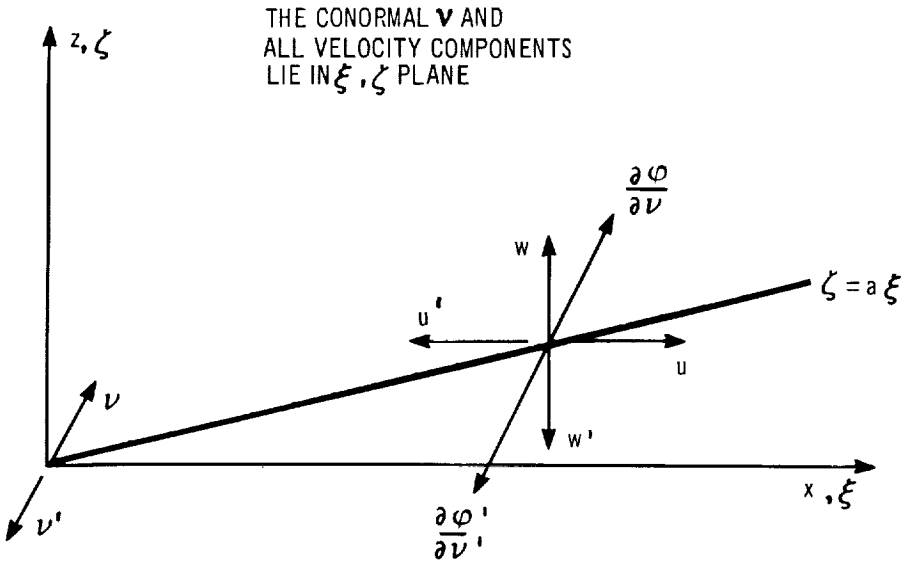

The second term in equation (12) then vanishes, and

$$\frac{\partial \varphi}{\partial \nu} + \frac{\partial \varphi'}{\partial \nu'} = \frac{2}{\sqrt{1 + a^2}} (\bar{w} + \beta^2 \, a \, \bar{u}) \tag{15}$$

where the bars denote the values of the velocity components on the surface .

If the quantity $(\bar{w} + \beta^2 \, a \, \bar{u})$ is constant, it can be taken outside the integral. If, in addition, the partial derivative of σ with respect to x is taken through the double integral, which is a legitimate operation in this case, equation (12) reduces to

$$\varphi(x, y, z) = - \frac{\bar{w} + \beta^2 \, a \, \bar{u}}{\pi} \int_0^{\eta_3} d\eta \int_{\xi_1}^{\xi_2} \frac{d\xi}{\sqrt{(x - \xi)^2 - \beta^2 (y - \eta)^2 - \beta^2 (z - a \, \xi)^2}} \tag{16}$$

For the special case a = 0, this expression reverts to the usual integral form for the potential due to a surface distribution of sources in the ξ, η plane. The integral will be evaluated in its most general form, however, as the resulting

functions will be used later in the derivation of the potential due to a constant pressure difference across the surface S.

Applying the integration formulae appearing in Appendix A, and simplifying, the following result is obtained for the case $\beta\sqrt{a^2 + m^2} < 1$ (subsonic leading edge):

$$\varphi(x, y, z) = \frac{\bar{w} + \beta^2 a \bar{u}}{\pi\sqrt{1 - \beta^2 a^2}} \int_0^{\eta_3} \cosh^{-1} \frac{(1 - \beta^2 a^2)\eta - m(x - \beta^2 az)}{\beta m\sqrt{(1 - \beta^2 a^2)(\eta - y)^2 + (z - ax)^2}}\, d\eta$$

$$= \frac{\bar{w} + \beta^2 a \bar{u}}{\pi} \left\{ \frac{z - ax}{1 - \beta^2 a^2} \tan^{-1} \frac{m(z - ax)\sqrt{x^2 - \beta^2(y^2 + z^2)}}{y[(y - mx) - \beta^2 a(ay - mz)] + (z - ax)^2} \right.$$

$$+ \frac{(1 - \beta^2 a^2) y - m(x - \beta^2 az)}{(1 - \beta^2 a^2)\sqrt{1 - \beta^2(a^2 + m^2)}} \cosh^{-1} \frac{x - \beta^2(my + az)}{\beta\sqrt{(y - mx)^2 + (z - ax)^2 - \beta^2(ay - mz)^2}}$$

$$\left. - \frac{y}{\sqrt{1 - \beta^2 a^2}} \cosh^{-1} \frac{x}{\beta\sqrt{y^2 + z^2}} \right\} \qquad (17)$$

If $\beta\sqrt{a^2 + m^2} \geq 1$ (sonic or supersonic leading edge), the inverse hyperbolic cosine is replaced by the inverse cosine [see equation (43)].

The perturbation velocity components may now be obtained by differentiation.

$$u = \frac{\partial\varphi}{\partial x} = \frac{-(\bar{w} + \beta^2 a \bar{u})}{\pi(1 - \beta^2 a^2)} \left\{ a \tan^{-1} \frac{m(z - ax)\sqrt{x^2 - \beta^2(y^2 + z^2)}}{y[(y - mx) - \beta^2 a(ay - mz)] + (z - ax)^2} \right.$$

$$\left. + \frac{m}{\sqrt{1 - \beta^2(a^2 + m^2)}} \cosh^{-1} \frac{x - \beta^2(my + az)}{\beta\sqrt{(y - mx)^2 + (z - ax)^2 - \beta^2(ay - mz)^2}} \right\}$$

$$v = \frac{\partial\varphi}{\partial y} = \frac{-(\bar{w} + \beta^2 a \bar{u})}{\pi} \left\{ \frac{1}{\sqrt{1 - \beta^2 a^2}} \cosh^{-1} \frac{x}{\beta\sqrt{y^2 + z^2}} \right.$$

$$\left. - \frac{1}{\sqrt{1 - \beta^2(a^2 + m^2)}} \cosh^{-1} \frac{x - \beta^2(my + az)}{\beta\sqrt{(y - mx)^2 + (z - ax)^2 - \beta^2(ay - mz)^2}} \right\}$$

$$w = \frac{\partial \varphi}{\partial z} = \frac{(\bar{w} + \beta^2 a \bar{u})}{\pi(1 - \beta^2 a^2)} \left\{ \tan^{-1} \frac{m(z - ax)\sqrt{x^2 - \beta^2(y^2 + z^2)}}{y[(y - mx) - \beta^2 a(ay - mz)] + (z - ax)^2} \right.$$

$$\left. + \frac{\beta^2 a m}{\sqrt{1 - \beta^2(a^2 + m^2)}} \cosh^{-1} \frac{x - \beta^2(my + az)}{\beta\sqrt{(y - mx)^2 + (z - ax)^2 - \beta^2(ay - mz)^2}} \right\} \quad (18)$$

It should be noted that $\varphi = xu + yv + zw.$ (19)

The results may be quickly verified by evaluating u and w on the surface $z = ax$.

Noting that

$$\tan^{-1} \frac{m(z - ax)\sqrt{x^2 - \beta^2(y^2 + z^2)}}{y[(y - mx) - \beta^2 a(ay - mz)] + (z - ax)^2} \quad (20)$$

$$= \pi \quad \text{for} \quad z = ax, \quad \text{and} \quad 0 < y < mx$$

$$= 0 \quad \text{for} \quad z = ax, \quad \text{and} \quad y < 0, \quad y > mx$$

Then, for $0 < y < mx$,

$$\bar{u} = \frac{-(\bar{w} + \beta^2 a \bar{u})}{\pi(1 - \beta^2 a^2)} \left\{ a\pi + \frac{m}{\sqrt{1 - \beta^2(a^2 + m^2)}} \cosh^{-1} \frac{x(1 - \beta^2 a^2) - \beta^2 my}{\beta\sqrt{1 - \beta^2 a^2}\,|y - mx|} \right\}$$

$$\bar{w} = \frac{(\bar{w} + \beta^2 a \bar{u})}{\pi(1 - \beta^2 a^2)} \left\{ \pi + \frac{\beta^2 a m}{\sqrt{1 - \beta^2(a^2 + m^2)}} \cosh^{-1} \frac{x(1 - \beta^2 a^2) - \beta^2 my}{\beta\sqrt{1 - \beta^2 a^2}\,|y - mx|} \right\}$$

Therefore $\bar{w} + \beta^2 a \bar{u} \equiv \frac{(\bar{w} + \beta^2 a \bar{u})}{(1 - \beta^2 a^2)\pi} (1 - \beta^2 a^2)\pi$ (21)

Thus the resulting flow satisfies the imposed boundary conditions on the semi-infinite triangular surface illustrated in figure 2. Off this surface, in the plane $z = ax$, the quantity $(\bar{w} + \beta^2 a \bar{u}) = 0$.

Two special cases of these results deserve attention, as they will be used later in the numerical analysis. In the first, for $a = 0$, the velocity components due to a surface distribution of sources in the x, y plane are simply obtained from equations (18):

$$u_1 = -\frac{\bar{w}}{\pi} m \left[\frac{1}{\sqrt{1-\beta^2 m^2}} \cosh^{-1} \frac{x - \beta^2 my}{\beta\sqrt{(mx-y)^2 + (1-\beta^2 m^2) z^2}} \right]$$

$$v_1 = \left(\frac{\bar{w}m}{\pi}\right) \left\{ \frac{1/m}{\sqrt{1-\beta^2 m^2}} \cosh^{-1} \frac{x - \beta^2 my}{\beta\sqrt{(mx-y)^2 + (1-\beta^2 m^2) z^2}} - \frac{1}{m} \cosh^{-1} \frac{x}{\beta\sqrt{y^2+z^2}} \right\}$$

$$w_1 = \left(\frac{\bar{w}m}{\pi}\right) \left[\frac{\tan^{-1}}{m} \frac{mz\sqrt{x^2 - \beta^2(y^2+z^2)}}{y^2 + z^2 - mxy} \right] \qquad (22)$$

In the second special case, the velocity components due to a line source along the x axis will be derived. The term $m\bar{w}/\pi$ is taken as a constant (for $m \to 0$) in the equations for the velocity components given by equation (22), and the limit of the resulting expressions evaluated as m approaches zero. The result is given below:

$$u_{S1} = -k \cosh^{-1} \frac{x}{\beta\sqrt{y^2+z^2}}$$

$$v_{S1} = \frac{k\,y}{\sqrt{y^2+z^2}} \sqrt{x^2 - \beta^2(y^2+z^2)}$$

$$w_{S1} = \frac{k\,z}{\sqrt{y^2+z^2}} \sqrt{x^2 - \beta^2(y^2+z^2)} \qquad (23)$$

where $k = \lim_{m \to 0} \frac{m\bar{w}}{\pi}$ = constant, and the subscript S1 refers to a line source having a linear variation with x.

These velocity components will be used later to represent the flow surrounding a circular cone at zero incidence centered on the x axis. The potential function corresponding to this flow is

$$\varphi_{S1} = k \left\{ x \cosh^{-1} \frac{x}{\beta\sqrt{y^2+z^2}} - \sqrt{x^2 - \beta^2(y^2+z^2)} \right\} \qquad (24)$$

Potential function for linearly varying source distribution. —A good representation of wing thickness effects is obtained by a combination of constant and linearly varying source distributions, provided no discontinuity in slope occurs on the wing chord. The potential for a source distribution in which the normal component of velocity varies linearly with the distance from the leading edge may be obtained by substituting $(\xi - \eta/m)$ in the integrand of equation (16). For sources distributed in the x, y plane, a = 0, and the integral may be written

$$\varphi(x, y, z) = -\frac{\bar{w}_x}{\pi} \int_0^{\eta_1} d\eta \int_{\xi_1}^{\xi_2} \frac{(\xi - \eta/m)\, d\xi}{\sqrt{(x-\xi)^2 - \beta^2 (y-\eta)^2 - \beta^2 z^2}} \tag{25}$$

where the limits of integration are given by equations (10) and (11) with $a = 0$.

For regions having a subsonic leading edge, $\beta m < 1$,

$$\varphi(x, y, z) = \frac{-\bar{w}_x}{2\pi m} \left\{ \frac{(mx - y)^2 - (1-\beta^2 m^2) z^2}{\sqrt{1-\beta^2 m^2}} \cosh^{-1} \frac{x - \beta^2 my}{\beta\sqrt{(mx - y)^2 + (1 - \beta^2 m^2) z^2}} \right.$$

$$- (y^2 - z^2 - 2mxy) \cosh^{-1} \frac{x}{\beta\sqrt{y^2 + z^2}} - my\sqrt{x^2 - \beta^2 (y^2 + z^2)}$$

$$\left. - 2z\,(mx - y) \tan^{-1} \frac{mz\sqrt{x^2 - \beta^2 (y^2 + z^2)}}{y^2 + z^2 - mxy} \right\} \tag{26}$$

For regions having a sonic or supersonic leading edge $\beta m \geq 1$, the inverse hyperbolic cosine term must be replaced by equations (42) or (43).

The velocity components are obtained by differentiation, as before.

$$u_2 = -\frac{\bar{w}_x}{\pi} \left\{ \frac{(mx - y)}{\sqrt{1 - \beta^2 m^2}} \cosh^{-1} \frac{x - \beta^2 my}{\beta\sqrt{(mx - y)^2 + (1 - \beta^2 m^2) z^2}} + y \cosh^{-1} \frac{x}{\beta\sqrt{y^2 + z^2}} \right.$$

$$\left. - z \tan^{-1} \frac{mz\sqrt{x^2 - \beta^2 (y^2 + z^2)}}{y^2 + z^2 - mxy} \right\}$$

$$v_2 = \frac{\bar{w}_x}{\pi m}\left\{(mx - y)\left[\frac{1}{\sqrt{1-\beta^2 m^2}}\cosh^{-1}\frac{x-\beta^2 my}{\beta\sqrt{(mx-y)^2+(1-\beta^2m^2)z^2}} - \cosh^{-1}\frac{x}{\beta\sqrt{y^2+z^2}}\right] + m\sqrt{x^2-\beta^2(y^2+z^2)} - z\tan^{-1}\frac{z\sqrt{x^2-\beta^2(y^2+z^2)}}{y^2+z^2-mxy}\right\}$$

$$w_2 = \frac{\bar{w}_x}{\pi m}\left\{z\left[\sqrt{1-\beta^2m^2}\cosh^{-1}\frac{x-\beta^2my}{\beta\sqrt{(mx-y)^2+(1-\beta^2m^2)z^2}} - \cosh^{-1}\frac{x}{\beta\sqrt{y^2+z^2}}\right] + (mx-y)\tan^{-1}\frac{mz\sqrt{x^2-\beta^2(y^2+z^2)}}{y^2+z^2-mxy}\right\} \quad (27)$$

In the plane $z = 0$

$$w_2 = \bar{w}_x\,(x - y/m) \qquad \text{for } 0<y<mx$$

$$= 0 \qquad \text{for } y<0,\ y>mx$$

Thus, for constant y, $\bar{w}_x$ can be interpreted as the rate of change of w in the x direction.

Potential function for constant pressure surface. — In equation (12), Ω is set equal to the perturbation velocity u on the upper surface of S. The desired solution will have a constant difference in u everywhere on S, that is $\Delta u = u - u' = \text{constant}$. Before introducing this condition into equation (12), the derivative of u and u' with respect to the conormal is investigated. Following the same procedure used in deriving equation (6),

$$\frac{\partial u}{\partial \nu} = \frac{\beta^2 a}{\sqrt{1 + a^2}} \frac{\partial u}{\partial \xi} + \frac{1}{\sqrt{1 + a^2}} \frac{\partial u}{\partial \zeta}$$

$$\frac{\partial u'}{\partial \nu'} = \frac{-\beta^2 a}{\sqrt{1 + a^2}} \frac{\partial u'}{\partial \xi} - \frac{1}{\sqrt{1 + a^2}} \frac{\partial u'}{\partial \zeta} \tag{28}$$

Summing these expressions, the following result is obtained:

$$\frac{\partial u}{\partial \nu} + \frac{\partial u'}{\partial \nu'} = \frac{1}{\sqrt{1 + a^2}} \left[\beta^2 a \frac{\partial}{\partial \xi} (u - u') + \frac{\partial}{\partial \zeta} (u - u') \right] = 0,$$

since $(u - u')$ is constant on the surface S. Therefore the first term in equation (12) vanishes, and the equation reduces to

$$u(x, y, z) = \frac{\Delta u}{2\pi} \frac{\partial}{\partial x} \int_0^{\eta_3} d\eta \int_{\xi_1}^{\xi_2} \frac{-\beta^2 a + \dfrac{(x - \xi)(z - a\xi)}{(y - \eta)^2 + (z - a\xi)^2}}{\sqrt{(x - \xi)^2 - \beta^2 (y - \eta)^2 - \beta^2 (z - a\xi)^2}} d\xi \tag{29}$$

Since $u = \partial\varphi/\partial x$, an expression for the potential function may be obtained by integrating equation (29) with respect to x. Since the potential is zero everywhere ahead of the envelope of Mach cones defined by the leading edge of the surface S, the constant of integration is zero, and the potential function, in integral form, becomes

$$\varphi(x, y, z) = \frac{-1}{4\pi}\left(\frac{\Delta p}{q_\infty}\right)\int_0^{\eta_3} d\eta \int_{\xi_1}^{\xi_2} \frac{-\beta^2 a + \dfrac{(x-\xi)(z-a\xi)}{(y-\eta)^2 + (z-a\xi)^2}}{\sqrt{(x-\xi)^2 - \beta^2(y-\eta)^2 - \beta^2(z-a\xi)^2}}\, d\xi \tag{30}$$

where Δu has been replaced by $-\Delta p/2q_\infty$. Δp is the pressure difference across the lifting surface S, and q_∞ is the dynamic pressure $\gamma\, p_\infty\, M^2/2$, where p_∞ is the static pressure in the undisturbed flow. Equation (30) thus gives the potential function corresponding to the oblique triangular region of constant lifting pressure illustrated in figure 2.

Equation (30) breaks down naturally into two double integrals as follows:

$$\varphi(x, y, z) = \frac{\beta^2 a}{4\pi}\left(\frac{\Delta p}{q_\infty}\right)\int_0^{\eta_3} d\eta \int_{\xi_1}^{\xi_2} \frac{d\xi}{\sqrt{(x-\xi)^2 - \beta^2(y-\eta)^2 - \beta^2(z-a\xi)^2}}$$

$$- \frac{1}{4\pi}\left(\frac{\Delta p}{q_\infty}\right)\int_0^{\eta_3} d\eta \int_{\xi_1}^{\xi_2} \frac{(x-\xi)(z-a\xi)\, d\xi}{\left[(y-\eta)^2 + (z-a\xi)^2\right]\sqrt{(x-\xi)^2 - \beta^2(y-\eta)^2 - \beta^2(z-a\xi)^2}} \tag{31}$$

The integration with respect to ξ is carried out first, making use of the integration formulae in Appendix A. It should also be noted that the first integral is identical to that in equation (16) for the surface distribution of sources. After some simplification, the following result is obtained:

$$\varphi(x, y, z) = \frac{-\beta^2 a}{4\pi}\left(\frac{\Delta p}{q_\infty}\right)\int_0^{\eta_3} \frac{1}{\sqrt{1-\beta^2 a^2}} \cosh^{-1} \frac{(1-\beta^2 a^2)\eta - m(x-\beta^2 az)}{\beta m\sqrt{(1-\beta^2 a^2)(\eta-y)^2 + (z-ax)^2}}\, d\eta$$

$$- \frac{1}{4\pi a}\left(\frac{\Delta p}{q_\infty}\right)\int_0^{\eta_3} \left[\cosh^{-1} \frac{y - mx}{\beta\sqrt{(a\eta - mz)^2 + m^2(\eta - y)^2}}\right.$$

$$\left. - \frac{1}{\sqrt{1-\beta^2 a^2}} \cosh^{-1} \frac{(1-\beta^2 a^2)\eta - m(x-\beta^2 az)}{\beta m\sqrt{(1-\beta^2 a^2)(\eta-y)^2 + (z-ax)^2}}\right] d\eta$$

and combining terms

$$\varphi(x,y,z) = \frac{-1}{4\pi a}\left(\frac{\Delta p}{q_\infty}\right)\int_0^{\eta_3}\left[\cosh^{-1}\frac{y - mx}{\beta\sqrt{(a\eta - mz)^2 + m^2(\eta - y)^2}}\right.$$

$$\left. - \sqrt{1 - \beta^2 a^2}\,\cosh^{-1}\frac{(1 - \beta^2 a^2)\,\eta - m(x - \beta^2 az)}{\beta m\sqrt{(1 - \beta^2 a^2)\,(\eta - y)^2 + (z - ax)^2}}\right] d\eta \qquad (32)$$

By repeated application of the integration formulae in Appendix A, the integration with respect to η may be completed, after some lengthy computation, giving the final result:

$$\varphi(x,\,y,\,z) = \frac{-1}{4\pi}\left(\frac{\Delta p}{q_\infty}\right)\left\{x\tan^{-1}\frac{m(z - ax)\sqrt{x^2 - \beta^2(y^2 + z^2)}}{y\left[(y - mx) - \beta^2 a(ay - mz)\right] + (z - ax)^2}\right.$$

$$- \frac{y}{a^2 + m^2}\left[a\sqrt{1 - \beta^2(a^2 + m^2)}\,\cosh^{-1}\frac{x - \beta^2(my + az)}{\beta\sqrt{(mx - y)^2 + (ax - z)^2 - \beta^2(ay - mz)^2}}\right.$$

$$+ m\tan^{-1}\frac{(ay - mz)\sqrt{x^2 - \beta^2(y^2 + z^2)}}{x(my + az) - y^2 - z^2}$$

$$+ \frac{1}{a}\left(m^2\tanh^{-1}\frac{\sqrt{x^2 - \beta^2(y^2 + z^2)}}{x}\right.$$

$$\left.\left. - (a^2 + m^2)\sqrt{1 - \beta^2 a^2}\,\tanh^{-1}\frac{\sqrt{(1 - \beta^2 a^2)\left(x^2 - \beta^2(y^2 + z^2)\right)}}{x - \beta^2 az}\right)\right]$$

$$+ \frac{z}{a^2 + m^2}\left[m\sqrt{1 - \beta^2(a^2 + m^2)}\,\cosh^{-1}\frac{x - \beta^2(my + az)}{\beta\sqrt{(mx - y)^2 + (ax - z)^2 - \beta^2(ay - mz)^2}}\right.$$

$$- m\tanh^{-1}\frac{\sqrt{x^2 - \beta^2(y^2 + z^2)}}{x}$$

$$+ \frac{1}{a}\left(m^2\tan^{-1}\frac{(ay - mz)\sqrt{x^2 - \beta^2(y^2 + z^2)}}{x(my + az) - y^2 - z^2}\right.$$

$$\left.\left.\left. - (a^2 + m^2)\tan^{-1}\frac{m(z - ax)\sqrt{x^2 - \beta^2(y^2 + z^2)}}{y\left[(y - mx) - \beta^2 a(ay - mz)\right] + (z - ax)^2}\right)\right]\right\} \qquad (33)$$

This equation is valid only if $\beta\sqrt{a^2 + m^2} < 1$ (subsonic leading edge). If $\beta\sqrt{a^2 + m^2} \geq 1$ (sonic or supersonic edge), the inverse hyperbolic cosine is replaced by the inverse cosine[(see equation 43)].

The velocity components may now be obtained by differentiating equation (30), where $u = \frac{\partial \varphi}{\partial x}$, $v = \frac{\partial \varphi}{\partial y}$, $w = \frac{\partial \varphi}{\partial z}$

The evaluation of these derivatives is rather lengthy: however, it can be proved that u, v, w are merely the coefficients of x, y, z respectively in the expression $\varphi(x, y, z)$, given by equation (33). Thus,

$$\varphi(x, y, z) = xu + yv + zw \tag{34}$$

and u, v, w may be obtained from equation (33) by inspection[(cf. equations (18) and (19)].

The results may be verified by evaluating u on the surface z = ax. Substituting equation (20) into the first term of equation (33), then,

$$\bar{u} = \frac{-\Delta p}{4 q_\infty} = -\frac{p - p'}{4 q_\infty} \quad \text{for} \quad 0 < y < mx$$

$$= 0 \quad \text{for} \quad y < 0, \quad \text{or} \quad y > mx$$

Thus the horizontal component of velocity on the upper surface exactly equals one quarter of the pressure difference between the lower and upper surfaces, divided by q_∞. Since the horizontal component of velocity on the lower surface $\bar{u}'$ is equal and opposite to $\bar{u}$, the pressure coefficient on the lower surface must also be equal and opposite to that on the upper. That is,

$$C_{P_{upper}} = \frac{p}{q_\infty} = -2\bar{u} \tag{35}$$

$$C_{P_{lower}} = \frac{p'}{q_\infty} = -2\bar{u}' = 2\bar{u}$$

The velocity components will now be written out for the special case a = 0, in which the triangular region of constant pressure is located in the x, y plane. Two terms in each of the u and w velocity component formulae require special attention. The limits of these two terms as a goes to zero are written out below:

$$\lim_{a\to 0}\left\{\frac{1}{a}\left[m^2 \tanh^{-1}\frac{\sqrt{x^2-\beta^2(y^2+z^2)}}{x} - (a^2+m^2)\sqrt{1-\beta^2 a^2}\tanh^{-1}\frac{\sqrt{(1-\beta^2 a^2)\left(x^2-\beta^2(y^2+z^2)\right)}}{x-\beta^2 az}\right]\right\}$$

$$= -\frac{m^2 z}{y^2+z^2}\sqrt{x^2-\beta^2(y^2+z^2)} \qquad (36)$$

$$\lim_{a\to 0}\left\{\frac{1}{a}\left[m^2 \tan^{-1}\frac{(ay-mz)\sqrt{x^2-\beta^2(y^2+z^2)}}{x(my+az)-(y^2+z^2)} - (a^2+m^2)\tan^{-1}\frac{m(z-ax)\sqrt{x^2-\beta^2(y^2+z^2)}}{y\left[(y-mx)-\beta^2 a(ay-mz)\right]+(z-ax)^2}\right]\right\}$$

$$= -\frac{m^2 y}{y^2+z^2}\sqrt{x^2-\beta^2(y^2+z^2)} \qquad (37)$$

The velocity components for this special case ($a = 0$) may now be written:

$$u_3 = -\frac{\Delta p}{4\pi q_\infty}\tan^{-1}\frac{mz\sqrt{x^2-\beta^2(y^2+z^2)}}{y^2+z^2-mxy}$$

$$v_3 = \frac{\Delta p}{4\pi q_\infty}\left\{\frac{1}{m}\tan^{-1}\frac{mz\sqrt{x^2-\beta^2(y^2+z^2)}}{y^2+z^2-mxy} - \frac{z}{y^2+z^2}\sqrt{x^2-\beta^2(y^2+z^2)}\right\}$$

$$w_3 = -\frac{\Delta p}{4\pi q_\infty}\left\{\frac{1}{m}\left[\sqrt{1-\beta^2 m^2}\cosh^{-1}\frac{x-\beta^2 my}{\beta\sqrt{(mx-y)^2+(1-\beta^2 m^2)z^2}} - \cosh^{-1}\frac{x}{\beta\sqrt{y^2+z^2}}\right] - \frac{y}{y^2+z^2}\sqrt{x^2-\beta^2(y^2+z^2}\right\} \qquad (38)$$

This expression for w_3, with $z = 0$, agrees with the downwash function presented by other investigators for a triangular plate with uniform loading. [(See, for example, equation (32) of reference 9)].

Classification of the velocity functions. — It is apparent from the preceding analysis that certain functions appear repeatedly in the equations for the perturbation velocity components and potential functions, equations (18), (22), (23), (33), and (38). These functions are listed below:

$$F1 = \tan^{-1} \frac{m(z - ax)\sqrt{x^2 - \beta^2(y^2 + z^2)}}{y\left[(y - mx) - \beta^2 a(ay - mz)\right] + (z - ax)^2}$$

$$F2 = \frac{1}{\sqrt{1 - \beta^2(a^2 + m^2)}} \cosh^{-1} \frac{x - \beta^2(my + az)}{\beta\sqrt{(y - mx)^2 + (z - ax)^2 - \beta^2(ay - mz)^2}}$$

$$F3 = \tan^{-1} \frac{(ay - mz)\sqrt{x^2 - \beta^2(y^2 + z^2)}}{x(my + az) - (y^2 + z^2)}$$

$$F4 = \left(F3 - (1 + a^2/m^2)\ F1\right)\ (m/a)$$

$$F5 = \tanh^{-1} \frac{\sqrt{x^2 - \beta^2(y^2 + z^2)}}{x}$$

$$F6 = \sqrt{1 - \beta^2 a^2}\ \tanh^{-1} \frac{\sqrt{(1 - \beta^2 a^2)\left(x^2 - \beta^2(y^2 + z^2)\right)}}{x - \beta^2 az}$$

$$F7 = \left(F5 - (1 + a^2/m^2)\ F6\right)\ (m/a) \qquad (39)$$

These functions may all be conveniently rewritten in terms of inverse cosines, or inverse hyperbolic cosines, as follows:

$$F1 = \frac{z - ax}{|z - ax|} \cos^{-1} \frac{y\left[(y - mx) - \beta^2 a(ay - mz)\right] + (z - ax)^2}{\sqrt{\left[(z - ax)^2 + (1 - \beta^2 a^2)y^2\right]\left[(y - mx)^2 + (z - ax)^2 - \beta^2(ay - mz)^2\right]}}$$

$$F2 = \frac{1}{\sqrt{1 - \beta^2(a^2 + m^2)}} \cosh^{-1} \frac{x - \beta^2(my + az)}{\beta\sqrt{(y - mx)^2 + (z - ax)^2 - \beta^2(ay - mz)^2}}$$

$$F3 = \frac{mz - ay}{|mz - ay|} \cos^{-1} \frac{-x(my + az) + (y^2 + z^2)}{\sqrt{(y^2 + z^2)\left[(y - mx)^2 + (z - ax)^2 - \beta^2(ay - mz)^2\right]}}$$

$$F4 = \left(F3 - (1 + a^2/m^2)\ F1\right)\ (m/a)$$

$$F5 = \cosh^{-1} \frac{x}{\beta\sqrt{y^2 + z^2}}$$

$$F3 = \pi \text{ for } z \geq a/my$$
$$= -\pi \text{ for } z < a/my \tag{46}$$

In addition, F4 and F7 are unchanged, and F5 and F6 are zero. Thus an unsymmetric two-dimensional flow region is defined in which the velocity components are constant.

The perturbation velocity components may now be expressed very simply in terms of these new functions. For example:

Constant source distribution (a = 0)

$$u_1 = -\frac{\overline{w}}{\pi} m \, F2$$
$$v_1 = \frac{\overline{w}}{\pi} (F2 - F5)$$
$$w_1 = \frac{\overline{w}}{\pi} F1 \tag{47}$$

Linearly varying source distribution (a = 0)

$$u_2 = \frac{\overline{w}_x}{\pi} \left[(mx - y) \, F2 + yF5 - zF1 \right]$$
$$v_2 = \frac{\overline{w}_x}{\pi m} \left[(mx - y) \, (F2 - F5) - \frac{(y^2 + z^2)}{y} \, F4 - zF1 \right]$$
$$w_2 = \frac{\overline{w}_x}{\pi m} \left[(mx - y) \, F1 + z \left[(1 - \beta^2 m^2) \, F2 - F5 \right] \right] \tag{48}$$

Oblique constant-pressure lifting surface

$$u_3 = -\frac{\Delta p}{4\pi q_\infty} F1$$
$$v_3 = \frac{\Delta p}{4\pi q_\infty} \frac{1}{a^2 + m^2} \left[a \left(1 - \beta^2 (a^2 + m^2) \right) F2 + m \, (F3 + F7) \right]$$
$$w_3 = \frac{-\Delta p}{4\pi q_\infty} \frac{m}{a^2 + m^2} \left[\left(1 - \beta^2 (a^2 + m^2) \right) F2 - F5 + F4 \right] \tag{49}$$

Visualization of constant pressure velocity components. — The following figures depict the three components of velocity corresponding to oblique, constant-pressure lifting surfaces in supersonic flow. For the case $a = 0$ where the pressure discontinuity is located in the x-y plane (figures 3 to 5), the velocity components are given for triangular regions having subsonic, sonic, and supersonic leading edges. The dominant effect of the vortex-like flow around the side edge of the triangles is clearly visible, as is the narrow upwash field in the leading edge region of the subsonic leading-edge wing.

For the nonplanar case, $a = 0.2$, (figures 6 and 7), the velocity components are given only for subsonic and supersonic leading-edges. The flow disturbance is now seen to be centered about the plane $z = ax$, and is no longer symmetrical about the x-y plane. An additional discontinuity occurs in the v and w velocity components in the plane $z = (a/m)y$ (the plane through the x axis that just touches the leading edge), which corresponds to a sheet of vorticity being shed aft of the leading edge. It should also be noted that, for the supersonic leading-edge case, the sidewash and downwash are no longer equal and opposite above and below the plane of wing in the "two-dimensional region" forward of the Mach cone from the apex.

The velocity field in a plane perpendicular to the free-stream direction located one unit behind the apex of a subsonic leading edge, constant-pressure delta wing is presented in figure 8. The vortex sheet trailing from points along the leading edge can be seen to generate a circulatory type of flow on the suction side of the wing. This circulation above the wing may be comparable to the "ram's horn" vortex observed experimentally above the upper surface of highly swept delta wings.

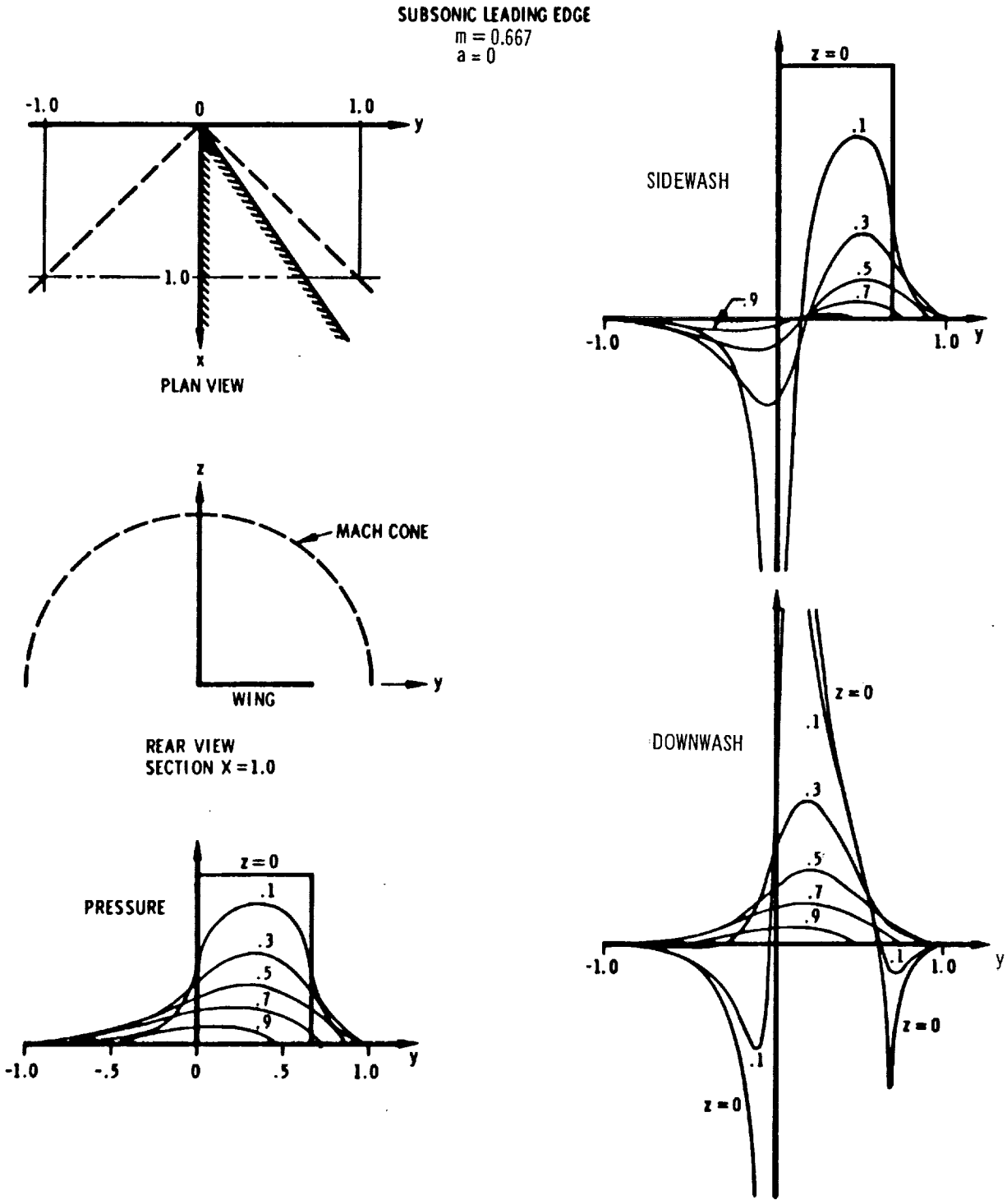

FIGURE 3 VELOCITY COMPONENTS – SUBSONIC LEADING EDGE

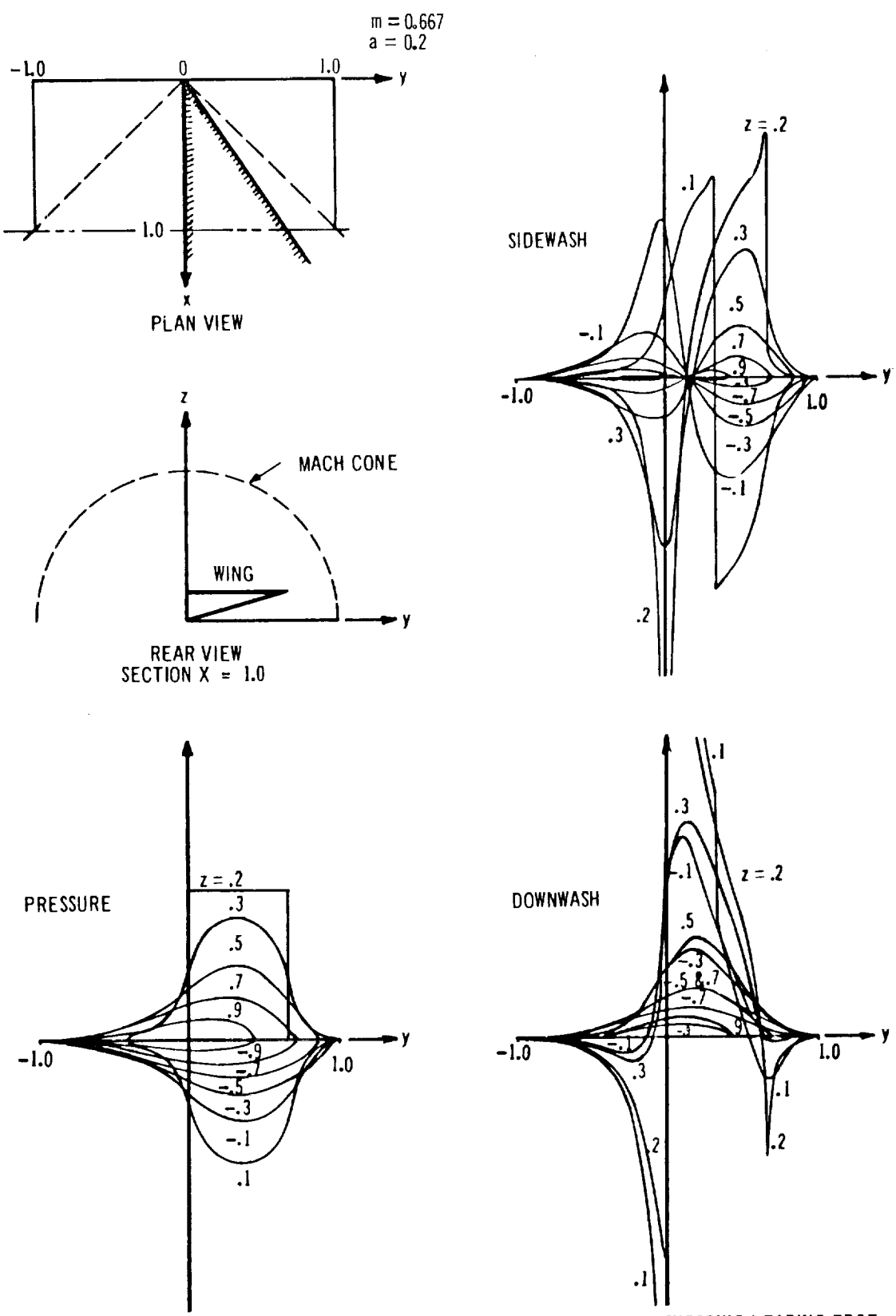

FIGURE 6 VELOCITY COMPONENTS FROM INCLINED SINGULARITY SURFACE – SUBSONIC LEADING EDGE

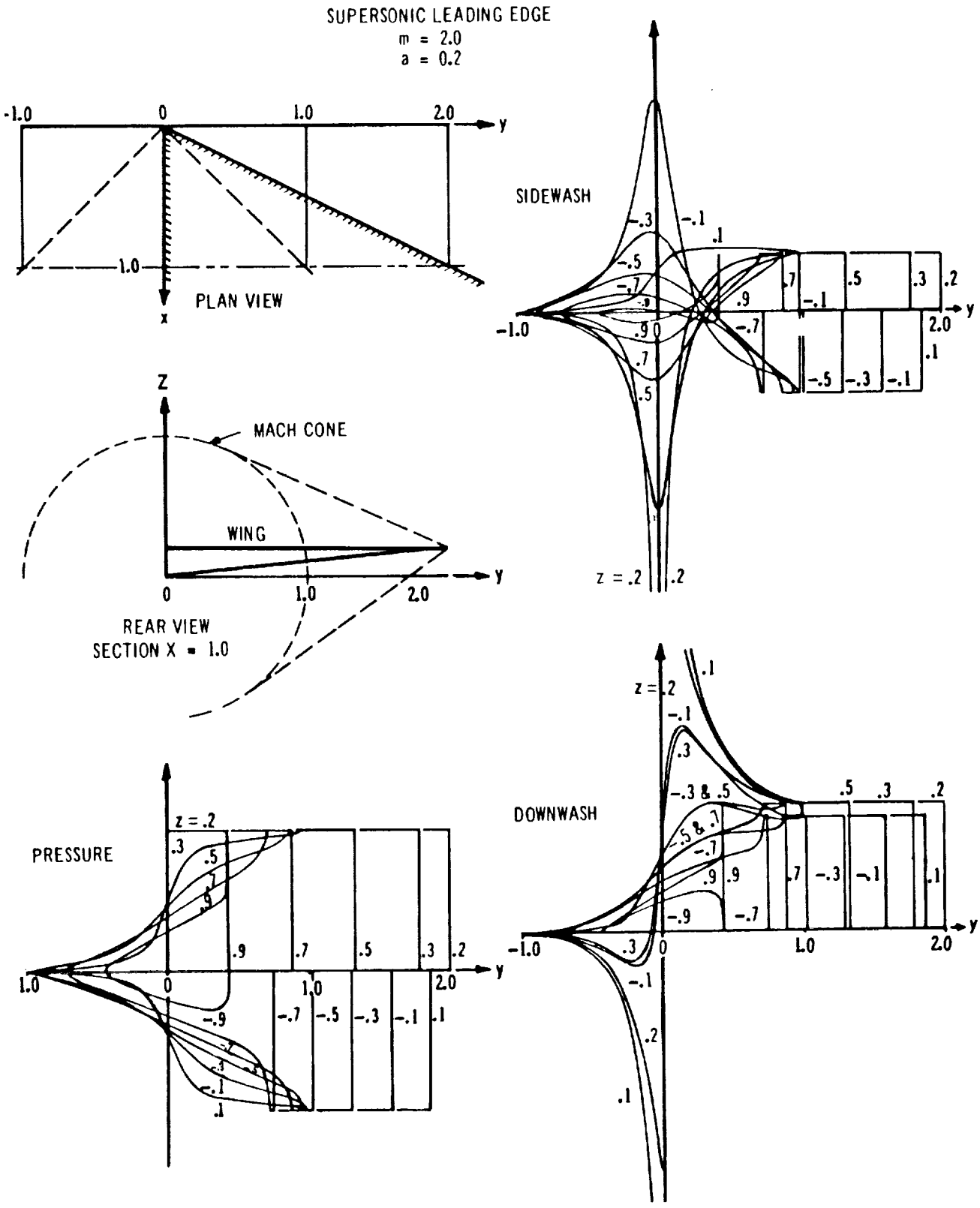

FIGURE 7 VELOCITY COMPONENTS FROM INCLINED SINGULARITY SURFACE – SUPERSONIC LEADING EDGE

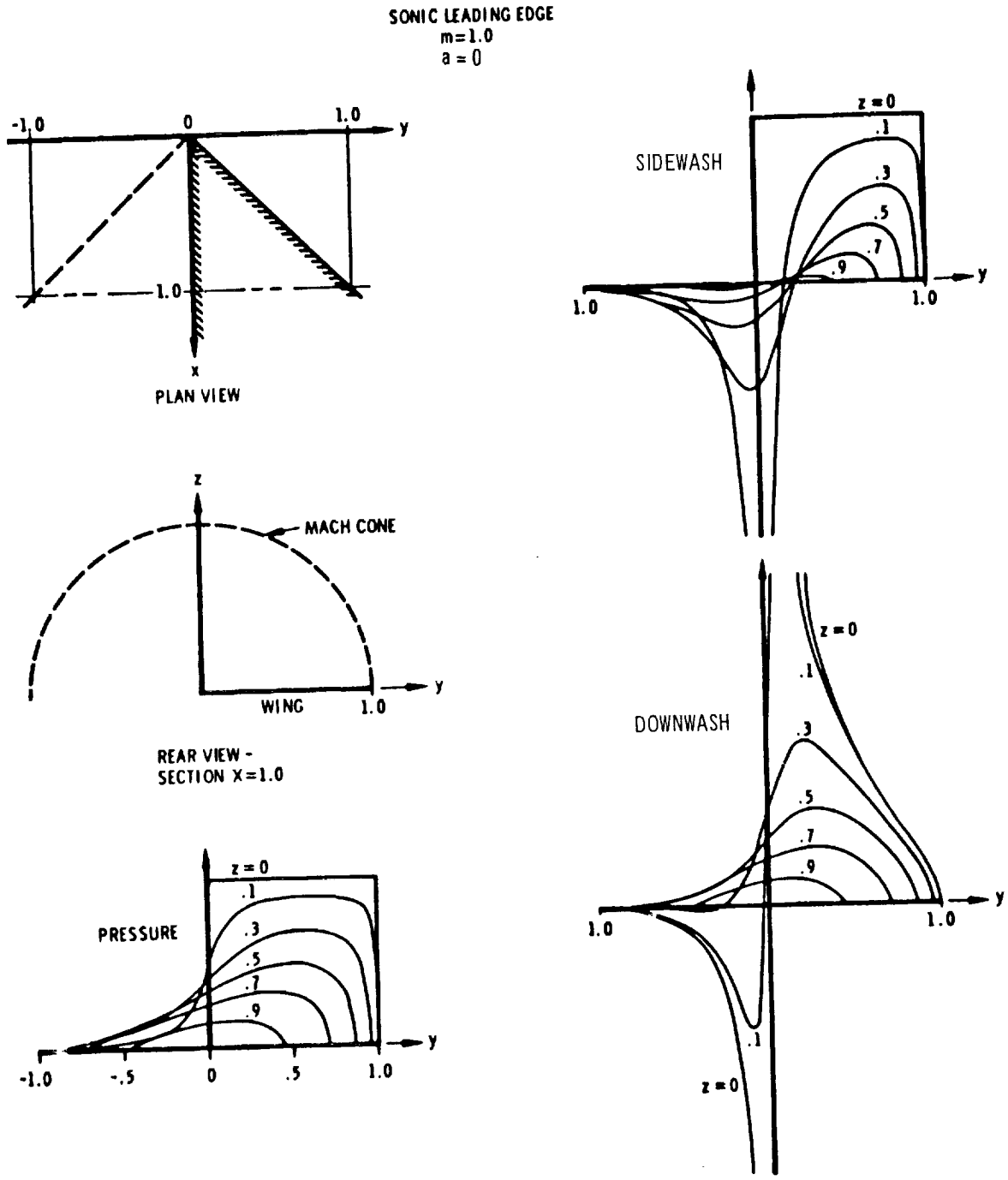

FIGURE 4 VELOCITY COMPONENTS – SONIC LEADING EDGE

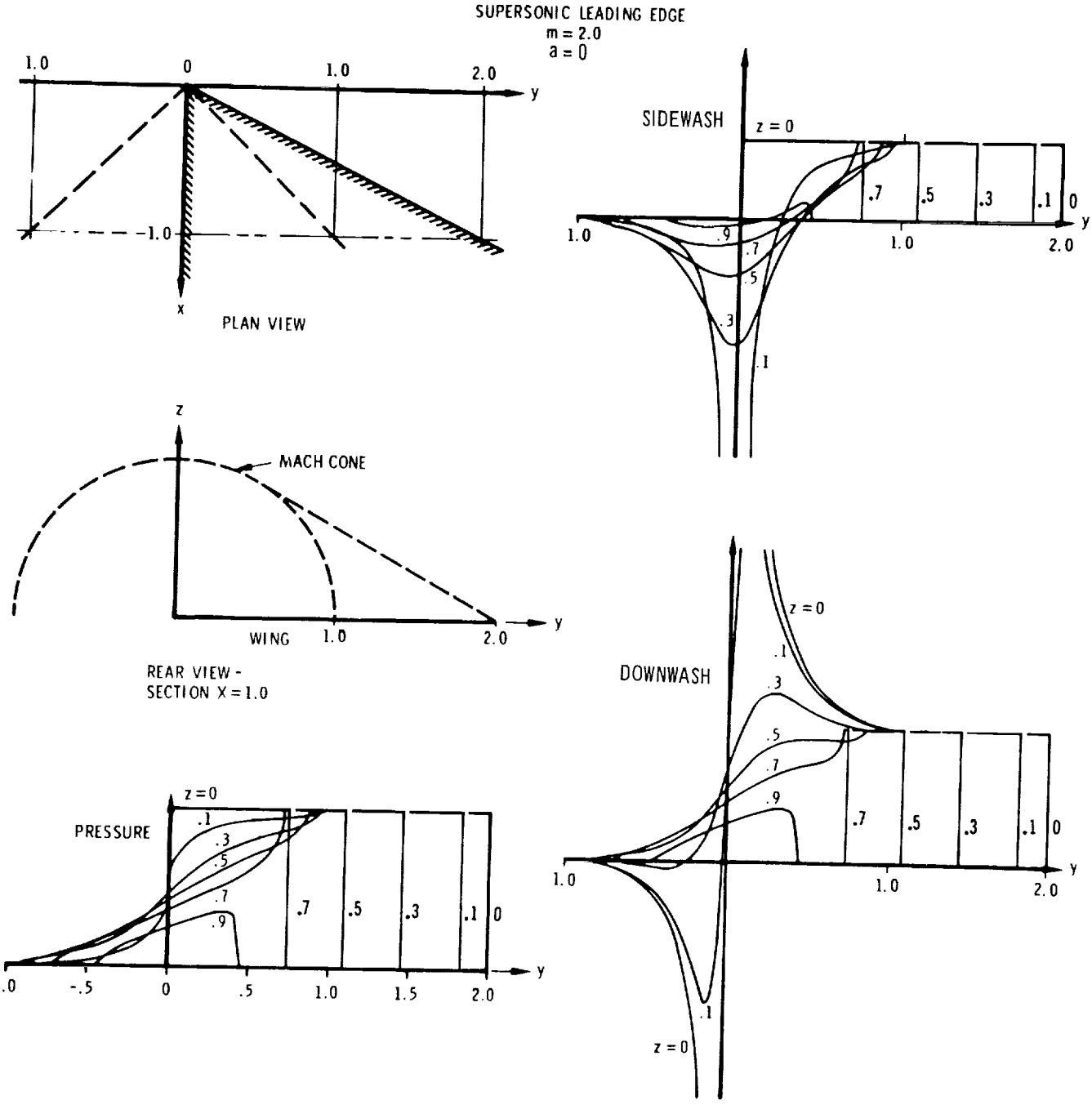

FIGURE 5 VELOCITY COMPONENTS– SUPERSONIC LEADING EDGE

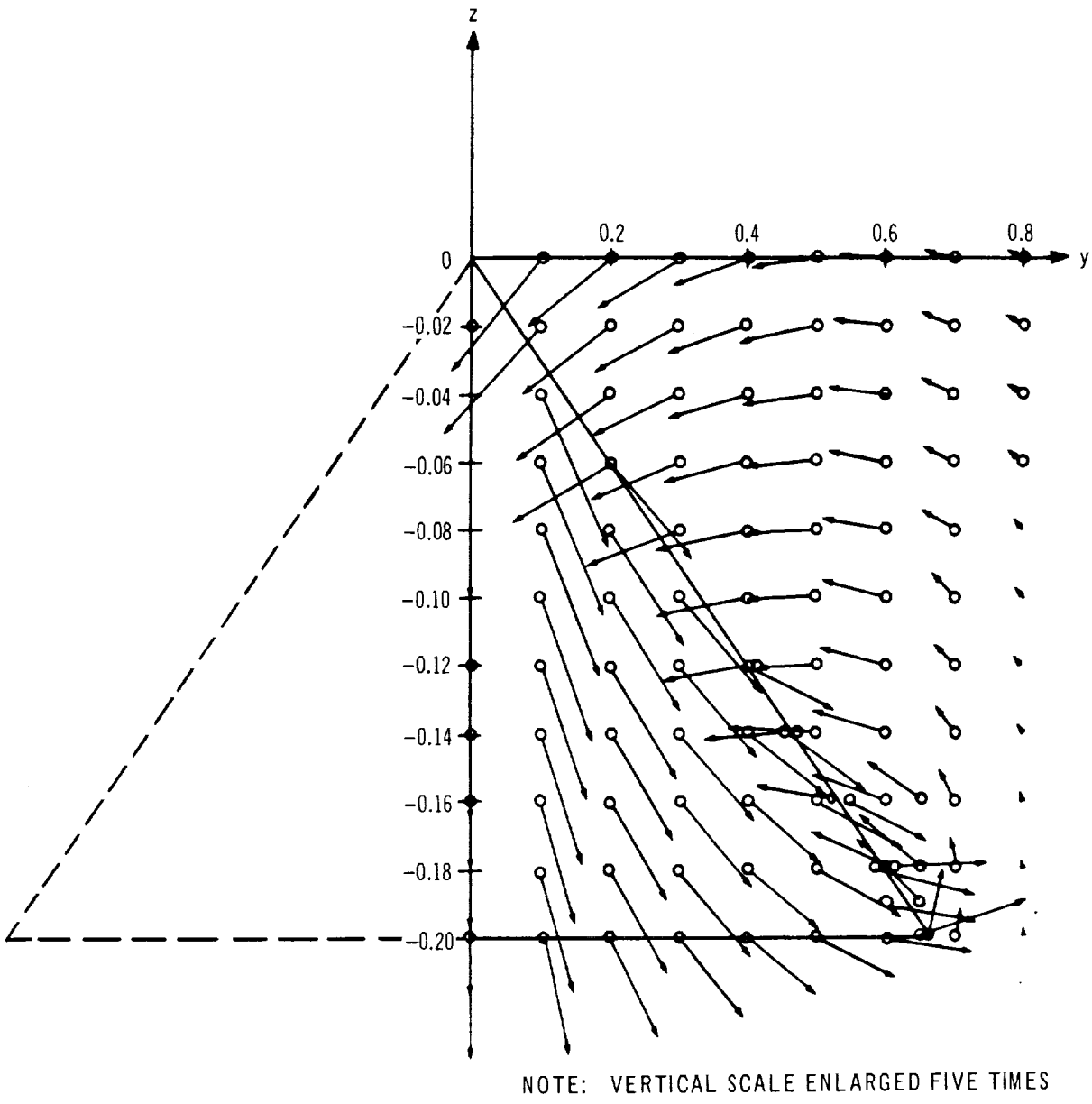

FIGURE 8 FLOW VISUALIZATION – CONSTANT-PRESSURE DELTA WING

4.3 Calculation of Velocity Components—Line Singularities

Derivation of potential equation. —Equation (1) may be rewritten in terms of the cylindrical coordinates x, r, and θ as follows:

$$\beta^2 \varphi_{xx} = \varphi_{rr} + \varphi_r/r + \varphi_{\theta\theta}/r^2 \tag{50}$$

To solve this equation, the perturbed flow will be resolved in two components: the axial component, defined by the axially symmetrical potential φ_S; and the cross component, defined by the potential φ_D. Place

$$\varphi = \varphi_S + \varphi_D \tag{51}$$

Then, for the axially symmetric flow,

$$\beta^2 \varphi_{S_{xx}} = \varphi_{S_{rr}} + \varphi_{S_r}/r \tag{52}$$

and for the cross flow,

$$\beta^2 \varphi_{D_{xx}} = \varphi_{D_{rr}} + \varphi_{D_r}/r + \varphi_{D_{\theta\theta}}/r^2 \tag{53}$$

The potential functions for the axially symmetric flow and the cross flow will be determined separately.

Potential function and velocity components for line sources. —The solution to equation (52) is well known, and is given in reference 10 as follows:

$$\varphi_S(x, r) = -\int_0^{\xi_1} \frac{f(\xi)\, d\xi}{\sqrt{(x-\xi)^2 - \beta^2 r^2}} \tag{54}$$

where $\xi_1 = x - \beta r$ is the intersection of the Mach forecone from P(x, r) with the x axis, and in the slender-body approximation $f(\xi) = \frac{dS_B(\xi)}{d\xi}$ where $S_B(\xi)$ is the body cross-sectional area.

For the distribution

$$S_B(\xi) = \mu(\xi)\left[1 - H(\xi - \ell)\right] + \mu(\ell)\, H(\xi - \ell) \tag{55}$$

where $H(\xi - \ell)$ represents a unit step function starting at $\xi = \ell$, the solution will represent the flow about an arbitrary body of revolution up to $\xi = \ell$ followed by a semi-infinitely long cylinder of cross section equal to $\mu(\ell)$. Since

$$f(\xi) = \frac{dS_B}{d\xi}$$

then

$$f(\xi) = \frac{d\mu}{d\xi}\left[1 - H(\xi - \ell)\right] - \mu(\xi)\,\delta(\xi - \ell) + \mu(\ell)\,\delta(\xi - \ell) \tag{56}$$

where $\delta(\xi - \ell)$ represents a delta function at $\xi = \ell$. Replacing $f(\xi)$ in equation (54) by equation (56) yields

$$\varphi_S(x, r) = -\int_0^{\xi_1} \frac{\frac{d\mu}{d\xi}\left[1 - H(\xi - \ell)\right] - \mu(\xi)\,\delta(\xi - \ell) + \mu(\ell)\,\delta(\xi - \ell)}{\sqrt{(x - \xi)^2 - \beta^2 r^2}} \tag{57}$$

which becomes for $\xi_1 \leq \ell$

$$\varphi_S(x, r) = -\int_0^{\xi_1} \frac{\frac{d\mu}{d\xi}\,d\xi}{\sqrt{(x - \xi)^2 - \beta^2 r^2}} \tag{58}$$

or for $\xi_1 > \ell$

$$\varphi_S(x, r) = -\int_0^{\ell} \frac{\frac{d\mu}{d\xi}\,d\xi}{\sqrt{(x - \xi)^2 - \beta^2 r^2}} \tag{59}$$

If ℓ is taken to represent the end of the body, then equation (58) governs the flow ahead of the Mach cone from the end of the body. Equation (59) governs the flow behind the Mach cone from the end of the body.

For the case $\frac{d\mu}{d\xi} = k_S \xi$, equation (57) represents the potential due to a line source of linearly varying strength distributed along the x axis from $x = 0$ to $x = \ell$. The solution to equation (57) for this case is given as

$$\varphi_{S_1} = k_S \left\{ - x \cosh^{-1} \frac{x}{\beta r} + \sqrt{x^2 - \beta^2 r^2} \right\} - k_S H(\xi_1 - \ell) \left\{ - x \cosh^{-1} \frac{x - \ell}{\beta r} + \sqrt{(x - \ell)^2 - \beta^2 r^2} \right\} \tag{60}$$

Note that the unit step function lies along the Mach cone from the end of the body. Ahead of the Mach cone,only the first two terms of equation (60) make up the potential, while behind the Mach cone additional terms are necessary.

The velocity components corresponding to the linearly varying line source may be obtained by differentiating the potential function and are listed below:

$$u_{S1} = \frac{\partial \varphi_{S1}}{\partial x} = -k_S \cosh^{-1}\frac{x}{\beta r} + k_S H(\xi_1 - \ell)\left\{\cosh^{-1}\frac{x-\ell}{\beta r} + \frac{\ell}{\sqrt{(x-\ell)^2 - \beta^2 r^2}}\right\}$$

$$v_{r_{S1}} = \frac{\partial \varphi_{S1}}{\partial r} = \frac{k_S}{r}\sqrt{x^2 - \beta^2 r^2} - \frac{k_S}{r} H(\xi_1 - \ell)\left\{\sqrt{(x-\ell)^2 - \beta^2 r^2} + \frac{\ell(x-\ell)}{\sqrt{(x-\ell)^2 - \beta^2 r^2}}\right\}$$

$$v_{\theta_{S1}} = \frac{1}{r}\frac{\partial \varphi_{S1}}{\partial \theta} = 0 \qquad (61)$$

Similarly, for the case $\frac{d\mu}{d\xi} = k_S \xi^2$, equation (57) represents the potential due to a line source of quadratically varying strength distributed along the x axis from $x = 0$ to $x = \ell$. The solution to equation (57) for this case is given as

$$\varphi_{S2} = k_S\left\{\frac{3}{2} x\sqrt{x^2 - \beta^2 r^2} - \left(x^2 + \frac{\beta^2 r^2}{2}\right)\cosh^{-1}\frac{x}{\beta r}\right\}$$

$$- k_S H(\xi_1 - \ell)\left\{\frac{3x+\ell}{2}\sqrt{(x-\ell)^2 - \beta^2 r^2} - \left(x^2 + \frac{\beta^2 r^2}{2}\right)\cosh^{-1}\frac{x-\ell}{\beta r}\right\} \qquad (62)$$

The velocity components are

$$u_{S2} = \frac{\partial \varphi_{S2}}{\partial x} = k_S\left\{2\sqrt{x^2 - \beta^2 r^2} - 2x\cosh^{-1}\frac{x}{\beta r}\right\}$$

$$- k_S H(\xi_1 - \ell)\left\{2\sqrt{(x-\ell)^2 - \beta^2 r^2} - 2x\cosh^{-1}\frac{x-\ell}{\beta r} - \frac{\ell^2}{\sqrt{(x-\ell)^2 - \beta^2 r^2}}\right\}$$

$$v_{S2} = \frac{\partial \varphi_{S2}}{\partial r} = \frac{k_S}{r}\left\{x\sqrt{x^2 - \beta^2 r^2} - \beta^2 r^2 \cosh^{-1}\frac{x}{\beta r}\right\}$$

$$- \frac{k_S}{r} H(\xi_1 - \ell)\left\{(x + \ell)\sqrt{(x - \ell)^2 - \beta^2 r^2} - \beta^2 r^2 \cosh^{-1}\frac{x - \ell}{\beta r}\right.$$

$$\left. + \frac{\ell^2 (x - \ell)}{\sqrt{(x - \ell)^2 - \beta^2 r^2}}\right\} \qquad (63)$$

$$v_{\theta_{S2}} = \frac{1}{r}\frac{\partial \varphi_{S2}}{\partial \theta} = 0$$

Potential function and velocity components for line doublets. —The solution to equation (53) is also given in reference 10:

$$\varphi_D(x, r, \theta) = \frac{\cos\theta}{r}\int_0^{\xi_1} \frac{m(\xi)(x - \xi)\, d\xi}{\sqrt{(x - \xi)^2 - \beta^2 r^2}} \qquad (64)$$

wherein the slender-body approximation $m(\xi) = \frac{dS_B(\xi)}{d\xi}$

For the cross-sectional area distribution given by equation (55),

$$m(\xi) = \frac{d\eta}{d\xi}\left[1 - H(\xi - \ell)\right] - \eta(\xi)\,\delta(\xi - \ell) + \eta(\ell)\,\delta(\xi - \ell) \qquad (65)$$

Replacing $m(\xi)$ in equation (64) by equation (65) yields

$$\varphi_D(x, r, \theta) = \frac{\cos\theta}{r}\int_0^{\xi_1} \frac{\frac{d\eta}{d\xi}\left[1 - H(\xi - \ell)\right] - \eta(\xi)\,\delta(\xi - \ell) + \eta(\ell)\,\delta(\xi - \ell)\,(x - \xi)\, d\xi}{\sqrt{(x - \xi)^2 - \beta^2 r^2}} \qquad (66)$$

which becomes for $\xi_1 \leq \ell$

$$\varphi_D(x, r, \theta) = \frac{\cos\theta}{r} \int_0^{\xi_1} \frac{\frac{d\eta}{d\xi}(x - \xi)\, d\xi}{\sqrt{(x - \xi)^2 - \beta^2 r^2}} \tag{67}$$

or for $\xi_1 > \ell$

$$\varphi_D(x, r, \theta) = \frac{\cos\theta}{r} \int_0^{\ell} \frac{\frac{d\eta}{d\xi}(x - \xi)\, d\xi}{\sqrt{(x - \xi)^2 - \beta^2 r^2}} \tag{68}$$

For the case $\frac{d\eta}{d\xi} = k_D \xi$, equation (66) represents the potential due to a line doublet of linearly varying strength distributed along the x axis from $x = 0$ to $x = \ell$. The solution to equation (66) for this case is

$$\varphi_{D_1} = k_D \frac{\cos\theta}{2r} \left\{ x \sqrt{x^2 - \beta^2 r^2} - \beta^2 r^2 \cosh^{-1} \frac{x}{\beta r} \right\}$$
$$- k_D \frac{\cos\theta}{2r} H(\xi_1 - \ell) \left\{ (x + \ell) \sqrt{(x - \ell)^2 - \beta^2 r^2} - \beta^2 r^2 \cosh^{-1} \frac{x - \ell}{\beta r} \right\} \tag{69}$$

The velocity components corresponding to this case may also be obtained by differentiation and are listed below:

$$u_{D1} = \frac{\partial \varphi_{D1}}{\partial x} = \frac{k_D \cos\theta}{r} \sqrt{x^2 - \beta^2 r^2}$$
$$- k_D \frac{\cos\theta}{r} H(\xi_1 - \ell) \left\{ \sqrt{(x - \ell)^2 - \beta^2 r^2} + \frac{\ell (x - \ell)}{\sqrt{(x - \ell)^2 - \beta^2 r^2}} \right\}$$

$$v_{D1} = \frac{\partial \varphi_{D1}}{\partial r} = \frac{-k_D \cos\theta}{2r^2} \left\{ \beta^2 r^2 \cosh^{-1} \frac{x}{\beta r} + x \sqrt{x^2 - \beta^2 r^2} \right\}$$

$$+\frac{k_D \cos\theta}{2r^2} H(\xi_1 - \ell) \left\{ \beta^2 r^2 \cosh^{-1} \frac{x-\ell}{\beta r} + (x+\ell)\sqrt{(x-\ell)^2 - \beta^2 r^2} + \frac{2\beta^2 r^2 \ell}{\sqrt{(x-\ell)^2 - \beta^2 r^2}} \right\}$$

$$v_{\theta_{D1}} = \frac{1}{r}\frac{\partial \varphi_{D1}}{\partial \theta} = -\frac{k_D \sin\theta}{2r^2} \left\{ x\sqrt{x^2 - \beta^2 r^2} - \beta^2 r^2 \cosh^{-1} \frac{x}{\beta r} \right\}$$

$$+\frac{k_D \sin\theta}{2r^2} H(\xi_1 - \ell) \left\{ (x+\ell)\sqrt{(x-\ell)^2 - \beta^2 r^2} - \beta^2 r^2 \cosh^{-1} \frac{x-\ell}{\beta r} \right\} \tag{70}$$

Similarly for the case $\frac{d\eta}{d\xi} = k_D \xi^2$, equation (66) represents the potential due to a line doublet of quadratically varying strengths along the x axis from $x = 0$ to $x = \ell$. The solution to equation (66) for this case is

$$\varphi_{D2} = \frac{k_D \cos\theta}{r} \left\{ \frac{x^2 + 2\beta^2 r^2}{3} \sqrt{x^2 - \beta^2 r^2} - x\beta^2 r^2 \cosh^{-1} \frac{x}{\beta r} \right\}$$

$$- \frac{k_D \cos\theta}{r} H(\xi_1 - \ell) \left\{ \frac{x^2 + x\ell + \ell^2 + 2\beta^2 r^2}{3} \sqrt{(x-\ell)^2 - \beta^2 r^2} - x\beta^2 r^2 \cosh^{-1} \frac{x-\ell}{\beta r} \right\} \tag{71}$$

The velocity components are

$$u_{D2} = \frac{\partial \varphi_{D2}}{\partial x} = \frac{k_D \cos\theta}{r} \left\{ x\sqrt{x^2 - \beta^2 r^2} - \beta^2 r^2 \cosh^{-1} \frac{x}{\beta r} \right\}$$

$$- \frac{k_D \cos\theta}{r} H(\xi_1 - \ell) \left\{ \frac{2x+\ell}{3}\sqrt{(x-\ell)^2 - \beta^2 r^2} - \beta^2 r^2 \cosh^{-1} \frac{x-\ell}{\beta r} + \frac{x(x^2 - \beta^2 r^2) - \ell(\ell^2 + 2\beta^2 r^2)}{3\sqrt{(x-\ell)^2 - \beta^2 r^2}} \right\}$$

$$v_{D2} = \frac{\partial \varphi_{D2}}{\partial r} = \frac{-k_D \cos\theta}{r^2}\left\{\frac{x^2 - 4\beta^2 r^2}{3}\sqrt{x^2 - \beta^2 r^2} + x\beta^2 r^2 \cosh^{-1}\frac{x}{\beta r}\right\}$$

$$+ \frac{k_D \cos\theta}{r^2} H(\xi_1 - \ell)\left\{\frac{x^2 + x\ell + \ell^2 - 2\beta^2 r^2}{3}\sqrt{(x-\ell)^2 - \beta^2 r^2}\right.$$

$$\left. + x\beta^2 r^2 \cosh^{-1}\frac{x-\ell}{\beta r} + \frac{(-2x^2 + 4x\ell + \ell^2 + 2\beta^2 r^2)\beta^2 r^2}{3\sqrt{(x-\ell)^2 - \beta^2 r^2}}\right\}$$

$$v_{\theta_{D2}} = \frac{1}{r}\frac{\partial \varphi_{D2}}{\partial \theta} = \frac{-k_D \sin\theta}{r^2}\left\{\frac{x^2 + 2\beta^2 r^2}{3}\sqrt{x^2 - \beta^2 r^2} - x\beta^2 r^2 \cosh^{-1}\frac{x}{\beta r}\right\}$$

$$+ \frac{k_D \sin\theta}{r^2} H(\xi_1 - \ell)\left\{\frac{x^2 + x\ell + \ell^2 + 2\beta^2 r^2}{3}\sqrt{(x-\ell)^2 - \beta^2 r^2}\right.$$

$$\left. - xB^2 r^2 \cosh^{-1}\frac{x-\ell}{\beta r}\right\} \qquad (72)$$

It should be noted that although some slender body theory notation has been used in deriving the above line singularities, their strengths are calculated by the classical Von Karman-Moore method (reference 11) in which the appropriate boundary conditions are satisfied on the body surface (equation (98)) and not on the body axis as in slender body theory.

4.4 Formation of the Aerodynamic Matrix

Geometrical considerations. — A detailed description of the geometry of the wing-body combination is deferred until section 5. In this section, only sufficient geometrical description will be given to continue the development of the aerodynamic theory.

Briefly, the wing and body geometry is specified with respect to an arbitrary coordinate system, or "defining axes" X, Y, Z, as illustrated in the following sketch. The defining axes may be inclined at an angle of attack α_D to the free stream.

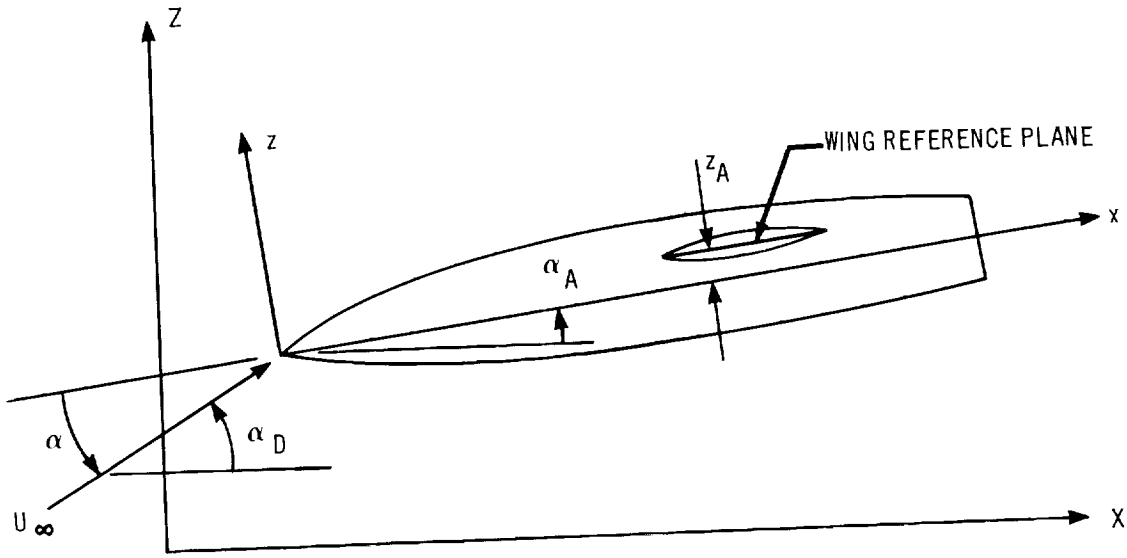

The body is restricted to have circular, or nearly circular, cross sections, but may have arbitrary camber and incidence. The wing may have any planform that can be approximated by straight-line segments and can be mounted at any height above or below the body axis. The effect of dihedral is not included. The wing sections may have arbitrary camber, twist, incidence, and thickness distributions.

The "body axes" x, y, z are established by the geometry definition program so that the x axis passes through the centroids of the body cross sections at the nose and base, while the y axis remains parallel to the Y axis. The body coordinate system is therefore related to the defining axes by a simple transformation involving a translation of the body in the X-Z plane, followed by a rotation about the Y axis through the angle α_A. For most configurations, the wing and body can be specified most simply in terms of the body axes directly.

Referring to the sketch, it can be seen that in general the x-y plane will be inclined at an angle $\alpha = \alpha_D - \alpha_A$ with respect to the free stream. The component of the free-stream velocity parallel to the x axis is $U_\infty \cos \alpha$, and the component parallel to the z axis is $U_\infty \sin \alpha$. In the following analysis, it will be assumed that α is sufficiently small so that $\cos \alpha \simeq 1$ and $\sin \alpha \simeq \alpha$. Therefore, for all practical purposes the axial component of the free-stream velocity may be set equal to the free-stream velocity U_∞, while the cross component, which represents the additional effects of an angle of attack, is set equal to $U_\infty \alpha$. This approximation is consistent with the underlying assumptions of linear theory and introduces considerable simplification into the analysis.

The transformed body is now approximated by an equivalent body of revolution about the x axis. Each section of the equivalent body has the same cross-sectional area as the original body, while the body camber is defined by the heights of the centroids of the original sections above the x axis. The transformed wing is defined to lie in a plane parallel to the x–y plane, located at an average height z_A above or below that plane. The line of intersection of this planar wing and the transformed body is calculated within the program.

Finally, the surfaces of the transformed wing and body are subdivided into a large number of rectilinear panels. The leading and trailing edges of these panels may be swept forward or back in an arbitrary way, but the side edges must be constrained to lie in planes parallel to the x axis. To meet this latter requirement, each panel may be further subdivided into two or three parts, to be described later. The panels are defined by the x, y, z coordinates of the four

corner points. A typical panel arrangement on a wing-body combination is illustrated in figure 1 (page 11).

A primed system of coordinates is now introduced, originating at a specified corner point k of panel j. The x' axis is defined to be parallel to the x axis, while the y' axis is defined to lie in the plane of the panel as in figure 1. It can be seen that, in general, the x'-y' plane is inclined at an angle θ_j to the x-y plane. It should be noted that the panel may also be inclined to an angle $\alpha_j = dz'/dx'$ with respect to the x'-y' plane, as illustrated in the following sketch.

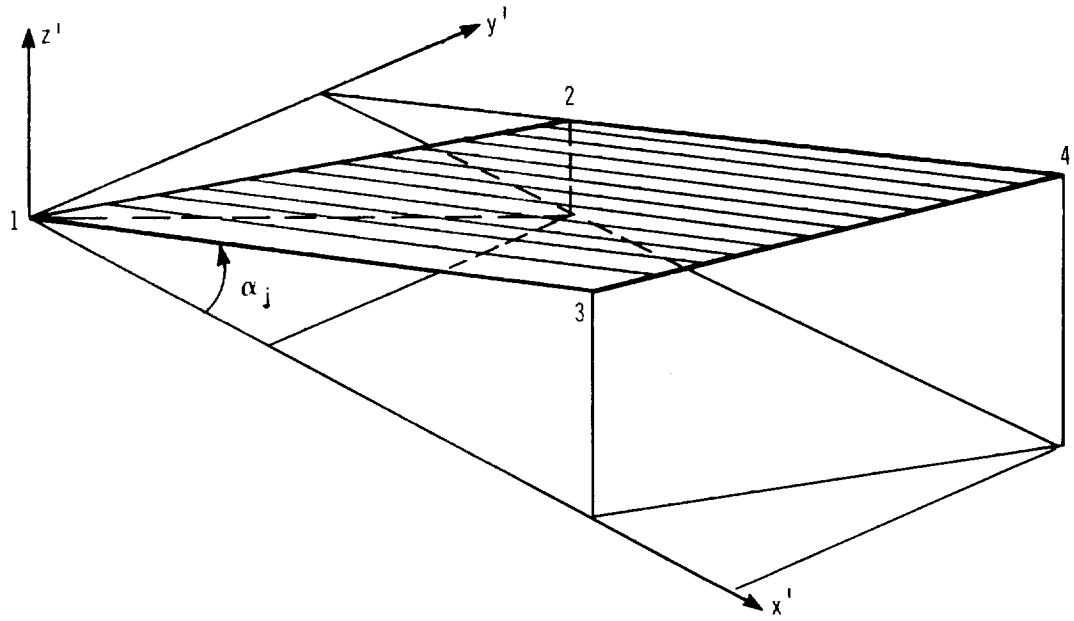

The panel corner point-numbering convention is shown on the sketch. The leading edge lies between points 1 and 2, and the trailing edge between points 3 and 4. The projection of the leading edge in the x'-y' plane has the slope m_{j1}, while the projection of the trailing edge in the x'-y' plane has the slope m_{j3}. Note that $m_{j1} = m_{j2}$ and $m_{j3} = m_{j4}$. The side edge between points 1 and 3 always lies in the x'-z' plane, and the side edge between points 2 and 4 always lies in a plane parallel to the x'-z' plane.

The coordinates of a point i (x_i, y_i, z_i) may be expressed in terms of the primed system of coordinates originating at corner k of panel j as follows:

$$x'_{ijk} = x_i - x_{jk}$$

$$y'_{ijk} = (y_i - y_{jk}) \cos \theta_j + (z_i - z_{jk}) \sin \theta_j$$

$$z'_{ijk} = (z_i - z_{jk}) \cos \theta_j - (y_i - y_{jk}) \sin \theta_j \qquad (73)$$

where $\cos \theta_j = \dfrac{C_j}{\sqrt{B_j^2 + C_j^2}}$; $\sin \theta_j = \dfrac{B_j}{\sqrt{B_j^2 + C_j^2}}$

and

$$B_j = \begin{vmatrix} x_{j1} & z_{j1} & 1 \\ x_{j2} & z_{j2} & 1 \\ x_{j3} & z_{j3} & 1 \end{vmatrix} \quad ; \qquad C_j = \begin{vmatrix} x_{j1} & y_{j1} & 1 \\ x_{j2} & y_{j2} & 1 \\ x_{j3} & y_{j3} & 1 \end{vmatrix}$$

In general, the point i will be located at the control point of panel i. Note that $\theta = 0$ for all wing panels is a linearizing assumption.

Superposition of the velocity components for the surface singularities. — Formulae for the three velocity components u, v, w are given in section 4.2 for the three types of surface singularities chosen: constant and linearly varying surface distributions of sources and surface distributions of vortices. The velocity components are derived for the elementary case in which the surface singularities are located on semi-infinite triangular regions and are expressed in terms of the coordinate system originating at the apex of this triangular region.

The velocity components induced by a distribution of singularities over a finite panel may now be obtained by combining four such elementary solutions originating at each of the four corner points of the panel using the method of superposition. The procedure is illustrated by the following sketch:

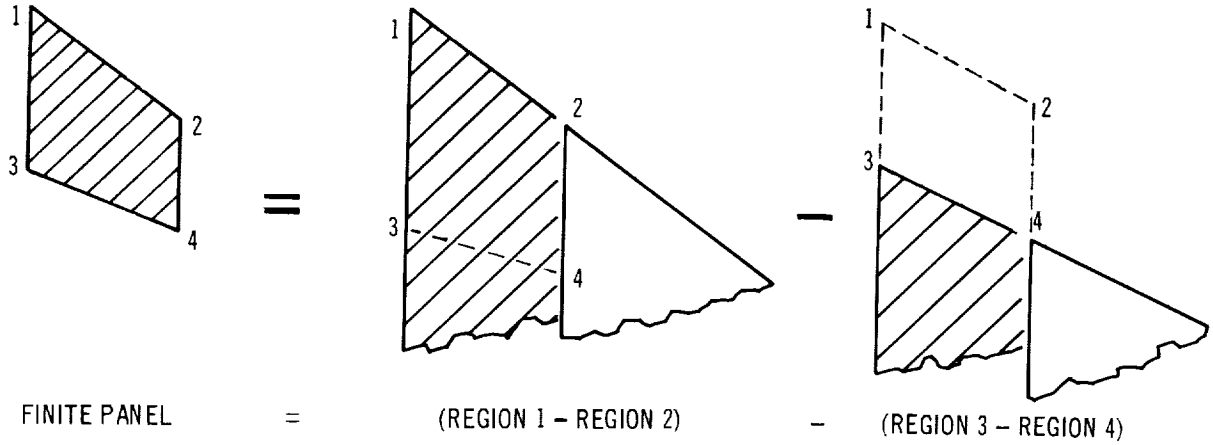

The effect of a semi-infinite strip of singularities having the same width as the panel is obtained by subtracting the triangular region with origin at corner point 2 from that originating at corner point 1. Both regions must have the same leading-edge slope and constant singularity strengths. The singularity strength everywhere outside this strip is now zero. If the semi-infinite strip corresponding to the difference between the triangular regions originating at corner points 3 and 4 is now subtracted from the original strip, then it can be seen that the constant singularity strength will be limited to the area enclosed by the panel and will be zero elsewhere. It is not necessary for the second strip to have the same leading-edge slope as the first, but it must have equal strength.

In the method of aerodynamic influence coefficients, all the singularity distributions are defined to have unit strengths; consequently, the superposition of the velocity components corresponding to the elementary surface singularities may proceed directly. For example, the velocity components at the control point of panel i due to a distribution of singularities on panel j may be written as follows:

$$\begin{aligned} u'_{ij} &= q_{ij1} - q_{ij2} - q_{ij3} + q_{ij4} \\ v'_{ij} &= r_{ij1} - r_{ij2} - r_{ij3} + r_{ij4} \\ w'_{ij} &= c_{ij1} - c_{ij2} - c_{ij3} + c_{ij4} \end{aligned} \tag{74}$$

where

$$\begin{aligned} q_{ijk} &= P(a'_j,\ b'_{jk},\ \xi'_{ijk},\ y'_{ijk},\ z'_{ijk}) \\ r_{ijk} &= \beta\, S(a'_j,\ b'_{jk},\ \xi'_{ijk},\ y'_{ijk},\ z'_{ijk}) \\ c_{ijk} &= \beta\, D(a'_j,\ b'_{jk},\ \xi'_{ijk},\ y'_{ijk},\ z'_{ijk}) \end{aligned} \tag{75}$$

and

$$a'_j = \beta \tan \alpha_j = \beta \frac{(z_{j3} - z_{j1}) \cos \theta_j - (y_{j3} - y_{j1}) \sin \theta_j}{x_{j3} - x_{j1}} \tag{76}$$

$$b'_{jk} = \frac{1}{\beta\, m_{jk}} = \frac{x_{j2} - x_{j1}}{\beta\left[(y_{j2} - y_{j1}) \cos \theta_j + (z_{j2} - z_{j1}) \sin \theta_j\right]},\ k = 1,\ 2 \tag{77}$$

$$= \frac{x_{j4} - x_{j3}}{\beta\left[(y_{j4} - y_{j3}) \cos \theta_j + (z_{j4} - z_{j3}) \sin \theta_j\right]},\ k = 3,\ 4$$

Also, $\xi'_{ijk} = x'_{ijk}/\beta$ where x'_{ijk}, y'_{ijk}, and z'_{ijk} are defined by equation (73).

The functions P, S, and D in equation (75) are written out in full in Appendix B for each type of surface singularity.

Calculation of the aerodynamic influence coefficients for surface singularities. — The velocity component that is both normal to the body axis and in a plane which is parallel to the body axis and perpendicular to each panel surface through its control point is required. The magnitude of this normal velocity component induced at control point i by the distribution of singularities of unit strength on panel j is defined to be the aerodynamic influence coefficient a_{ij}. An expression for the aerodynamic influence coefficients may be derived by an examination of the projections of the velocity components in a double-primed system of coordinates associated with panel i, as illustrated in the following sketch:

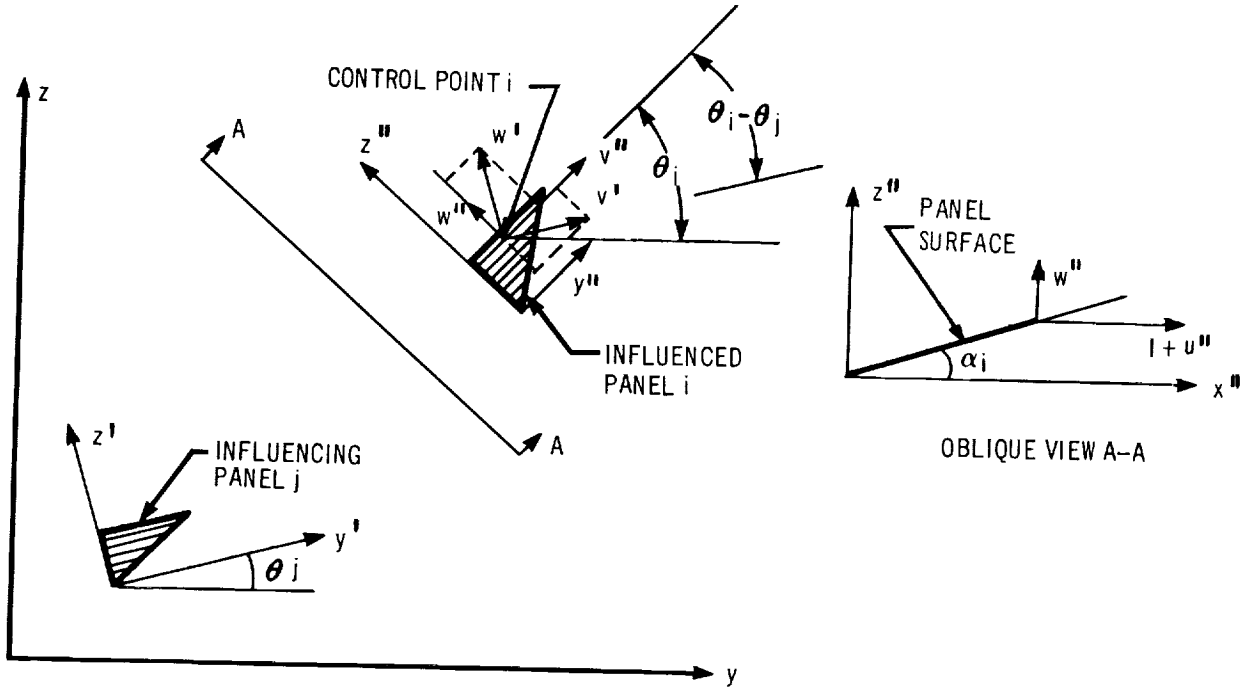

Then
$$a_{ij} = w''_{ij} = w'_{ij} \cos(\theta_i - \theta_j) - v'_{ij} \sin(\theta_i - \theta_j) \tag{78}$$
The other two components of velocity may be written

$$u''_{ij} = u'_{ij}$$

$$v''_{ij} = v'_{ij} \cos(\theta_i - \theta_j) + w'_{ij} \sin(\theta_i - \theta_j) \tag{79}$$
where u', v', and w' are given by equation (74).

Additional subscripts are used to classify the aerodynamic influence coefficients according to the location of the control point i on the wing or body, the location of the influencing panel j, and the type of singularity the panel contains. For example, the influence on wing panel i by a surface distribution of vorticity on body panel j is denoted by $a_{WBV_{ij}}$, and the influence on body panel i by a surface distribution of sources on wing panel j is denoted by $a_{BWS_{ij}}$.

Certain special cases will now be considered so that the formulation of the aerodynamic influence coefficients can be completed.

Multiple-part panels: There are certain areas on the wing and body where the panels cannot be represented by a single planar region in which both side edges lie in planes parallel to, or coincident with, x'-z' plane. These areas may occur at wing tips, along wing-body intersections, and on the surfaces of opening or closing bodies. In these areas, the panels must be further subdivided into two or three parts, each part of which meets the side-edge requirement, as illustrated below. It should be noted that a triangular part is considered to have a side edge of zero length.

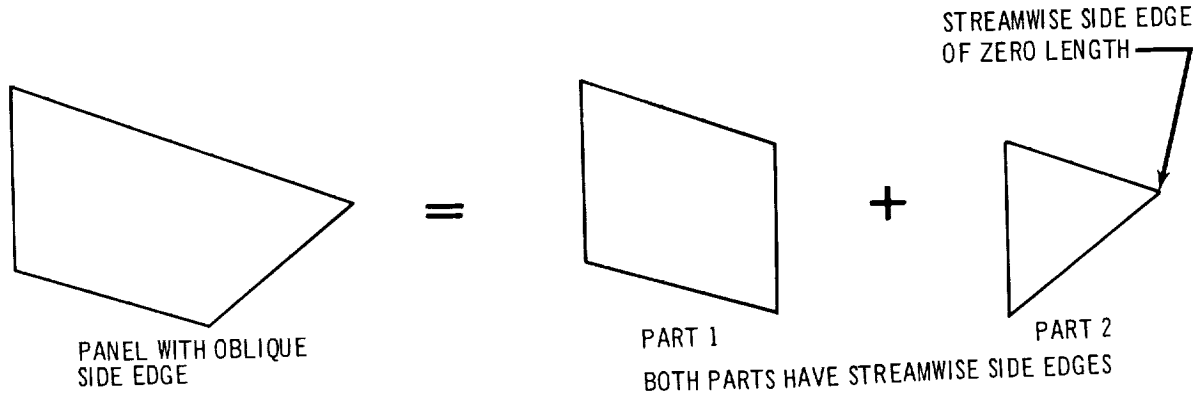

In case a multiple part panel is an influencing panel, the velocity components induced by each of the parts at a given control point are calculated separately, and the total contribution is determined by adding these individual components together. The influence coefficient is then formed from these velocity components as before. If the influenced panel is a multiple-part panel, the velocity components and

influence coefficient are calculated at a single control point representing the combined areas.

Panels having negative slopes: The formulae for the velocity components have been presented only for the case in which the semi-infinite triangular region containing the singularities has a positive leading-edge slope ($m_{jk} \geq 0$). These formulae may be extended to the case in which the region has a negative leading-edge slope by applying a slight variation in the superposition procedure used to calculate the effect of a finite panel as sketched.

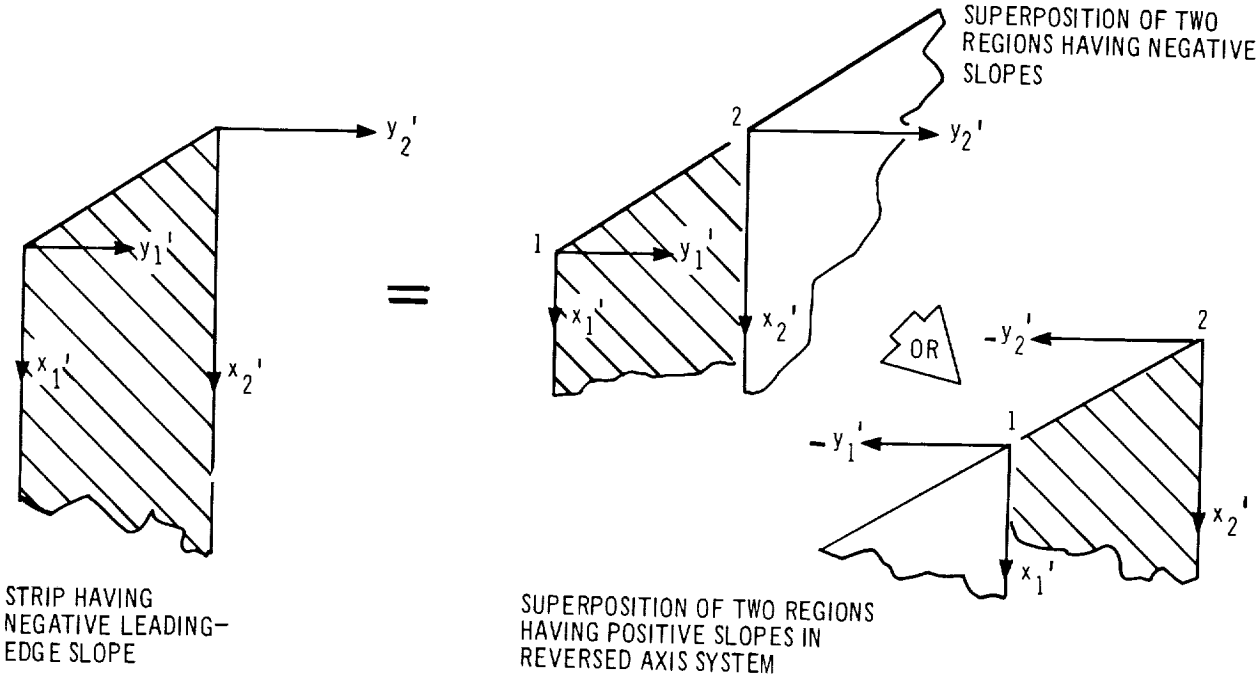

The influence of a semi-infinite strip of constant pressure at a given point i may be calculated by taking the difference of the influences of the two semi-infinite triangular regions of negative slope having vertices at corners 1 and 2, as before. However, this case is calculated in an equivalent manner by taking the difference between the influences of the two semi-infinite triangular regions having positive leading-edge slopes as shown in the right part of the sketch, where the order of subtraction and the direction of the y' axes from the corner points must be reversed. The velocity components are still given by the formulae of

equation (58), with the following modifications to the terms q_{ijk}, r_{ijk}, and c_{ijk}:

$$\begin{aligned} q_{ijk} &= \pm P\ (a'_j, \pm b'_{jk},\ \xi'_{ijk}, \pm y'_{ijk},\ z'_{ijk}) \\ r_{ijk} &= \beta\ S\,(a'_j, \pm b'_{jk},\ \xi'_{ijk}, \pm y'_{ijk},\ z'_{ijk}) \\ c_{ijk} &= \pm\beta\ D(a'_j, \pm b'_{jk},\ \xi'_{ijk}, \pm y'_{ijk},\ z'_{ijk}) \end{aligned} \qquad (80)$$

where + is for $m_{jk} \geq 0$

and − is for $m_{jk} < 0$

Panel symmetry effects: For configurations having panels located symmetrically on the right and left side of the x-z plane, it is possible to introduce considerable simplification into the computer program by calculating these symmetrical panels in pairs. The formulae for the velocity components in the double-primed system of coordinates associated with panel i have been given by equations (78) and (79). If panel i has an image panel $\bar{i}$ associated with it, located on the opposite side of the x-z plane, the velocity components in the double-primed system of this image panel may be written

$$\begin{aligned} \bar{w}''_{ij} &= \bar{w}'_{ij} \cos(\theta_i + \theta_j) + \bar{v}'_{ij} \sin(\theta_i + \theta_j) \\ \bar{v}''_{ij} &= \bar{w}'_{ij} \sin(\theta_i + \theta_j) - \bar{v}'_{ij} \cos(\theta_i + \theta_j) \end{aligned} \qquad (81)$$

The sketch on the following page illustrates the geometrical relationship between the panel i and its image panel $\bar{i}$, and the location of the influencing panel j. It can easily be seen that the velocity components for both cases can be expressed by the single pair of formulae as follows:

$$\begin{aligned} w''_{ij} &= w'_{ij} \cos(\theta_i \pm \theta_j) \quad \pm \quad v'_{ij} \sin(\theta_i \pm \theta_j) \\ v''_{ij} &= w'_{ij} \sin(\theta_i \pm \theta_j) \quad \pm \quad v'_{ij} \cos(\theta_i \pm \theta_j) \end{aligned} \qquad (82)$$

provided that the y'_{ijk} and z'_{ijk} coordinates used in equations (75) or (80) are replaced by

$$y'_{ijk} = (\pm y_i - y_{jk}) \cos \theta_j + (z_i - z_{jk}) \sin \theta_j$$

$$z'_{ijk} = (z_i - z_{jk}) \cos \theta_j - (\pm y_i - y_{jk}) \sin \theta_j \qquad (83)$$

where the upper sign is used for i and j on the same side of the x-y plane and the lower sign is used for i and j on the opposite side of the x-y plane (image panel $\bar{i}$) in both of the above equations.

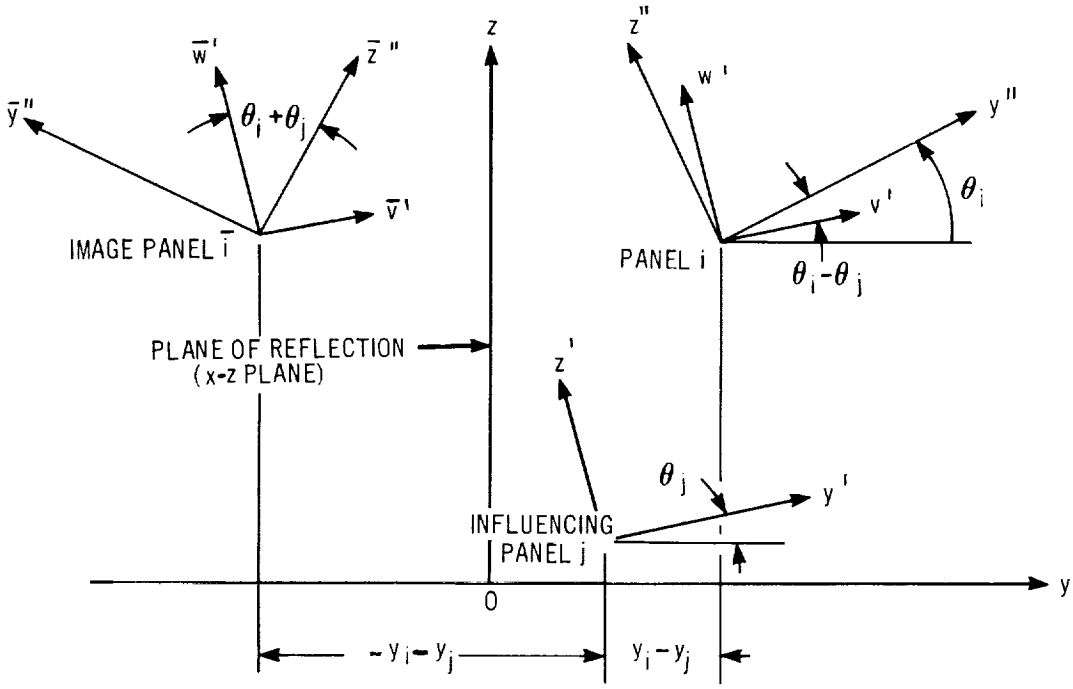

Calculation of the aerodynamic influence coefficients for line singularities. — The line singularities used to represent the effects of the body thickness, camber, and incidence are located along the positive x axis. The component of velocity induced by these singularities which is normal to the x axis and in a plane parallel to this axis and perpendicular to the surface at a control point is required. The magnitude of this velocity component induced at control point i by the k^{th} singularity of unit strength is defined to be the aerodynamic influence coefficient a_{ik}. The following sketch illustrates the geometry for a control point on the surface of the body and for a control point on an arbitrary panel:

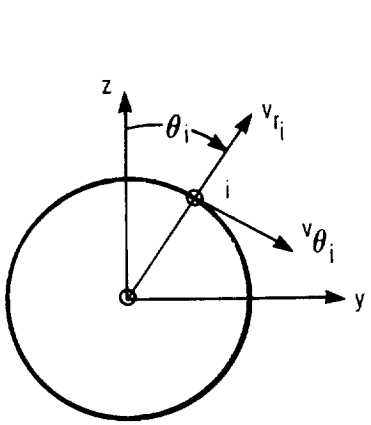

CONTROL POINT ON BODY SURFACE

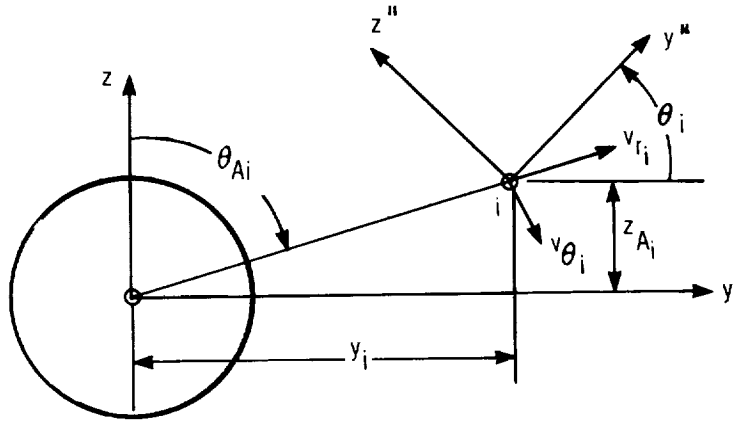

CONTROL POINT ON ARBITRARY (WING OR BODY) PANEL

On the surface of the body, θ_i is given by the angular position of point i, measured from the x-z plane. On wing (or body) panels θ_i is given by the inclination of the x"-y" plane to the x-y plane as before.

On the surface of the body,

$$a_{ik} = v_{r_{ik}} \tag{84}$$

On the surface of a panel,

$$a_{ik} = v_{r_{ik}} \cos(\theta_i + \theta_A) - v_{\theta_{ik}} \sin(\theta_i + \theta_A) \tag{85}$$

where

$$\theta_{A_i} = \tan^{-1} \frac{y_i}{z_{A_i}}$$

$$v_{r_{ik}} = v_{r_{S1_{ik}}} = \frac{\sqrt{(x_i - x_k)^2 - \beta^2 r_i^2}}{r_i} \quad \text{for line sources of linear variation,}$$

$$v_{r_{ik}} = v_{r_{S2_{ik}}} = \frac{1}{r_i}\left\{(x_i - x_k)\sqrt{(x_i - x_k)^2 - \beta^2 r_i^2} - \beta^2 r_i^2 \cosh^{-1}\frac{x_i - x_k}{\beta r_i}\right\}$$

for line sources of quadratic variation,

$$v_{r_{ik}} = v_{r_{D1_{ik}}} = \frac{\cos\theta_i}{2r_i^2}\left\{\beta^2 r_i^2 \cosh^{-1}\frac{x_i - x_k}{\beta r_i} + (x_i - x_k)\sqrt{(x_i - x_k)^2 - \beta^2 r_i^2}\right\}$$

for line doublets of linear variation, and

$$v_{r_{ik}} = v_{r_{D2_{ik}}} = \frac{-\cos\theta_i}{v_i^2}\left\{\left[\frac{(x_i - x_k)^2 - 4\beta^2 r_i^2}{3}\right]\sqrt{(x_i - x_k)^2 - \beta^2 r_i^2} + (x_i - x_k)\,\beta^2 r_i^2 \cosh^{-1}\frac{x_i - x_k}{\beta r_i}\right\} \quad \text{for line doublets} \tag{86}$$

of quadratic variation. Similarly,

$$v_{\theta_{ik}} = v_{\theta_{S1_{ik}}} = v_{\theta_{S2_{ik}}} = 0 \quad \text{for line sources,}$$

$$v_{\theta_{ik}} = v_{\theta_{D1_{ik}}} = \frac{-\sin\theta}{2r_i^2}\left\{(x_i - x_k)\sqrt{(x_i - x_k)^2 - \beta^2 r^2} - \beta^2 r_i^2 \cosh^{-1}\frac{x_i - x_k}{\beta r_i}\right\}$$

and

$$v_{\theta_{ik}} = v_{\theta_{D2_{ik}}} = \frac{-\sin\theta}{r_i^2}\left\{\left[\frac{(x_i - x_k)^2 + 2\beta^2 r_i^2}{3}\right]\sqrt{(x_i - x_k)^2 - \beta r_i^2} - (x_i - x_k)\,\beta^2 r_i^2 \cosh^{-1}\frac{x_i - x_k}{\beta r_i}\right\} \quad \text{for line doublets, and}$$

x_k = x coordinate of the origin of the k^{th} line singularity. (87)

The control points i are restricted to lie ahead of the Mach cone from the end of the body; i.e., $\xi_1 \leq \ell$.

The aerodynamic influence coefficients induced by the line singularities are also classified by the use of subscripts in a manner similar to that used for the surface singularities. For example, the influence on wing panel i by the k^{th} line source of linear variation is denoted by $a_{WBS1_{ik}}$, and the influence on body control point i by the k^{th} line doublet of quadratic variation is denoted by $a_{BBD2_{ik}}$.

Resultant normal velocity at a control point.—The resultant normal velocity at control point i may now be obtained by adding the normal velocities induced by local cross flow to those induced by the various singularities. The local cross-flow velocity normal to the surface, nondimensionalized by the freestream velocity U_∞, is $\alpha \cos \theta_i$. On the body, the local angle of attack is assumed to be the difference between the angle of attack α and the slope of the body camber line.

The resultant normal velocity on body panel i may be expressed as follows:

$$n_{B_i} = \left(\alpha - \frac{dz_c}{dx}\right) \cos \theta_i + n_{BBS_i} + n_{BBD_i} + n_{BBV_i} + n_{BWV_i} + n_{BWS_i} \qquad (88)$$

where

$$n_{BBS_i} = a_{BBS1_{i1}} T_{S_1} + \sum_{k=1}^{K} a_{BBS2_{ik}} T_{S2_k} \quad \text{(due to body line sources)}$$

$$n_{BBD_i} = a_{BBD1_{i1}} T_{D1} + \sum_{k=1}^{K} a_{BBD2_{ik}} T_{D2_k} \quad \text{(due to body line doublets)}$$

$$n_{BBV_i} = \sum_{j=1}^{N_B} a_{BBV_{ij}} p_{B_j} \quad \text{(due to surface distribution of vorticity on body)}$$

$$n_{BWV_i} = \sum_{j=1}^{N_W} a_{BWV_{ij}} p_{W_j} \quad \text{(due to surface distribution of vorticity on wing)}$$

$$n_{BWS_i} = \sum_{j=1}^{N_T} a_{BWS_{ij}} \alpha_{T_j} \quad \text{(due to surface distribution of sources on wing)}$$

As indicated above, the normal velocities induced by the various singularities may be expressed as the sum of the products of the influence coefficients with their respective singularity strengths. The influence coefficients have been described previously; the singularity strengths are defined below:

T_{S1} = strength of linearly varying body line source 1

T_{S2_k} = strength of quadratically varying body line source k

T_{D1} = strength of linearly varying body line doublet 1

T_{D2_k} = strength of quadratically varying body line doublet k

p_{B_j} = pressure difference across body panel j

P_{W_j} = pressure difference across wing panel j

$\alpha_{T_j} = \left(\frac{dz_T}{dx}\right)_j$ = thickness slope at leading edge of wing panel j

For the summation limits above, there are $K \leq 50$ line sources and doublets, $N_B \leq 100$ body panels, and $N_W \leq 100$ wing panels. The number of wing thickness singularities $N_T = N_W + N_C$, where N_C is the number of chordwise columns of panels on the wing. The number of singularities used may be chosen arbitrarily for each problem.

Likewise, the resultant normal velocity on wing panel i may be written

$$n_{W_i} = \alpha + n_{WBS_i} + n_{WBD_i} + n_{WBV_i} + n_{WWV_i} + n_{WWS_i} \qquad (89)$$

where $n_{WBS_i} = a_{WBS1_{i1}} T_{S1} + \sum_{k=1}^{K} a_{WBS2_{ik}} T_{S2_k}$ (due to body line sources)

$n_{WBD_i} = a_{WBSD_{i1}} T_{D1} + \sum_{k=1}^{K} a_{WBD2_{ik}} T_{D2_k}$ (due to body line doublets)

$n_{WBV_i} = \sum_{j=1}^{N_B} a_{WBV_{ij}} p_{B_j}$ (due to surface distribution of vorticity on body)

$n_{WWV_i} = \sum_{j=1}^{N_W} a_{WWV_{ij}} p_{W_j}$ (due to surface distribution of vorticity on wing)

$n_{WWS_i} = \sum_{j=1}^{N_T} a_{WWS_{ij}} \alpha_{T_j}$ (due to surface distribution of sources on wing)

Note that, by definition, $\theta_i = \theta_j = 0$ on all wing panels.

Boundary conditions.—The boundary conditions equate the local flow direction to the slope of the surface at the control points, where the local flow direction is defined as the ratio of the resultant normal velocity to the axial velocity. For example, the boundary condition at control point i on the wing may be expressed

$$n_{W_i} = \left(\frac{dz}{dx}\right)_i \tag{90}$$

and on the body

$$\frac{n_{B_i}}{1 + u_{B_i}} = \left(\frac{dr}{dx}\right)_i \tag{91}$$

The resultant normal velocities n_{B_i} and n_{W_i} are defined by equations (88) and (89), respectively. The resultant axial velocity, expressed as a fraction of the free-stream velocity, is assumed to be unity on the wing. On the body, however, it is customary to include the axial velocity perturbations due to the line sources and doublets. Correspondingly,

$$u_{B_i} = u_{BBS_i} + u_{BBD_i} \tag{92}$$

All other axial velocity perturbations are assumed to be small and are neglected.

The boundary conditions may be used to determine the strengths of the various singularities representing the wing-body combination. In this report, the body geometry, wing thickness distribution, and planform are always specified in advance. The wing camber and twist distribution either may be given or will be determined by specifying the lifting pressure distribution or minimum drag condition. As a result, the boundary conditions are most easily satisfied by solving equations (90) and (91) in three steps.

In the first step, the boundary conditions on the wing are divided into two parts, one associated with the lifting effects, the other with the thickness effects. The surface slope of the wing may be expressed as follows:

$$\left(\frac{dz}{dx}\right)_i = \left(\frac{dz_c}{dx}\right)_i \pm \left(\frac{dz_T}{dx}\right)_i \tag{93}$$

where the upper sign refers to the upper surface, and the lower to the lower surface. Substituting equations (87) and (89) into equation (90):

$$\left(\frac{dz_c}{dx}\right)_i \pm \left(\frac{dz_T}{dx}\right)_i = \alpha + n_{WBS_i} + n_{WBD_i} + n_{WBV_i} + n_{WWV_i} + n_{WWS_i} \qquad (94)$$

The wing thickness effects are represented by a combination of constant and linearly varying distributions of sources on the panels, as shown in this sketch:

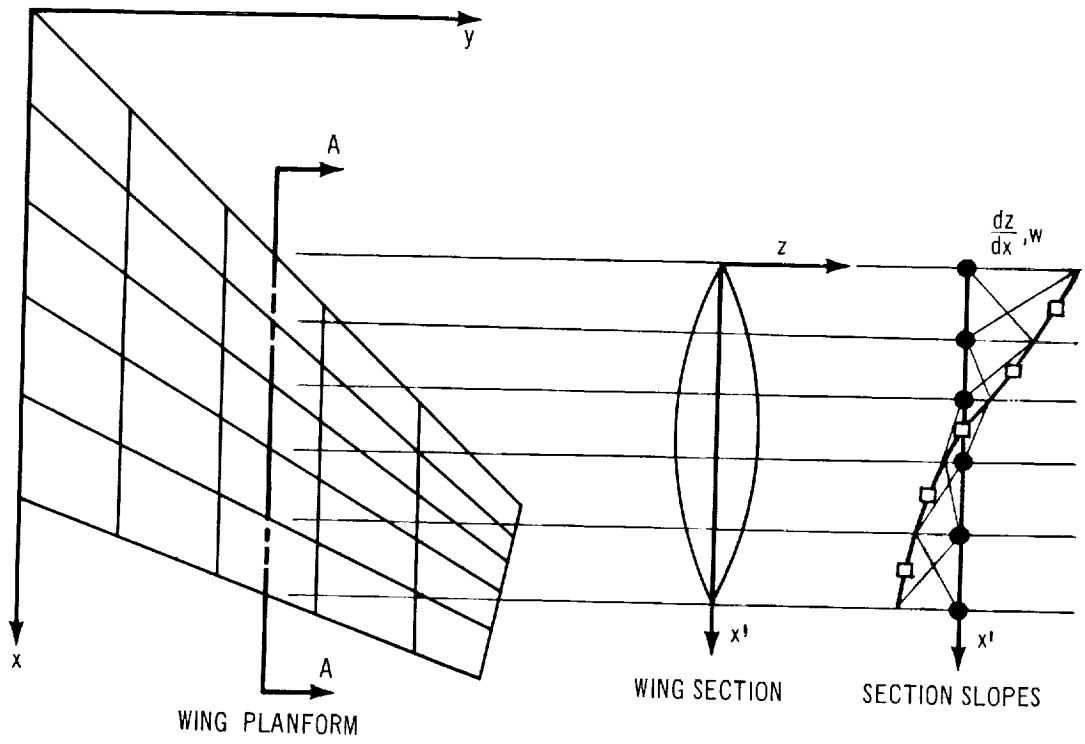

For each chord, the wing section is approximated by a series of parabolic arcs having continuous slopes along the panel edges. This is achieved by superimposing linearly varying source distributions across the chord so that the section slopes are exactly satisfied at the panel edges. Other constant source distributions are located along the leading and trailing edges of the wing to simulate the discontinuity of the section slope at these points. The method is restricted to wing sections with a finite slope that does not exceed the Mach angle at the leading edge.

The normal velocity at control point i may be expressed as

$$n_{WWS_i} = \sum_{j=1}^{N_T} a_{WWS_{ij}} \left(\frac{dz_T}{dx}\right)_j$$

$$= \pm \left(\frac{dz_T}{dx}\right)_i \tag{95}$$

since $a_{WWS_{i,j}} = \pm (1 - k_i)$ for source j originating along the leading edge of panel i

$a_{WWS_{i,j+1}} = \pm k_i$ for source j + 1 originating along the trailing edge of panel i

$a_{WWS_{i,j}} = 0$ for all other sources on the wing. k_i is the chord fraction of the control point location. The geometry is shown below (from sketch on previous page):

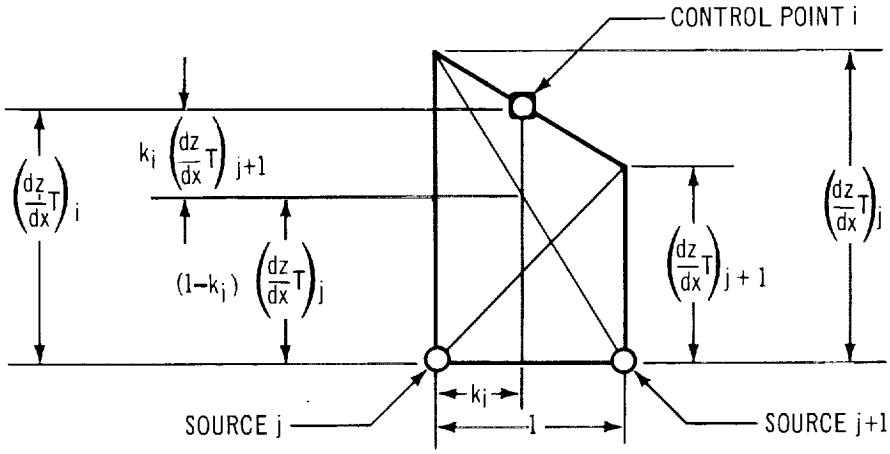

Thus, it can be seen that the given slope of the thickness distribution at control point i, $(dz_T/dx)_i$, is in fact the desired strength of the surface source distribution on wing panel i and satisfies exactly the wing thickness boundary condition on both surfaces. Equation (93) may now be expressed in terms of the slope of the wing camber surface alone, as follows:

$$\left(\frac{dz_c}{dx}\right)_i = \alpha + n_{WBS_i} + n_{WBD_i} + n_{WBV_i} + n_{WWV_i} \tag{96}$$

The various normal velocity components are written out in terms of the aerodynamic influence coefficients following equation (89).

In the second step, the strengths of the line sources and doublets are determined that completely satisfy the given boundary conditions on the body, assuming no interference effects from the wing. For this step, equation (91) is written as follows:

$$\left(\frac{dr}{dx}\right)_i (1 + u_{BBS_i}) + \left(\frac{dr}{dx}\right)_i u_{BBD_i} = \left(\alpha - \frac{dz_c}{dx}\right) \cos \theta_i + n_{BBS_i} + n_{BBD_i} + n_{BBV_i} + n_{BWV_i} + n_{BWS_i} \quad (97)$$

This equation is now broken down into three parts so that the unknown singularity strengths, T_{S_k} and T_{D_k}, can be determined independently.

For the line sources,

$$\left(\frac{dr}{dx}\right)_i (1 + u_{BBS_i}) = n_{BBS_i} \quad (98)$$

For the line doublets,

$$\left(\frac{dr}{dx}\right)_i u_{BBD_i} = n_{BBD_i} + \left(\alpha - \frac{dz_c}{dx}\right) \cos \theta_i \quad (99)$$

The remainder of equation (96) then expresses the condition that the resultant normal velocity components on the body due to the wing must be canceled by the distribution of vorticity on the body panels; that is,

$$n_{BBV_i} = - (n_{BWV_i} + n_{BWS_i}) \quad (100)$$

The various normal velocity components appearing in equations (97), (98), (99), and (100) are written out in terms of the aerodynamic influence coefficients following equation (88). The third step is to solve equations (100) and (96) simultaneously to yield the pressure differences across the wing and body panels that will satisfy the remaining boundary conditions on the wing, once the strengths of the line sources and doublets on the axis are determined from equations (98) and (99).

Determination of line sources and doublets.—The strengths of the body line sources may be determined by a modified version of the classical Von Karman-Moore approach (reference 11). In the Von Karman-Moore method, the solution assumes a singularity distribution made up of a series of linearly varying singularities with various starting points along the x axis. The

solution may be made smoother by adding quadratically varying singularities to approximate the singularity strength. This was found necessary by Van Dyke (reference 12) in obtaining his second-order solution, and has been useful in obtaining smooth first-order solutions in the field around a body of revolution. The method is outlined in the following sketch:

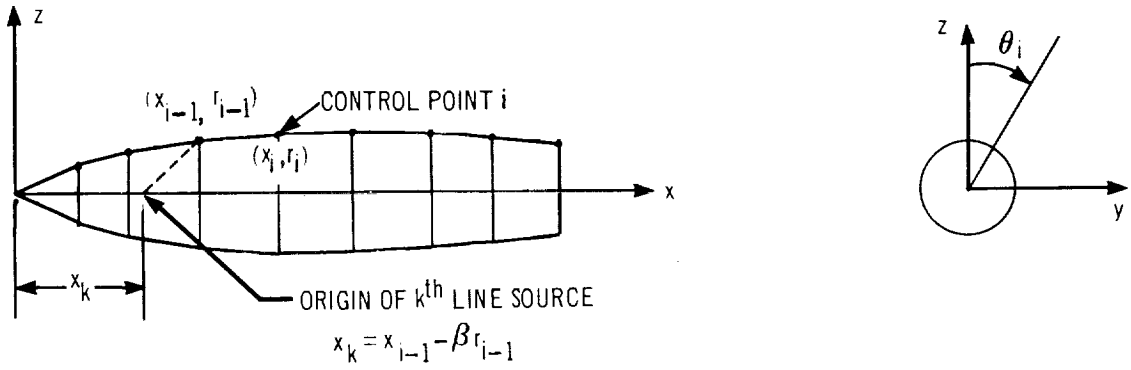

The body is considered to be made up of a series of parabolic arcs and is defined by an array of radii and stations which act as control points.

A linearly varying strength source is placed at origin k = 1 to give the proper conical tip. The strength of this source is determined by the tangency condition at the nose of the body.

$$T_{S1} = \frac{\tan \delta_N}{\sqrt{\cot^2 \delta_N - \beta^2} + \tan \delta_N \cosh^{-1}\left(\frac{\cot \delta_N}{\beta}\right)} \tag{101}$$

where δ_N is the semivertex angle of the nose.

A quadratically varying source is also placed with its origin at the tip; it satisfies the boundary condition (equation 98) at i = 1.

$$a_{BBS1} T_{S1} + a_{BBS2_{11}} T_{S2_1} = \left(\frac{dr}{dx}\right)_1 \left[1 + u_{BBS1} T_{S1} + u_{BBS2_{11}} T_{S2_1}\right]$$

which yields

$$T_{S2_1} = \frac{\left(\frac{dr}{dx}\right)_1 - \left[a_{BBS1_{11}} - \left(\frac{dr}{dx}\right)_1 u_{BBS1_{11}}\right] T_{S1}}{a_{BBS2_{11}} - \left(\frac{dr}{dx}\right)_1 u_{BBS2_{11}}} \tag{102}$$

where a_{BBS1} and $a_{BBS2_{ik}}$ have previously been defined by equation (87),

$$U_{BBS1_{ik}} = -\cosh^{-1}\frac{x_i - x_k}{\beta r_i} \quad \text{for linearly varying sources, and}$$

$$U_{BBS2_{ik}} = 2\sqrt{(x_i - x_k)^2 - \beta^2 r_i^2} - 2(x_i - x_k)\cosh^{-1}\frac{x_i - x_k}{\beta r_i} \tag{103}$$

for quadratically varying sources.

At subsequent stations the expression for quadratically varying sources is

$$T_{S2_i} = \frac{\left(\frac{dr}{dx}\right)_i - \left[a_{BBS1_{i1}} - \left(\frac{dr}{dx}\right)_i u_{BBS1_{i1}}\right] T_{S1} - \sum_{k=1}^{i-1}\left[a_{BBS2_{ik}} - \left(\frac{dr}{dx}\right)_i u_{BBS2_{ik}}\right] T_{S2_k}}{a_{BBS2_{ii}} - \left(\frac{dr}{dx}\right)_i u_{BBS2_{ii}}} \tag{104}$$

The end of a closing body presents a special problem, since the influence coefficients cannot be evaluated on the axis. The boundary condition used is that the net source strength at the end of a closing body must be zero. The manner in which the source strength varies along the x axis is known, as well as the strengths of the previously evaluated singularities. Therefore, at the end of the body, $i = K$, $r_i = 0$.

$$(x_K - x_1) T_{S1} + \sum_{k=1}^{K} (x_K - x_k)^2 T_{S2_k} = 0$$

which yields

$$T_{S2_K} = \frac{-(x_K - x_1) T_{S1} - \sum_{k=1}^{K-1} (x_K - x_k)^2 T_{S2_k}}{\left[x_K - (x - \beta r)_{K-1}\right]^2} \tag{105}$$

In this analysis the k^{th} line source originates at the distance $x_k = (x - \beta r)_{i-1}$ from the nose of the body.

The strength of the body doublets may be found by a method similar to that used for the sources. The boundary condition [equation (99)] may be written in terms of the aerodynamic influence coefficients

$$\left(\frac{dr}{dx}\right)_i \left[u_{BBD1_{i1}} T_{D1} + \sum_{k=1}^{K} u_{BBD2_{ik}} T_{D2_k}\right] = a_{BBD1_{i1}} T_{D1} + \sum_{k=1}^{K} a_{BBD2_{ik}} T_{D2_k} + \left(\alpha - \frac{dz_c}{dx}\right)_i \cos\theta_i \tag{106}$$

where $\left(\alpha - \frac{dz_c}{dx}\right)$ is the local angle of attack, $a_{BBD1_{ik}}$ and $a_{BBD2_{ik}}$ have been previously defined by equation (87), and

$$u_{BB1_{ik}} = \frac{\cos\theta}{r_i}\sqrt{(x_i - x_k)^2 - \beta^2 r_i^2}$$

for linearly varying doublets, and

$$u_{BBD2_{ik}} = \frac{\cos\theta}{r_i}\left\{(x_i - x_k)\sqrt{(x_i - x_k)^2 - \beta^2 r_i^2} - \beta^2 r_i^2 \cosh^{-1}\frac{x_i - x_k}{\beta r_i}\right\} \quad (107)$$

for quadratically varying doublets.

Now both $u_{BBD_{ik}}$ and $a_{BBD_{ik}}$ contain $\cos\theta_i$ internally, which is eliminated from equation (106) by placing

$$u'_{BBD_{ik}} = \frac{u_{BBD_{ik}}}{\cos\theta_i}$$

and

$$a'_{BBD_{ik}} = \frac{a_{BBD_{ik}}}{\cos\theta_i}$$

The result may be written

$$\left(\alpha - \frac{dz_c}{dx}\right)_i = -\left[a'_{BBD1_{i1}} - \left(\frac{dr}{dx}\right)_i u'_{BBD1_{i1}}\right] T_{D1} - \sum_{k=1}^{K}\left[a'_{BBD2_{ik}} - \left(\frac{dr}{dx}\right)_i u'_{BBD2_{ik}}\right] T_{D2_k} \quad (108)$$

Following the same procedure as before, a linearly varying doublet is placed at the nose of the body with strength

$$T_{D1} = \frac{-\left(\alpha - \frac{dz_c}{dx}\right)_{nose}}{\frac{\beta}{2}\left[\sqrt{\cot^2\delta_N - \beta^2} + \beta\cosh^{-1}\left(\frac{\cot\delta_N}{\beta}\right) + \tan\delta\left(\sqrt{\cot^2\delta_N - \beta^2}\right)\right]} \quad (109)$$

Also placed at the nose is a quadratically varying doublet with strength

$$T_{D2_1} = \frac{-\left(\alpha - \frac{dz_c}{dx}\right)_1 + \left[a'_{BBD1_{11}} - \left(\frac{dr}{dx}\right)_1 u'_{BBD1_{11}}\right] T_{D1}}{a'_{BBD2_{11}} - \left(\frac{dr}{dx}\right)_1 u'_{BBD2_{11}}} \tag{110}$$

and at subsequent stations

$$T_{D2_i} = \frac{-\left(\alpha - \frac{dz_c}{dx}\right)_i + \left[a'_{BBD1_{i1}} - \left(\frac{dr}{dx}\right)_i u'_{BBD1_{i1}}\right] T_{D1} + \sum_{k=1}^{i-1} \left[a'_{BBD2_{ik}} - \left(\frac{dr}{dx}\right)_i u'_{BBD2_{ik}}\right] T_{D2_i}}{a'_{BBD2_{ii}} - \left(\frac{dr}{dx}\right)_i u'_{BBD2_{ii}}} \tag{111}$$

At the end of a closing body, $i = K$, $r_i = 0$.

$$T_{D2_K} = \frac{-(x_K - x_1)\, T_{D1} - \sum_{k=1}^{K-1} (x_K - x_k)^2\, T_{D2_k}}{\left[x_K - (x - \beta r)_{K-1}\right]^2} \tag{112}$$

Calculation of lift distribution on the wing. —As stated earlier, equations (96) and (100) may now be solved for the magnitudes of the pressure differences required across the wing and body panels to satisfy the remaining boundary conditions. On the wing,

$$n_{WBV_i} + n_{WWV_i} = \left(\frac{dz_c}{dx}\right)_i - \alpha - n_{WBS_i} - n_{WBD_i} \tag{113}$$

where the last two terms represent the normal velocity on the wing due to the body-line sources and doublets. To simplify the following analysis, these two terms are combined

$$n_{WB_i} = n_{WBS_i} + n_{WBD_i} = a_{WBS1_{i1}} T_{S1} + \sum_{k=1}^{K} a_{WBS2_{ik}} T_{S2_k} + a_{WBD1_{i1}} T_{D1} + \sum_{k=1}^{K} a_{WBD2_{ik}} T_{D2_k} \tag{114}$$

On the body,

$$n_{BBV_i} + n_{BWV_i} = - n_{BWS_i} = - \sum_{j=1}^{N_T} a_{BWS_{ij}} \alpha_{T_j} \tag{115}$$

The last term represents the normal velocity on the body resulting from the wing sources.

Equation (115) is the general expression for the normal velocity on the i^{th} body-panel control point. There are $N_B \leq 100$ such equations. Similarly, equation (92) is the general expression for the normal velocity at the i^{th} wing panel control point, resulting in another $N_W \leq 100$ equations. This combined system of $N_B + N_W$ equations is sufficient to determine the N_B values of P_{B_j} and the N_W values of p_{W_j}. For example, the equations may be written out as follows:

$$\begin{aligned}
&\sum_{j=1}^{N_B} a_{BBV_{1j}} \cdot p_{B_j} + \sum_{j=1}^{N_W} a_{BWV_{1j}} \cdot p_{W_j} = - n_{BWS_1} \\
&\sum_{j=1}^{N_B} a_{BBV_{2j}} \cdot p_{B_j} + \sum_{j=1}^{N_W} a_{BWV_{2j}} \cdot p_{W_j} = - n_{BWS_2} \\
&\qquad \vdots \qquad\qquad\qquad\qquad \vdots \\
&\sum_{j=1}^{N_B} a_{BBV_{N_B j}} \cdot p_{B_j} + \sum_{j=1}^{N_W} a_{BWV_{N_B j}} \cdot p_{W_j} = - n_{BWS_{N_B}} \\
&\sum_{j=1}^{N_B} a_{WBV_{1j}} \cdot p_{B_j} + \sum_{j=1}^{N_W} a_{WWV_{1j}} \cdot p_{W_j} = \left(\frac{dz_c}{dx}\right)_1 - \alpha - n_{WB_1} \\
&\sum_{j=1}^{N_B} a_{WBV_{2j}} \cdot p_{B_j} + \sum_{j=1}^{N_W} a_{WWV_{2j}} \cdot p_{W_j} = \left(\frac{dz_c}{dx}\right)_2 - \alpha - n_{WB_2} \\
&\qquad \vdots \qquad\qquad\qquad\qquad \vdots \\
&\sum_{j=1}^{N_B} a_{WBV_{N_W j}} \cdot p_{B_j} + \sum_{j=1}^{N_W} a_{WWV_{N_W j}} \cdot p_{W_j} = \left(\frac{dz_c}{dx}\right)_{N_W} - \alpha - n_{WB_{N_W}}
\end{aligned} \tag{116}$$

This system of equations is more simply expressed in the following matrix form:

$$\left[\begin{array}{cccc|cccc} {}^{a}_{BBV_{11}} & {}^{a}_{BBV_{12}} & \cdots & {}^{a}_{BBV_{1N_B}} & {}^{a}_{BWV_{11}} & {}^{a}_{BWV_{12}} & \cdots & {}^{a}_{BWV_{1N_W}} \\ {}^{a}_{BBV_{21}} & {}^{a}_{BBV_{22}} & & & & & & {}^{a}_{BWV_{2N_W}} \\ \vdots & & & & & & & \vdots \\ {}^{a}_{BBV_{N_B1}} & & & & & & & \\ \hline {}^{a}_{WBV_{11}} & & & & {}^{a}_{WWV_{11}} & & & \\ {}^{a}_{WBV_{21}} & & & & & & & \\ \vdots & & & & & & & \\ {}^{a}_{WBV_{N_W1}} & & \cdots & & & & & {}^{a}_{WWV_{N_WN_W}} \end{array}\right] \left\{\begin{array}{c} {}^{p}_{B_1} \\ {}^{p}_{B_2} \\ \vdots \\ {}^{p}_{B_{N_B}} \\ {}^{p}_{W_1} \\ {}^{p}_{W_2} \\ \vdots \\ {}^{p}_{W_{N_W}} \end{array}\right\} = \left\{\begin{array}{c} -{}^{n}_{BWS_1} \\ -{}^{n}_{BWS_2} \\ \vdots \\ -{}^{n}_{BWS_{N_B}} \\ \left(\frac{dz_c}{dx}\right)_1 - \alpha - {}^{n}_{WB_1} \\ \left(\frac{dz_c}{dx}\right)_2 - \alpha - {}^{n}_{WB_2} \\ \vdots \\ \left(\frac{dz_c}{dx}\right)_{N_W} - \alpha - {}^{n}_{WB_{N_W}} \end{array}\right\} \tag{117}$$

The matrix of aerodynamic influence coefficients is normally referred to as the aerodynamic matrix. This matrix can be conveniently partitioned into four parts, as indicated, one giving the influence of the body on the body $\left[A_{BB}\right]$, the next giving the influence of the body on the wing $\left[A_{WB}\right]$, the next giving the influence of the wing on the body $\left[A_{BW}\right]$, and the last giving the influence of the wing on the wing $\left[A_{WW}\right]$. In terms of these submatrices, equation (117) becomes

$$\left[\begin{array}{cc} \left[A_{BB}\right] & \left[A_{BW}\right] \\ \left[A_{WB}\right] & \left[A_{WW}\right] \end{array}\right] \left\{\begin{array}{c} p_B \\ p_W \end{array}\right\} = \left\{\begin{array}{c} -n_{BWS} \\ \frac{dz_c}{dx} - \alpha - n_{WB} \end{array}\right\} \tag{118}$$

This matrix equation may now be solved for $\left\{p_B\right\}$ and $\left\{p_W\right\}$ as though it were a system of two linear algebraic equations, as indicated below:

$$\begin{aligned} \left[A_{BB}\right]\left\{p_B\right\} + \left[A_{BW}\right]\left\{p_W\right\} &= -\left\{n_{BWS}\right\} \\ \left[A_{WB}\right]\left\{p_B\right\} + \left[A_{WW}\right]\left\{p_W\right\} &= \left\{\frac{dz_c}{dx} - \alpha - n_{WB}\right\} \end{aligned} \tag{119}$$

The first equation gives:

$$\left\{ p_B \right\} = - \left[A_{BB} \right]^{-1} \left\{ \left\{ n_{BWS} \right\} + \left[A_{BW} \right] \left\{ p_W \right\} \right\} \tag{120}$$

Substituting this into the second equation,

$$\left[\left[A_{WW} \right] - \left[A_{WB} \right] \left[A_{BB} \right]^{-1} \left[A_{BW} \right] \right] \left\{ p_W \right\} = \left\{ \left[A_{WB} \right] \left[A_{BB} \right]^{-1} \left\{ n_{BWS} \right\} + \left\{ \frac{dz_c}{dx} - \alpha - n_{WB} \right\} \right\}$$

which yields the lift distribution on the wing, provided the slope of the camber surface and angle of attack are specified:

$$\left\{ p_W \right\} = \left[A_R \right]^{-1} \left\{ \left[A_{WB} \right] \left[A_{BB} \right]^{-1} \left\{ n_{BWS} \right\} + \left\{ \frac{dz_c}{dx} - \alpha - n_{WB} \right\} \right\} \tag{121}$$

where $$\left[A_R \right] = \left[\left[A_{WW} \right] - \left[A_{WB} \right] \left[A_{BB} \right]^{-1} \left[A_{BW} \right] \right] \tag{122}$$

is referred to as the "reduced" aerodynamic matrix.

The pressure difference across the body panels, $\left\{ p_B \right\}$, may now be determined from equation (120). This completes the determination of all the singularity strengths for a wing-body combination of given geometry.

4.5 Calculation of Pressures, Forces, and Moments

Pressure coefficients. —The pressure coefficient is defined as

$$C_p = \frac{p - p_\infty}{1/2\,\rho_\infty u_\infty^2} = \frac{2}{\gamma M_\infty^2}\,\frac{p - p_\infty}{p_\infty} \tag{123}$$

For isentropic flow, this may be rewritten as

$$C_p = \frac{2}{\gamma M_\infty^2}\left\{\left[1 + \frac{\gamma-1}{2} M_\infty^2 \left(1 - (1+u)^2 + v^2 + w^2\right)\right]^{\frac{\gamma}{\gamma-1}} - 1\right\} \tag{124}$$

where u, v, and w are nondimensional perturbation velocities in the x, y, and z directions; γ is the ratio of specific heats for air (1.40); and M_∞ is the free-stream Mach number. Equation (124) will be referred to as the 'exact' formula for the isentropic pressure coefficient.

By expanding the terms inside the brackets in equation (124) and neglecting higher-order terms, one can derive two other formulas from which to calculate pressure coefficients. For flow over axially symmetric or elongated bodies, the following 'nonlinear' formula is sometimes recommended:

$$C_p = -2u + \beta^2 u^2 - v^2 - w^2 \tag{125}$$

For two-dimensional and planar flows, the 'linear' formula is consistent with the approximations made in first-order theory:

$$C_p = -2u \tag{126}$$

The user may use any of the above formulas to calculate pressure coefficients in the computer program.

The pressure coefficients on the body resulting from line sources and doublets are calculated separately from those on the wing and body panels. The combined pressure coefficient on the body in the presence of the wing is the sum of these two calculations.

The velocity components on the body resulting from line sources and doublets are calculated by the formulae

$$u_{B_i} = u_{BBS1_{i1}} T_{S1} + \sum_{k=1}^{K} u_{BBS2_{ik}} T_{S2_k} + u_{BBD1_{i1}} T_{D1} + \sum_{k=1}^{K} u_{BBD2_{ik}} T_{D2_k}$$

$$v_{r_{B_i}} = v_{r_{BBS1_{i1}}} T_{S1} + \sum_{k=1}^{K} v_{r_{BBS2_{i1}}} T_{S2_k} + v_{r_{BBD1_{i1}}} T_{D1} + \sum_{k=1}^{K} v_{r_{BBD2_{ik}}} T_{D2_k}$$

$$v_{\theta_{B_i}} = v_{\theta_{BBS1_{i1}}} T_{S1} + \sum_{k=1}^{K} v_{\theta_{BBS2_{i1}}} T_{S2_k} + v_{\theta_{BBD1_{i1}}} T_{D1} + \sum_{k=1}^{K} v_{\theta_{BBD2_{ik}}} T_{D_k}$$

$$v_{B_i} = v_{r_{B_i}} \sin\theta_i + v_{\theta_{B_i}} \cos\theta_i$$

$$w_{B_i} = v_{r_{B_i}} \cos\theta_i - v_{\theta_{B_i}} \sin\theta_i \qquad (127)$$

The velocity components on the body panels resulting from surface distributions of singularities on the body and wing are given by

$$u_{B_i} = u_{BBV_i} + u_{BWV_i} + u_{BWS_i} \qquad (128)$$

where

$$u_{BBV_i} = \sum_{j=1}^{N_B} u_{BBV_{ij}} p_{B_j}$$

$$u_{BWV_i} = \sum_{j=1}^{N_W} u_{BWV_{ij}} p_{W_j}$$

$$u_{BWS_i} = \sum_{j=1}^{N_T} u_{BWS_{ij}} \alpha_{T_j};$$

and

$$v_{B_i} = v_{BBV_i} + v_{BWV_i} + v_{BWS_i} \tag{129}$$

where

$$v_{BBV_i} = \sum_{j=1}^{N_B} (v_{BBV_{ij}} \cos \theta_j - w_{BBV_{ij}} \sin \theta_j)\, p_{B_j}$$

$$v_{BWV_i} = \sum_{j=1}^{N_W} (v_{BWV_{ij}} \cos \theta_j - w_{BWV_{ij}} \sin \theta_j)\, p_{W_j}$$

$$v_{BWS_i} = \sum_{j=1}^{N_T} (v_{BWS_{ij}} \cos \theta_j - w_{BWS_{ij}} \sin \theta_j)\, \alpha_{T_j} ;$$

and

$$w_{B_i} = w_{BBV_i} + w_{BWV_i} + w_{BWS_i} \tag{130}$$

where

$$w_{BBV_i} = \sum_{j=1}^{N_B} (w_{BBV_{ij}} \cos \theta_j + v_{BBV_{ij}} \sin \theta_j)\, p_{B_j}$$

$$w_{BWV_i} = \sum_{j=1}^{N_W} (w_{BWV_{ij}} \cos \theta_j + v_{BWV_{ij}} \sin \theta_j)\, p_{W_j}$$

$$w_{BWS_i} = \sum_{j=1}^{N_T} (w_{BWS_{ij}} \cos \theta_j + v_{BWS_{ij}} \sin \theta_j)\, \alpha_{T_j}$$

The various velocity coefficients are given by equation (74), selected according to the type of singularity considered.

Finally, the velocity components on the wing panels are calculated by

$$u_{W_i} = u_{WBS_i} + u_{WBD_i} + u_{WBV_i} + u_{WWV_i} + u_{WWS_i} \tag{131}$$

where

$$u_{WBS_i} = u_{WBS1_{i1}}\, T_{S1} + \sum_{k=1}^{K} u_{WBS2_{ik}}\, T_{S2_k}$$

$$u_{WBD_i} = u_{WBD1_{ik}} T_{D1} + \sum_{k=1}^{K} u_{WBD2_{ik}} T_{D2_k}$$

$$u_{WBV_i} = \sum_{j=1}^{N_B} u_{WBV_{ij}} p_{B_j}$$

$$u_{WWV_i} = \sum_{j=1}^{N_W} u_{WWV_{ij}} p_{W_j}$$

$$u_{WWS_i} = \sum_{j=1}^{N_T} u_{WWS_{ij}} \alpha_{T_j};$$

and

$$v_{W_i} = v_{WBS_i} + v_{WBD_i} + v_{WBV_i} + v_{WWV_i} + v_{WWS_i} \qquad (132)$$

where

$$v_{WBS_i} = (v_{r_{S1_{i1}}} \sin \theta_{A_i} + v_{\theta_{S1_{i1}}} \cos \theta_{A_i}) T_{S1} + \sum_{k=1}^{K} (v_{r_{S2_{ik}}} \sin \theta_{A_i} + v_{\theta_{S2_{ik}}} \cos \theta_{A_i}) T_{S2_k}$$

$$v_{WBD_i} = (v_{r_{D1_{i1}}} \sin \theta_{A_i} + v_{\theta_{D1_{i1}}} \cos \theta_{A_i}) T_{D1} + \sum_{k=1}^{K} (v_{r_{D2_{ik}}} \sin \theta_{A_i} + v_{\theta_{D2_{iD}}} \cos \theta_{A_i}) T_{D2_k}$$

$$v_{WBV_i} = \sum_{j=1}^{N_B} (v_{WBV_{ij}} \cos \theta_j - w_{WBV_{ij}} \sin \theta_j) p_{B_j}$$

$$v_{WWV_i} = \sum_{j=1}^{N_W} (v_{WWV_{ij}} \cos \theta_j - w_{WWV_{ij}} \sin \theta_j) p_{W_j}$$

$$v_{WWS_i} = \sum_{j=1}^{N_T} (v_{WWS_{ij}} \cos \theta_j - w_{WWS_{ij}} \sin \theta_j) \alpha_{T_j};$$

and

$$w_{W_i} = w_{WBS_i} + w_{WBD_i} + w_{WBV_i} + w_{WWV_i} + w_{WWS_i} \quad (133)$$

where

$$w_{WBS_i} = (v_{r_{S1}} \cos\theta_{A_i} - v_{\theta_{S1}} \sin\theta_{A_i}) T_{S1} + \sum_{k=1}^{K} (v_{r_{S2_{ik}}} \cos\theta_{A_i} - v_{\theta_{S2_{ik}}} \sin\theta_{A_i}) T_{S2_k}$$

$$w_{WBD_i} = (v_{r_{D1}} \cos\theta_{A_i} - v_{\theta_{D1}} \sin\theta_{A_i}) T_{D1} + \sum_{k=1}^{K} (v_{r_{D2_{ik}}} \cos\theta_{A_i} - v_{\theta_{D2_{ik}}} \sin\theta_{A_i}) T_{D2_k}$$

$$w_{WBV_i} = \sum_{j=1}^{N_B} (w_{WBV_{ij}} \cos\theta_j + v_{WBV_{ij}} \sin\theta_j) p_{B_j}$$

$$w_{WWV_i} = \sum_{j=1}^{N_W} (w_{WWV_{ij}} \cos\theta_j + v_{WWV_{ij}} \sin\theta_j) p_{W_j}$$

$$w_{WWS_i} = \sum_{j=1}^{N_T} (w_{WWS_{ij}} \cos\theta_j + v_{WWS_{ij}} \sin\theta_j) \alpha_{T_j}.$$

Forces and moments on the isolated body. —The lift, drag, and pitching moments on the body caused by the line sources and doublets alone are calculated by integrating the pressures over the body. Interference effects from the wing are ignored at this point and are added later.

The aerodynamic forces acting on a body can be easily resolved into an axial force X, a normal force F, and a pitching moment about the nose M. The corresponding dimensionless coefficients are given by

$$C_{X_B} = \frac{X}{qS_W} = \frac{1}{S_W} \int_0^1 r(x) \frac{dr(x)}{dx} \int_0^{2\pi} C_P(x, r, \theta) \, d\theta dx$$

$$C_{N_B} = \frac{F}{qS_W} = \frac{1}{S_W} \int_0^1 r(x) \int_0^{2\pi} C_P(x, r, \theta) \cos\theta d\theta dx$$

$$C_{M_{B_0}} = \frac{M}{qS_W\bar{c}} = \frac{1}{S_W\bar{c}} \int_0^1 xr(x) \int_0^{2\pi} C_P(x,r,\theta) \cos\theta d\theta dx \quad (134)$$

These coefficients may be evaluated by numerical integration, first with respect to θ, then with respect to x.

The lift, pressure drag, and pitching moments about some arbitrary point may now be obtained by a resolution of forces. For example,

$$\begin{aligned} C_{L_B} &= C_{N_B} \cos\alpha - C_{X_B} \sin\alpha \\ C_{B_B} &= C_{N_B} \sin\alpha + C_{X_B} \cos\alpha \\ C_{M_B} &= C_{M_{B_0}} + \bar{x}C_{N_B} - \bar{z}C_{X_B} \end{aligned} \quad (135)$$

where the moments are computed about the point $(\bar{x}, \bar{z})$, $\bar{c}$ is a reference chord and S_W is the reference wing area. The forces and moments are computed for the half-body only.

Forces and moments on the wing. — The forces and moments acting on the wing are determined by calculation of the forces and moments acting on the upper surface of the wing and adding them to those acting on the lower surface. The pressure coefficient on a wing panel is usually given by equation (126). The normal force on the surface of a panel is the product of the dynamic pressure, the pressure coefficient, and the panel area.

$$F_i = q\, C_{p_i}\, A_i \quad (136)$$

Resolution of this force into components normal and parallel to the free-stream direction yields

$$\begin{aligned} L_i &= -F_i \\ D_i &= F_i\left[\left(\frac{dz}{dx}\right)_i - \alpha\right] \end{aligned} \quad (137)$$

where $$\left(\frac{dz}{dx}\right)_i = \left(\frac{dz_c}{dx}\right)_i \pm \left(\frac{dz_T}{dx}\right)_j$$

is the slope of the panel with respect to the x-y plane. The upper sign refers to the upper surface, the lower to the lower surface.

The pitching moment with respect to a point $(\bar{x}, 0, \bar{z})$ is:

$$M_i = - L_i (x_i - \bar{x}) + D_i (z_i - \bar{z}) \tag{138}$$

The sum of the forces and moments on the upper and lower surfaces, divided by the product of the dynamic pressure and the reference wing area, results in the lift, drag, and pitching moment coefficients for the wing:

$$C_{L_W} = \frac{1}{q\ S_W} \sum_{i=1}^{N_W} (L_{U_i} - L_{L_i})$$

$$C_{D_W} = \frac{1}{q\ S_W} \sum_{i=1}^{N_W} (D_{U_i} + D_{L_i}) \tag{139}$$

$$C_{M_W} = \frac{1}{q\ S_W\ \bar{c}} \sum_{i=1}^{N_W} (M_{U_i} + M_{L_i})$$

where the subscripts U and L refer to the upper and lower surfaces.

Interference forces and moments on body panels. — The forces and moments on the body panels are similarly calculated. The normal force on the panel surface is given by equation (136). The interference lift and drag may now be calculated, making due allowance for the inclination of the panel:

$$L_i = - F_i \cos \theta_i$$

$$D_i = F_i \left[\left(\frac{dz'}{dx} \right)_i - \alpha \cos \theta_i \right] \tag{140}$$

where dz'/dx is the slope of the panel with respect to the primed system of coordinates having its origin in the foremost panel corner, as illustrated in figure 1 (page 11). As before, the pitching moment is given by equation (138).

The lift, drag, and pitching moment coefficients are given by equation (139), omitting the terms with subscript L.

Forces and moments on wing-body combination. — The resultant lift, drag, and pitching moment coefficients may now be obtained by adding the isolated body coefficients [equation (134)] to the wing coefficients and the body interference coefficients, both from equation (139). This completes the determination of the forces and moments on the wing-body combination at a given angle of attack.

Spanwise force distributions on wings. —Spanwise distributions of lift and drag on the wings may also be calculated. The lift on a wing may be written in the following form:

$$L = 2q \iint_{\text{half wing}} \left(C_{p_L} - C_{p_u} \right) dS \tag{140A}$$

Dividing by ΔY_i and writing in difference form:

$$\left(\frac{\Delta L}{\Delta Y} \right)_i = 2q \sum_{i=1}^{N_W} \left(C_{p_{L_i}} - C_{p_{U_i}} \right) \frac{\Delta S_i}{\Delta Y_i} \tag{140B}$$

For a chordwise strip of panels at some streamwise location k,

$$\left(\frac{\Delta L}{\Delta Y} \right)_k = 2q \sum_{i=N_{row_k}}^{N_{row_{k+1}}-1} \left(C_{p_{L_i}} - C_{p_{U_i}} \right) \frac{\Delta S_i}{\Delta Y_i} \tag{140C}$$

where: N_{row_k} = leading edge panel number for row k

ΔS_i = A_i - panel area

ΔY_i = panel width

Multiplying both sides of equation (139C) by b/2q yields

$$\left[\left(\frac{b}{2q} \right) \left(\frac{\Delta L}{\Delta Y} \right) \right]_k = b \sum_{i=N_{row_k}}^{N_{row_k}-1} \left(C_{p_{L_i}} - C_{p_{U_i}} \right) \frac{A_i}{\Delta Y_i} \tag{140D}$$

Similarly,

$$\left[\left(\frac{b}{2q} \right) \left(\frac{\Delta D}{\Delta Y} \right) \right]_k = \sum_{i=N_{row_k}}^{N_{row_k}-1} \left(C_{p_{L_i}} - C_{p_{U_i}} \right) \left[\left(\frac{dz}{dx} \right)_i - \alpha \right] A_i \tag{140E}$$

where b = wing semispan.

Note that

$$C_L = \sum_{k=1}^{N_R} \left[\left(\frac{b}{2q} \right) \left(\frac{\Delta L}{\Delta Y} \right) \right]_k \qquad (140F)$$

and

$$C_D = \sum_{k=1}^{N_R} \left[\left(\frac{b}{2q} \right) \left(\frac{\Delta D}{\Delta Y} \right) \right]_k$$

where N_R = number of rows on wing.

4.6 Applications to Specific Problems

The method of aerodynamic influence coefficients can be applied to a wide variety of aerodynamic problems involving supersonic flows about wing-body combinations. The generality of the method is primarily due to the matrix formulation of the problem, which introduces considerable simplification into the algebraic manipulations involved. For example, either the direct problem of determining the pressures, forces, and moments on configurations of given geometry, or the inverse problem of determining the geometry which will result in certain desired aerodynamic properties, can be solved with equal ease. In particular, the wing camber and twist required to minimize the drag of a wing-body combination under given constraints of lift, or lift and pitching moment, may be determined by additional straightforward operations on the aerodynamic matrix. The various applications will be outlined in the following sections.

Direct problems. — The determination of the aerodynamic pressures, forces, and moments acting on a wing-body combination of given geometry has been outlined in section 4.5. Briefly, the problem is solved in three steps, beginning with the analysis of the isolated body, followed by the analysis of the wing in the presence of the body, and completed by calculation of the interference effects of the wing on the body. This technique is fundamental to the solution of both direct and inverse problems, once the geometry of the configuration has been defined. The specific direct problems that can be treated with this method are outlined below. Examples giving results for selected cases are presented in section 4.7.

Body alone: Given a body having circular or nearly circular cross sections, and having arbitrary camber and angle of attack, determine the pressures, forces, and moments.

Wing alone: Given a wing planform that can be approximated by a series of straight-line segments and having arbitrary angle of attack, camber, twist, and thickness distributions, determine the pressures, forces, and moments. This problem can be solved at a number of angles of attack to give the theoretical lift and moment curves and the drag polar.

Special cases include the calculation of plane wings at incidence, non-lifting thick wings, and the effect of control surface deflections.

Wing-body combinations: All cases described above may be calculated for the combined wing and body, taking into account all the interference effects of one on the other. In particular, the effects of symmetrical body contouring may be included in the analysis.

Inverse problems. — Inverse problems fall into two categories. The first category includes the determination of the wing camber and twist distribution required to support a given lift distribution. In the second category, the wing camber and twist are found that will satisfy the condition of minimum drag under given constraints of lift and pitching moment. These two categories are described in detail below.

Given lift distribution: The slope of the camber surface that will support a given lift distribution p_W may be determined by inverting equation (121) thus:

$$\left\{\frac{dz_c}{dx}\right\} = \alpha + \left\{n_{WB}\right\} + \left[A_R\right]\left\{p_W\right\} - \left[A_{WB}\right]\left[A_{BB}\right]^{-1}\left\{n_{WBS}\right\} \qquad (141)$$

where $\left\{n_{WB}\right\}$ is the normal velocity distribution induced on the wing by the body-line sources and doublets, $\left[A_R\right]$ is the reduced aerodynamic matrix given by equation (122), and $\left[A_{WB}\right]\left[A_{BB}\right]^{-1}\left\{n_{WBS}\right\}$ is the normal velocity component induced on the wing by the cancellation of the normal velocity components induced by the wing-thickness distribution on the body.

A special case results when the lift distribution on the wing is constant. In this case, however, if additional pressures are introduced by the wing and body thickness distributions or body camber and angle of attack effects, then the pressure distributions on the upper and lower surfaces of the wing will not be constant.

Minimum drag for given lift and pitching moment: The wing camber and twist required to minimize the drag of a wing-body combination under given constraints of lift and pitching moment may be determined by applying the calculus of variations to the drag equation. The problem is formulated by defining a

function F in terms of the N_W variables p_{W_i} and the two auxiliary variables, or Lagrange multipliers, λ_1 and λ_2. The function F is chosen so it will be equal to the drag when the wing lift and pitching moment are equal to their constrained values $\bar{L}$ and $\bar{M}$, respectively. One such function is

$$F = D + \lambda_1 (L - \bar{L}) + \lambda_2 (M - \bar{M}) \tag{142}$$

where

$$L = - \sum_{i=1}^{N_W} A_i \, p_{W_i}$$

$$D = \sum_{i=1}^{N_W} L_i \left(\frac{dz_c}{dx}\right)_i = - \sum_{i=1}^{N_W} A_i \left(\frac{dz_c}{dx}\right)_i p_{W_i}$$

$$M = - \sum_{i=1}^{N_W} L_i \, (x_i - \bar{x}) = \sum_{i=1}^{N_W} A_i \, (x_i - \bar{x}) \, p_{W_i}$$

and

A_i = the area of panel i

p_{W_i} = the pressure difference across panel i

$\left(\frac{dz_c}{dx}\right)_i$ = the surface slope of panel i

x_i = the coordinate of the centroid of panel i

$\bar{x}$ = the x coordinate of the moment center

It is assumed that the moment center lies on the centerline of the configuration and in the wing reference plane.

The $N_W + 2$ conditions for minimum drag may now be written

$$\frac{\partial F}{\partial p_{W_i}} = \frac{\partial D}{\partial p_{W_i}} + \lambda_1 \frac{\partial L}{\partial p_{W_i}} + \lambda_2 \frac{\partial M}{\partial p_{W_i}} = 0, \qquad i = 1, \cdots N_W$$

$$\frac{\partial F}{\partial \lambda_1} = L - \bar{L} = 0$$

$$\frac{\partial F}{\partial \lambda_2} = M - \bar{M} = 0 \tag{143}$$

To evaluate these partial derivatives it is necessary to express the camber surface slopes $(dz_c/dx)_i$ in terms of the pressure differences across the wing panels p_{W_i}. The boundary conditions on the wing require that the slope of the camber surface be equal to the resultant normal velocity component at each point. Therefore,

$$\left(\frac{dz_c}{dx}\right)_i = n_{WB_i} + n_{WBV_i} + n_{WWV_i} \tag{144}$$

where n_{WB_i}, the normal velocity on the wing due to the body-line sources and doublets, is given by equation (114) for a specified body shape. Expressions for n_{WBV_i} and n_{WWV_i} are given following equation (89) and are repeated below for convenience. The normal velocity on the wing due to the distributions of vorticity on the wing panels is given directly in terms of p_{W_i} as follows:

$$n_{WWV_i} = \sum_{j=1}^{N_W} a_{WWV_{ij}} p_{W_j} \tag{145}$$

However, the normal velocity on the wing due to the distributions of vorticity on the body panels is given in terms of the pressure difference across the body panels p_{B_i} as follows:

$$n_{WBV_i} = \sum_{j=1}^{N_B} a_{WBV_{ij}} p_{B_j} \tag{146}$$

Thus an expression is required relating p_{B_i} to p_{W_i}. Equation (120) gives the desired result in matrix notation.

$$\left\{p_B\right\} = -\left[A_{BB}\right]^{-1}\left\{n_{BWS}\right\} - \left[A_{BB}\right]^{-1}\left[A_{BW}\right]\left\{p_W\right\} \tag{147}$$

where $\left\{n_{BWS}\right\}$ is an array giving the normal velocity components on the body panels due to the wing thickness distribution. For wings without thickness, this term will not appear in the above equation.

Finally by substituting equations (145) and (146) into equation (144) and simplifying, the desired result is obtained:

$$\left(\frac{dz_c}{dx}\right)_i = n_{WB_i} - \sum_{j=1}^{N_B} b_{ij}\, n_{BWS_j} + \sum_{j=1}^{N_W} a_{R_{ij}}\, p_{W_j} \tag{148}$$

where b_{ij} is an element of the matrix:

$$\left[B_{ij}\right] = \sum_{k=1}^{N_W} \left[A_{WB_{ik}}\right] \left[A_{BB_{kj}}\right]^{-1}$$

and $a_{R_{ij}}$ is an element of the reduced aerodynamic matrix given by equation (122):

$$\left[A_{R_{ij}}\right] = \left[\left[A_{WW}\right] - \left[A_{WB}\right] \left[A_{BB}\right]^{-1} \left[A_{BW}\right]\right]$$

In the above expressions, $\left[A_{WB}\right]$ is the matrix of the influence coefficients $a_{WBV_{ij}}$, $\left[A_{BB}\right]$ is the matrix of the influence coefficients $a_{BBV_{ij}}$, and so on, as described following equation (117).

The partial derivatives indicated in equation (143) may now be evaluated.

The expression for the drag becomes

$$D = \sum_{i=1}^{N_W} D_i = - \sum_{i=1}^{N_W} A_i \, p_{W_i} \left(n_{WB_i} - \sum_{j=1}^{N_B} b_{ij} \, n_{BWS_j} + \sum_{j=1}^{N_W} a_{R_{ij}} \, p_{W_j} \right) \tag{149}$$

Therefore,

$$\frac{\partial D}{\partial p_{W_i}} = - \left[A_i \left(n_{WB_i} - \sum_{j=1}^{N_B} b_{ij} \, n_{BWS_j} + \sum_{j=1}^{N_W} a_{R_{ij}} \, p_{W_j} \right) + \sum_{j=1}^{N_W} A_j \, a_{R_{ji}} \, p_{W_j} \right]$$

$$= - A_i \left(n_{WB_i} - \sum_{j=1}^{N_B} b_{ij} \, n_{BWS_j} \right) - \sum_{j=1}^{N_W} \left(A_i \, a_{R_{ij}} + A_j \, a_{R_{ji}} \right) p_{W_j} \tag{150}$$

Also,

$$\frac{\partial L}{\partial p_{W_i}} = - A_i$$

$$\frac{\partial M}{\partial p_{W_i}} = A_i \, (x_i - \bar{x}) \tag{151}$$

Similarly,

$$\frac{\partial F}{\partial \lambda_1} = - \sum_{j=1}^{N_W} A_i \, p_{W_i} - \overline{L}$$

$$\frac{\partial F}{\partial \lambda_2} = \sum_{j=1}^{N_W} A_i \, p_{W_i} \, (x_i - \bar{x}) - \overline{M} \tag{152}$$

Substituting these partial derivatives into equation (143) gives a system of $N_W + 2$ linear equations. This system of equation may be written in matrix form, as follows, where N_W has been replaced by N for simplicity:

$$\begin{bmatrix} -(A_1{}^aR_{11} - A_1{}^aR_{11}) - (A_1{}^aR_{12} - A_2{}^aR_{21}) \cdots - A_1 (x_1 - \bar{x}) A_1 \\ -(A_2{}^aR_{21} - A_1{}^aR_{12}) - (A_2{}^aR_{22} + A_2{}^aR_{22}) \cdots - A_2 (x_2 - \bar{x}) A_2 \\ -(A_3{}^aR_{31} + A_1{}^aR_{13}) \\ \vdots \\ -(A_N{}^aR_{N1} - A_1{}^aR_{1N} \cdots - A_N (x_N - \bar{x}) A_N \\ -A_1 \quad -A_2 \cdots 0 \quad 0 \\ (x_1 - \bar{x}) A_1 \quad (x_2 - \bar{x}) A_2 \quad 0 \quad 0 \end{bmatrix} \begin{Bmatrix} p_{W_1} \\ p_{W_2} \\ \vdots \\ p_{W_N} \\ \lambda_1 \\ \lambda_2 \end{Bmatrix} = \begin{Bmatrix} A_1 (n_{WB_1} - \sum_{j=1}^{N} b_{1_j} n_{BWS_j}) \\ A_2 (n_{WB_2} - \sum_{j=1}^{N} b_{2_j} n_{BWS_j}) \\ \vdots \\ A_N (n_{WB_N} - \sum_{j=1}^{N} b_{N_j} n_{BWS_j}) \\ \bar{L} \\ \bar{M} \end{Bmatrix} \quad (153)$$

The wing pressure distribution for minimum drag may be found by inverting the matrix and postmultiplying it by the array on the right-hand side of the equation. If the lift only is to be constrained, the row and column of the matrix corresponding to λ_2 is omitted before the inversion. Finally, the optimum camber shape may be calculated by equation (141).

The method of Lagrange multipliers outlined above may be extended to include many other cases of interest. Examples of cases that have been determined by this method, but not reported here, are:

1) Optimization of the wing camber surface while keeping the total lift, or total lift and pitching moment, of the wing plus body constrained to given values.

2) Optimization of the wing twist for a given camber and lift (or lift and pitching moment) on the wing.

3) Optimization of any consecutively numbered group of panels on the wing, while constraining the camber and twist of the remaining panels, and the wing lift, or lift and pitching moment. This case may be useful for determining optimum flap settings at given cruise conditions.

4) Calculation of the incidence at which a given cambered wing will achieve a given lift coefficient.

4.7 Theoretical Comparisons

In this section results of the method of aerodynamic influence coefficients are compared with linear theory calculations published by other investigators. Theoretical solutions for isolated wings, bodies, and wing-body combinations are compared. The form of the pressure distributions and the prediction of the lift and drag of the examples studied are emphasized. In particular, the reasons underlying the choice of the various control points used in the calculations are discussed.

Pressure distributions on flat plate wings.—Pressure distributions have been calculated for delta, double delta, arrow, and constant-chord wings over a range of supersonic Mach numbers and compared with linearized theory results published by other investigators.

It was found that location of the panel control points had a dominant effect on the form of the wing pressure distributions obtained. Figure 9 shows the calculated chordwise pressure distributions (corresponding to two control-point locations) on an inclined, planar, constant-chord wing with sonic leading edges. The upper plot shows the result obtained when the control point is located at the panel centroids. A strong oscillatory tendency in the chordwise pressure distribution is observed that does not agree with the exact linear theory solution, except towards the trailing edge of the wing. The plot on the lower right shows the result obtained for control points located at 95 percent of the streamwise chord through the panel centroid. The chordwise pressure distributions are now smooth, and they follow the linear theory solution closely, except very near the leading edge and in the region of the strong discontinuity introduced by the wing-tip Mach wave.

The effect of the control point location on the pressures calculated for three panels on the inboard row of this wing is shown in the sketch on the lower left of the illustration. Here the pressures converge smoothly towards the correct linear theory value as the control point is moved towards the trailing edge of the panel. This is true for panels having sonic or supersonic trailing edges. For panels having subsonic trailing edges, however, the normal velocity at the trailing edge is infinite, and the panel pressure becomes indeterminate. To avoid this difficulty, and to maintain a good approximation to the exact linear theory pressure coefficients, the control points have been arbitrarily located

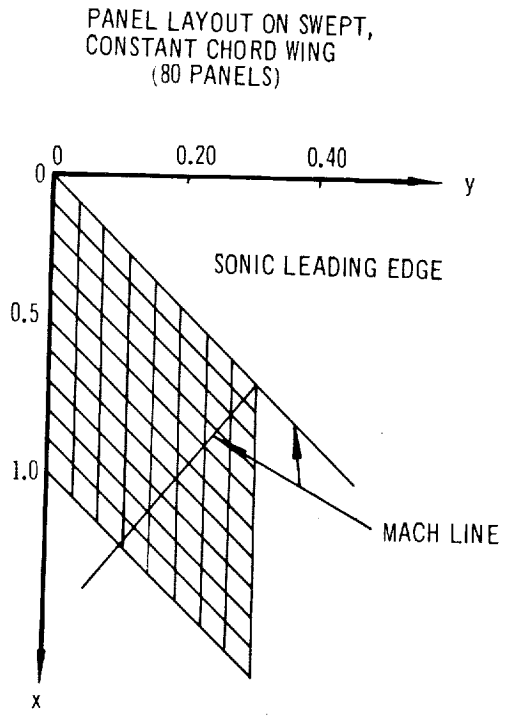

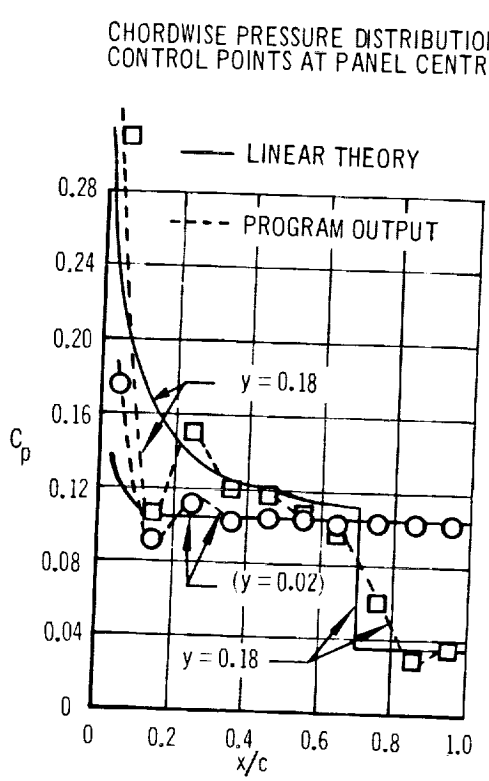

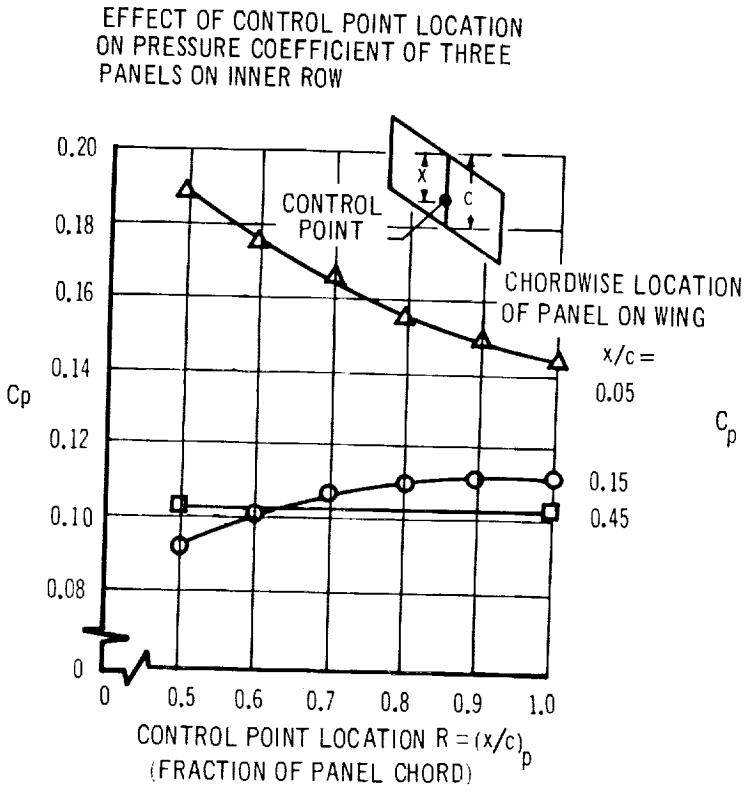

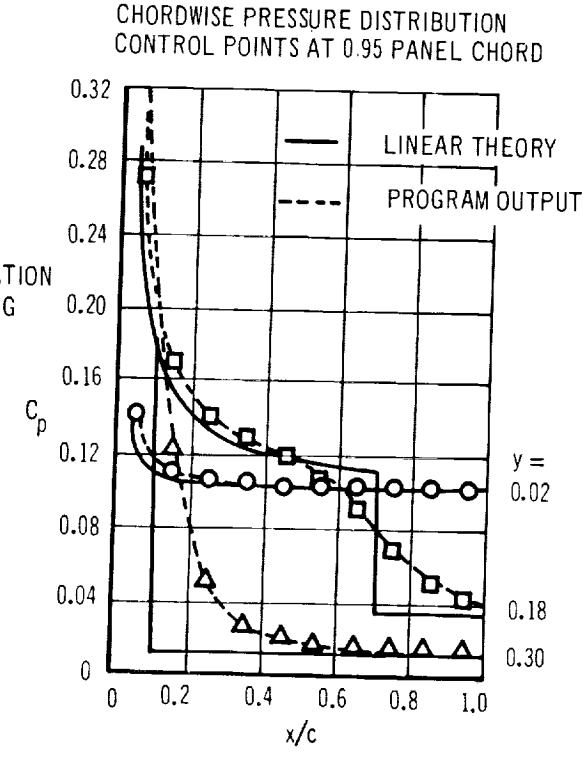

FIGURE 9 EFFECT OF CONTROL POINT LOCATION

at 95 percent of the streamwise chord through the panel centroid. This choice of control point location has given an adequate representation of the pressure distribution for all cambered or uncambered lifting wings so far investigated.

Examples illustrating the results obtained for isolated wings are presented on the following pages. In all these examples, the wing has been subdivided into 100 panels, spaced evenly in 10-percent increments in both chordwise and spanwise directions. Each wing has an incidence $\alpha = 0.1$ radian.

Figure 10 shows the pressure distribution calculated for flat-plate delta wing at incidence, compared to an exact linearized theory solution. The wing planform corresponds to that of example II of reference 13 and has a subsonic leading edge with $\tan \Lambda / \beta = 1.2$. The present theory agrees reasonably well with the exact result, except in the region of the wing tip or near the leading edge. The overall lift curve slope of the wing is 3.58, compared to the exact value of 3.62. The wing center of pressure is correctly located at a point two thirds of the root chord from the apex.

Figure 11 shows the pressure distribution calculated for a flat-plate arrow wing at incidence. These results are compared with both the exact linear theory solution and to another influence coefficient method recently published by Carlson and Middleton (reference 5). The wing has a subsonic leading edge and supersonic trailing edge at Mach 2.0. This particular wing planform has been studied extensively at the NASA Langley Research Center and as a result, both theoretical and experimental data are available for comparison. The present method agrees reasonably well with both the exact linear theory result and the cited numerical method.

The final example, showing the pressure distribution of a flat-plate, double-delta wing, is shown in figure 12. This was chosen to illustrate the application of the method to more general planforms. The exact linear theory analysis of this planform, based on a superposition procedure, was presented in reference 14. This particular planform was also analyzed by Middleton and Carlson in reference 2. The illustration shows the spanwise pressure distributions at two stations on the wing, which were obtained by interpolating chordwise pressure distribution plots. The pressure distribution shows the same magnitude and trends as the exact solution, but does not reproduce the pressure discontinuities predicted by the method of superposition.

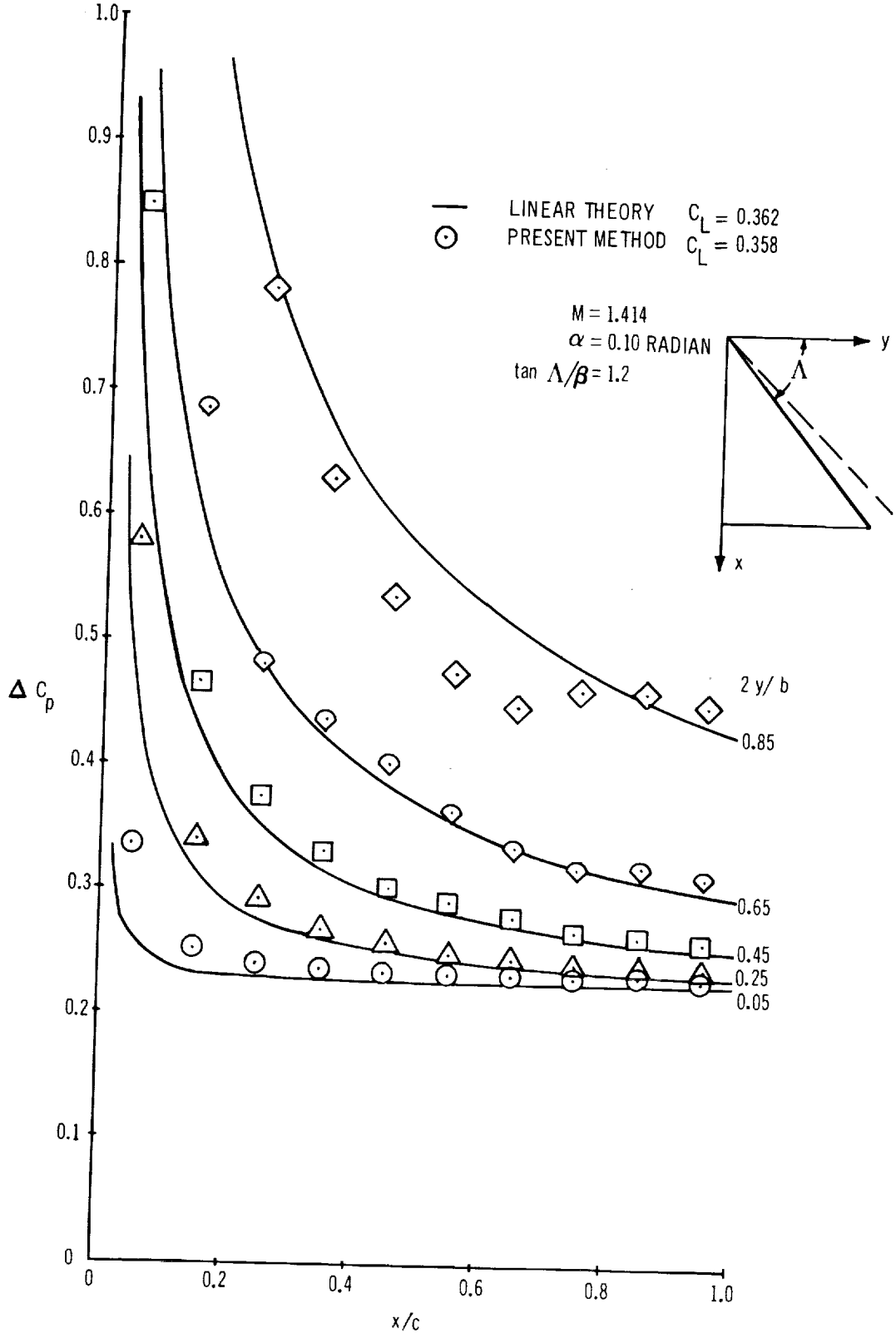

FIGURE 10 PRESSURE DISTRIBUTION – FLAT-PLATE DELTA WING

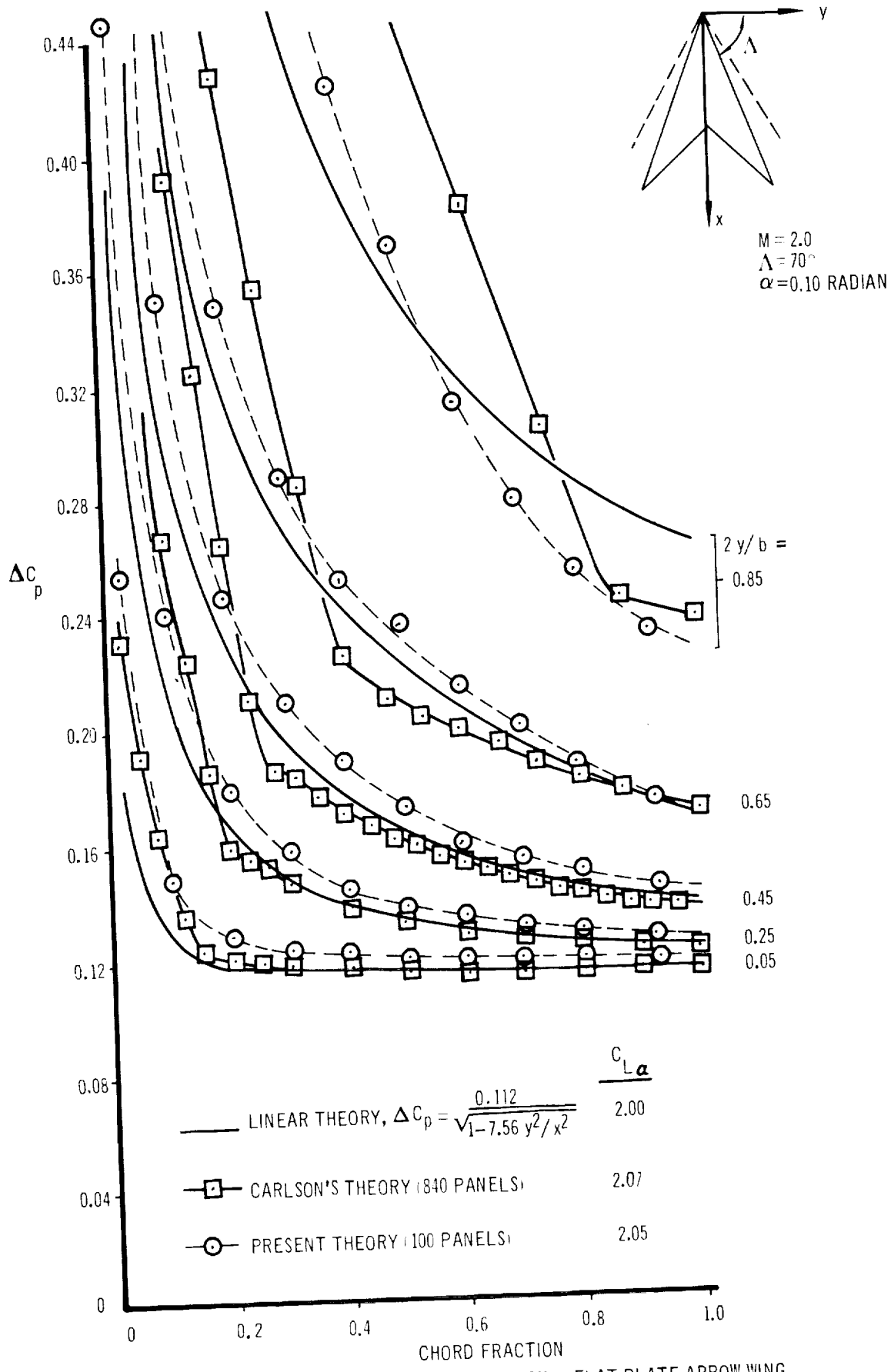

FIGURE 11 PRESSURE DISTRIBUTION – FLAT-PLATE ARROW WING

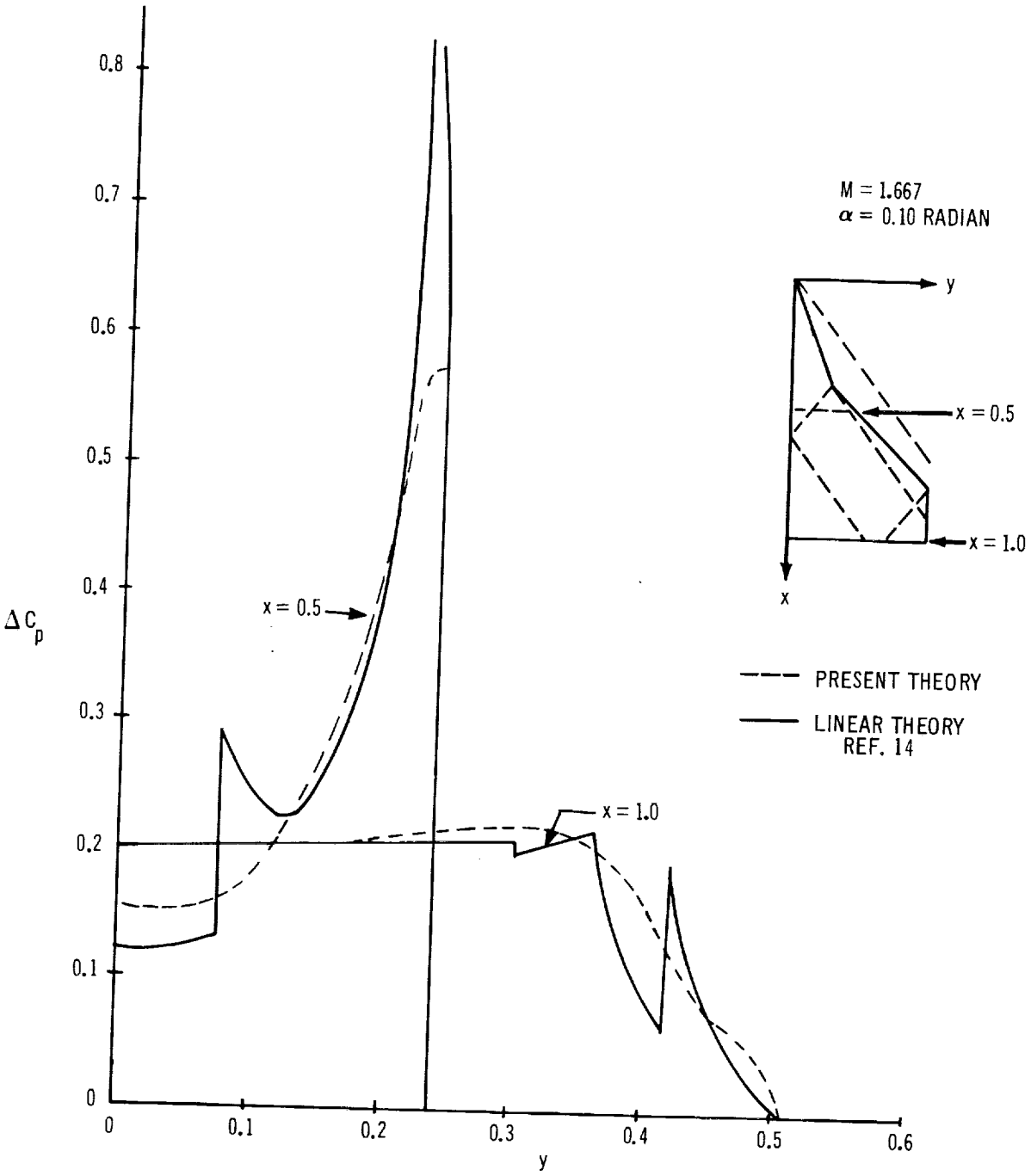

FIGURE 12 PRESSURE DISTRIBUTION — FLAT-PLATE DOUBLE-DELTA WING

The lift curve slope (per degree) and center of pressure at two Mach numbers were estimated with reasonable precision, however, and are presented for comparison in the following table:

Method	M = 1.414		M = 1.667	
	C_{L_α}	X_{CP}	C_{L_α}	X_{CP}
Superposition Analysis (14)	0.0514	0.682	0.0461	—
Present Method	0.0516	0.691	0.0448	0.697
Carlson and Middleton (2)	0.0507 (per degree)	0.687	0.0449 (per degree)	0.686

Pressure distribution due to wing thickness. —Wing-thickness effects are simulated by a combination of constant and linearly varying distributions of sources on the panels. The behavior of these singularities is sufficiently different from the constant distributions of vorticity used to represent the lifting surfaces that a new control point must be defined for calculating the velocity components and pressures resulting from thickness. Best results were obtained when the thickness control points were located at the centroids of the panels.

An example of the thickness pressures calculated for a subsonic leading-edge arrow wing of 6 percent biconvex section is given for $\alpha = 0°$ in figure 36, page 197. Good correlation with experiment is obtained, except near the trailing edge at the tip. The pressure distributions calculated by this method showed no tendency to oscillate at any point on the wing chord; this improves upon previous methods based on distributions of constant-strength sources.

Pressure distribution on cambered wings. —The pressure distribution on cambered wings is calculated in the same manner as the pressure distribution for flat wings at incidence. However, the slope of the camber surface must be calculated at the panel control points. A sample calculation showing the chordwise pressure distributions on a cambered arrow wing with thickness at three angles of attack is given in figure 37, page 198.

The inverse problem of calculating the camber surface corresponding to a given pressure distribution is numerically simpler than the preceding problem and yields excellent results. An example giving the camber surface of a delta wing planform corresponding to a linearly varying chordwise pressure distribution is shown in figure 13. The camber surface agrees closely to the predicted by the method of reference 13.

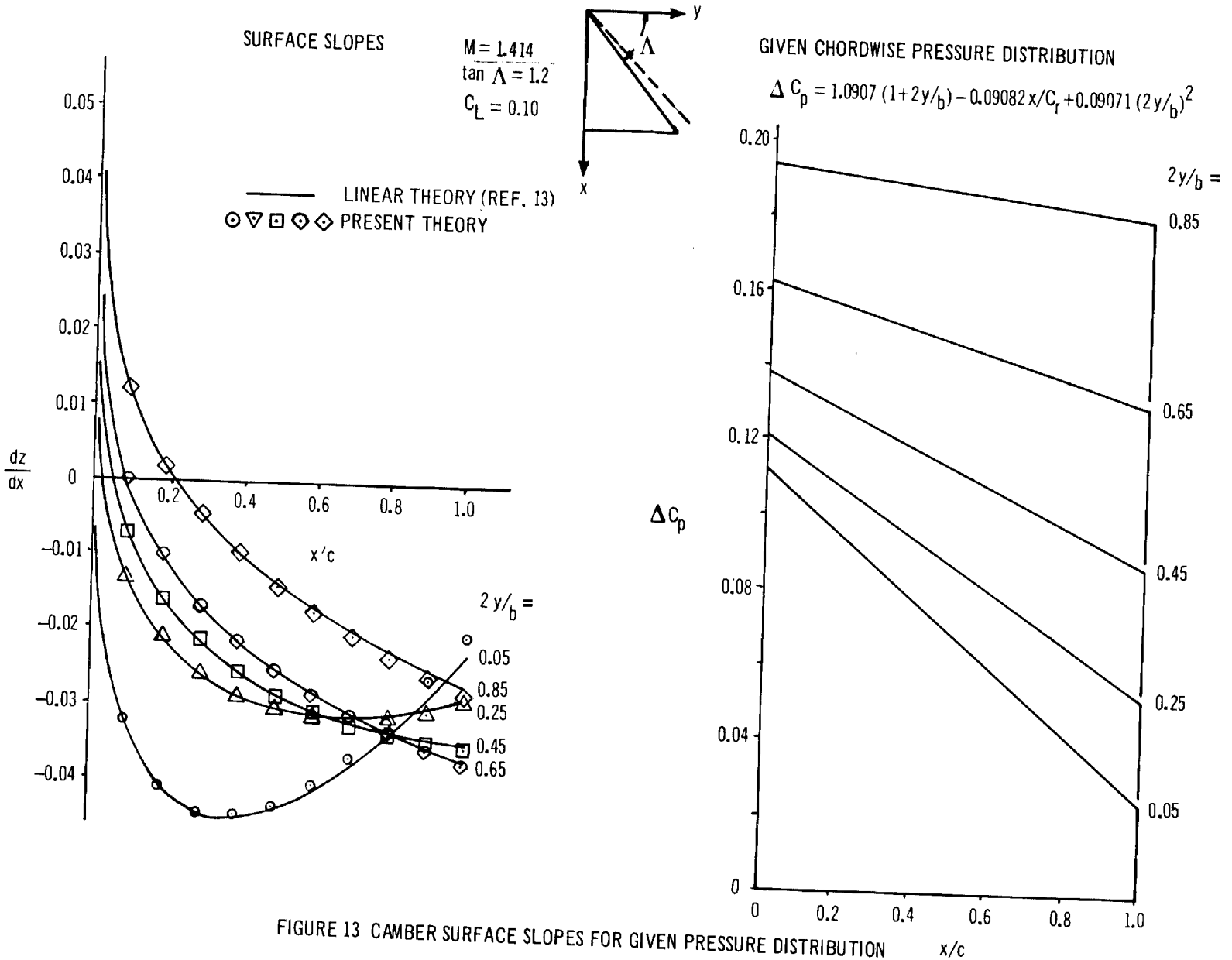

FIGURE 13 CAMBER SURFACE SLOPES FOR GIVEN PRESSURE DISTRIBUTION

Drag of cambered wings. — The pressure drag of a cambered surface is given by the double integral of the product of the surface pressure and slope, evaluated over the wing area:

$$D = -q \int_{-b/2}^{b/2} \int_{LE}^{TE} C_p \left(\frac{dz}{dx}\right) dx\, dy \tag{154}$$

In equation (137), this integral is replaced by a summation over the wing panels as follows.

$$D = -q \sum_{i=1}^{N_W} C_{p_i} \left(\frac{dz}{dx}\right)_i A_i \tag{155}$$

where the slope of each panel is defined at its control point. This formula is adequate to calculate the drag of uncambered wings, because the pressure on each panel is assumed to be constant and the surface slope is constant between control points. For cambered wings, on the other hand, the surface slope of the wing varies continuously between control points and may even approach infinity near the leading edge, as illustrated in figure 13. As a result, equation (155) will not in general yield a good approximation to the drag unless the term $(dz/dx)_i$ is replaced by the average slope of panel i.

As illustrated in figure 14, the slope of a cambered wing is approximated by a series of straight lines through the control points. The slope at any point on a given panel is estimated by a linear interpolation formula. If the panel lies along the leading edge, the slope is estimated by a linear extrapolation of the slope of the first two panels. The formulae are given below:

For leading-edge panels,

$$\left(\frac{\overline{dz}}{dx}\right)_1 = \left(\frac{dz}{dx}\right)_1 + \frac{\overline{R} - R}{1 + R\left(\frac{c_2}{c_1} - 1\right)}\left[\left(\frac{dz}{dx}\right)_2 - \left(\frac{dz}{dx}\right)_1\right] \tag{156}$$

For the remaining panels,

$$\left(\frac{\overline{dz}}{dx}\right)_i = \left(\frac{dz}{dx}\right)_i + \frac{\overline{R} - R}{1 + R\left(\frac{c_i}{c_{i-1}} - 1\right)} \cdot \frac{c_i}{c_{i-1}} \cdot \left[\left(\frac{dz}{dx}\right)_i - \left(\frac{dz}{dx}\right)_{i-1}\right] \tag{157}$$

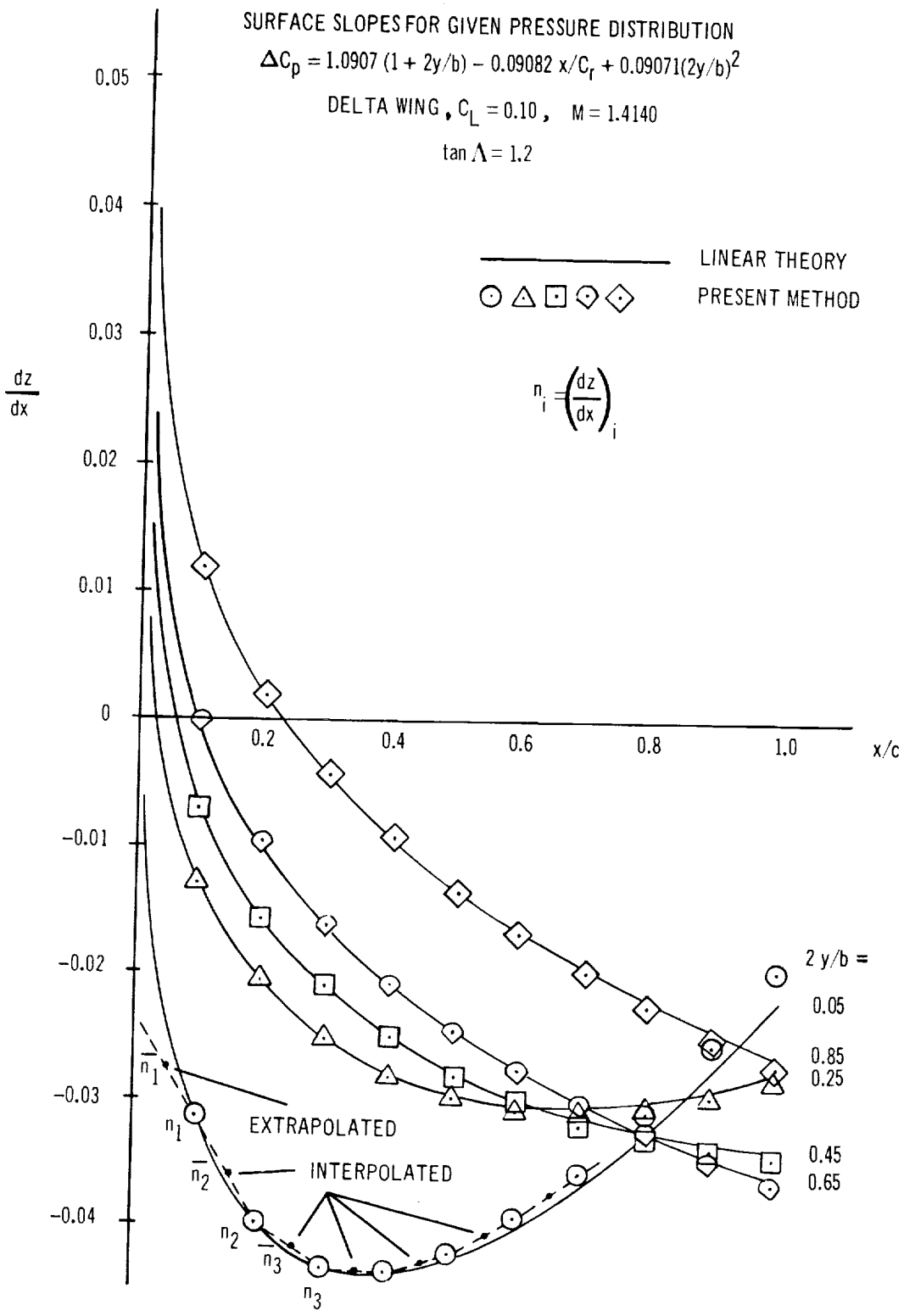

FIGURE 14 DETERMINATION OF SURFACE SLOPES FOR DRAG CALCULATION

where R is panel chord fraction defining the location of the panel control point

$\overline{R}$ is the panel chord fraction defining the average slope

c_i is the panel chord

c_{i-1} is the chord of the preceding panel

In equation (156) the subscripts 1 and 2 refer to the first and second panels along the leading edge in any given row.

The value of $\overline{R}$ has been chosen by making a comparison between the drag given by the program for a constant pressure delta wing, and the exact linear theory solution for this wing, which is:

$$C_D = \frac{\beta C_L^2}{4}\left[1 - \frac{2}{\pi}\left(b \cosh^{-1} b - \cos^{-1}\frac{1}{b} - \sqrt{b^2 - 1}\,\cosh^{-1}\frac{b^2+1}{2b}\right)\right] \quad \text{for } b = \frac{\tan\Lambda}{\beta} > 1.0$$

$$= \frac{\beta C_L^2}{4} \quad \text{for } b \leq 1.0 \qquad (158)$$

The results are presented in figure 15. It can be seen that the drag given by the program varies linearly with $\overline{R}$, and increases as the point used for defining the slope moves towards the trailing edge of the panels. For subsonic leading-edge delta wings, agreement occurs for $0.675 < \overline{R} < 0.825$, depending on the wing aspect ratio. It should be emphasized that the drag given by the program deviates very little from the exact value over the entire range of R for wings having sonic leading edges, but that the deviation increases as the sweep-back increases. Wings having supersonic leading edges showed results almost independent of the choice of $\overline{R}$.

Additional correlations of this kind are required to confirm the validity of this method for calculating the drag of cambered wings. On the basis of the present limited study, however, it was decided to use the value of $\overline{R} = 0.75$ in the program for computing the effective panel slope used in the drag calculations. This choice of $\overline{R}$ gives values of $C_D/\beta C_L^2$ which differ by less than 2 percent for wings having the lowest aspect ratios studied, and less than 1 percent for the sonic leading-edge planform.

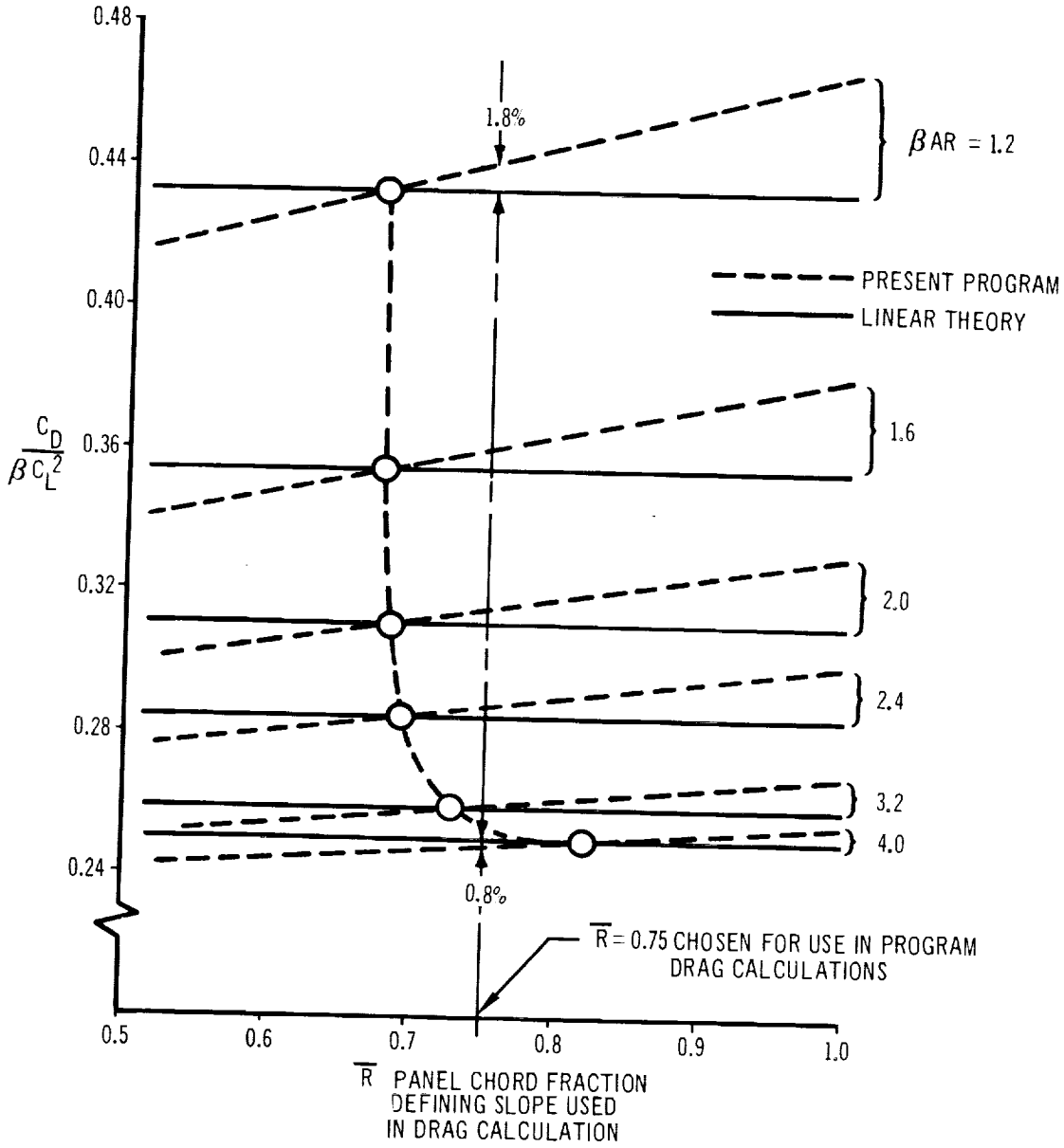

FIGURE 15 EFFECT OF SURFACE SLOPE INTERPOLATION ON DRAG OF CONSTANT PRESSURE DELTA WING

Wing camber for minimum drag. — Plots showing the minimum drag of a family of isolated delta and clipped-tip arrow wings are presented in figures 16 and 17 for comparison with data presented in reference 3. The present theory calculates the surface shape for minimum drag by first calculating the optimum pressure distribution by inverting the matrix of equation (153), and then substituting this result into equation (141) to obtain the corresponding panel slopes. Both the aerodynamic matrix and the panel slopes are calculated for control points located at 95 percent of the local panel chords, to avoid undesirable oscillations in the results. The slope interpolation formulae developed in the previous section are then applied to calculate the drag of the resulting cambered wing. The interpolated panel slope corresponding to $\bar{R} = 0.75$ was used in the drag calculations shown in the figures.

Figure 16 shows the results obtained for a family of delta wings. The minimum drag calculated by the present program is somewhat higher than that estimated by the methods of reference 3 for wings having subsonic leading edges. On the other hand, the results do agree reasonably well with the predictions of the aerodynamic influence coefficient method of reference 1. The drag predicted for the flat-plate wing without leading-edge suction agrees closely in all three methods, however.

Figure 17 shows similar results for a family of clipped-tip arrow wings. As indicated on the figure, excellent agreement is obtained between this result and the minimum drags estimated by the methods of both references 1 and 3.

It is apparent from an examination of these results that further correlations between the present theory and other known minimum drag solutions will be very desirable in order to obtain confidence in the range of application of the method. In the meantime it is sufficient to say that the method gives good agreement with other accepted procedures for determining the wing camber surface for minimum drag.

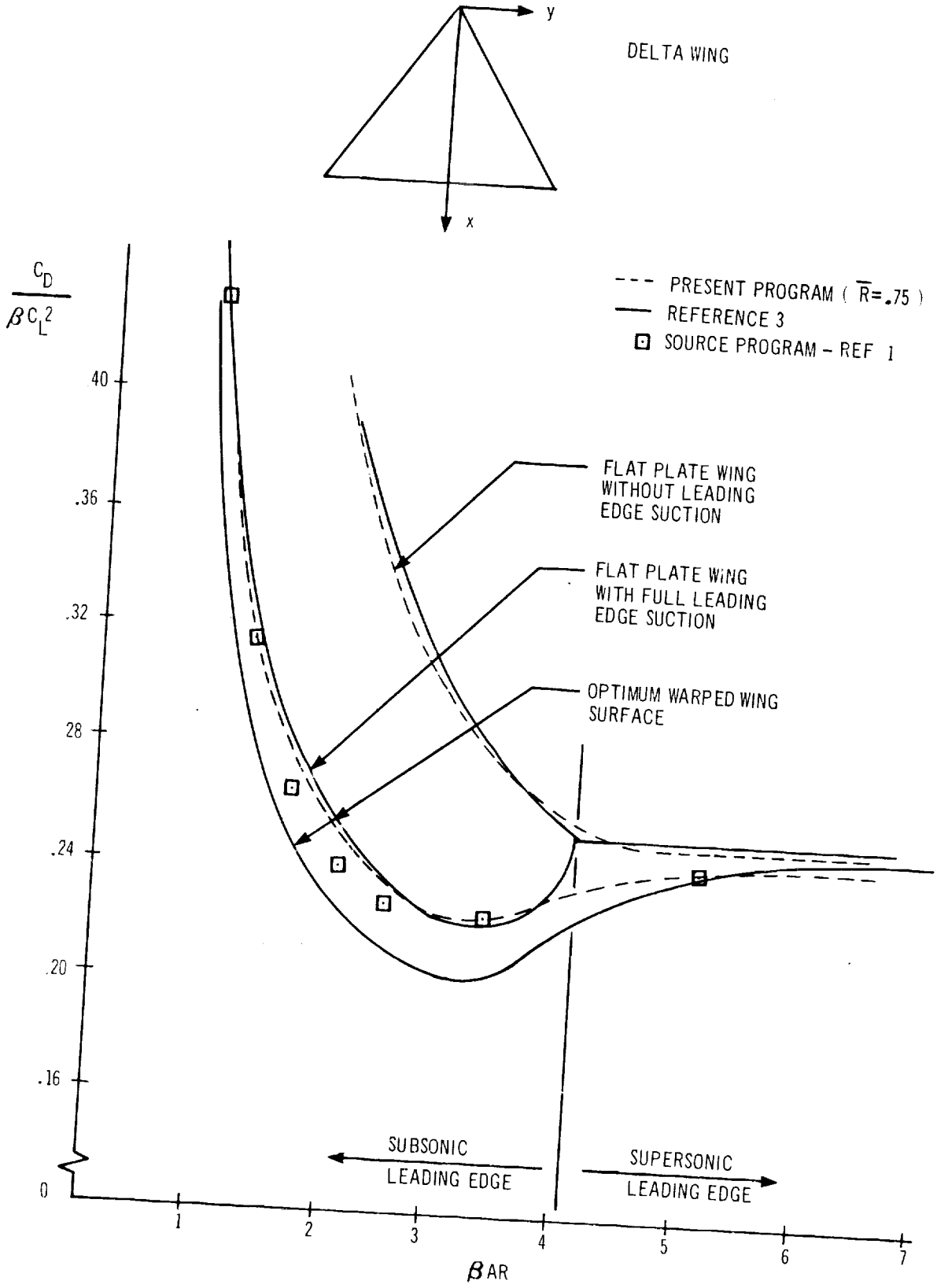

FIGURE 16 MINIMUM DRAG OF DELTA WINGS

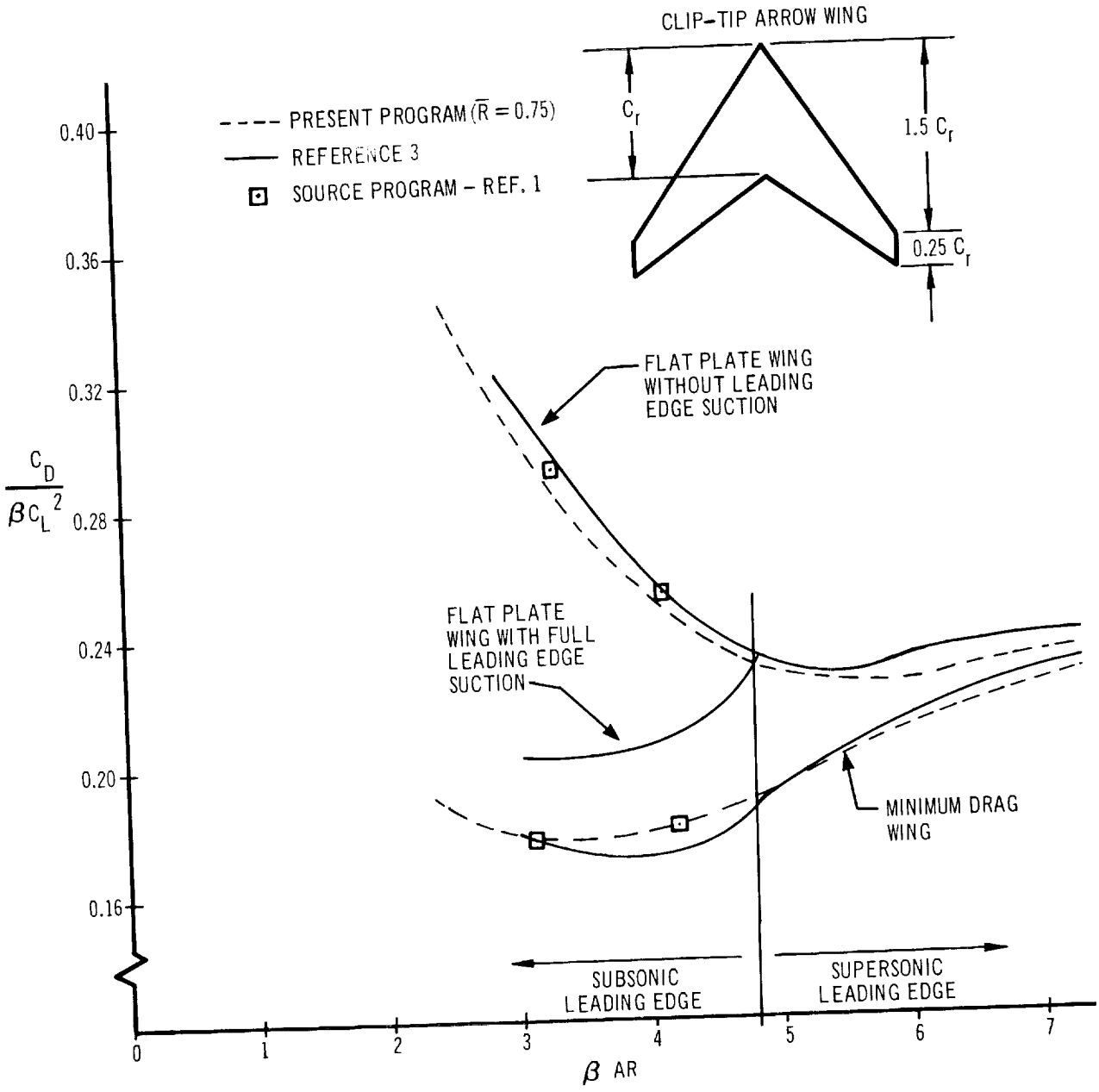

FIGURE 17 MINIMUM DRAG OF CLIPPED-TIP ARROW WINGS

Pressure distribution on a cone. —Figure 18 shows the circumferential pressure distribution at Mach 2.0 for a 10-degree circular cone at an incidence of 0.10 radian. The pressure distributions are identical for all sections along the length of the cone. The results obtained with all three pressure-coefficient formula options are given. On the basis of the nonlinear formula equation (125), the program predicts a lift coefficient only half the exact theoretical value of 0.185 given by the cone tables. Use of the linear formula equation (126), gives a better lift coefficient of 0.160, but use of the 'exact' isentropic pressure coefficient formula equation (124), gives the most accurate value, 0.183.

At zero incidence, the linear formula best approximates the exact value. The cone tables give the value $C_P = 0.104$, whereas the linear formula gives $C_P = 0.114$, the nonlinear formula $C_P = 0.087$, and the exact isentropic formula $C_P = 0.068$.

For bodies of revolution of arbitrary shape, the exact isentropic formula best approximates the experimental results at both zero incidence and zero angle of attack. Figure 34 (page 194) gives an example comparing the theoretical and experimental pressure distributions on a parabolic body of revolution.

Pressure distribution on wing-fin combination. —The pressure distributions calculated for a rectangular wing in the presence of an inclined rectangular fin are presented in figure 19, and compared with the linear theory solution given by Snow in reference 15.

The theoretical solution for the case in which the wing has an incidence α and zero fin incidence, is given below:

On the wing

$$C_p = 2\alpha \left[\frac{B}{\gamma} + \frac{2}{\pi} \tan^{-1} \frac{R^{\pi/\gamma} \sin \pi B/\gamma}{1 - R^{\pi/\gamma} \cos \pi B/\gamma} \right] \tag{159}$$

On the fin

$$C_p = 2\alpha \left[\frac{B}{\gamma} + \frac{2}{\pi} \tan^{-1} \frac{R^{\pi/\gamma} \sin \pi B/\gamma}{1 + R^{\pi/\gamma} \cos \pi B/\gamma} \right] \tag{160}$$

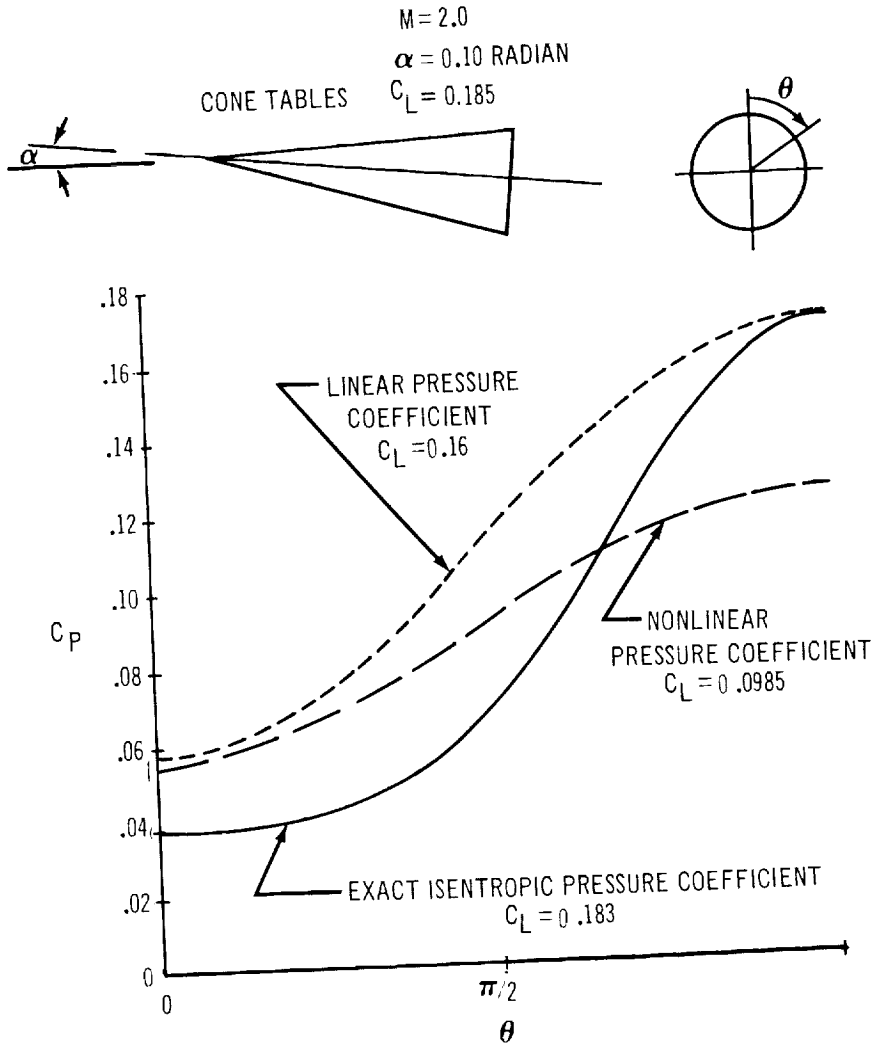

FIGURE 18 THEORETICAL PRESSURE DISTRIBUTIONS ON 10-DEGREE CONE AT INCIDENCE

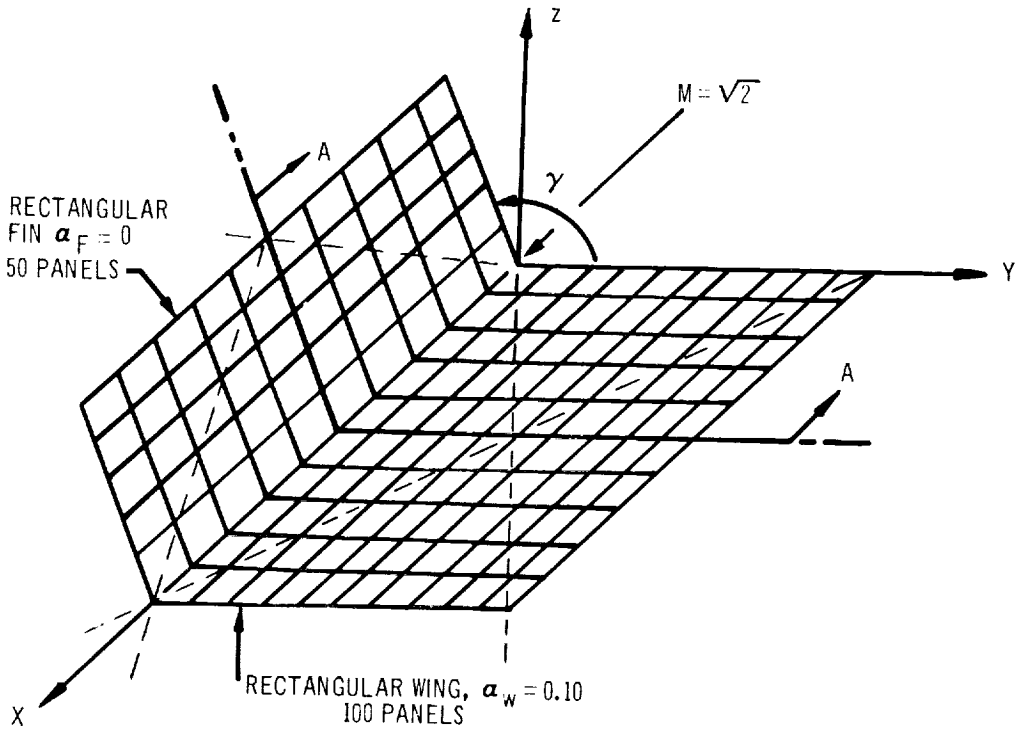

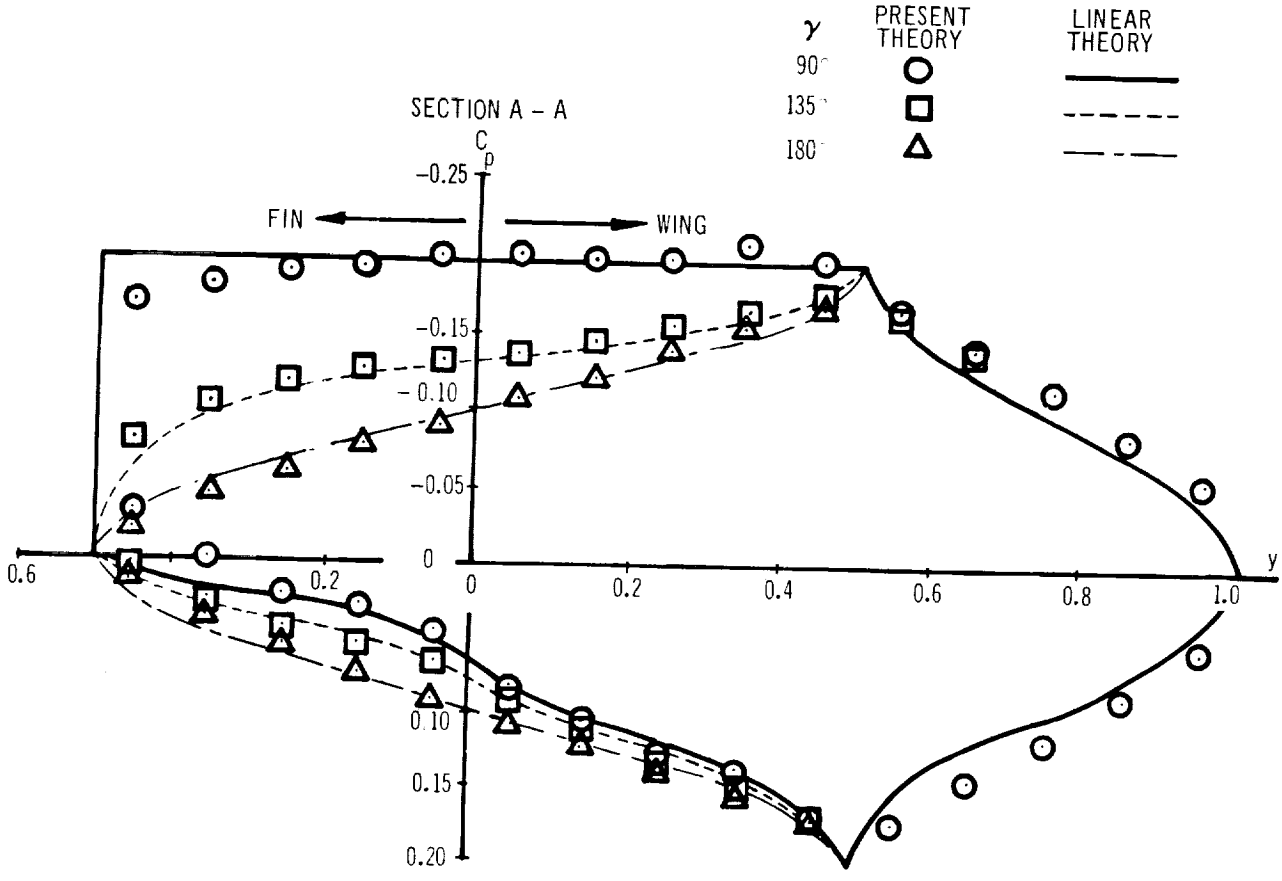

FIGURE 19 PRESSURE DISTRIBUTION ON WING-FIN COMBINATION

where $B = \cos^{-1}\left(\frac{\tan \Lambda}{\beta}\right)$

$R = \left(1 - \sqrt{1 - r^2}\right)/r$

$r = \beta \sqrt{y^2 + z^2}/x$

In the figure, the spanwise pressure distributions at the midchord are compared for three fin inclinations. The agreement is excellent.

The program, in its present form, will no longer admit cases involving wing-fin combinations as shown. This is the result of specializing the geometry definition and paneling sections of the program, which restricts its application to configurations composed of wings and circular bodies only.

Pressure distributions on wing-body combinations.—Wing and body pressure distributions calculated at Mach 1.48 for a configuration composed of an unswept rectangular wing centrally mounted on a circular body are presented in figures 39 through 42 (pages 201 through 204). The pressure distributions calculated by Nielsen (reference 16) are presented in terms of an incremental pressure coefficient P, obtained by taking the difference between the local pressure coefficients for the lifting case and the non-lifting case ($\alpha_W = \alpha_B = 0$). In this way, the effect of the nose shape on pressure distributions is eliminated. It should be remarked that the present theory calculates the surface pressure distributions including the effect of the nose shape; consequently, the results presented are the difference between two calculations. The incremental pressure coefficients calculated on the wing and body agree favorably with Nielsen's theoretical results, both for wing only at incidence and for the case in which both wing and body are at incidence.

Figure 20 shows the pressure distributions calculated for a rectangular wing-rectangular body combination analyzed by Lu Ting in reference 17. The calculated pressure coefficients oscillate above and below the theoretical results published by Lu Ting, particularly in the area of the wing-body intersection. The reason for this oscillatory behavior is not known at present, although an instability inherent in the numerical analysis is suspected. It is interesting to note that similar instabilities did not occur for the polygonal bodies used to approximate bodies of revolution in the other examples presented in this report.

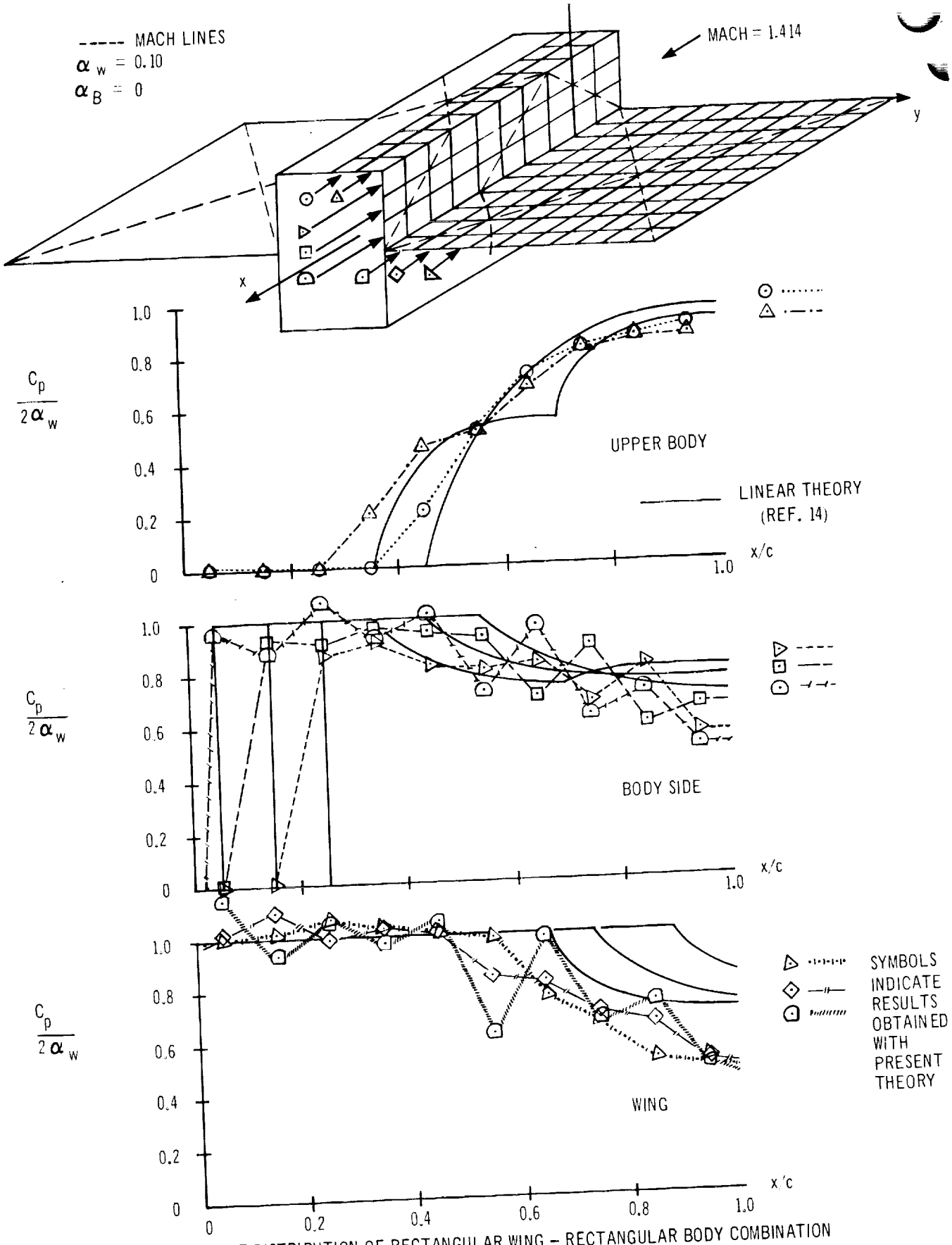

FIGURE 20 PRESSURE DISTRIBUTION OF RECTANGULAR WING – RECTANGULAR BODY COMBINATION

4.8 Calculation of Field Velocity Components and Streamlines

The method of aerodynamic influence coefficients is also applicable to the calculation of field velocity components and streamlines. The perturbation velocities in the field may be expressed as a sum of the products of elementary velocity components and their appropriate singularity strengths. These perturbation velocities will be valid to first order.

Local flow directions, pressure distributions, and streamlines in the field can be calculated from the perturbation velocities. However, the resulting flow field will not be uniformly valid to first order. This is because linearized supersonic theory, upon which the solution is based, postulates that the flow disturbances will be propagated along the undisturbed or zero-order Mach lines, rather than the curved first-order Mach lines.

Velocity perturbations in the field.—The flow-field solution depends on a valid body solution; the strengths of all the singularities and their locations, which make up the wing-body solution, must be known. These may be found by solving the 'direct' or 'inverse' problems outlined in section 4.6. The perturbation velocities at point P_n in the field are the sum of the products of all the elemental velocity components and their respective singularity strengths. Only the singularities that lie inside the Mach cone facing forward from the point in question will influence that point, as shown in the sketch below.

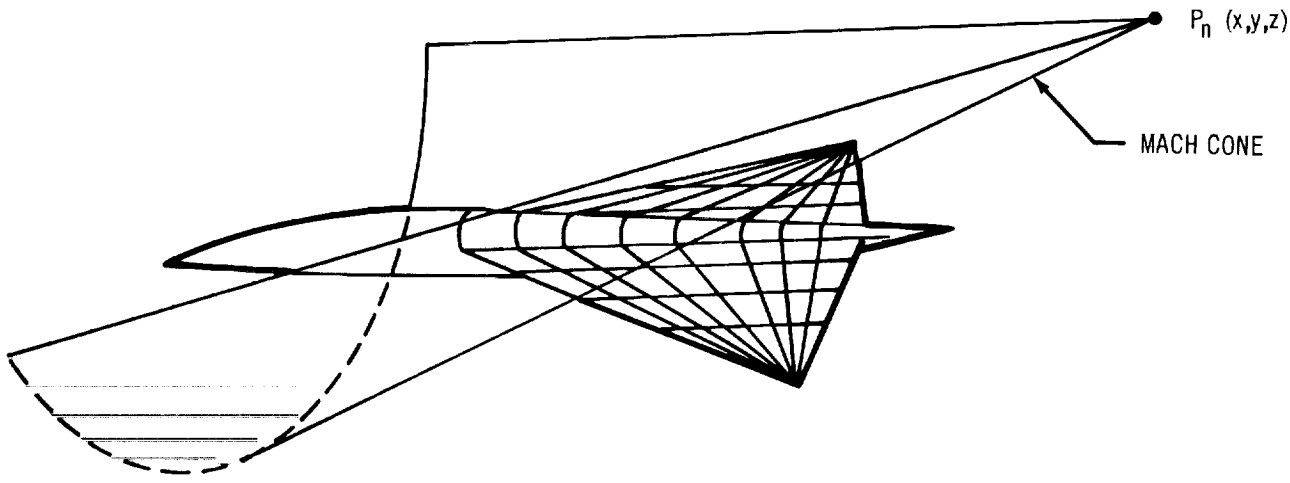

Equations (61), (62), (70), and (72) and Appendix B give expressions for the elemental velocity components (for wing and body panels) of the singularities that lie in the forward-facing Mach cone with apex on field point P_n. These are the same elemental components as in the wing-body solution, except that the coordinates apply to the field point in question instead of a given control point. The elemental velocity components for the singularities outside the forward-facing Mach cone are identically zero.

The resulting perturbation velocities at point P_n are:

$$u_n = u_{BS1_{n1}} T_{S1} + \sum_{j=1}^{K} u_{BS2_{nj}} T_{S2_j} + u_{BD1_{n1}} T_{D1} + \sum_{j=1}^{K} u_{BD2_{nj}} T_{D2_j} + \sum_{j=1}^{N_T} u_{WS_{nj}} \alpha_{T_j} + \sum_{j=1}^{N_w} u_{WV_{nj}} P_{W_j} + \sum_{j=1}^{N_B} u_{BV_{nj}} P_{Bj}$$

$$v_n = v_{BS1_{n1}} T_{S1} + \sum_{j=1}^{K} v_{BS2_{nj}} T_{S2_j} + v_{BD1_{n1}} T_{D1} + \sum_{j=1}^{K} v_{BD2_{jn}} T_{D2_j} + \sum_{j=1}^{N_T} v_{WS_{nj}} \alpha_{T_j} + \sum_{j=1}^{N_w} v_{WV_{nj}} P_{wj} + \sum_{j=1}^{N_B} v_{BV_{nj}} P_{B_j}$$

$$w_n = w_{BS1_{n1}} T_{S1} + \sum_{j=1}^{K} w_{BS2_{nj}} T_{S2_j} + w_{BD1_{n1}} T_{D1} + \sum_{j=1}^{K} w_{BD2_{nj}} T_{D2_j} + \sum_{j=1}^{N_T} W_{WS_{nj}} \alpha_{T_j} + \sum_{j=1}^{N_w} w_{WV_{nj}} P_{W1} + \sum_{j=1}^{N_B} w_{BV_{nj}} P_{B_j} \quad (161)$$

Local flow directions and pressures. — The total nondimensional velocity at a point is given by the vector sum of its velocity components:

$$\vec{V} = \vec{u} + \vec{v} + \vec{w} \tag{162}$$

where

$$\vec{u} = (u + \cos\alpha)\,\vec{i}$$

$$\vec{v} = v\,\vec{j}$$

$$\vec{w} = (w + \sin\alpha)\,\vec{k}$$

$\vec{i}, \vec{j}, \vec{k}$ are unit vectors along the transformed body coordinate axis.

The velocity vector components fully define the flow direction in the field. The pressure coefficient in the field is given by the same formulas used on the wing-body, equations (124), (125), and (126). The computer program is designed to allow use of any of the three formulas in calculating the pressure distributions. To aid the user, the program includes a method to generate two- and three-dimensional grids in the field; velocities and pressures will be calculated at the corner points of these grids. This method is described in section 5.2.

Streamline calculations. —The contour of a streamline in the flow field about some wing-body configuration is obtained by finding the coordinates of a series of points on the streamline. Beginning with an initial point (x_0, y_0, z_0) through which the desired streamline is to pass, the coordinates (x, y, z) of any other point on the streamline may be found as

$$x = x_0 + \int_{s_0}^{s_0 + \Delta s} \frac{|\tilde{u}|}{\sqrt{|\tilde{u}|^2 + |\tilde{v}|^2 + |\tilde{w}|^2}}\, ds$$

$$y = y_0 + \int_{s_0}^{s_0 + \Delta s} \frac{|\tilde{v}|}{\sqrt{|\tilde{u}|^2 + |\tilde{v}|^2 + |\tilde{w}|^2}}\, ds$$

$$z = z_0 + \int_{s_0}^{s_0 + \Delta s} \frac{|\tilde{w}|}{\sqrt{|\tilde{u}|^2 + |\tilde{v}|^2 + |\tilde{w}|^2}}\, ds \tag{163}$$

where Δs is the distance along the streamline between (x_0, y_0, z_0) and (x, y, z), and $s_0 = s_0(x_0, y_0, z_0)$.

These equations may be solved numerically by a digital computer using the Adams-Moulten variable-step-size method. This is a predictor-corrector method. The equations must be in the form $Y_{n_x} = f_{n_x}(s, Y_1, Y_2, Y_3 \cdots Y_n)$ and are given as

$$\frac{dx}{ds} = \frac{|\vec{u}|}{\frac{ds}{dt}}$$

$$\frac{dy}{ds} = \frac{|\vec{v}|}{\frac{ds}{dt}}$$

$$\frac{dz}{ds} = \frac{|\vec{w}|}{\frac{ds}{dt}} \qquad (164)$$

where $$\frac{ds}{dt} = \sqrt{|\vec{u}|^2 + |\vec{v}|^2 + |\vec{w}|^2}$$

This method can be used to calculate the contour of a streamline by proceeding step by step upstream or downstream from an initial point.

Flow field about a parabolic spindle. —Figure 21 shows pressure distributions and streamlines about a body of revolution of parabolic profile. The upper half of the figure shows several stream tubes enclosing the body. Comparison of the cross-sectional areas of the stream tubes ahead of the body and at one body length behind the body shows the areas to be nearly equal. This is consistent with the one-dimensional continuity equation and indicates the good agreement between the calculated stream tube and theory.

The lower half of figure 21 shows the pressure distributions on the body surface and at several radii away from the body. The pressure distributions agree well with those given by other methods. However, the location of the pressure distributions in the field are valid only to zero order and do not reflect any Mach-line curvature effects.

Flow field about a lifting arrow wing. —The flow field behind a lifting arrow wing (Carlson wing, reference 18) was calculated by using the grid interrogation technique. The interrogation grid was placed behind the wingtip and aligned normal to the flow. Figure 22 shows the flow field calculated. The circular

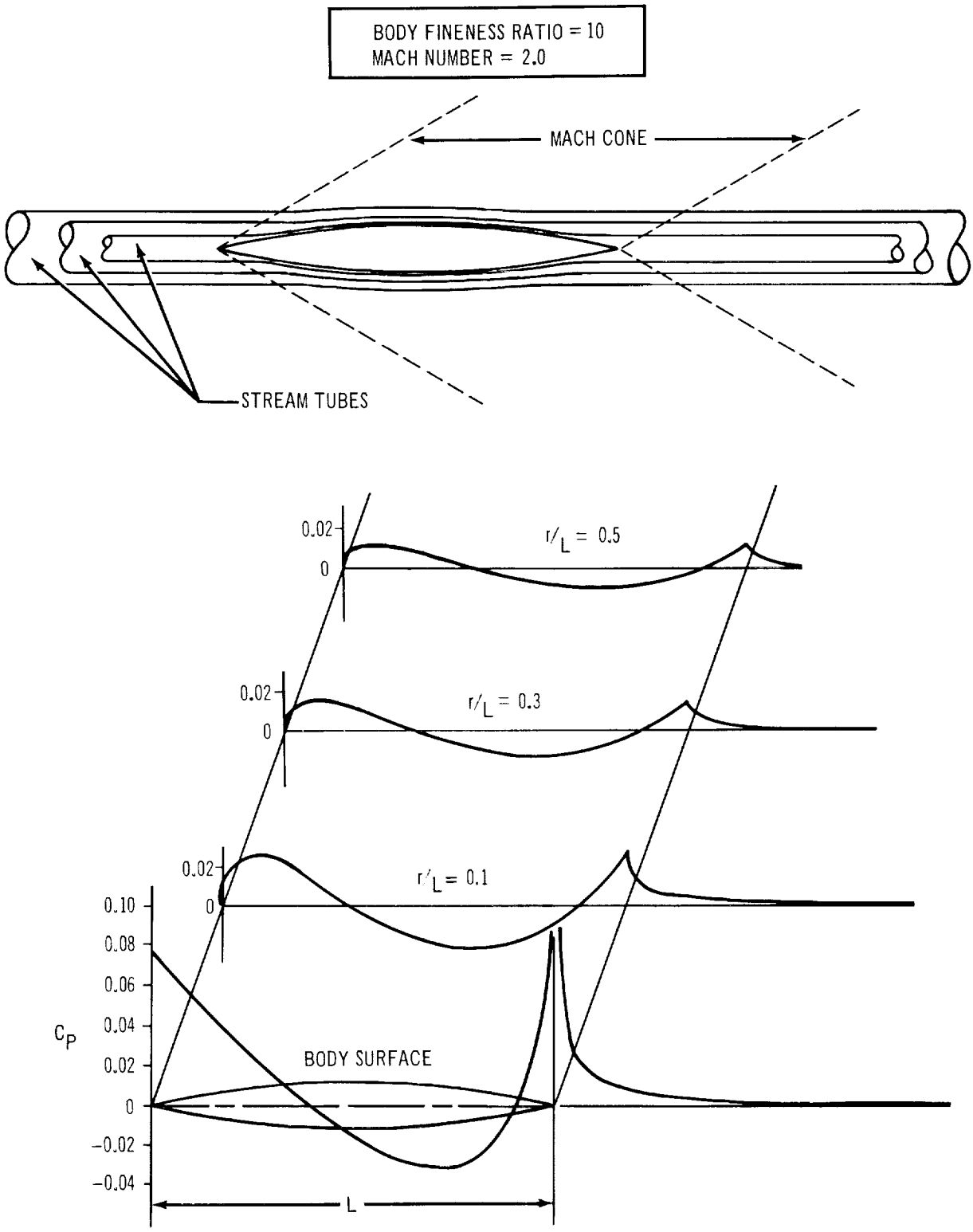

FIGURE 21 STREAM TUBES AND PRESSURE DISTRIBUTION ABOUT A PARABOLIC BODY OF REVOLUTION

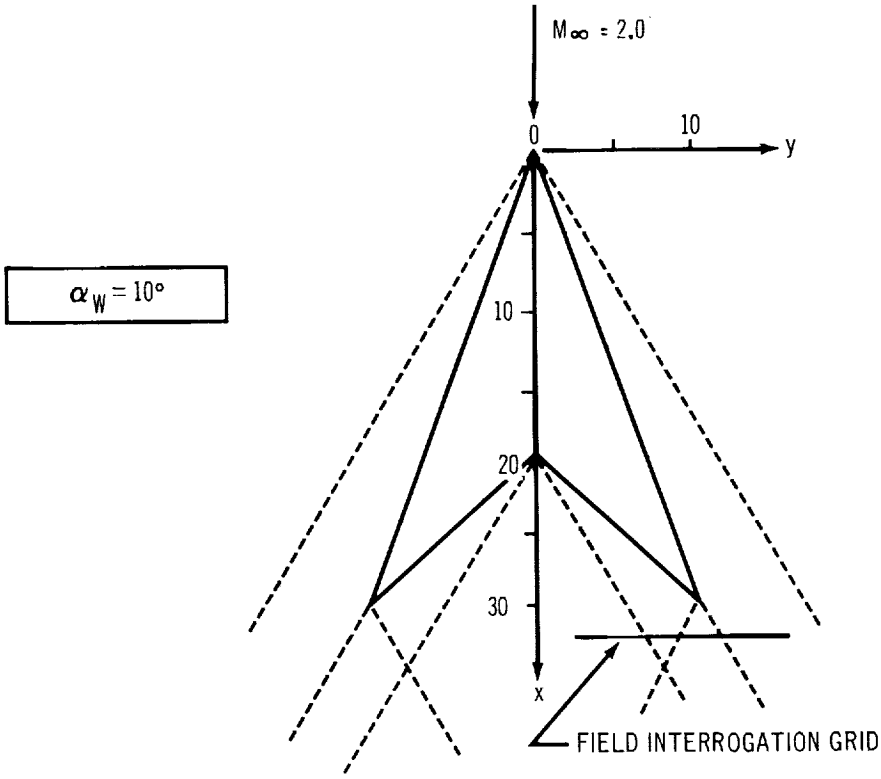

VELOCITY VECTORS IN z – y PLANE

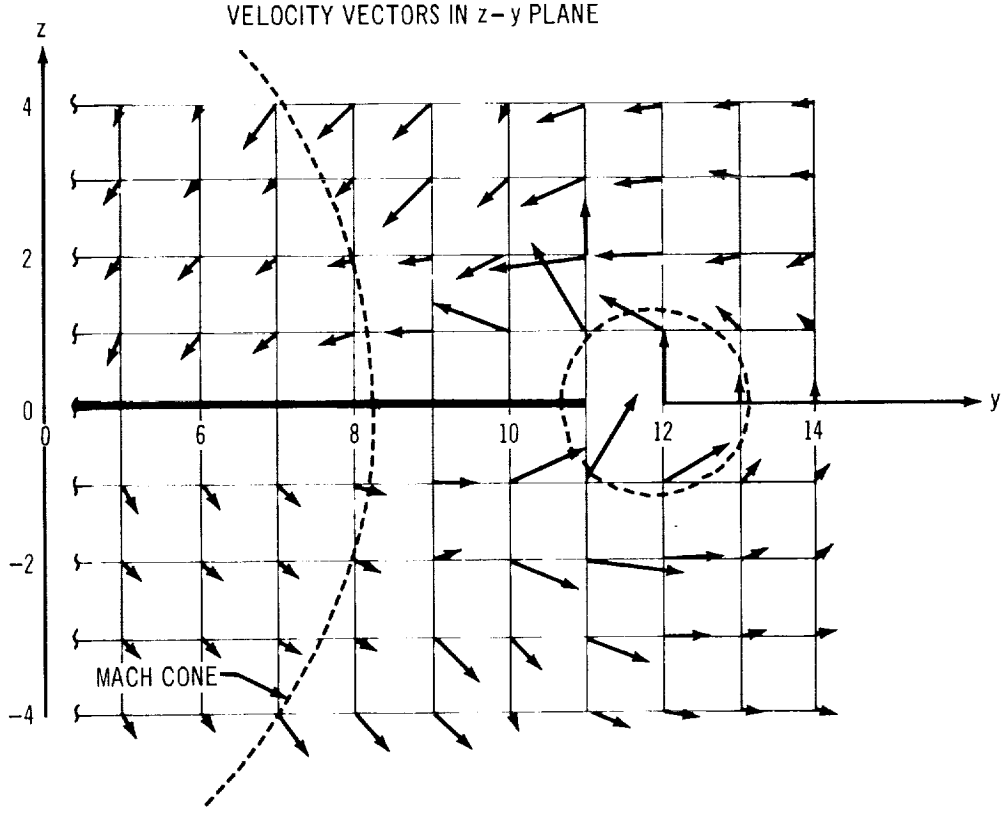

FIGURE 22 FLOW BEHIND A LIFTING ARROW WING

motion typical of the shed vortex behind the wing is clearly evident. Also evident is the antisymmetric character of the flow, predicted by linear theory.

The flow in this region is characterized by the separate zones of influence defined by the Mach cones from the nose and tail apexes and the wingtip. Some of the fluctuations in the spanwise distribution of downwash may be explained by the theory, which allows concentrated vortices to be shed from the streamwise edges of the wing panels. These vortices are shed along panel edges interior to the wingtip whenever the spanwise load is not constant.

Flow field about a wing-body combination. —Figures 23, 24, and 25 show flow field calculations for a wing-body combination at Mach 1.8 and 6-degree angle of attack. The configuration, fully described in section 6.4, has a constant chord swept wing, and cylindrical body.

The grid interrogation technique was used to calculate the field between the body and the wing's trailing edge. The grid was placed parallel to the flow in a region where a horizontal tailplane might be located; figure 23 shows the calculated downwash distributions. The downwash variation both spanwise and chordwise could affect the design of a tailplane in this region.

Streamline calculations (figure 24) show some typical characteristics. Streamlines like number 1, which pass over a lifting sweptback wing, tend to curve inward toward the root. Those like number 2, which pass under a lifting sweptback wing, are deflected toward the wingtip. Streamline 3 shows the effect of closeness to the body; as it passes over the wing, the body constrains its inward curve.

The portion of a streamline that passes through the wing chord plane aft of the wing's leading edge should be discounted. The wing chord plane in that area represents a discontinuity in the field and accounts for the field's anti-symmetric character. In linear theory, this discontinuous plane represents the shed vortex sheet from the wing. Crossing of this sheet by the streamlines indicates that the sheet is not properly positioned in the field; but linear theory does not allow for the proper wake position.

Perturbation velocity components were also calculated around an inlet ring directly beneath the wing; figure 25 shows the flow directions around this ring. These directions give a good approximation of the flow angularity in this region, which must be known to design the inlet properly.

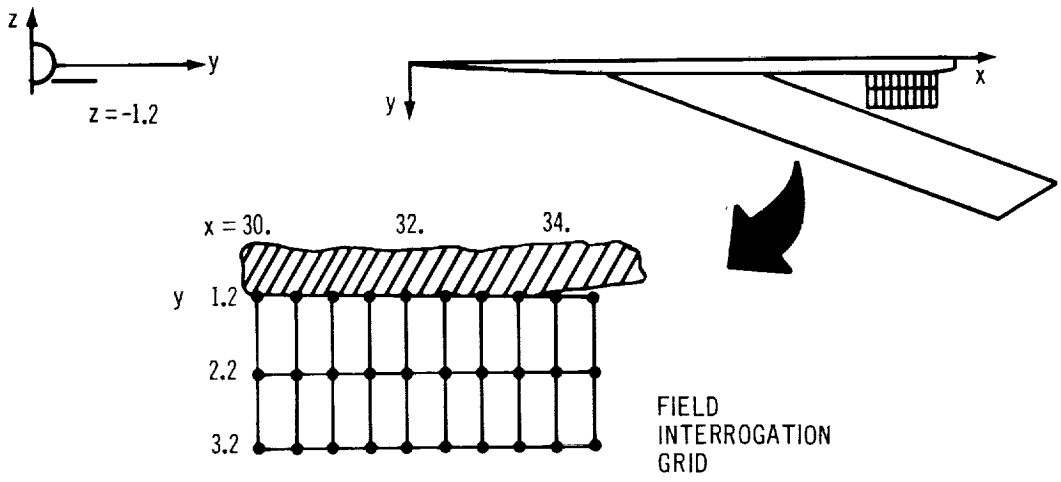

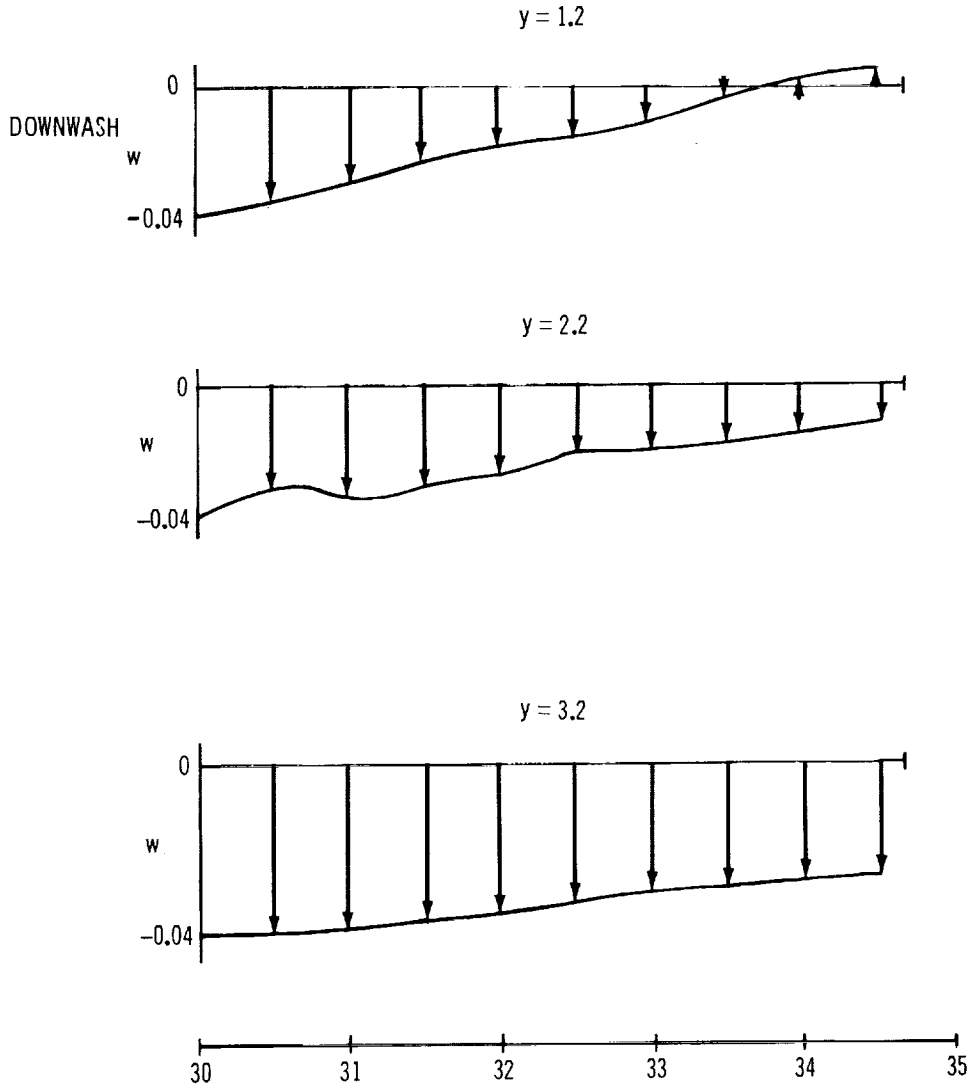

FIGURE 23 DOWNWASH ON A TAILPLANE LOCATION

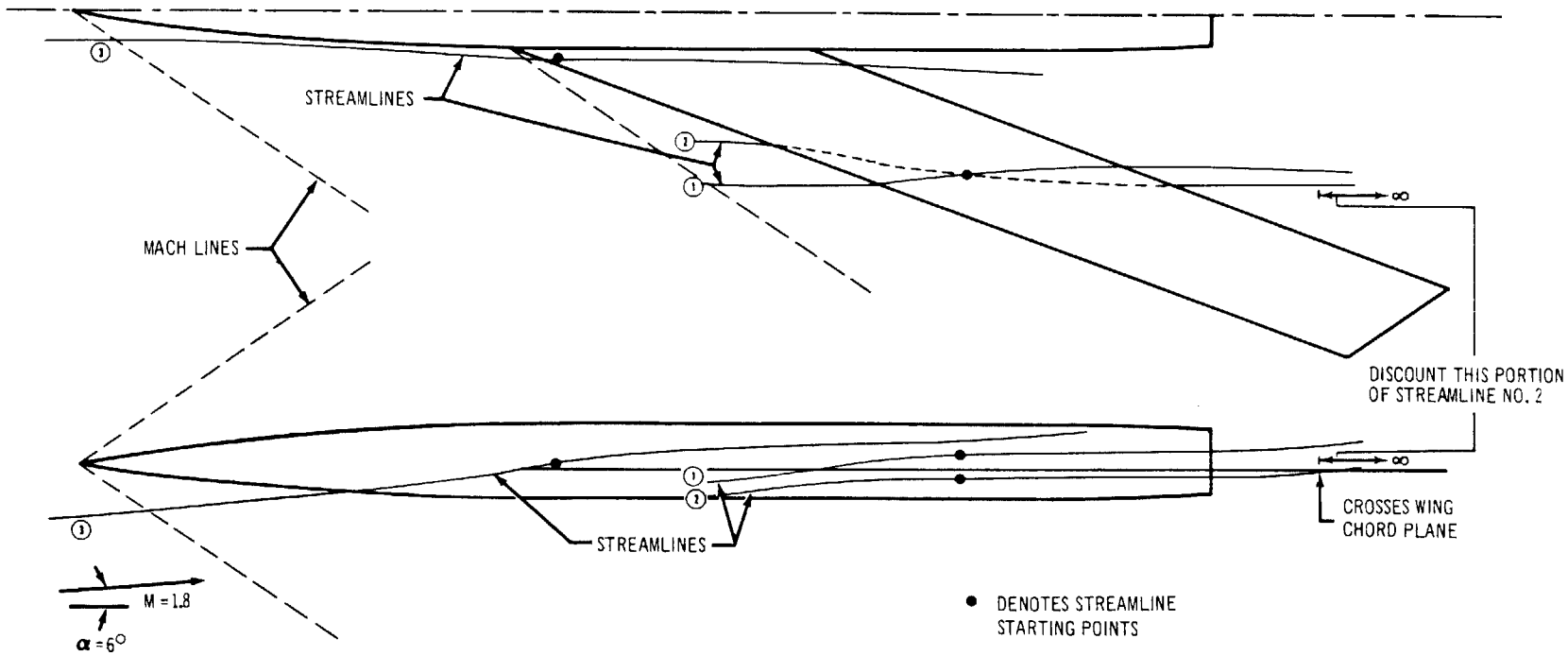

FIGURE 24 STREAMLINES ABOUT BOEING WING-BODY COMBINATION

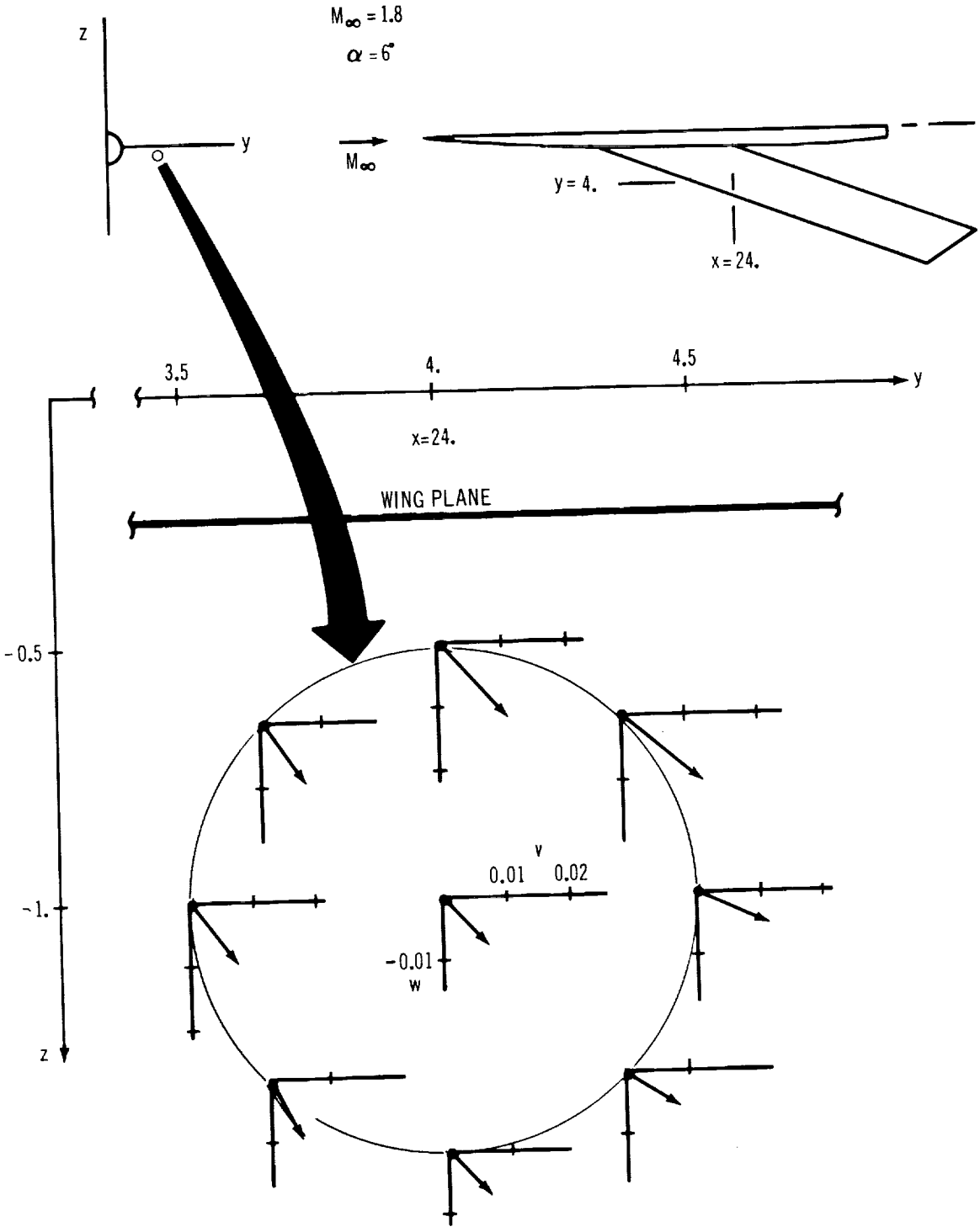

FIGURE 25 FLOW DIRECTIONS AROUND AN INLET RING

The grid interrogation technique was also used to calculate pressure distributions parallel to the body axis at three angular positions (θ = 0° , 90° , and 180°). These one-dimensional interrogation lines are located at a radius of one body length. The calculated pressure distributions (figure 26) show two distinct characteristics. One, the pressure distributions change greatly with changes in angular position. This is primarily due to the change of influence of each singularity with changes in angular position, particularly for those singularities associated with the lifting effects. Two, the pressure distributions at each position are somewhat irregular or bumpy. This is due to the limited number of singularities used to describe the wing-body configuration and their spacial distribution.

Figure 27 shows the contributions of the various types of singularities in making up the pressure distribution along a given interrogation line. The contributions are relatively smooth in themselves, but may combine in such a way that the resultant pressure distribution is not smooth. Since all disturbances propagate along straight Mach lines, there can be no coalescence of Mach waves. The pressure distributions are calculated in the near field and do not necessarily represent the asymptotic values in the far field. It would be of interest to compare these or similar distributions with those given by sonic boom theory for an equivalent distribution of singularities along the body axis.

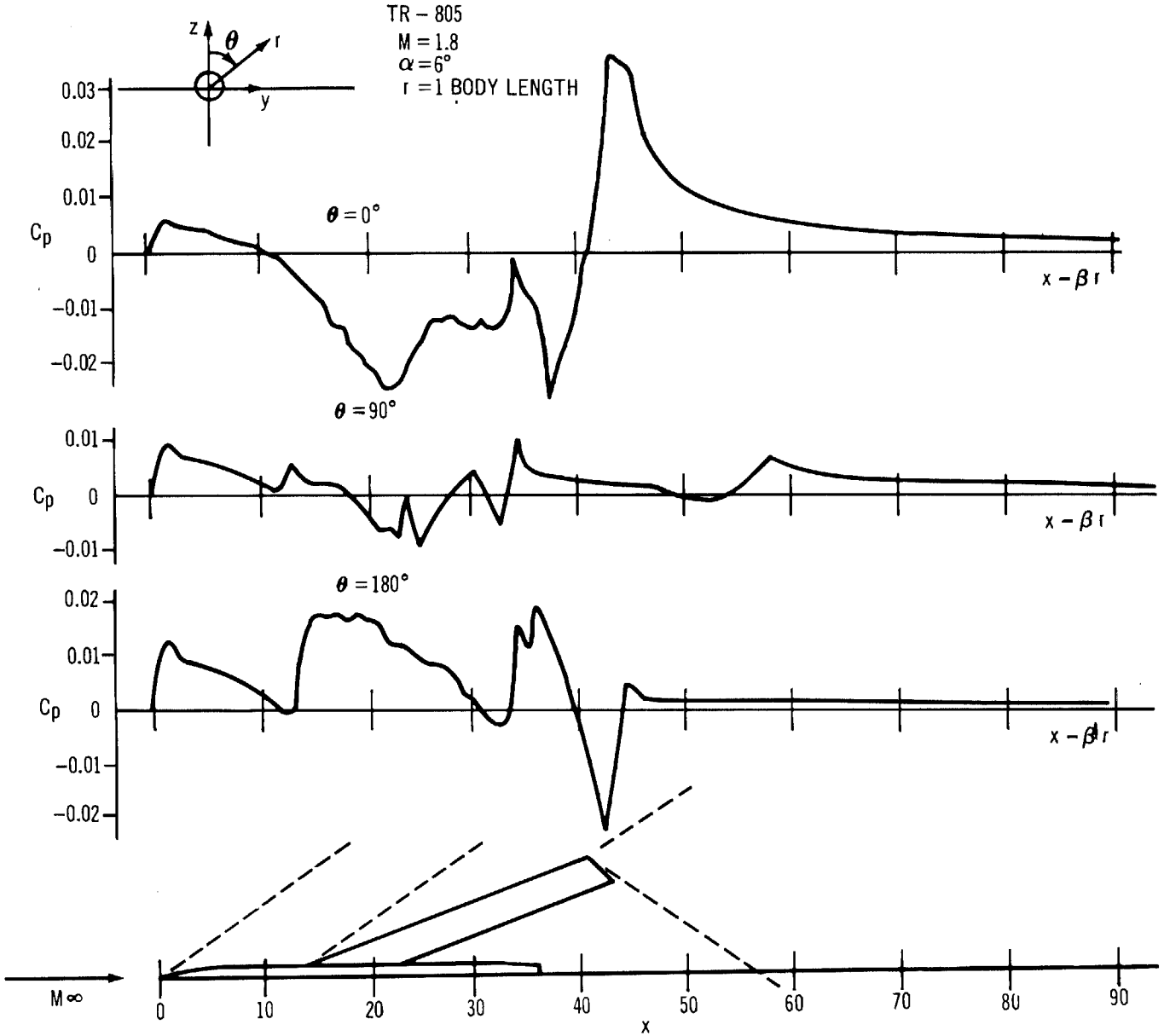

FIGURE 26 NEAR FIELD PRESSURE DISTRIBUTIONS

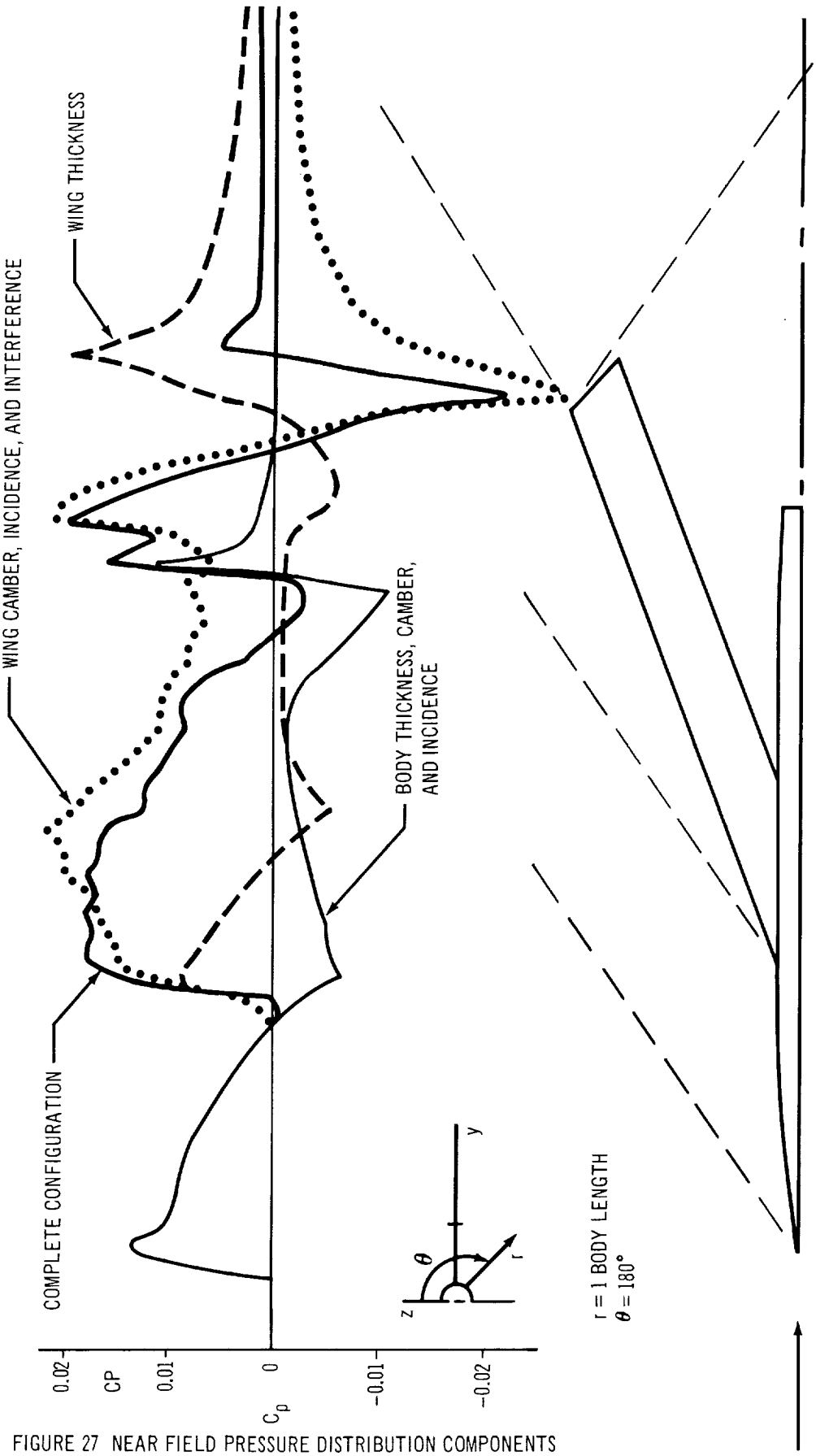

FIGURE 27 NEAR FIELD PRESSURE DISTRIBUTION COMPONENTS

5. COMPUTER PROGRAM

5.1 Description

The digital computer program described in this section has been developed to solve the problem of optimization of wing camber surfaces for wing-body combinations at supersonic speeds. It can also solve direct and other indirect aerodynamic problems.

The program is coded in FORTRAN IV and MAP languages for the IBM 7090/7094 (32K) digital computer under the Systems Monitor, IBSYS Version 13. It is compatible with the NASA-Ames direct-coupled IBM 7040/7094 computer system. Because the program exceeds the capacity of a single core load, the Loader Overlay feature is used to allow the complete program to be subdivided into smaller segments or links. The links are processed in a specific order to solve a particular problem.

The Overlay feature uses one system unit as the input-output tape on which the overlay links are written. Besides the input-output tape, the program uses seven tape units for scratch purposes. The choice of units to be used depends on the particular computer installation; tapes must be changed as needed. A special subroutine, OPCAMI, initializes all the tape units and assigns a logical number to each. Tape changes are made by merely changing the logical designations in this subroutine (see Part II).

The complete program consists of five sections: Geometry Definition, Geometry Transformation, Geometry Paneling, Aerodynamic Calculations, and Flow Visualization (see flow chart, figure 28). The first two sections provide a suitable geometric description of the configuration, and the third section subdivides the configuration into panels. The fourth section performs all aerodynamic calculations and solves the problem. The Flow Visualization section computes velocities at points in the field and constructs streamlines about the configuration.

Program execution is controlled by the subroutine OPCAM, a control program located in link 0 under the Overlay structure. Those control cards within the data deck that determine which program sections are used to process the case are read by the subroutine OPCAM and lower-level subroutines in five program sections:

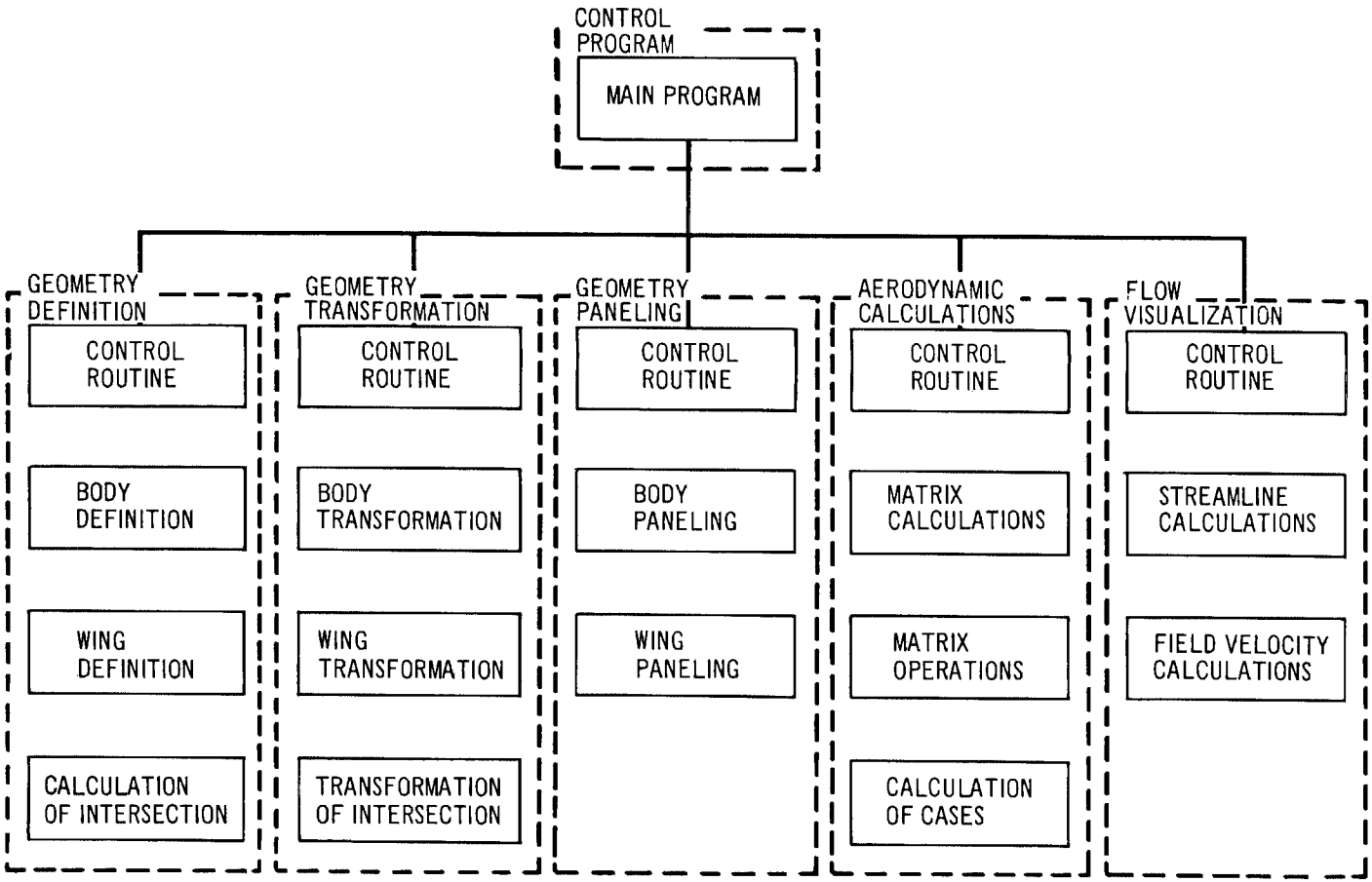

FIGURE 28 PROGRAM FLOW CHART

1. GEOMD in link 5 (Geometry Definition)
2. TFLAT in link 11 (Geometry Transformation)
3. PANEL in link 12 (Geometry Paneling)
4. AERO in link 20 (Aerodynamic Calculations)
5. FLOVIZ in link 38 (Flow Visualization)

Multiple cases, each involving a different wing-body configuration, can be run. When a nonsystems error occurs during processing within a section of the program, an error message appears. Execution of the case is terminated, a partial data printout is given, and the next case is processed.

Execution time averages 10 minutes for a typical (100 panels) body-alone or wing-alone case and 20 to 25 minutes for a wing-body combination of 200 panels. The computer time and number of printout lines for a single configuration can be estimated from the following equations based on experience with an IBM 7094/M2.

Time (minutes) $= 2.5 + 0.3G + (4. \times 10^{-4} \times P^2) \times A + 0.6C + 0.1F$

where G indicates type of paneling:

= 0., no paneling

= 1., wing paneling only

= 2., wing and body paneling

P is number of panels (if no paneling is required, use P=10)

A indicates aerodynamic calculations:

= 0., no aerodynamic calculations

= 1., aerodynamic calculations requested

C is number of aerodynamic cases. Each of the following is a case:

Wing optimization case

Direct aerodynamic case

Indirect aerodynamic case

Each angle of a polar series

F is the total number of field points, grid points, and streamline points required for flow-visualization calculations.

$$\text{Output (lines)} = 100 + \left[500 + (10 \times P^{\frac{1}{2}}) \times V \times C\right] \times T + F$$

where V indicates velocity component printout:

= 1., no velocity component printout

= 2., velocity components requested

T indicates type of case:

= 1., wing-alone case

= 2., body-alone case

= 3., wing-body case

5.2 Program Usage

The computer program solves a problem in four steps. In the first step, the configuration geometry (wing alone, body alone, or wing-body combination) is defined and transformed to a more convenient representation. In the second step, the configuration is paneled and required geometric data are calculated. Figure 29 illustrates the definition and paneling sequence.

Some paneling information is input to the definition part of the program. For example, the body meridian lines that define the body for a wing-body combination also determine the streamwise edges of the body panels. Likewise, some information can be input to the paneling part of the program to help complete the definition. For example, to obtain desired wing-tip geometry, a paneling input can be used to truncate the wing inboard of the tip-defining chord.

The third step performs the aerodynamic calculations (coefficients of lift, drag, moment and pressure) for each case requested. The fourth step performs the flow visualization calculations (field pressure coefficients, velocity components, and streamlines); this step is optional.

The following subsections discuss problem solving for body-alone, wing-alone, and wing-body cases. The discussions include recommended methods for inputting problems to the program. These recommendations will almost always yield reasonable aerodynamic results, and are a good beginning for exploring the program's capabilities. They are summarized at the end of this section (page 144).

Body alone. - For the body-alone case, no paneling is done. The entire body is represented as an equivalent body of circular cross section by a series of equally spaced line sources and doublets. The user may define a

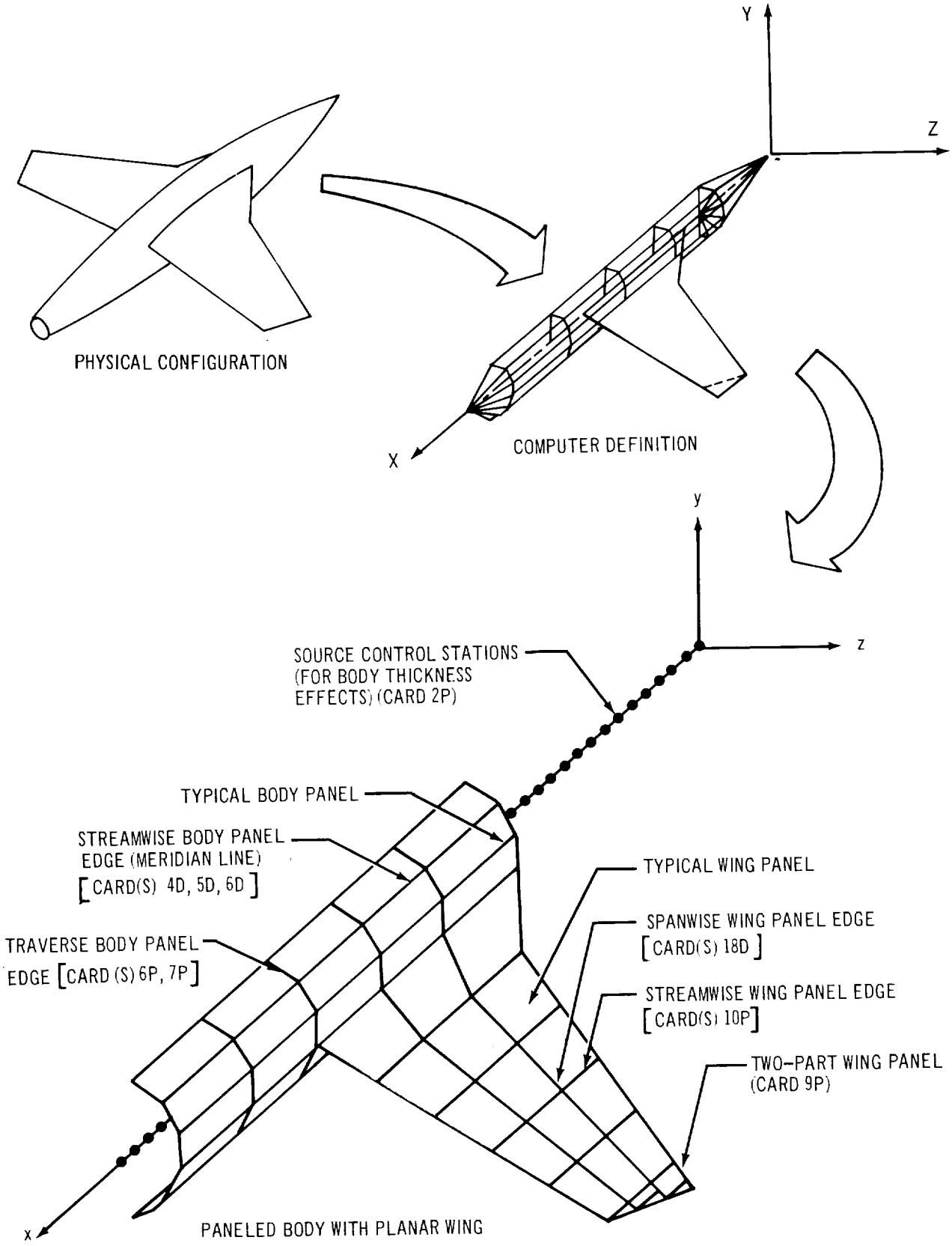

FIGURE 29 PANELING: NOMENCLATURE, DEFINITION, AND SEQUENCE

cambered body with arbitrary cross section and have the program determine the equivalent body of revolution; or an equivalent body may be input with its thickness and camber specified separately in the aerodynamic section. (See the data input formats, section 5.3.)

Boundary conditions for the analysis are satisfied not on the input body surface, but on the surface of an equivalent body of revolution with a straight axis. Body camber and angle of attack are simulated by an equivalent cross-flow imposed by the line doublets. The equivalent body's x-axis stations and the corresponding camber and radii values are printed out at the beginning of the aerodynamic section's output (see Appendix C). It is this information that is used by the aerodynamic section in its analysis.

The user specifies the body by a number of X-stations at which an array of radii (ρ) and angles (θ) are given. A maximum of 50 body stations may be specified (Card 4D).* The program assumes that all bodies are symmetrical about the vertical plane. Therefore, only data for half-bodies is specified; that is, 0 degrees $\leq \theta \leq$ 180 degrees where the top meridian line corresponds to $\theta = 0$ degrees and the bottom meridian line corresponds to $\theta = 180$ degrees. Alternate techniques for specifying body stations are presented in the discussion of card input format, section 5.3.

A "body definition" axis is set parallel to the computer-reference x-axis by specifying a (y, z) coordinate pair through which it must pass. Points from which the $\rho - \theta$ arrays generate body sections are specified in relation to this body definition axis at each defining station [Card(s) 5D for SCODE = 1., 2., or 3.]. At least seven theta values should be specified (BTHETA $\geq$ 7., Card 4D), and these values should provide even circumferential spacing of the meridian lines.

---

*Input data cards noted in parentheses in this section are explained in section 5.3, page 146.

After the $\rho - \theta$ array is computed, the program constructs longitudinal meridian lines through sets of radii end points. The resulting computer definition looks like this:

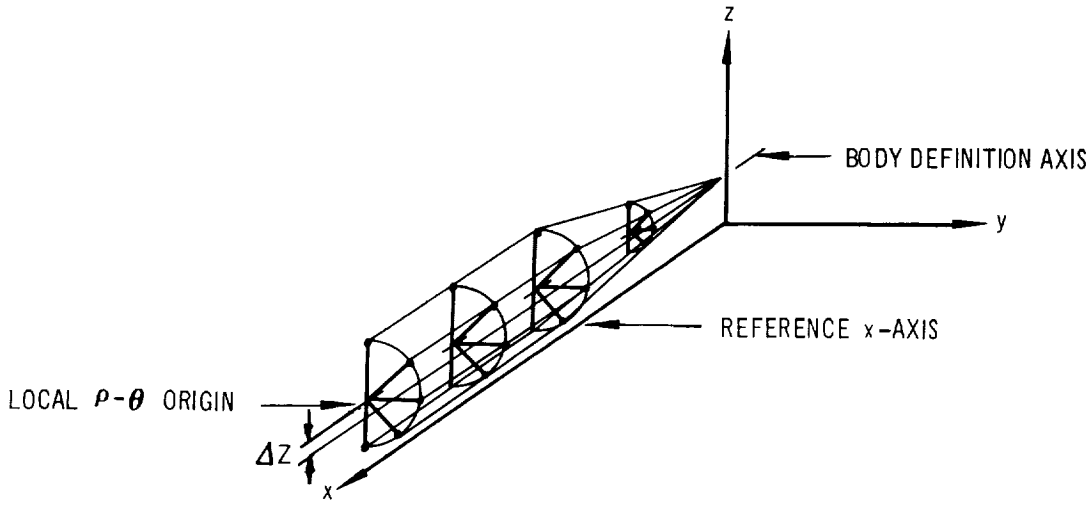

The program then locates the cross-section centroids of the aft body station and the forward body station. The section area and centroid depend on the interpolation chosen to define the fairing between the given points. Linear interpolation produces a polygonal area; biquadratic interpolation forms a partly curved figure, as shown in the following sketch.

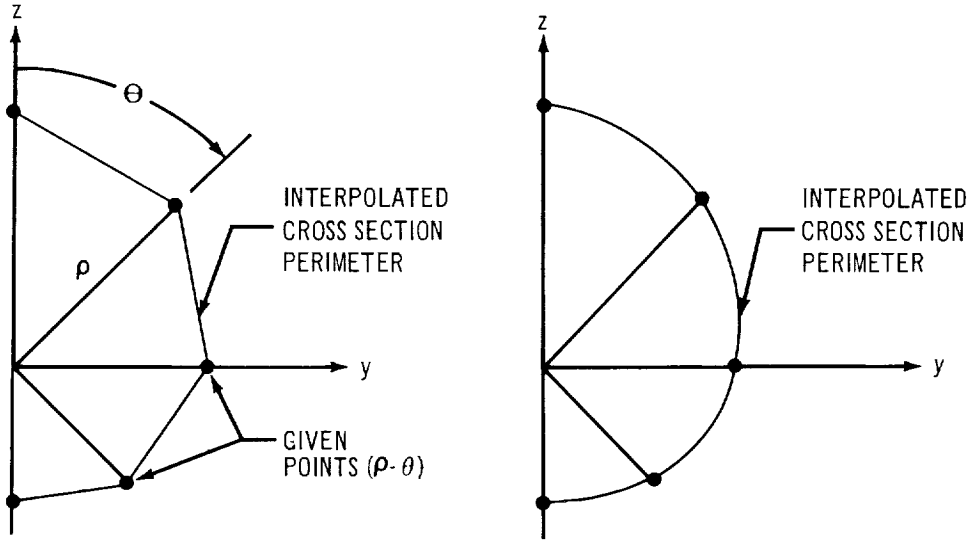

If a body of revolution is being defined (constant ρ at each station), a symmetrical θ-array must be specified to locate the centroid correctly. The following sketch shows how an asymmetrical θ-array can cause an error in the centroid location.

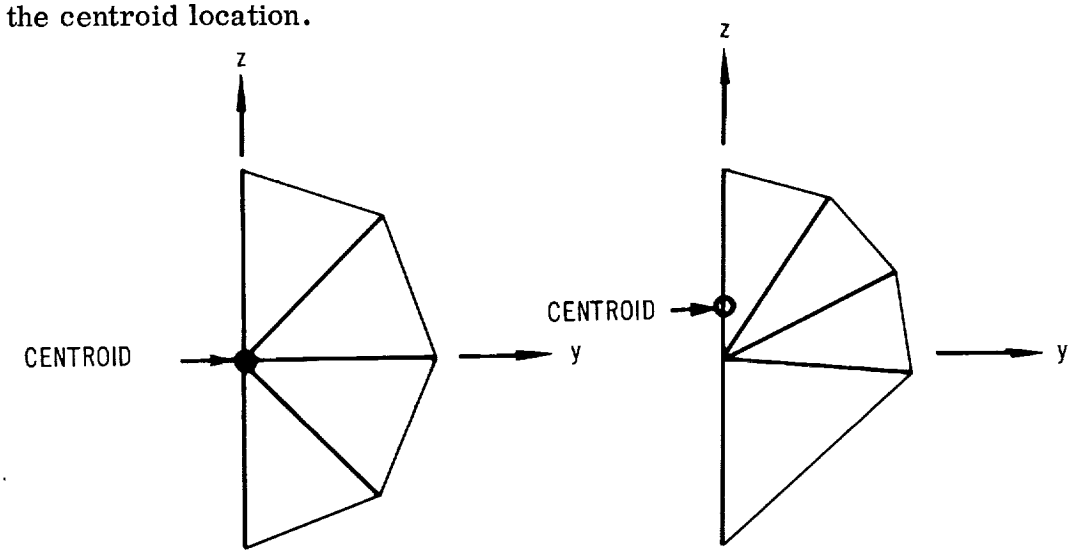

CONSTANT ρ:
SYMMETRICAL θ-ARRAY

CONSTANT ρ:
ASYMMETRICAL θ-ARRAY

After centroids are located for the fore and aft sections, these centroids are used to construct a new body axis (the x-axis) on which all remaining calculations are based. An equivalent body of revolution about the x-axis is determined. The number of stations (Card 2P) along the new body axis at which line sources and doublets are located is specified. Because these stations are evenly spaced along the body length, specifying the number of sources establishes their locations. The body meridians are cut at each source control station by transverse planes. Centroid locations relative to the body axis are determined from the body sections resulting from these transverse cuts.

The average of the radii connecting the x-axis with meridian lines at each source control station is used as the radius of the equivalent body with circular cross sections. The aerodynamic section uses these radii to determine the body source strengths.

The aerodynamic section now determines the axial and circumferential velocities and pressure coefficients at source control stations. Total C_L, C_D, and C_M are determined for the specified Mach number and angle of

attack. A sample program input for a parabolic body with a fineness ratio of 11 is given on page 180 in section 5.4.

Wing alone. - The wing planform must first be defined by specifying the coordinates of all corner points and break points. Control chords, except perhaps the wing-tip control chord, are defined through each corner point and break point. The wing apex must be on the X-axis. A minimum of two control chords must be specified. A pointed wing tip is considered a control chord of zero length. The wing planform is defined by projecting the actual wing into the X , Y plane as shown in the following sketch.

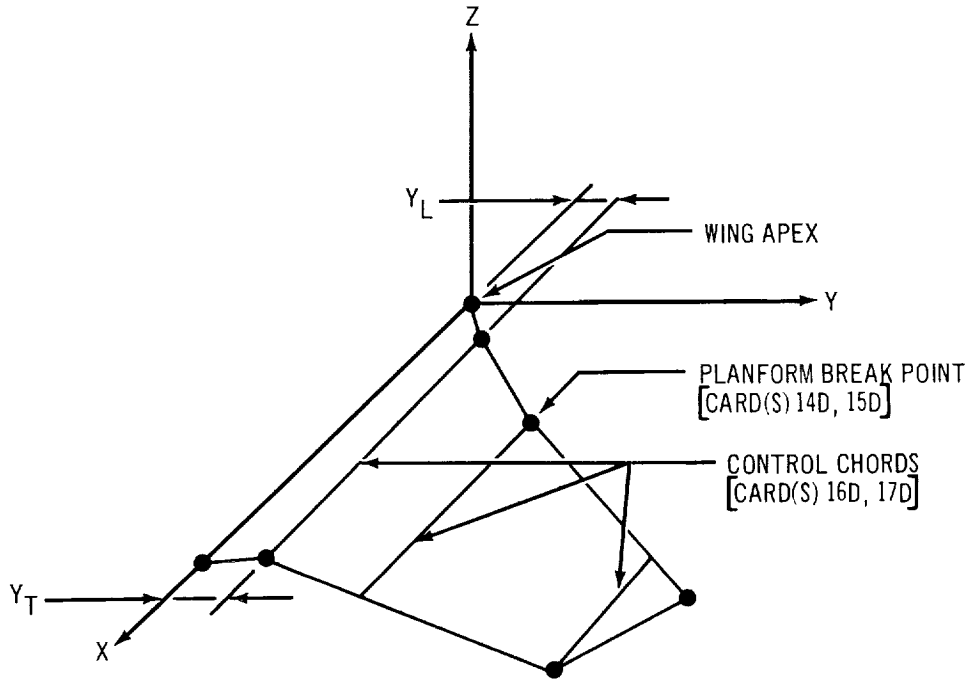

In planning the definition of the wing configuration, the effect of the planform definition and control chords on the wing paneling must be considered.

The wing panels are defined by constant-percent-chord lines [Card(s) 18D] and streamwise wing buttock lines [Card(s) 10P]. The constant-percent-chord lines are calculated in reference to the control chords. If the control chords are yawed with respect to the mainstream, the streamwise percent-chord positions of panel centroids and control points will vary spanwise on a spanwise panel row. Plotting and interpreting wing pressure data will then involve tedious hand calculations. It is therefore recommended that streamwise

control chords be used throughout the wing [Card(s) 17D, BETA = 0. or $Y_L = Y_T$].

There are three ways to panel the wing tip, as shown in these sketches:

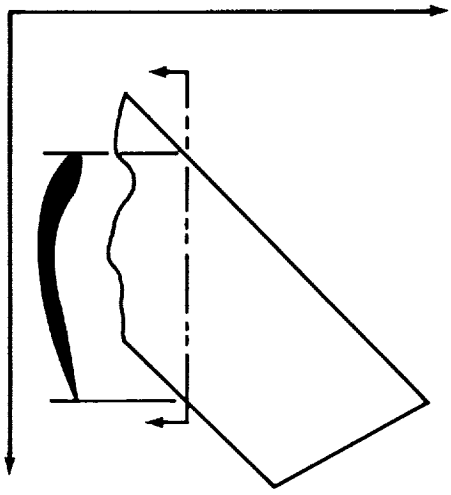

GIVEN CONFIGURATION

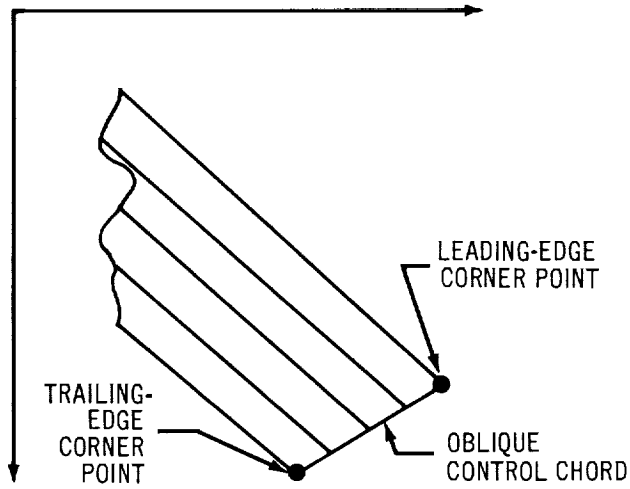

OBLIQUE CONTROL CHORD METHOD

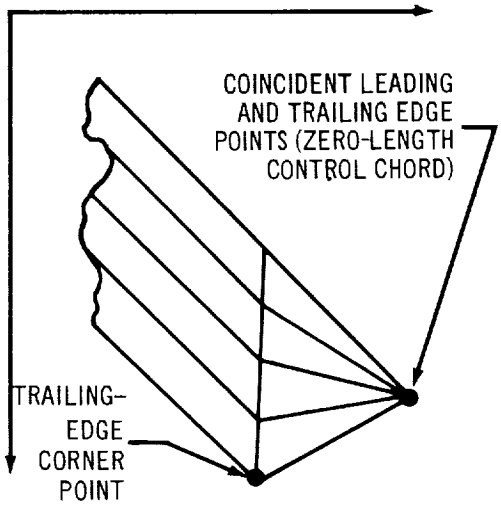

COINCIDENT EDGES METHOD

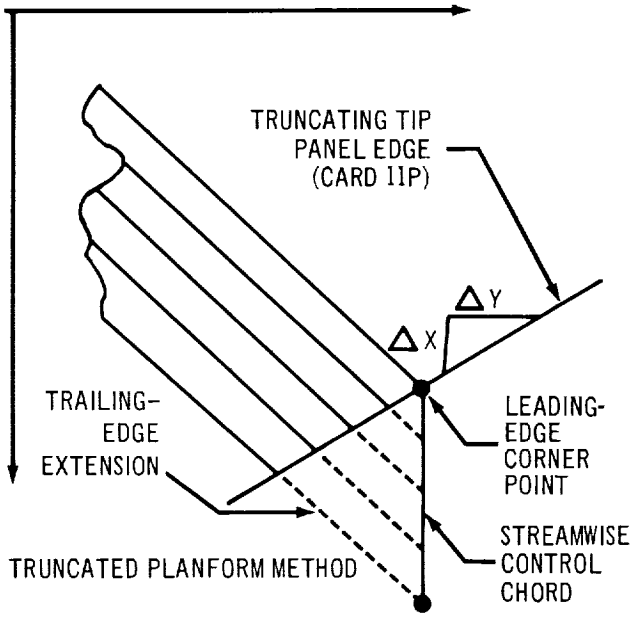

TRUNCATED PLANFORM METHOD

Tip paneling is partly controlled by the wing definition technique. If a planform corner point on the trailing edge is joined to a corner point on the leading edge by a wing-tip control chord of finite length, the spanwise panel edges form quadrilateral tip panels. If the planform leading- and trailing-edge tip points are coincident, the tip has triangular panels. For the oblique-control-chord method, hand calculations are needed to locate the streamwise percent-chord

positions of the tip panel centroids; this difficulty was discussed above for yawed control chords in the wing. The triangular panels of the coincident-edges method avoid this difficulty, but do not yield a good solution for a wing optimization analysis [CASE (Card 5A) = 3.].

The truncated-planform method, which avoids both of these difficulties, is recommended. The planform's leading edge is input coincident with the given wing. The trailing edge is input coincident with the given wing's trailing edge on the wing's inboard side; outboard, however, it extends spanwise and terminates exactly streamwise of the tip's leading edge (see sketch, page 130). Thus the tip control chord is streamwise. The tip paneling card (Card 11P) is used to input the oblique edge.

With this method, the panel centroids of all the chordwise rows are in the same streamwise percent-chord position, from the root-chord row to and including the tip row. Also, the tip is paneled with quadrilateral panels which yield reasonable optimization solutions.

The streamwise wing buttock lines, which define the wing panel's streamwise edges [Card(s) 10P], should be input so that each streamwise row is the same width. At an oblique tip, the mean width of the row should match the width of the other streamwise rows. The constant-percent-chord lines, which define the wing panel's leading and trailing edges [Card(s) 18D], should be spaced at a constant interval for optimization solutions. For given-configuration solutions, smaller panels may be placed in the region where the wing section changes most rapidly (e.g., leading edge). Panels there should have significantly shorter chords than panels farther aft. For wing camber optimization, the wing's inboard panels should be approximately as long as they are wide.

A maximum of 110 wing panels can be specified. Except for problems that are very simple aerodynamically, all 110 panels should be used.

Wing thickness can be specified by tables of upper- and lower-surface airfoil ordinates (Cards 12P and 13P), or as thickness slopes in the aerodynamic section [Card(s) 14A and 14AB]. Camber and twist can either be included in these ordinates or input as slopes in the aerodynamic section. The airfoils, one for each streamwise column of panels, must be oriented streamwise at spanwise locations corresponding to the y-centroid of each column. A nondimensional airfoil-ordinate array can be specified, because the program scales every array to fit the chord length at the specified span

location. Furthermore, for wings having no twist and the same airfoil from root to tip, only one ordinate table is needed. The program will scale the airfoils and correctly locate them across the span.

The following sketch is a sample paneling of a wing with these recommendations applied.

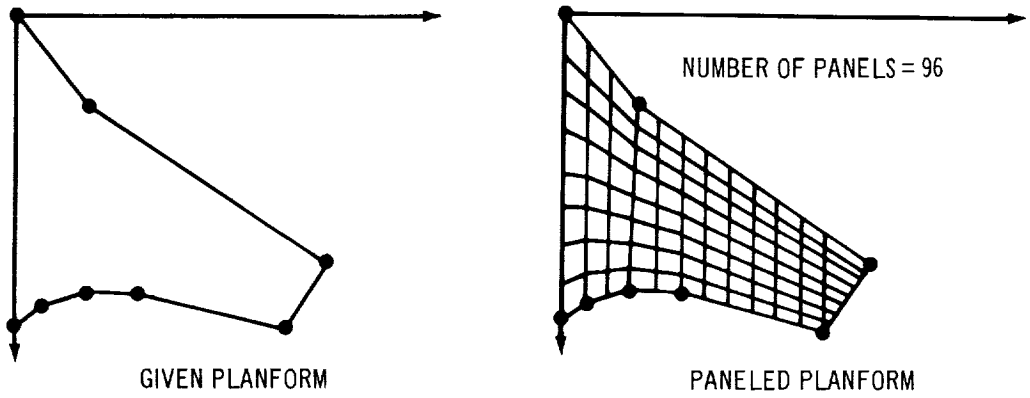

Program inputs for an arrow wing with camber, twist, and thickness are shown in section 5.4 (page 181). The aerodynamic section calculates pressure and force coefficient data for the specified wing geometry at Mach 2.05 for an angle-of-attack series (α = 0, 2, and 6 degrees). In addition, the wing camber shape, pressure coefficients, and force coefficients for a wing with identical planform and thickness distribution are determined for two cases. One has a constant ΔC_p distribution, and the other is a minimum-drag wing. Both are constrained to a total $C_L = 0.1$.

Wing-Body Combination. — The wing-body case, the most complex both geometrically and aerodynamically, requires full use of the program. The wing and body are defined as in the previous discussions on wing alone and body alone. However, because the wing's effect on the body is desired, the body must be paneled aft of its intersection with the wing's leading edge. The wing's effect on the body is determined by the influence-coefficient method. Body pressures caused by body thickness and camber are determined by the source-doublet method as in the body-alone case. A maximum of 100 body panels and 110 wing panels may be specified.

The program panels the defined body. If for some reason it is desired that the equivalent body of circular cross section be paneled, the body defined must be the equivalent body. Note that in a body-alone case, the radii and station centroid locations determined by the definition and transformation sections are passed directly to the aerodynamic section to calculate the source and doublet strengths. This procedure bypasses the paneling section.

The geometry definition of the body proceeds the same way as in the body-alone case. The meridian lines constructed in the definition section form the streamwise body-panel edges. Therefore, the desired body paneling must be known when the body definition is being established, because the θ-array determines the radial location of meridian lines. The transverse body panel edges are specified in the paneling section [Card(s) 6P, 7P].

Wing paneling is handled the same as for the wing-alone case except that the inboard wing-panel edges formed by the wing-body intersection are determined by the program. The wing definition should extend into the body to ensure that the program will find a wing-body intersection. Only the exposed wing planform is paneled.

The procedure of establishing a body axis system through the forward and aft body-station centroids is the same as for the body-alone case. In addition, the wing is oriented parallel to the x-y plane. The wing height, z_A, is computed by the program as the average of the leading- and trailing-edge heights above the x-y plane.

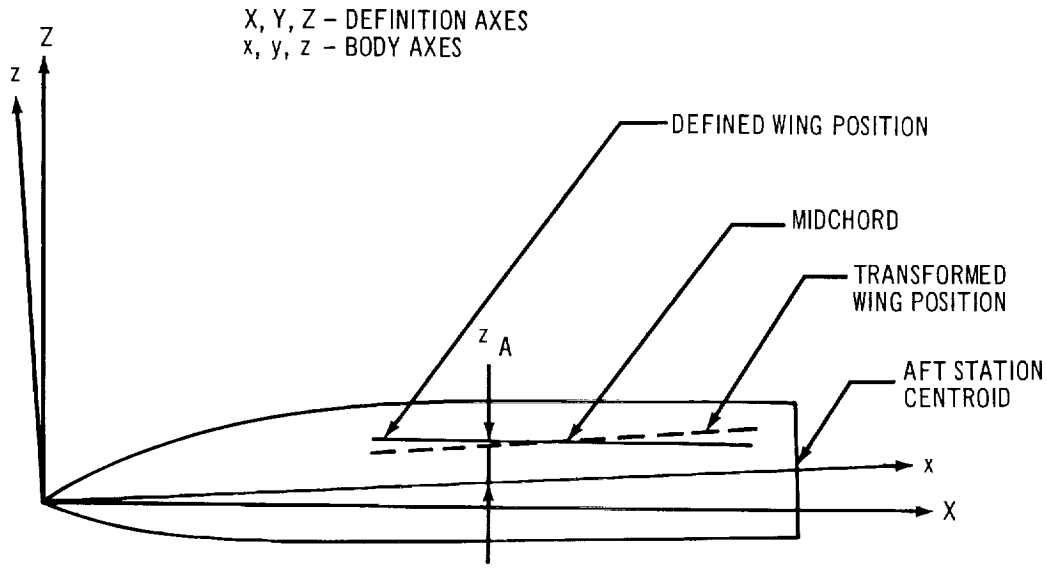

This transformed wing-body combination in the body axis system is the configuration that is paneled. All panel corner points, centroids, and control points are determined relative to the body axis system. Any wing incidence desired relative to the x-axis may be given by specifying an airfoil ordinate table with the correct incidence, or may be input as slopes in the aerodynamic section [Card(s) 12A and 12AC]. Wing thickness may be input by specifying an airfoil ordinate table, or by inputting thickness slopes to the aerodynamic section [Card(s) 14A and 14AB]. The entire wing shape may be pitched in relation to the wing axis by an input to Card 11A. The paneling is not affected by the airfoil ordinate tables, the wing incidence, or the aerodynamic slopes.

The wing intersection must not cross a body-definition meridian line. This can be prevented by choosing a θ-array, or a set of (Y, Z)-points on Card(s) 9D for SCODE[Card(s) 6D] = 6, that causes the meridian lines to straddle the wing intersection region. Specifying a meridian line coincident with the wing intersection also prevents a body meridian from crossing the wing intersection.

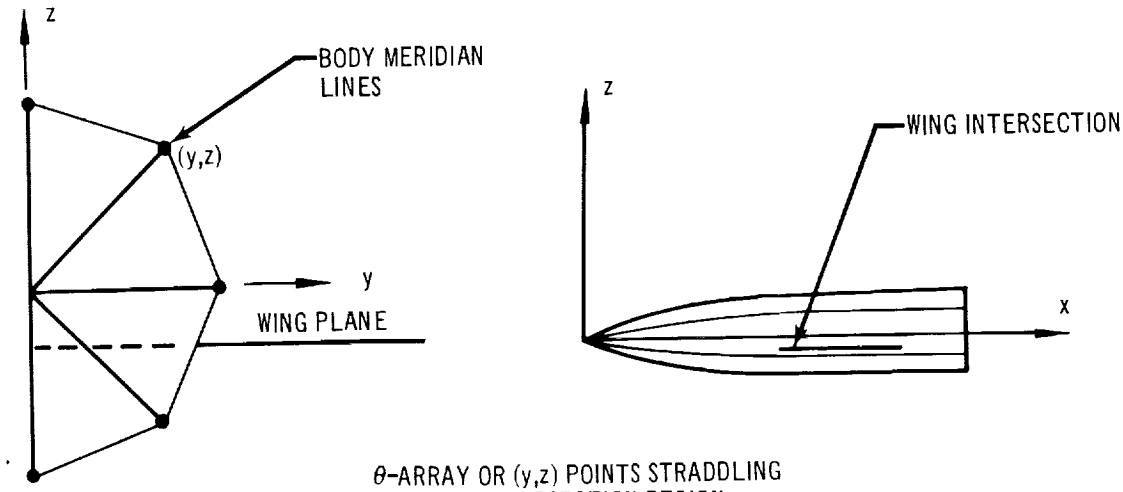

θ-ARRAY OR (y,z) POINTS STRADDLING THE WING INTERSECTION REGION

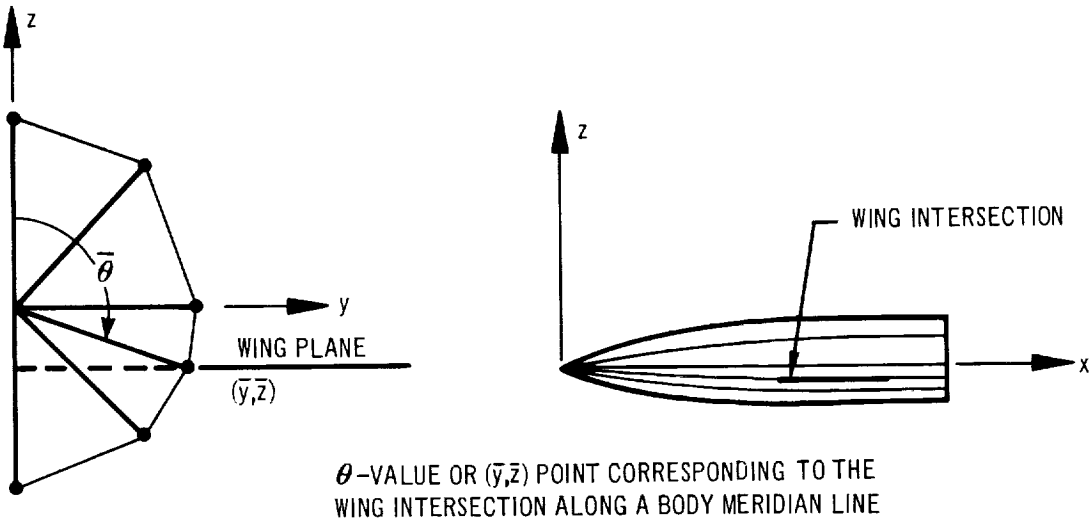

θ-VALUE OR $(\bar{y},\bar{z})$ POINT CORRESPONDING TO THE WING INTERSECTION ALONG A BODY MERIDIAN LINE

If the body is defined with the wing intersection between meridian lines, the paneling section constructs another longitudinal panel edge running aft from the wing's trailing edge (see the following sketch). Note that this meridian line is displaced in the θ-direction just aft of the wing's trailing edge, so that it is halfway between the input "straddling" meridian lines on the aft-body panels. This completes the added body-panel strip formed by the wing intersection. The number of panels around the body is the same at all stations, and the extra panels created by this procedure must be included within the maximum of 100 body panels.

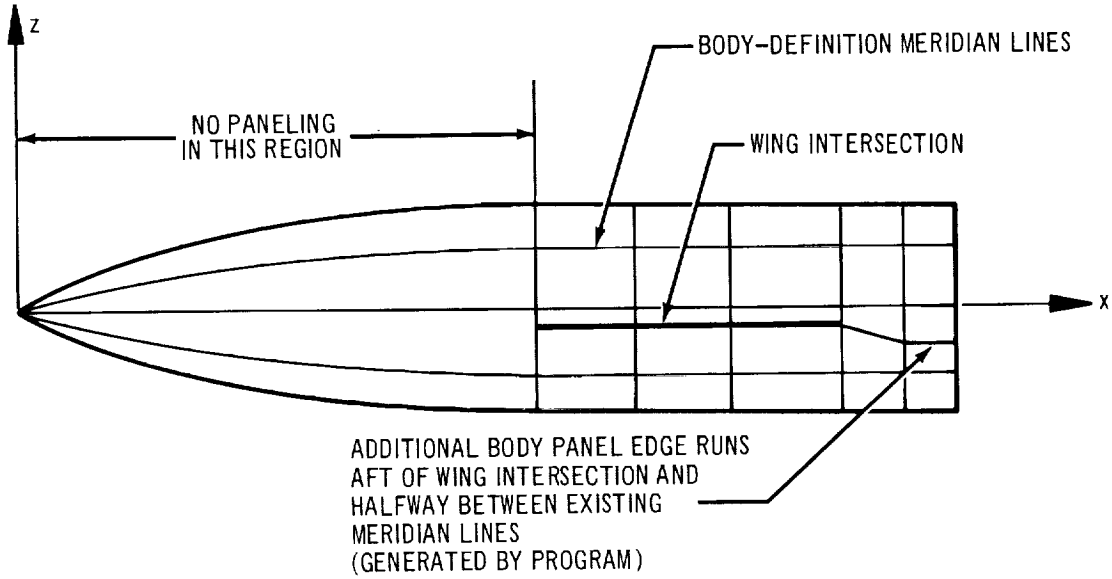

Body pressures due to thickness are determined from a set of equivalent body radii and body camber (z-centroid) values.

Transverse body panel edges in the wing intersection region must coincide with the spanwise wing panel edges, but do not have to be as numerous as the spanwise edges. The body panel edges in this region are specified by a table of integers that identify those spanwise wing panel edges that continue around the body to form transverse body panel edges. The spanwise wing panel edges are numbered consecutively from leading edge to trailing edge, as sketched below. The integers corresponding to those edges that continue around the body appear in sequence in the table. The table must always start with the integer 1 and terminate with the wing trailing-edge number.

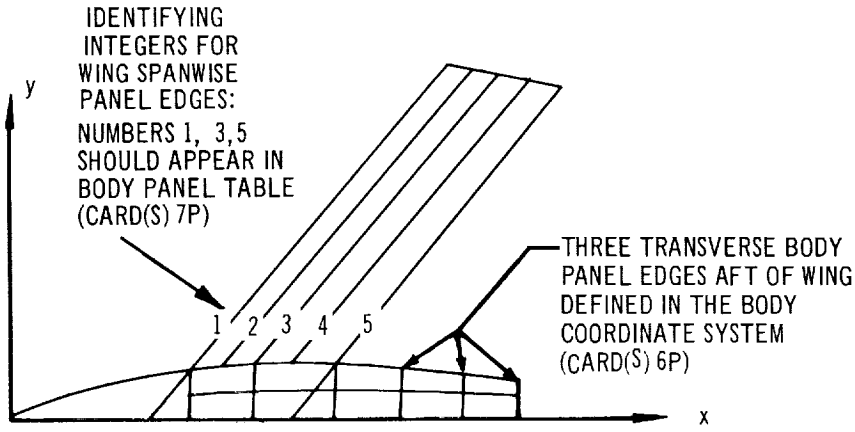

Transverse body panel edges aft of the wing trailing edge are defined in the body coordinate system.

Paneling the body is more complex than paneling a wing planform, since many multipart panels may occur. Two-part panels also can occur on some wing tips and along the inboard strip of wing panels if the wing intersects the body in a region of closure as shown below.

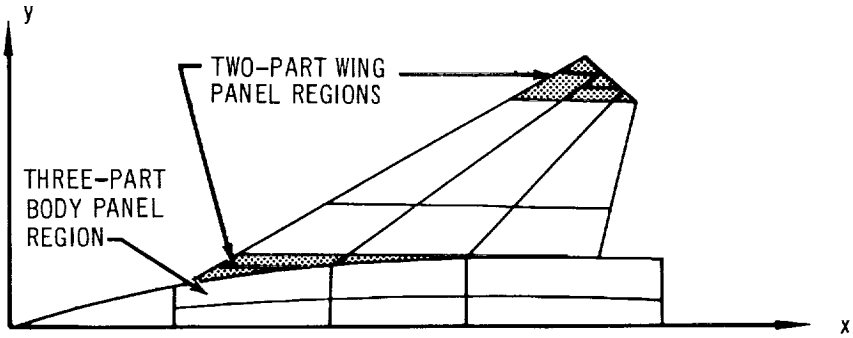

Body panels occurring in regions of closure are three-part panels. All wing and body panels must be quadrilateral with two streamwise edges. When paneling situations occur that do not satisfy these conditions, a multipart panel whose individual parts satisfy the conditions is constructed internally by the program (Card 5P, TOLB). A typical body panel and its parts are shown here:

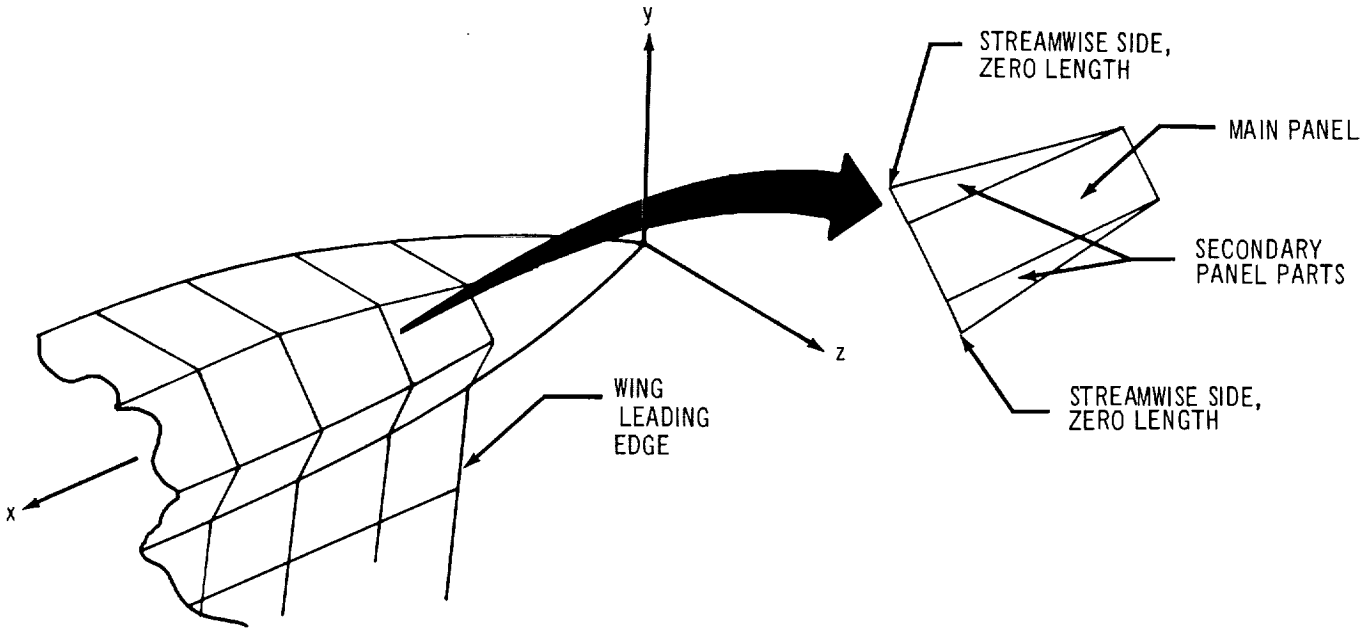

Most supersonic bodies do not have regions of rapid closure (hypersonic blunt bodies are not adaptable to the linearized analysis techniques of this program); therefore, the secondary body panel parts are usually very small. If these secondary areas are nearly zero, the matrix of influence coefficients can become singular, preventing matrix inversion. A tolerance control on the leading-edge slope of these secondary panel parts can be used to avoid this matrix problem. This tolerance is specified in the paneling section. The same matrix problem can result from secondary wing panel parts. A control tolerance on these wing panel parts also is specified in the paneling section. Program input illustrating the use of these tolerance controls (TOLB on Card 5P and TOLW on Card 9P, respectively) is contained in section 5.4 (pages 188 and 189).

Experience with the program has shown that it will not always successfully analyze a configuration that makes full use of the definition, transformation, and paneling sections. In particular, a paneled wing-body combination may not be properly defined and analyzed if it uses a contoured body, a cambered body, a body of "radical" cross section, or a shoulder-mounted or very-low-mounted wing. Pressure calculations on the body and wing panels may be erratic, and drag and lift figures may be incorrect.

These difficulties can be partly overcome by the following techniques: The primary effect of body thickness and camber is obtained by inputting equivalent body radii and camber (z-centroids) to the aerodynamic section directly. Only a cylindrical uncambered shell of body panels is then input to the definition section; these panels account for the wing-on-body interference, a secondary effect.

A zero-radius section is input at the nose. The body-definition enriching tolerance, CHDB (Card 4D), is set to zero. A cross section representing the configuration's body in the region of the wing-body intersection is determined. This cross section is then input by using SCODE (Card 4D) = 6. just ahead of the intersection. A meridian line is defined at the intended height of the wing, and other meridian lines are positioned along the cross-section perimeter as evenly as possible. Using SCODE = 0., other stations are placed throughout the region to be paneled; the last defining section should be just aft of the last (planned) transverse body panel's trailing edge. The last body cross section is a zero-radius station at the body tail. The body is defined at its true length so that the source control stations will be located correctly.

The nomenclature and paneling sequence is shown in figure 29.

The wing is input in the manner used for wing-alone configurations. The wing-alone recommendations also apply to the wing-body configuration. In inputting the streamwise wing-buttock lines (panel edges), note that the program sets the wing-body intersection as the inboard streamwise edge of the wing root panels; no input is required for this panel edge.

The body radii and camber (z-centroid) values generated by the geometry and paneling for the source control stations should not be used in the aerodynamic section. These values must be replaced by choosing Option B on aerodynamic Cards 8A and 9A and inputting the true equivalent radii and

camber values on Card(s) 8AB and Card(s) 9AB respectively. These values may be calculated by using the program in the following way:

The configuration body is input to the definition and paneling sections as a body-alone case; the data is terminated after Card 2P with an END OF DATA card. Equivalent body radii and camber values are thus generated. If the geometry transformation is done without rotation, the camber values may be used directly. If any rotation occurs, the camber values must be adjusted to be relative to an x-axis running through the nose, parallel to the definition X-axis. The following sketch shows the adjustment.

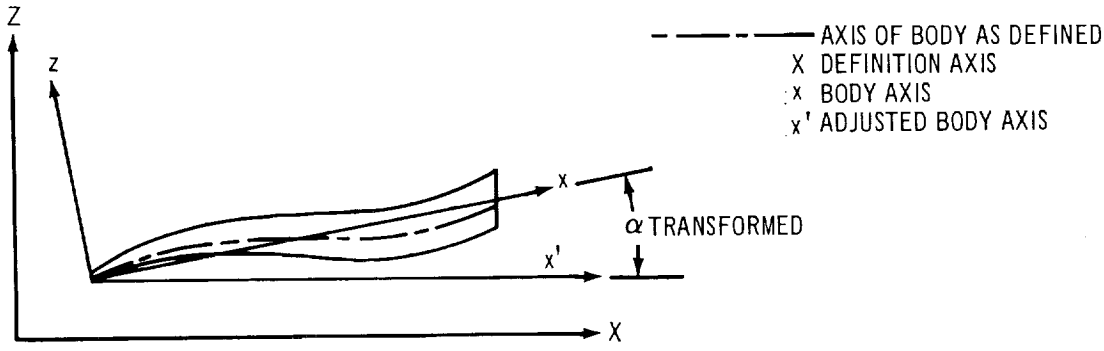

$$z\text{-CAMBER}_{ADJUSTED} = Z\text{-CAMBER}_{BODY} + (X_{BODY}) \sin (\alpha_{TRANSFORMED})$$

Aerodynamic save tape. - Sections 4.3 and 4.4 show that the aerodynamic matrix [the square matrix on the left side of equation(117)]depends only on paneling and Mach number. The right side's ultimate variables, wing thickness slopes [equation 93)], wing camber and angle of attack, and body thickness and camber are completely independent of Mach number. The "solution" to equation(117), the column matrix of panel pressures, is obtained by inverting the left-side square matrix and multiplying it by the right side. The left-side square matrix is termed the "aerodynamic matrix."

About four-fifths of the computing time is used in forming and inverting the aerodynamic matrix. It is often desired to analyze a given configuration with different wing cambers and thicknesses (or none at all) or with different body shapes. For this reason the inverted aerodynamic matrix is placed on a tape which can be saved for repeated use.

In addition to the inverted aerodynamic matrix the "aerodynamic tape" also saves, for optional use: the wing camber, twist, and thickness from the paneling section; body source control stations and body camber and thickness from the definition section; and data needed to calculate lift, drag, and moment coefficients. A complete and detailed description of the information saved on the aerodynamic tape is found in Format 5 of Appendix D in Part II.

The following illustration shows the inputs required for saving and reusing the aerodynamic tape. At the end of a computer run in which an aerodynamic tape is to be saved, the computer operator removes the reel of tape from the appropriate tape unit (Unit B6 in the example), assigns it an identifying number, and stores it. The identifying number is given to the user. When the user wishes to re-use the tape, he begins his data with Card 1A (AERODYNAMIC), selects the USE TAPE option for Card 2A, and enters the identifying tape number on the appropriate program control card.

The aerodynamic save tape control card (Card 2A) is repeated here from section 5.3 for easy reference. As indicated in the definition, each option for Card 2A requires a particular tape usage card. As shown below, the arrow ⇨ indicates one of the tape usage cards.

Card 2A	Select and input one of the following data control cards.		
	1-7	COMPUTE	The aerodynamic matrices and geometry data are not saved on computer tape; this card is used when a defined and paneled configuration is input. Use the word SCRATCH on the tape usage card.*
	1-9	SAVE TAPE	The aerodynamic matrices and geometry data are saved on tape for repeated analysis. The body and wing thickness and camber from the geometry section are also saved for optional use. This card is used when a defined and paneled configuration is input. Use the word SAVE* on the tape usage card.

*Peculiar to Boeing system.

1-8	USE TAPE	A previously saved aerodynamic computer tape is to be used; no definition nor paneling data are input when this option is selected. Use the word MOUNT on the tape usage card; also, input the appropriate tape number in Columns 15-21 and the word IN/OUT in Columns 34-39 of the tape usage card.*

Most of the data (such as body radii) on the aerodynamic tape can be superseded by selecting the appropriate option in the aerodynamic section and inputting the data desired. For example, selecting CASE (Card 5A) = 3. (the wing camber optimization) and inputting constraints on Card 13A automatically suppresses any camber input to Card(s) 12P and 13P in generating the aerodynamic tape. Such camber could be used by specifying CASE = 2. and inputting GIVEN on Card 12A.

```
      DATE     SEP 20, 1966              9411F        TAPE   9/12/66          TIME

      *JOB 57530B C RA2TEA17542/LARSEN, J.W.                    /LS80/5-0206/6-7000
      *     ACCT TIME 5
      *     XEQ
      *     PRINT ESTIMATE (5000. 100)
      *     USE    D072    C4    800, IN  ALTERNATE INPUT TAPE
      *     USE    SCRATCH C3    800, IN      IBJOB OVERLAY LINK TAPE
      *     SCRATCH        A4, A5, B2, B3, C1, C2, C9
      *     SCRATCH        B6
      *     STOP
      *     PAUSE
PAUSE SETUP TIME FROM 14.476 TO 14.480
      *     IBSYS

   BEGIN LOADING IBSYS                                        TIME 14.481
         ENTERING IBSYS BASIC MONITOR CONTROL                 STD 09/12/66
```

NOTE: THIS FORMAT PECULIAR TO BOEING SYSTEM

Flow visualization. - The flow visualization section provides a highly flexible means of visualizing the resultant flow field induced by the singularities' representation of the configuration.

*Peculiar to Boeing system.

The effects of the vorticity panels can be suppressed from the calculation by setting CAMN (Card 2F) = 1. in the data. If the only matter to be studied is wing thickness effects, selecting this code saves much computer time. However, thickness interference effects at a wing-body intersection will not be accounted for, and the body lifting effects due to line doublets will still be present.

There are three modes of visualizing flow: field interrogation, streamlines, and field point characteristics. The field interrogation mode uses a three-dimensional array of points established by the program. The program output at each point consists of point coordinates (relative to the transformed body axis), velocity components ($\vec{u}$, $\vec{v}$, and $\vec{w}$), and a pressure coefficient (C_p). Meaningful results cannot be expected for points inside the body, or near panel edges or the wing wake. A two-dimensional array is obtained by specifying a three-dimensional array with zero width in one direction. A two-dimensional skew array may also be specified as in section 5.3, page 176. The skew grid is defined in a plane which is defined by one of the coordinate axes (selected) and an axis with any specified orientation. The graduations on the coordinate axis are specified the same way as for the three-dimensional array. The graduations on the skew axis are determined by the intersections of a family of planes normal to a selected coordinate axis through its specified graduations (figure 30). The axis used to graduate the skew axis must be selected with care, because the forementioned family of planes must intersect the skew axis.

The second mode of visualizing flow is streamlines. A point is selected outside the body (not on the wing plane); the program then calculates the coordinates of the streamline by a step-by-step velocity-vector integration method, first upstream and then downstream of that point. The maximum and minimum step sizes that the integrator will take in locating successive streamline points is set for the XNS (Card 4FB) streamlines to be calculated. The initial step size XDELT (Card 4FC) is specified individually for each streamline. Printout consists of interpolated streamline coordinates beginning at XMIN (Card 4FC) and proceeding downstream in increments of the initial step size XDELT to XMAX (Card 4FC). An optional printout format may be used by setting PRINT equal to 1. (Card 4FA). This optional format consists of the

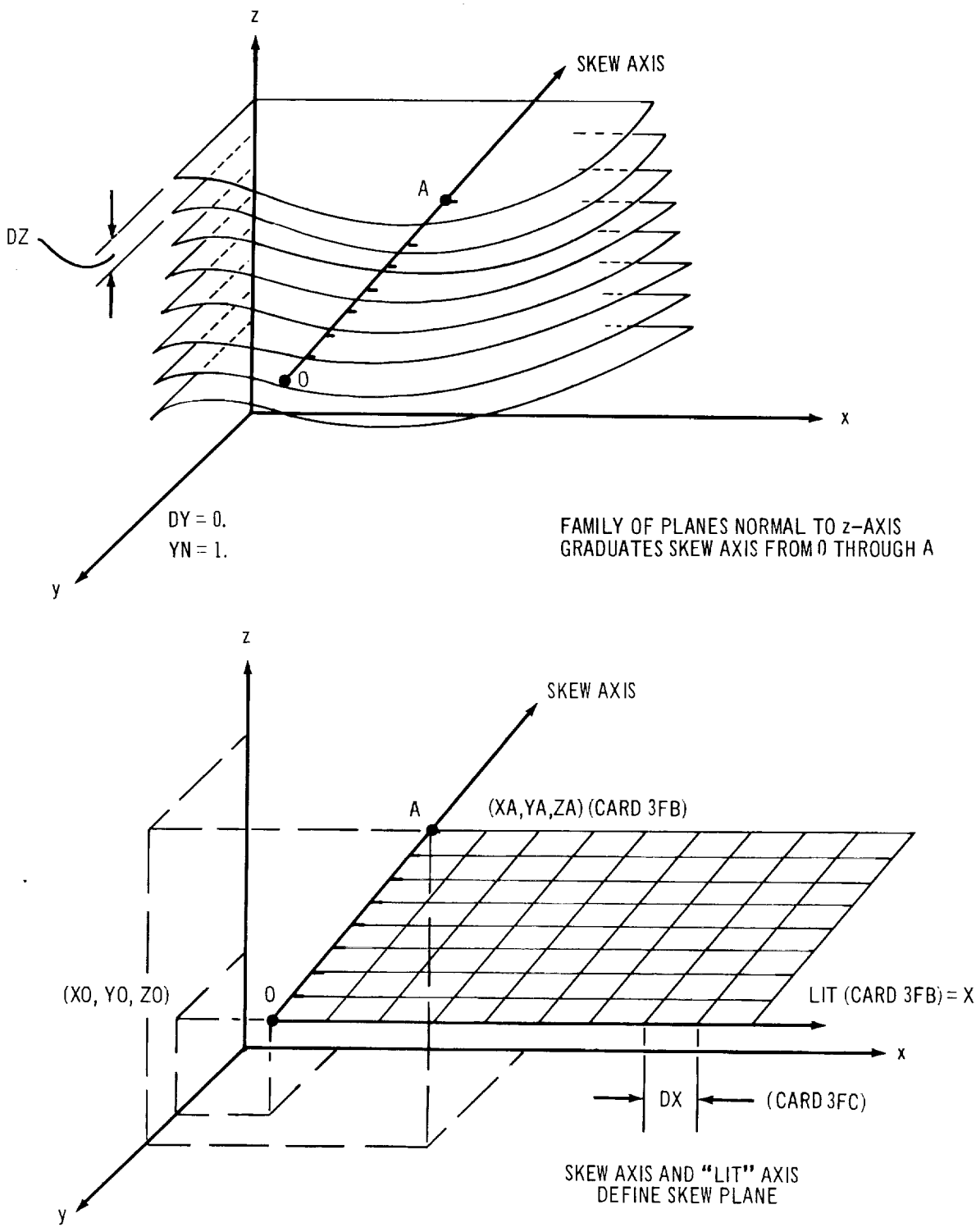

FIGURE 30 FLOW VISUALIZATION, SKEW GRID GRADUATIONS, AMD (CARD 3FC) = 4.

coordinates of the actual points calculated in generating the streamline, and the velocity components and pressure coefficients at each point.

The third and last mode of flow visualization is a calculation of perturbation velocity components (u , v , w), velocity components ($\vec{u}$, $\vec{v}$, $\vec{w}$), and a pressure coefficient (C_p) at specified points. The point coordinates are input directly. Just as with the grid mode, meaningful results cannot be expected at points inside the body or along panel edges.

Visualization calculations apply to the last angle of attack of the last aerodynamic analysis. A visualization of a configuration which has been previously saved on a "save tape" can be obtained by inputting Card 1A (AERODYNAMIC), Card 2A (the appropriate option), and the flow visualization cards beginning with Card 1F.

Summary of Usage Recommendations. - This summary of recommendations made in this section includes some added points which did not require explanation in the main text. Items 1 through 10 in this summary are listed by number; their application is shown by code in figure 31.

1. No body camber or cross-section variation is recommended in the body paneling of a wing-body combination; only a cylinder of characteristic cross section should be used.
2. Interior angles between body panels must be greater than 100 degrees and less than 175 degrees.
3. Body panels should be approximately equal in width.
4. Body panels should be approximately equal in length in the region of the wing intersection and downstream.
5. A body meridian line should be input coincident with the plane of the wing panels.
6. In a wing-body analysis, body thickness and camber should be input to the aerodynamic section directly.
7. The angle between the wing panels and the adjacent body panels must be not less than 45 degrees.
8. Root wing panels must be roughly the same size as the adjacent body panels; $1/2 \leq (\text{AREA}_{j_{body}} / \text{AREA}_{j_{wing}}) \leq 3$.
9. The wing should be defined with streamwise control chords from the

root to and including the tip. Oblique tips are paneled by truncating the planform.

10. Wing panel rows should be of equal width. The constant-percent-chord lines defining the panels' leading and trailing edges should be at an equal percent interval for a camber optimization analysis.
11. All but the simplest configurations should use as many panels as possible.
12. Whenever a configuration is to be analyzed more than once, an aerodynamic computer tape should be saved.
13. Whenever the flow visualization section studies only thickness effects, the option CAMN (Card 2F) = 1. should be selected.

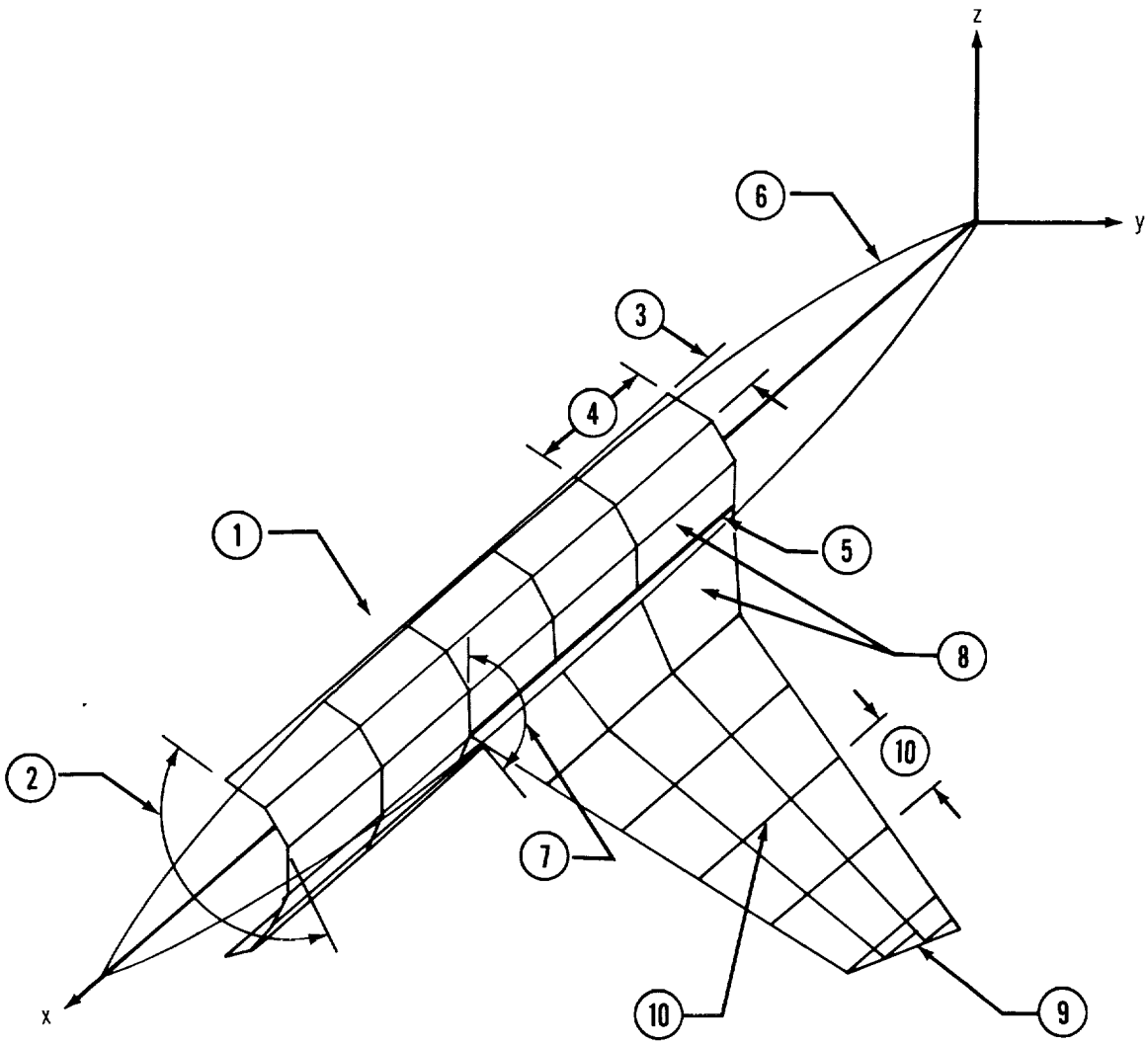

FIGURE 31 DIAGRAM OF RECOMMENDATIONS ON PROGRAM USAGE

5.3 Program Card Input Format

Aerodynamic cases that can be solved for the various configuration problems are the following:

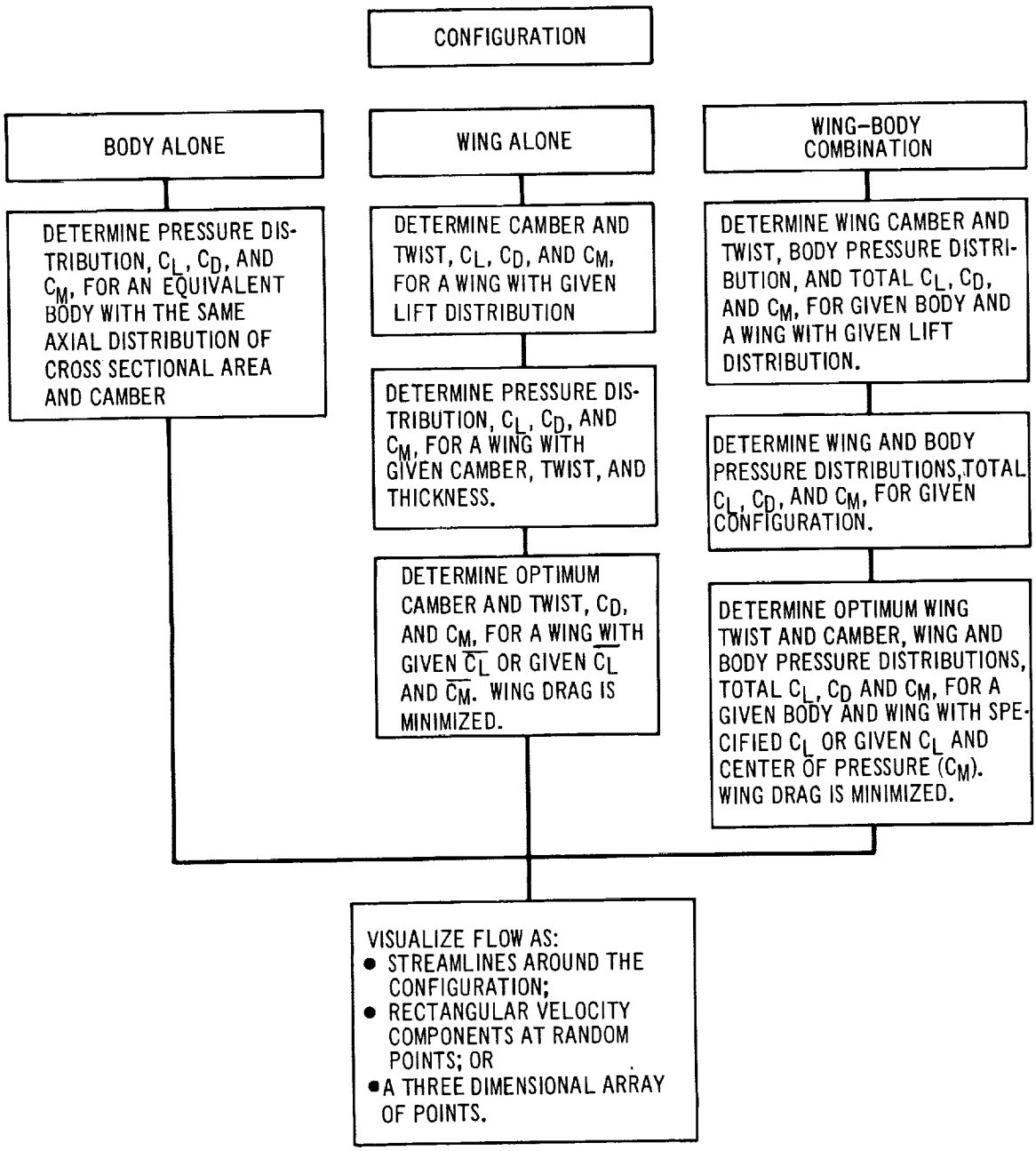

The corresponding input card sets needed to define and analyze a configuration are shown in figure 32. A completed input data deck resembles figure 33.

The cards are organized into four groups: definition, paneling, aerodynamics, and flow visualization. Each card's identifying code (columns 74 through 80) designates the group by the letter D, P, A, or F.

Multiple aerodynamic cases on a given geometry for a given Mach number may be requested in the aerodynamic set. If the Mach number or configuration is changed, the geometry must be redefined.

SUMMARY

The following chart summarizes the input data cards required to analyze each of the three basic configurations.

Geometry Definition Card Set	Wing-Alone	Body-Alone	Wing-Body
Card 1D	Yes	Yes	Yes
Cards 2D-9D	No	Yes	Yes
Cards 10D-18D	Yes	No	Yes
Cards 19D-20D	No	No	Yes
Card 21D	Opt	Opt	Opt
Card 22D	Yes	Yes	Yes

Geometry Paneling Card Set	Wing-Alone	Body-Alone	Wing-Body
Cards 1P-2P	Yes	Yes	Yes
Card 3P	Yes	No	Yes
Cards 4P-7P	No	No	Yes
Cards 8P-13P	Yes	No	Yes
Card 14P	Yes	No	Yes

Aerodynamic Card Set	Wing-Alone	Body-Alone	Wing-Body
Cards 1A-6A	Yes	Yes	Yes
Cards 7A, 8A-8AA, 9A-9AA	No	Yes	Yes
Cards 10A-10AA (or -10AB)	Opt (if CASE = 1.)	No	Opt
Cards 11A-11AA, 12A-12AA (or -12AC)	Opt (if CASE = 2.)	No	Opt
Card 13A	Opt (if CASE = 3.)	No	Opt
Cards 14A-14AA (or -14AB)	Opt (if THICK = 1.)	No	Opt
Cards 15A	Opt (if POLAR > 0.)	No	Opt
Card 16A	Yes	Yes	Yes

Flow Visualization Card Set	Wing-Alone	Body-Alone	Wing-Body
Cards 1F-2F	Yes	Yes	Yes
Cards 3F, 3FA, 3FB, 3FC	Opt (GRIDS option)	Opt	Opt
Cards 4F, 4FA, 4FB, 4FC	Opt (STREAMLINES option)	Opt	Opt
Cards 5F, 5FA	Opt (POINTS option)	Opt	Opt
Card 6F	Yes	Yes	Yes
Terminal Card	Yes	Yes	Yes

Note: For Aerodynamic section input data, only one of the following three card sets can be used per case:

1. Cards 10A-10AA (or -10AB). For CASE = 1. (design case), defines ΔC_p distribution.
2. Cards 11A-11AA, 12A-12AA (or -12AC). For CASE = 2. (analysis case), gives wing angle of attack, twist, and $\Delta z/\Delta x$ camber distribution.
3. Card 13A. For CASE = 3. (optimization case), gives constraints.

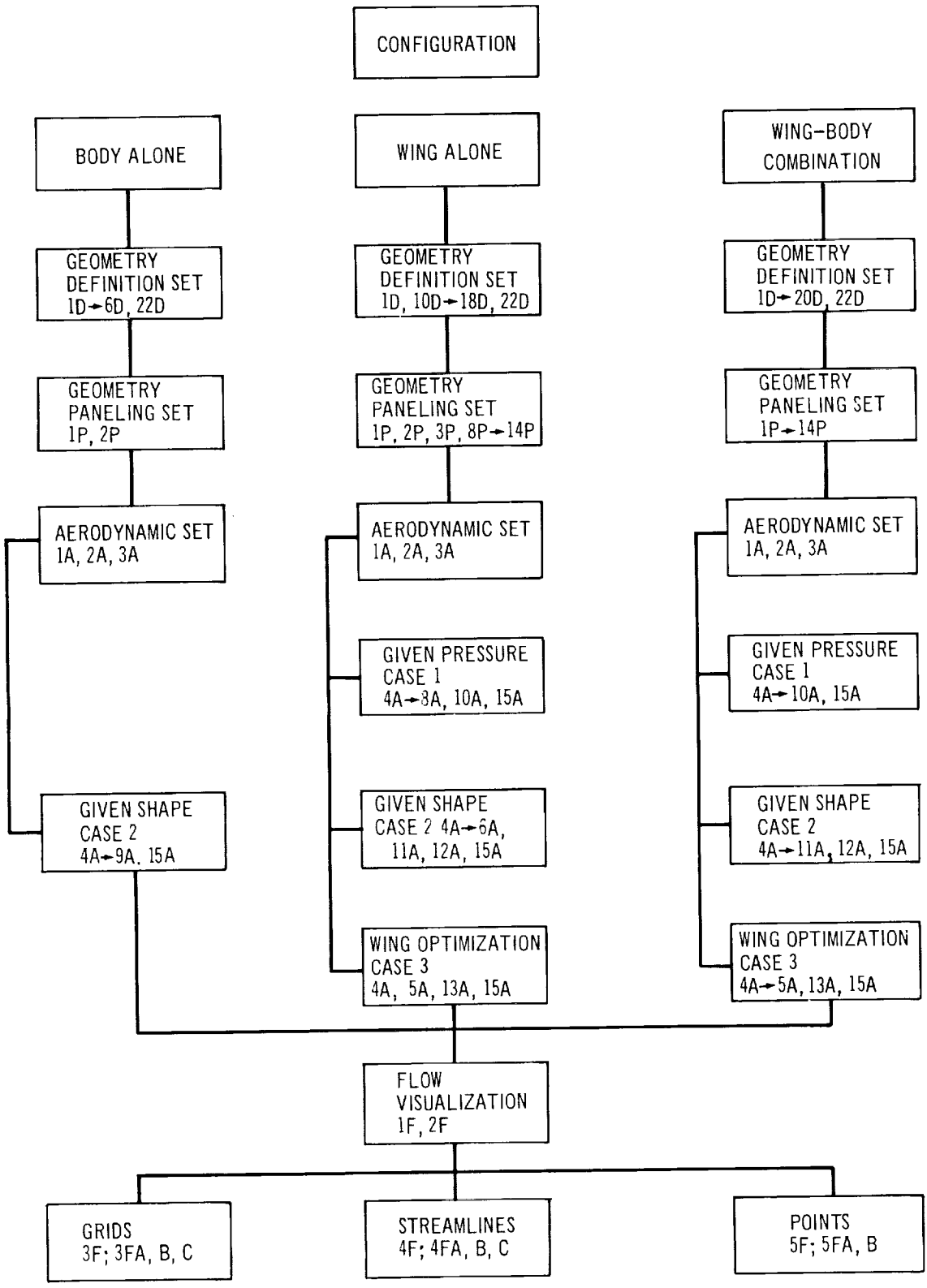

FIGURE 32 OUTLINE OF INPUT CARDS NEEDED TO DESCRIBE AND ANALYZE A CONFIGURATION

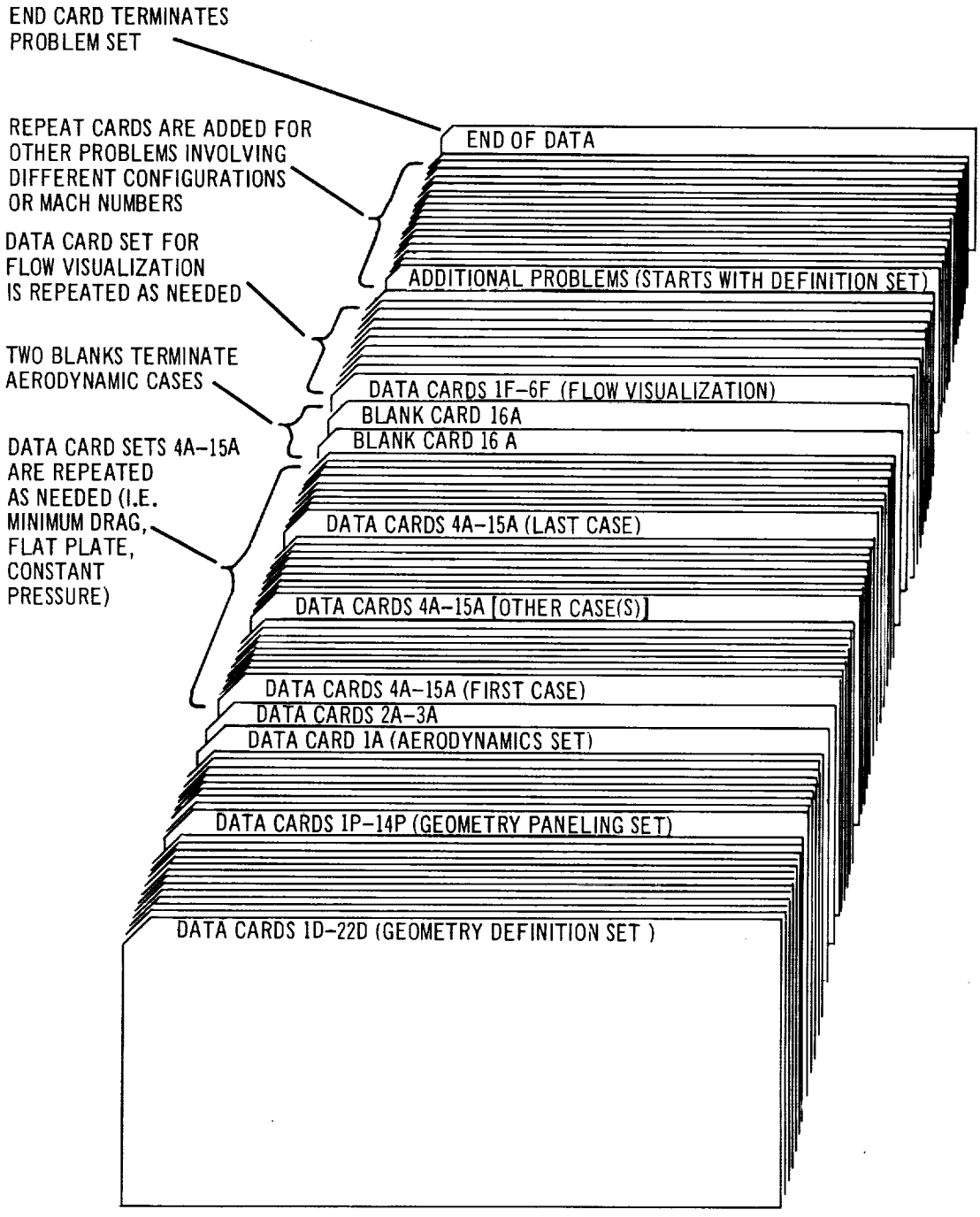

FIGURE 33 SAMPLE DATA DECK

GEOMETRY DEFINITION CARD SET

All geometry definition data, except title cards and literal statements, are punched in six-field, ten-digit format. A decimal point is required in each data field.

For a body-alone problem definition, Cards 10D through 19D are omitted. For a wing-alone problem definition, Cards 2D through 9D, 19D and 20D are omitted.

	Column	Code	Explanation
Card 1D	1-6	DEFINE	Columns 1-6 contain the word DEFINE.
Card 2D	1-4	BODY	Columns 1-4 contain the work BODY. Card 2D is used only when a body or wing-body combination is defined.
Card 3D	1-72	TITLE	Any desired title.
Card 4D	1-10	BNS	Number of defining body stations. $2. \leqslant \text{BNS} \leqslant 50.$.
	11-20	BTHETA	There is a defining-body cross section at each body station. This column gives number of points on each cross section; i.e., number of ρ, θ or Y, Z pairs per station. $3. \leqslant \text{BTHETA} \leqslant 10.$.
	21-30	AXIS (1)	Y-coordinate of body definition axis (cf. page 126).
	31-40	AXIS (2)	Z-coordinate of body definition axis (cr. page 126).
	41-50	CHDB	Dimensional tolerance to be used in generating additional body-meridian line points between given stations. If CHDB $\leqslant 0.$ or if BNS $< 4.$, no additional points will be generated. If $0. <$ CHDB $\leqslant 0.001$, then a value of 0.001 will be used (see page of Part II).
Card(s) 5D (2 cards maximum)	1-10 ⋮ 51-60 etc.	θ_1 ⋮ θ_6	Array of angles (θ), in degrees at each defining station. There must be exactly BTHETA angles $\leqslant 10$, six per card.
Card(s) 6D (50 maximum)	1-10	STA	X-coordinate of body station. (One card is needed for each defining station).

Column	Code	Explanation
11-20	YZ(1)	Δ Y-increment added to body definition axis to establish a local origin from which all ρ, θ for this station are measured.
21-30	YZ(2)	Δ Z-increment added to body definition axis to establish a local origin from which all ρ, θ for this station are measured (see page 127).
31-40	SCODE	= 0. this cross section is identical to previous section.
		= 1. this cross section is specified by BTHETA values of ρ (on cards 7D). The θ-array of card(s) 5D will be used.
		= 2. this cross section is a circle. (Radius given in columns 41-50.)
		= 3. this cross section is an ellipse. (Horizontal semi-axis is given in columns 41-50, the vertical in columns 51-60.)
		= 4. this cross section is circular (radius given in columns 41-50) with an angle array (on card(s) 8D) different from the θ-array on card(s) 5D. This option allows local deviations in the meridian lines.
		= 5. this cross section is specified by a set of ρ (on card(s) 7D) and by a nonstandard set of θ (on card(s) 8D).
		= 6. this cross section is given by a set of Y, Z pairs (on cards 9D).
41-50	RAD(1)	Radius of section if SCODE = 2. or 4.. Horizontal semi-axis if SCODE = 3.. Not used otherwise.
51-60	RAD(2)	Vertical semi-axis, if SCODE = 3.. Not used otherwise.

Note — if options 1, 4, 5, or 6 are designated, the added information card(s) 7D, 8D, or 9D must be inserted behind that station card 6D and before the next station card 6D.

	Column	Code	Explanation
Card(s) 7D	1-10	ρ_1	A set of body radii ρ if SCODE = 1. or 5.. There must be BTHETA $\leq$ 10 values of ρ.
	⋮	⋮	
	51-60	ρ_6	
	etc.		
Card(s) 8D (2 maximum per station)	1-10	θ_1	A set of θ if SCODE = 4. or 5.. There must be BTHETA $\leq$ 10 values of θ.
	⋮	⋮	
	51-60	θ_6	
	etc.		
Card 9D (3 maximum per station)	1-10	Y_1	Array of Y, Z coordinate pairs if SCODE = 6..
	11-20	Z_1	
	21-30	Y_2	
	31-40	Z_2	
	41-50	Y_3	
	51-60	Z_3	
	etc.		
Card 10D	1-4	WING	Columns 1-4 contain the word WING. This card is used whenever a wing is defined. For the case of a body alone, omit cards 10D through 19D. After reading a WING card, the program expects wing definition data.
Card 11D	1-72	TITLE	Any desired title.
Card 12D	1-10	PNLE	Number of corner or break points defining the planform leading edge (see page 129).

Notes:

1. There is a maximum of three Card(s) 7D and/or Card(s) 8D per station.

2. For inputting a body meridian exactly coincident with a wing's intersection, it is recommended that the cross-section option SCODE = 6. be used and that CHDB = 0.. The Z-height of the intersection's meridian [Card(s) 9D] is held constant and at exactly the same height as the wing [Card(s) 17D]. The aft-most body-defining station must be a zero-radius circle. (See pgs. 134 and 135 section 5.2.)

	Column	Code	Explanation
	11-20	PNTE	Number of corner or break points defining the planform trailing edge.
	21-30	AFN	Number of planform control chords. AFN $\geq$ 2., including the wing-tip control chord. AFN must equal the larger of PNLE and PNTE; that is, each control chord must begin or end at a planform defining point.
	31-40	PLN	Number of constant percent chord lines used to form spanwise panel edges. Wing leading and trailing edges are counted in this number.
	41-50	WUL	= 1.
	51-60	CHD	Must be left blank.
Card 13D	1-10	PCODE	= 1.
	11-20	ACODE	= 1.
	21-30	EPS	Must be left blank.
Card(s) 14D	1-10	X_1	Array of points defining the planform leading edge, arranged in order from inboard to outboard. There must be PNLE point pairs; three coordinates per card.
	11-20	Y_1	
	21-30	X_2	
	31-40	Y_2	For wing-body combinations, X_1 and Y_1 must lie inside the body so that an intersection can be calculated.
	41-50	X_3	
	51-60	Y_3	The X-axis defining these points originates at the nose of the configuration (for wing-body cases) as defined by the first Card 6D.
	etc.		
Card(s) 15D	1-10	X_1	Array of points defining the planform trailing edge, arranged in order from inboard to outboard. There must be PNTE point pairs; three coordinates per card.
	11-20	Y_1	
	21-30	X_2	
	31-40	Y_2	For wing-body combinations, X_1 and Y_1 must lie inside the body so that an intersection can be calculated.
	41-50	X_3	

Column	Code	Explanation
51-60	Y_3	
	etc.	

Cards 16D — Cards 16D and 17D always occur in pairs (unless AFNU = 0. on card 16D) to define each wing control chord. There must be AFN $\geq$ 2. pairs of 16D and 17D cards.

1-10	AFK	Code to indicate how the control chord is oriented on the planform. See sketches below.

WING CHORD DEFINITION

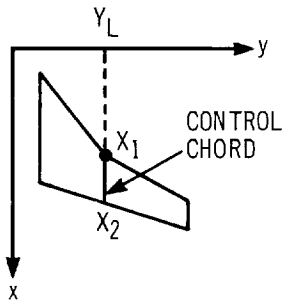

AFK = 1.

LEADING-EDGE POINT DEFINES CONTROL CHORD: The control chord leading point X_1 is at a planform leading-edge defining point.

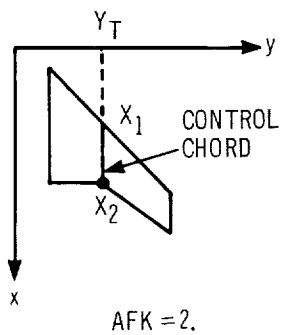

AFK = 2.

TRAILING-EDGE POINT DEFINES CONTROL CHORD: The control chord trailing point X_2 is at a planform trailing-edge defining point.

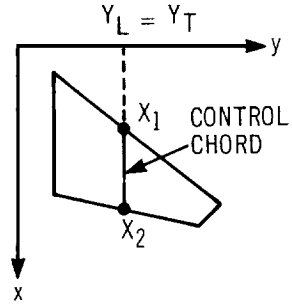

AFK = 3.

LEADING- AND TRAILING-EDGE POINTS BOTH DEFINE CONTROL CHORD: The control chord leading edge X_1 is at a planform leading-edge defining point

or

The control chord trailing point X_2 is at a planform trailing-edge defining point.

Both conditions must be satisfied at the tip.

WINGTIP CONTROL CHORD DEFINITION (OBLIQUE)

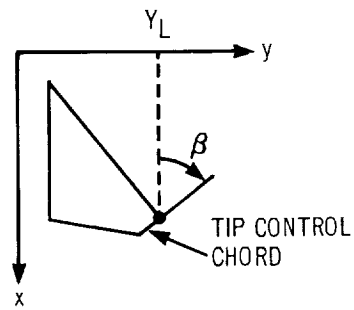

AFK = 1.

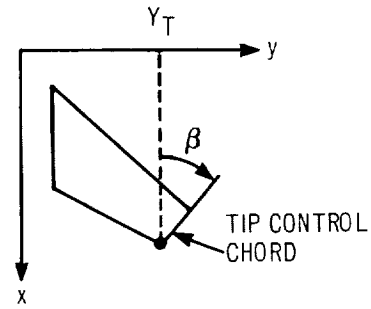

AFK = 2.

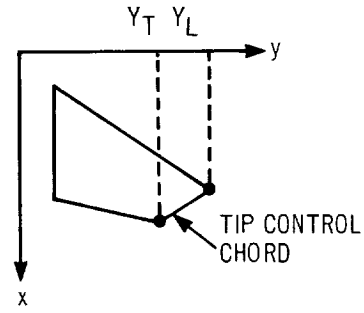

AFK = 3.

	Column	Code	Explanation
			Two of the three quantities Y_L, Y_T or β must be given. AFK indicates the appropriate pair. In summary: if AFK = 1., input Y_L and β; if AFK = 2., input Y_T and β; if AFK = 3., input Y_T and Y_L.
	11-20	BETA	The angle of yaw, β , in the diagram. If AFK = 1. or 2. and BETA = 0., the chord is streamwise. BETA is ignored if AFK = 3..
	21-30	Y_L	Y-coordinate of leading edge of control chord. If AFK = 1. or 3., Y_L is equal to the Y-coordinate of the corresponding planform leading-edge defining point. If AFK = 2., Y_L is ignored.
	31-40	Y_T	Y-coordinate of trailing edge of control chord. If AFK = 2. or 3., Y_T is equal to the Y-coordinate of the corresponding planform trailing-edge defining point. If AFK = 1., Y_T is ignored.
	41-50	AFNU	= 2. The height and control-chord true length are specified on the following card 17D. = 0. The previous 17D card values are used. Card 17D should not follow if AFNU = 0..
Card(s) 17D	1-10	X_O	= 0.
	11-20	Z_O	Z-coordinate at the leading edge of control chord.
	21-30	X_C	The control-chord true length. If $Z_O = Z_C = 0$, X_C may be given an arbitrary length, which is then scaled by the program to make X_C equal to the true chord length.
	31-40	Z_C	Z-coordinate of control chord at the trailing edge.

	Column	Code	Explanation
Notes:		1.	Z_O and Z_C specify the height of the wing. $Z_O = Z_C$, always; furthermore, the height of each control chord, including the tip, must be the same.
		2.	For wing-body configurations, $Z_O = Z_C$ must equal the height of the body meridian intended as the intersection meridian [Z-values, Card(s) 9D for SCODE = 6.] .
		3.	The control-chord true length X_C may be determined for AFK = 3. streamwise chords by subtracting the X-coordinates of the corresponding leading- and trailing-edge points (or by applying the right-triangle rule at an oblique chord). (See page 155).
			For AFK = 1. or 2., interpolation must be done along the planform edge to locate a point corresponding to the chord's associated planform defining point.
Card(s) 18D	1-10 : : 51-60 etc.	P_1 : : P_6	Array of constant percent chord values corresponding to the panel spanwise edges. The leading-edge value P_1 = 0.. There are PLN values required with the last value (for the trailing edge) = 100.
Card 19D	1-3	WBX	Columns 1-3 contain the letters WBX. This card indicates that a wing-body intersection is desired. For wing only or body alone cases, this card is omitted.
Card 20D	1-10		= 1. linear interpolation used on body station perimeters to compute additional points between meridian lines in the wing intersection region. See sketch on page 127 , which illustrates linear interpolation for the wing intersection.

	Column	Code	Explanation
			= 2. biquadratic interpolation used on body station perimeters to compute additional points between meridian lines in the wing intersection region.
	11-20		Dimensional intersection tolerance. Specifies the accuracy desired in locating wing-body intersection points. A value of 0.001 is suggested.
Card 21D	1-5	TDUMP	Columns 1-5 contain the letters TDUMP. This card is included if a dump of geometry definition and geometry transformation tapes is desired. See Appendix C of Part II for a detailed description of these tapes.
Card 22D	1-6	DEFEND	Columns 1-6 contain the word DEFEND. This card ends the definition set and must not be omitted.

GEOMETRY PANELING CARD SET

All paneling data, except title cards and literal statements, are punched in six-field, ten-digit format. A decimal point is required in each data field.

For body-alone case, cards 3P-14P are omitted.

For wing-alone case, cards 4P-7P are omitted.

	Column	Code	Explanation
Card 1P	1-5	PANEL	Columns 1-5 contain the word PANEL. This is the first card in the paneling link and must always follow the DEFEND card.
Card 2P	1-10		The number of source control stations at which the radius for an equivalent body of circular cross section and the actual body station centroid height are computed. A maximum of 50 stations may be requested. It is recommended that 50 stations be used. The radius at each control station is used to determine the source strength necessary to simulate the body thickness. The camber height at each control station and the body angle of attack (Card 7A) are used to determine the doublet strength necessary to simulate body camber and angle of attack.
NOTE: In a wing-alone problem, Card 2P is blank.			
	11-20		Dimensional tolerance applied to the additional points generated between meridian lines on the perimeter of body defining stations. This controls the area and centroid location calculations. A value of 0.001 is suggested.
	21-30		This field contains an interpolation code. The program first determines an equivalent radius, R, at each body defining section, X, and then establishes an R vs. X array. Interpolation for additional radii at other stations is

	Column	Code	Explanation
			performed on this array. The same technique is used to determine centroid locations. (See section 5.2, page 128.)
			= 1. linear interpolation for equivalent radii and centroid locations of the source control stations that are between body defining stations.
			= 2. biquadratic interpolation for equivalent radii and centroid locations at the source control stations that are between body defining stations.
	31-40		= 1. linear interpolation between meridian line points on the body definition sections.
			= 2. if biquadratic interpolation is desired.
	41-50		A dimensional tolerance value, E, such that if any equivalent radius length or centroid height, (z centroid), is less than E, its value will be set equal to zero. A value of 0.001 is suggested.
Card 3P	1-10	XPER	Fraction of local streamwise panel chord at which panel control point is located. 0. < XPER < 1..
			NOTE: XPER = .95 for all cases discussed in this report.
	11-20	YPER	Fraction of local panel width at which panel control point is located. 0. < YPER < 1..
			NOTE: YPER = 0. is a code used to locate the panel control point on the chord through the panel centroid. YPER = 0., for all cases discussed in this report.

	Column	Code	Explanation
Card 4P	1-10	BODY PANEL	Columns 1-10 contain the words BODY PANEL.
Card 5P	1-10	PLNB*	Number of transverse body panel edges aft of wing trailing edge-body intersection ≤ 21. See upper sketch on page 136. If PLNB = 0., omit card 6P.
	11-20	PLNW*	Number of transverse body panel edges within the wing body intersection region ≤ 16.
	21-30	TOLB	Slope tolerance on body secondary panel part leading edges. Panel parts with slopes $\left\|\frac{\Delta Y}{\Delta X}\right\|$ = TOLB in the local panel coordinate system) are eliminated. TOLB = 0.02 is suggested.
Card(s) 6P	1-10 ⋮ 51-60	$XCEPTB_1$ ⋮ $XCEPTB_6$ etc.	x-values of transverse body panel edges aft of the wing trailing edge - body intersection. There are PLNB values. Omit this card(s) if PLNB = 0. (See upper sketch, page 136.)
Card(s) 7P	1-10 ⋮ 51-60	$CODEBW_1$ ⋮ $CODEBW_6$ etc.	Each field contains an integer identifying those spanwise wing panel edges which continue around the body to form transverse body panel edges at the body intersection. The table must always start with the integer 1 and terminate with the wing trailing-edge number. See upper sketch on page 136. There are PLNW values.
Card 8P	1-10	WING PANEL	Columns 1-10 contain the words WING PANEL.
Card 9P	1-10	PLANE	Number of buttock lines which locate the streamwise wing panel edges specified by cards 10P and 11P. Wing-alone problem: PLANE is the number of buttock lines locating the streamwise panel edges including both

*(PLNB + PLNW) $\leq$ 21

Column	Code	Explanation
		the wing tip and centerline.
		Wing-body problem: PLANE is the number of buttock lines locating the streamwise panel edges, but does not include the inboard edge located by the program at the wing-body intersection. PLANE $\geq$ 2.. See sketches below.

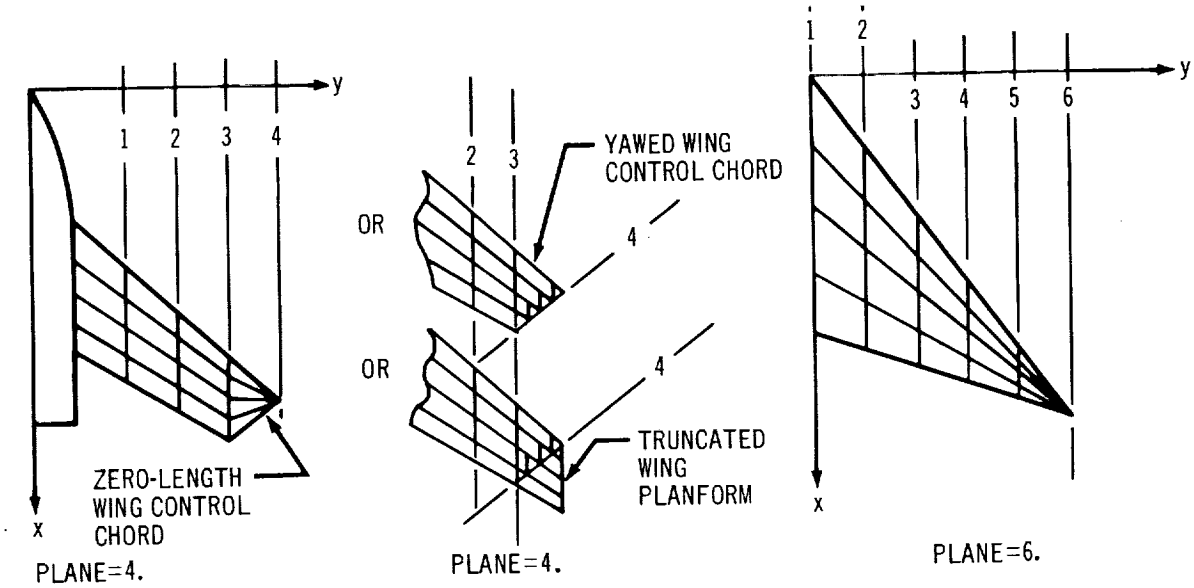

11-20	OPTF	= 1. upper and lower airfoil ordinates are read in (cards 12P and 13P) at each wing buttock line passing through the panel centroids. If the wing is untwisted and has the same airfoil section from root to tip, only one airfoil table is necessary. The program will scale this table to fit the appropriate chord.
		= 0. no tables are read in and the wing is a flat plate at zero incidence.
21-30	SNUM	Number of given airfoil ordinate tables.
		= 0., only if OPTF = 0.

	Column	Code	Explanation
			= 1., same airfoil section from wing root to tip.
			= (PLANE - 1), wing alone case airfoils specified.
			= PLANE, wing-body case airfoils specified.
	31-40	TOLW	Slope tolerance on wing secondary panel part leading edges. Panel parts with slopes $\left\lvert \frac{\Delta Y}{\Delta X} \right\rvert$ = TOLW are eliminated. TOLW = 0.01 is suggested.
Card(s) 10P	1-10 ⋮ 51-60 etc.	$YCEPT_1$ ⋮ $YCEPT_6$	Wing buttock line values at which streamwise panel edges are specified. There are (PLANE -1) values. The tip edge is specified on card 11P.
Card 11P	1-10	CPNT	Code indicating how the most outboard panel edge or wing tip is specified.

NOTE: This card controls the outboard panel edge and in no way influences the spanwise edges which are established by the geometry definition (see page 130). The outboard panel edge is usually made coincident with the definition wing tip, but it may be used to truncate the defined wing tip and the spanwise panel edges anywhere between the two outboard wing buttock lines specified by card 9P. If truncation is specified, the wing span and area are reduced.

= 0. X and Y coordinates of the wing tip leading and trailing edge are given. Use VALUE(1) through (4).

Column	Code	Explanation
		= 1. X and Y coordinates of the leading edge and the slope ($\Delta X/\Delta Y$) of the wing tip are given. Use VALUE(1), (2) and (5).
		= 2. X and Y coordinates of the trailing edge and the slope ($\Delta X/\Delta Y$) of the wing tip are given. Use VALUE(3), (4) and (5).
11-20	VALUE(1)	X-coordinate of wing tip leading edge if CPNT = 0. or 1..
21-30	VALUE(2)	Y-coordinate of wing tip leading edge if CPNT = 0. or 1..
31-40	VALUE(3)	X-coordinate of wing tip trailing edge if CPNT = 0. or 2..
41-50	VALUE(4)	Y-coordinate of wing tip trailing edge if CPNT = 0. or 2..
51-60	VALUE(5)	wing tip slope, $\frac{\Delta X}{\Delta Y}$, if CPNT = 1. or 2..

Card(s) 12P

Card(s) 12P and Card(s) 13P give the SNUM set of airfoil coordinates. These card sets (12P and 13P) are always used in pairs to define each airfoil; the coordinates apply at the centroid buttock line of each chordwise row of wing panels. The inboard row is read in first, then the next row outboard, then the next, etc. out to and including the tip row.

Chordwise biquadratic interpolation is used between input points. Thus it is recommended that XNUM (1) be 25., or nearly 25.; input points should be concentrated around regions of rapidly varying thickness and/or camber, such as the airfoil leading edge.

The card sets (12P and 13P) are omitted if OPTF = 0.

First Card	1-10	XNUM(1)	Number of points (X, Z coordinate pairs) in upper surface airfoil ordinate table. $4. \leq$ XNUM(1) $\leq 25.$.

	Column	Code	Explanation
Second Cards	1-10	$XFOIL_1$	Upper surface airfoil ordinate table. Local X and Z coordinates are given from leading edge to trailing edge. That is, the first values of ZFOIL and XFOIL entered are always zero. If the wing has no twist, an unscaled set of ordinates may be given and the program will scale the airfoil to the local chord. The section has no twist, if and only if, $ZFOIL_{upper,\ trailing\ edge} = -(ZFOIL_{lower,T.E})$
	11-20	$ZFOIL_1$	
	.	.	
	.	.	
	.	.	
	41-50	$XFOIL_3$	
	51-60	$ZFOIL_3$	
	etc.		
Cards 13P			
First Card	1-10	XNUM(2)	Number of points (X, Z coordinate pairs) in lower surface airfoil ordinate table. $4. \leq XNUM(2) \leq 25..$
Second Cards	1-10	$XFOIL_1$	Lower surface airfoil ordinate table. To input a completely uncambered section, it is recommended that XNUM(1) = XNUM(2) and that for I such that $1. \leq I \leq XNUM$, XFOIL(I), upper = XFOIL(I), lower and that ZFOIL(I), upper = - (ZFOIL(I), lower)
	11-20	$ZFOIL_1$	
	.	.	
	.	.	
	.	.	
	41-50	$XFOIL_3$	
	51-60	$ZFOIL_3$	
	etc.		
Card 14P	1-6	PANEND	Columns 1-6 contain the word PANEND. This card ends the paneling set and must be used whenever any paneling is performed. It is not needed for a body-alone problem.

AERODYNAMIC CARD SET

All aerodynamic data, except title cards and literal statements, are punched in seven-field, ten-digit format. A decimal point is required in each data field. Data Cards 1A and 2A are input only once for a given configuration and Mach number. The remaining aerodynamic data cards may be repeated as necessary to solve the selected aerodynamic cases.

	Column	Code	Explanation
Card 1A	1-11	AERO-DYNAMIC	Columns 1-11 contain the word AERODYNAMIC.
Card 2A	Select and input one of the following data control cards. (See p. 139.)		
	1-7	COMPUTE	The aerodynamic matrices and geometry data are not saved on computer tape; this card is used when a defined and paneled configuration is input. Use the word SCRATCH on the tape usage card. *
	1-9	SAVE TAPE	The aerodynamic matrices and geometry data are saved on tape for repeated analysis. The body and wing thickness and camber from the goemetry section are also saved for optional use. This card is used when a defined and paneled configuration is input. Use the word SAVE on the tape usage card. *
	1-8	USE TAPE	A previously saved aerodynamic computer tape is to be used; no definition nor paneling data are input when this option is selected. Use the word MOUNT on the tape usage card; also, input the appropriate tape number in Columns 15-21 and the word IN/OUT in Columns 34-39 of the tape usage card. *
Card 3A	1-10	XMACH	Mach number.
	11-20	SYM	= 0. the aerodynamic problem solved is asymmetric about the vertical X-Z plane (image panels not included, see page 56).
			= 1. the aerodynamic problem solved is symmetric about the vertical X-Z plane (image panels included, see page 56).

*Peculiar to Boeing system

	Column	Code	Explanation
Card 4A	1-72	TITLE	Any desired title.
Card 5A	1-10	CASE	= 1. calculates wing twist and camber for a given ΔC_p distribution on wing where $\Delta C_p = C_{p\ lower} - C_{p\ upper}$ = 2. calculates pressure distribution over the configuration. Wing and body camber can be changed within this option. = 3. optimizes wing twist and camber for minimum drag. NOTE: For body-alone problems, only case = 2. option is available.
	11-20	CPCALC	= 0. C_p calculations use linear equation; $C_p = -2u$. = 1. C_p calculations use nonlinear equation $C_p = -2u + \beta^2 u^2 - v^2 - w^2$ = 2. C_p calculations use the "exact" isentropic equation on the isolated body and the linear equation on the wing and body panels. The "exact" isentropic equation is $C_p = \frac{2}{\gamma M_\infty^2} \left\{ \left[1 + \frac{\gamma - 1}{2} M_\infty^2 \left(1 - (1+u)^2 + v^2 + w^2 \right) \right]^{\frac{\gamma}{\gamma - 1}} - 1 \right\}$ where M is the mainstream Mach number, U is the mainstream velocity and γ (1.4) is the coefficient of specific heats.
	21-30	POLAR	= 0. drag polar not requested. = 1. drag polar requested. A series of incremental angles of attack is specified on Card(s) 15A.
	31-40	THICK	= 0. wing thickness pressures are not calculated. = 1. wing thickness pressures are calculated.

	Column	Code	Explanation
	41-50	VOUT	= 0. the velocity components are not printed. = 1. the velocity components are printed.
Card 6A	1-10	RFAREA	Half-wing reference area. If this field is left blank, the program sums the wing panel areas to obtain the reference area which is the half-wing exposed area. For the body-alone problem, a value must be input, or a unit area is used.
	11-20	XP	x-coordinate about which the pitching moments are computed.
	21-30	ZP	z-coordinate about which the pitching moments are computed.
	31-40	CBAR	= 0. Unit (1.) reference chord length to be used in pitching-moment calculations. = CBAR, Reference chord length of CBAR to be used.
	41-50	SEMIS	= 0. Unit (1.) wing semispan to be used in spanwise C_L, C_D calculations. = SEMIS, Wing semispan of SEMIS to be used.

Card 7A — For configurations that include a body, the body angle of attack is specified on this card.

1-10	ARB	Body angle of attack (degrees).

Card 8A — For configurations that include a body, two options are available for specifying the body radii. The first word on the first card indicates the type of input. Omit this card set for wing-alone problems.

1-5	Option A = GIVEN. The body radii to be used are those calculated in the geometry definition section. No additional cards are needed.
1-72	Option B = Identifying title. Any title calls the option of inputting body radii directly. The radii from the geometry section are superseded.

Column	Code	Explanation
Card(s) 8AB (used only with Option B)		
1-10	R_1	The body radii are input on these cards. They are input from nose to tail and apply at the source control stations generated by the paneling section. There are XNRX radii required (Card 2P, columns 1-10).
11-20	R_2	
.	.	
:	:	
61-70	R_7	
etc.		

Card 9A — For configurations that include a body, two options are available for specifying body camber. The first word on the first card is the key to the type of input the program expects. Omit this card set for wing-alone problems.

1-5	GIVEN	Option A Columns 1-5 contain the word GIVEN.
7-80	Any additional identifying symbols	The program takes the body camber as that calculated in the geometry definition section. No additional cards are necessary for this option.
1-80	Any identifying symbols	Option B The first card contains any arbitrary identifying symbols (other than GIVEN or CONSTANT as the first word) to describe the body camber. The program expects more cards immediately to specify the body camber.

Card(s) 9AB (used only with Option B)		
1-10	Z_1	The body camber is input on these cards as Z-heights of body cross sections at the source control stations. The values are input from nose to tail; there are XNRX values required (Card 2P, columns 1-10).
11-21	Z_2	
.	.	
.	.	
.	.	
61-70	Z_7	
etc.		

Card 10A — Calculates wing twist and camber for a given wing ΔC_p distribution (CASE = 1., field 1 of Card 5A). Two options are available for specifying the ΔC_p distribution. These options are selected by the first word on the first card of this set. Omit this set for body-alone problems or CASE = 2. or 3.

Column	Code	Explanation
1-8	CONSTANT	Option A Columns 1-8 contain the word CONSTANT.
9-80	Any additional identifying symbols	This option restricts the wing to have a constant ΔC_p distribution. This constant value is specified on the following card. Recall that $\Delta C_p = C_{p\ lower} - C_{p\ upper}$
1-80	Any identifying symbols	Option B The first card contains appropriate identifying symbols (other than GIVEN or CONSTANT as the first word) to select Option B. ΔC_p for each panel is specified on the following card set.

Card 10AA (used only with Option A)

1-10	ΔC_p	ΔC_p for Option A.

Card(s) 10AB (used only with Option B)

1-10	ΔC_{p_1}	ΔC_p's for Option B. This array must be ordered starting with the inboard panel at the leading edge and running aft to the trailing edge, then proceeding outboard to the tip in the same manner. There must be the same number of values as there are wing panels. Values apply at panel centroids.
.	.	
.	.	
.	.	
.	.	
61-70	ΔC_{p_7}	
etc.		

Card 11A For configurations that include a wing and for which CASE (Card 5A) = 2, the wing angle of attack and an optional twist distribution are indicated on these cards.

1-10	ARW	Wing angle of attack (relative to body axis if wing-body configuration)
11-20	TWIST	= 0. No twist distribution to be given. = 1. Twist distribution to be specified on following cards.

Card(s) 11AA (used only if TWIST = 1.)

1-10	$ARWT_1$	Twist angle for successive wing panel columns; $ARWT_1$ applies to the inboard-most column.
11-20	$ARWT_2$	
.	.	
.	.	
61-70	$ARWT_7$	
etc.		

Column	Code	Explanation

NOTE: Card 11AA is repeated until an angle for each column of wing panels is given. Do not use Card 11AA if TWIST (Card 11A) = 0.

Card 12A Calculates the pressure distribution over the configuration (CASE = 2., field 1 of Card 5A). Three options are available for specifying the camber shape of the wing. The options are selected by the first word on the first card of this set. Omit this set for body-alone problems or CASE = 1. or 3..

		Option A
1-8	CONSTANT	Columns 1-8 contain the word CONSTANT. This option restricts the wing camber shape to have a constant slope for each wing panel. This constant value is specified on the following card.
9-80	Any other identifying symbols	
		Option B
1-5	GIVEN	The wing camber shape is specified by the input geometry. The panel slopes used are those generated in the paneling section of the program. In this case, no more cards are needed.
7-80	Any other identifying symbols	
		Option C
1-80	Any identifying symbols	Appropriate identifying symbols (other than GIVEN or CONSTANT as the first word) on the first card of this set are used to select this option. The wing camber shape is specified by a slope for each panel. Other cards must be input which contain the slope values.

Card 12AA (used only with Option A)

1-10	$\Delta Z/\Delta X$	The constant wing panel slope for Option A.

There is no auxiliary card for Option B.

Card(s) 12AC (used only with Option C)

1-10	$\Delta Z_1/\Delta X_1$	Wing panel slopes for Option C. The array must be ordered starting with the inboard panel at the leading edge and running aft to the trailing edge, then proceeding outboard to the tip in the same manner. There must be the same number of values as there are wing panels. Values apply to panel control points.
.	.	
.	.	
.	.	
61-70	$\Delta Z_7/\Delta X_7$	
etc.		

	Column	Code	Explanation
Card 13A			Optimized wing twist and camber for minimum drag (CASE = 3., field 1 of Card 5A). Two options are available. The first option optimizes the wing for a given wing-lift constraint, and the second option optimizes the wing for both the wing-lift and center-of-pressure constraints. Only one data card is required. Omit this card for a body-alone problem or CASE = 1. or 2.
	1-10	CONSNT	= 0. the wing is optimized for minimum drag with a wing-lift constraint. = 1. the wing is optimized for minimum drag with both wing-lift constraint and x-coordinate of the center-of-pressure constraint.
	11-20	CLBAR	Wing-lift-coefficient constraint.
	21-30	XCPBAR	The x-coordinate of the wing center-of-pressure constraint. If the center of pressure is not constrained, omit this field.
Card 14A			For configurations that include a wing and for which THICK (Card 5A) = 1., two options are available for specifying the wing thickness distribution. The first word on the first card indicates the type of input. Omit this set if THICK = 0.
	1-5		Option A = GIVEN. The wing thickness distribution to be used is that computed in the geometry paneling section. No more cards are needed.
	1-72		Option B = Identifying title. The wing thickness distribution is input on the following cards.
Card(s) 14AB (use only with Option B)			
	1-10	$ALPHAT_1$	Wing thickness slopes. For the purpose of these cards, wing thickness is the distance from the airfoil camber line to either airfoil surface. A leading-edge thickness slope (less than the tangent of the Mach angle) is given for the inboard wing-panel column and followed by thickness slopes for each panel in that column of the wing panels. This is repeated for each wing-panel column. The total number of input wing-thickness slopes equals the number of wing panels plus the number of panel columns.
	11-20	$ALPHAT_2$	
	21-30	$ALPHAT_3$	
	.	.	
	.	.	
	.	.	
	61-70	$ALPHAT_7$	

	Column	Code	Explanation
Card(s) 15A	1-10	DADEG	If drag polar is requested (POLAR = 1. on Card 5A), incremental angles of attack (in degrees) are specified on Card(s) 15A. A terminating blank card is used. Omit this card set if Polar option is not selected (POLAR = 0.) (one per card).
Card(s) 16A	1-72	(blank)	(This is a blank card.) To conduct an additional aerodynamic analysis, begin the new set of aerodynamic data with Card 4A. To terminate the data of the last analysis or to call the flow visualization section, place two Card(s) 16A after the terminating polar card.

If flow visualization of the last angle of attack of the last analysis is desired, place Card 1F of the Flow Visualization section in this position. If no visualization is desired, terminate with the following card.

Card 17A	1-11	END OF DATA	

FLOW VISUALIZATION CARD SET

All flow visualization data, except title cards and literal statements, are punched in seven-field, ten-digit format. A decimal point is required in each data field. This card-set instruction applies to any type of configuration and any type of aerodynamic analysis. Only the last angle of attack of the last aerodynamic analysis is visualized.

	Column	Code	Explanation
Card 1F	1-8	FLOW VIZ	Columns 1-8 contain the word FLOW VIZ. This card calls the Flow Visualization section of the program.
Card 2F	1-10	CPCALC	= 0. The linear C_p equation is used to calculate field pressure points. = 1. The nonlinear C_p equation is used. = 2. The "exact" isentropic equation is used. The C_p equations are defined for Card 5A of the aerodynamic set.
	11-20	CAMN	= 0. Influence of all singularities included in calculation of velocity components. = 1. Influence of wing and body constant pressure panels not included in calculation of velocity components. If lifting and interference effects are not of interest, selecting this option saves much computer time.
	21-30	POP	= 0. Perturbation velocity components are not printed. = 1. Perturbation velocity components are printed. NOTE: This printout option does not apply to any STREAMLINES case.

NOTE: The three modes of flow visualization (grids, streamlines, and points) may be called in any order and any number of times by inputting the appropriate literal card.

Card 3F	1-5	GRIDS	Columns 1-5 contain the word GRIDS. This card calls the grid mode of flow visualization.

	Column	Code	Explanation
Card 3FA	1-10	XNG	The number of two-dimensional or three-dimensional grid structures (an integer); any number may be requested.
Card 3FB	1-10	XO	The rectangular coordinates of the origin of the grid structure.
	11-20	YO	
	21-30	ZO	
	31-40	XA	The rectangular coordinates of a point which, together with the origin (above), defines an axis of a skew grid; the positive direction is from the origin to point A. (See figure 30.)
	41-50	YA	
	51-60	ZA	
			Enter values only if a skew grid is called; AMD (Card 3FC) = 4.
	61	LIT	= X Select and input the letter of the = Y coordinate axis which is used to- = Z gether with the skew axis defined above to define the two-dimensional skew grid.
			Enter a letter only if AMD = 4.
Card 3FC	1-10	DX	Values of increments which position points on the grid. If a two-dimensional grid is desired, set one of the increments to zero and the corresponding increment count (next three fields) to 1..
	11-20	DY	
	21-30	DZ	
	31-40	XN	The respective number of increments which position points on the grid (each an integer). If AMD = 1., YN × ZN $\leq$ 500. If AMD = 2., XN × ZN $\leq$ 500. If AMD = 3., XN × ZN $\leq$ 500.
	41-50	YN	
	51-60	ZN	
	61-70	AMD	This code controls the format in which the data is output. = 1. Data is output for all the (Y, Z) points at a given X-value; then the data for the next X-value, etc. Always select this code value when DX = 0. = 2. Data is output for all the (X, Z) points at a given Y-value; then the data for the next Y-value, etc. Always select this code value when DY = 0.

	Column	Code	Explanation
			= 3. Data is output for all the (X, Y) points at a given Z-value; then the data for the next Z-value, etc. Always select this code value when DZ = 0.
			= 4. A skew grid has been specified for the plane defined by LIT-axis and the line from the origin through point A. The following notes apply.

NOTES: 1. Increments and the number of increments determining points on a skew grid are input in the following way: The axis specified by LIT is input as if for a rectangular array. One of the other two axes is input with zero (0.) increment size and number. The remaining axis is input as if for a rectangular array also, but its graduations apply to the skew axis; planes are established normal to the remaining axis through each of its graduations. Where these planes intersect the skew axis, a skew-axis graduation is established. (See figure 30.)

2. Repeat Card 3FB and Card 3FC for each grid called. That is, there must be XNG sets of Cards 3FB-3FC.

Card 4F	1-11	STREAMLINES	This word appears in columns 1-11 and calls the streamlines option.
Card 4FA	1-10	DXMAX	The maximum permissible step size for the streamline's integrator. A value of 10. × XDELT is recommended.
	11-20	DXMIN	The minimum permissible step size for the streamline's integrator. DXMIN > 0., always. A value of 0.1 × XDELT is recommended.
	21-30	PRINT	The result is a series of points in rectangular coordinates (X, Y, Z) from XMIN through point S to XMAX. The values of X are determined by this code. (See Card 4FC.)
			= 0. Points are printed out in even increments of XDELT.
			= 1. Points are generated by the integrator and are printed out directly.

	Column	Code	Explanation
	NOTE:		If printout with PRINT = 1. shows that DXMIN is reached as an actual interval in printing out the results, the streamline may not be accurate. To ensure accuracy, reduce DXMIN and XDELT and repeat the calculation.
Card 4FB	1-10	XNS	The number of streamlines to be specified (an integer); any number may be requested.
Card(s) 4FC	1-10	XS	The streamlines' starting point, S. The streamline begins on the XMIN plane, proceeds downstream, passes through point S, and continues to the XMAX plane.
	11-20	YS	
	21-30	ZS	
	31-40	XMIN	The farthest point upstream and downstream to which the streamline will be calculated. The relationship XMIN $\leq$ XS $<$ XMAX must be observed.
	41-50	XMAX	
	51-60	XDELT	The initial step size for the streamline's integration. For configurations that include a wing, a value of 0.1 $\times$ (mean chord length) is recommended. For body-alone analyses, a value of 0.1 $\times$ (body length) is recommended. For streamlines passing very near the configuration, a smaller value should be used. DXMAX $>$ XDELT $>$ DXMIN, always.
			There must be exactly XNS number of Card(s) 4FC.
Card 5F	1-6	POINTS	Columns 1-6 contain the word POINTS. This card calls the points mode of the flow visualization.
Card 5FA	1-10	XP	The number of points requested (an integer); any number may be requested.
Card(s) 5FB	1-10	XF	Rectangular coordinates of point; there must be XP number of Card(s) 5FB.
	11-20	YF	
	21-30	ZF	

	Column	Code	Explanation
Card 6F	1-8	VIZEND	Columns 1-6 contain the word VIZEND. This card terminates the Flow Visualization section. The flow visualization calculations may be continued after the above data has been calculated and this card has been entered, by inputting Card 1F again and continuing the data.
Terminal Card	1-11	END OF DATA	If no further analysis is required, the run is terminated by an END OF DATA CARD.

5.4 Sample Input Formats

Program card input formats for three types of geometric configurations with successive aerodynamic cases are presented on the following pages:

Body alone. — A parabolic body of revolution with a fineness ratio of 11 is defined by 21 body stations. Ten equally spaced meridian lines are constructed. Because each body station is circular, only one radius per station is given and code 2. (on cards 6D, column 31) is used. On card 2P, 50 equally-spaced source control stations are requested. Although no body paneling is required, two panel cards (1P and 2P) are necessary to define the number of source stations and the method by which the equivalent body radii at the source stations are interpolated.

The two aerodynamic cases specified for the parabolic body are for CASE = 2. (card 4A), that is, calculations of pressure distribution over the given configuration. Both linear and exact C_p calculations are requested for two angles of attack (α = 0 degrees, is given automatically, $\Delta\alpha$ = 5 degrees is specified). Body camber is zero as given by the geometry description.

SEVEN FIELD, TEN DIGIT CRD FORMAT

1 10	11 20	21 30	31 40	41 50	51 60	61 69/70 71 72	IDENT 80
DEFINE							1D
BODY							2D
PARABOLIC BODY		L/D = 11.					3D
21.	10.	0.	0.	.001			4D
0.	20.	40.	60.	80.	100.		5D
120.	140.	160.	180.				5D
0.	0.	0.	2.	0.			6D
.05	0.	0.	2.	.00826			6D
.10	0.	0.	2.	.01569			6D
.15	0.	0.	2.	.02230			6D
.20	0.	0.	2.	.02808			6D
.25	0.	0.	2.	.03304			6D
.30	0.	0.	2.	.03717			6D
.35	0.	0.	2.	.04047			6D
.40	0.	0.	2.	.04295			6D
.45	0.	0.	2.	.04460			6D
.50	0.	0.	2.	.04543			6D
.55	0.	0.	2.	.04460			6D
.60	0.	0.	2.	.04295			6D
.65	0.	0.	2.	.04047			6D
.70	0.	0.	2.	.03717			6D
.75	0.	0.	2.	.03304			6D
.80	0.	0.	2.	.02808			6D
.85	0.	0.	2.	.02230			6D
.90	0.	0.	2.	.01569			6D
.95	0.	0.	2.	.00826			6D
1.	0.	0.	2.	0.			6D
DEFEND							22D
PANEL							1P
50.	.001	2.	2.				2P
AERODYNAMIC							1A
SAVE TAPE							2A
1.92	1.						3A
PARABOLIC BODY ONLY LINEAR CP							4A
2.	0.	1.	0.	1.			5A
0.	1.	0.					6A
0.							7A
GIVEN BODY RADII							8A
GIVEN BODY CAMBER							9A
5.							15A
							16A
PARABOLIC BODY ONLY EXACT CP							4A
2.	2.	1.	0.	1.			5A
0.	1.	0.					6A
							7A
GIVEN BODY RADII							8A
GIVEN BODY CAMBER							9A
5.							15A
							16A
							BLANK
							BLANK
END OF DATA							17A

TITLE PARABOLIC BODY ALONE NAME DATE PAGE 1 OF 1

Wing alone. — The input for a cambered and twisted arrow wing with thickness is shown on the following pages. The wing planform is defined by four points, two on the leading edge and two on the trailing edge (cards 14D, and 15D). Two points are coincident at the tip. Two control chords are given on cards 16D through 17D. The eleven constant-percent chord lines that form spanwise panel edges are specified on cards 18D. Wing buttock lines forming the ten streamwise panel edges are specified on cards 10P and 11P. A total of 100 wing panels are formed as shown in figure 35 (page 196). The remaining cards in the paneling set are airfoil ordinate tables, one table for each of the ten streamwise columns of panels. Each table specifies the thickness, camber, and twist by giving upper and lower airfoil ordinates along wing buttock lines through the spanwise centroid of each streamwise column of panels. Examples of three aerodynamic cases are given for this configuration. The first example illustrates the input card set for CASE = 1. (card 4A), calculation of wing twist and camber for constant pressure distribution, $C_L = .1$. An additional angle of attack of 5.73 degrees (0.1 radian) is also specified. The second example shows the input card set for CASE = 2., calculation of pressure distribution over a given configuration. Pressure distributions are determined at $\alpha = 0$ degrees, -2 degrees, 2 degrees, 6 degrees. The last example shows the input card set for CASE = 3., wing optimization. A constraint of $C_L = .1$ is specified; pressures and wing shape are determined for $\alpha = 0$ degrees and 5.73 degrees (0.1 radian). All the above aerodynamic cases specify linear C_p calculations.

SEVEN FIELD, TEN DIGIT CRD FORMAT

1 10	11 20	21 30	31 40	41 50	51 60	61	69/70	71	72	DENT 80
DEFINE										1D
WING										10D
CARLSON WING	2.									11D
2.	2.	2.	11.	1.	0.					12D
1.	1.	0.								13D
0.	0.	30.	10.919							14D
19.5	0.	30.	10.919							15D
3.	0.	0.	0.	2.						16D
0.	0.	1.	0.							17D
3.	0.	10.919	10.919	2.						16D
0.	0.	0.	0.							17D
0.	5.	15.	25.	35.	45.					18D
55.	65.	75.	85.	100.						18D
DEFEND										22D
PANEL										1P
0.	0.	0.	0.	0.						2P
.95	0.									3P
WING PANEL										8P
11.	1.	10.								9P
0.	.546	1.638	2.73	3.822	4.914					10P
6.005	7.097	8.189	9.281							10P
0.	30.	10.919	30.	10.919						11P
13.										12P
0.	.814	.4753	.817	.9506	.814					12P
1.9013	.80	3.8025	.75	5.7038	.655					12P
7.605	.532	9.5063	.388	11.4075	.212					12P
13.3088	0.	15.21	-.222	17.1113	-.485					12P
19.013	-.762									12P
13.										13P
0.	.814	.4753	.764	.9506	.706					13P
1.9013	.602	3.8025	.382	5.7038	.175					13P
7.605	-.0015	9.5063	-.183	11.4075	-.338					19P
13.3088	-.475	15.21	-.593	17.1113	-.668					13P
19.013	-.762									13P
13.										12P
0.	.367	.4388	.4047	.8775	.4329					12P
1.755	.463	3.51	.465	5.265	.4298					12P
7.02	.3562	8.775	.2539	10.53	.125					12P
12.285	-.0019	14.04	-.175	15.795	-.355					12P
17.55	-.5512									13P
13.										13P
0.	.376	.4388	.3574	.8775	.3319					13P
1.755	.273	3.51	.127	5.265	-.012					13P
7.02	-.15	8.775	-.2731	10.53	-.381					13P
12.285	-.461	14.04	-.513	15.795	-.5454					13P
17.55	-.5512									12P
13.										12P
0.	.132	.39	.1617	.78	.1938					12P
1.56	.2333	3.12	.2652	4.68	.2513					12P
6.24	.1668	7.8	.2244	9.36	.0829					12P
10.92	-.0211	12.48	-.1476	14.04	-.2899					12P
15.6	-.444									13P
13.										13P
0.	.132	.39	.1167	.78	.1038					

TITLE CAMBERED ARROW WING | NAME | DATE | PAGE 1 OF 1

AD 3778 81 8-8100

SEVEN FIELD, TEN DIGIT CRD FORMAT

1 10	11 20	21 30	31 40	41 50	51 60	61 69/70 71 72	DENT 80
1.56	.0643	3.12	-.0348	4.68	-.1317		13P
6.24	-.2245	7.8	-.3012	9.36	-.3861		13P
10.92	-.4141	12.48	-.4476	14.04	-.4589		13P
15.6	-.4476	14.04					13P
13.							12P
0.	.0408	.341	.0731	.6825	.1006		12P
1.365	.1431	2.73	.1863	4.095	.1984		12P
5.46	.1869	6.825	.152	8.19	.0925		12P
9.55	.0160	10.92	-.081	12.285	-.1935		12P
13.96	-.324						12P
13.							13P
0.	.0408	.341	.0341	.6825	.0226		13P
1.365	-.0039	2.73	-.076	4.095	-.146		13P
5.46	-.2061	6.825	-.2868	8.19	-.3285		13P
9.55	-.3525	10.92	-.343	12.285	-.3565		13P
13.65	-.324						13P
13.							12P
0.	.0544	.2925	.081	.585	.1055		12P
1.17	.1483	2.34	.2013	3.51	.2255		12P
4.68	.2235	5.85	.2107	7.02	.1683		12P
8.19	.1227	9.36	.053	10.53	-.0397		12P
11.7	-.144						12P
13.							13P
0.	.0544	.2925	.047	.585	.038		13P
1.17	.0813	2.34	-.0237	3.51	-.0695		13P
4.68	-.1035	5.85	-.1403	7.02	-.158		13P
8.19	-.1723	9.36	-.173	10.53	-.1667		13P
11.7	-.144						13P
13.							12P
0.	.0672	.2438	.0908	.4875	.112		12P
.975	.1485	1.95	.2031	2.925	.231		12P
3.9	.2365	4.875	.2265	5.85	.2005		12P
6.825	.159	7.8	.1031	8.775	.0333		12P
9.75	-.0512						12P
13.							13P
0.	.0672	.2438	.0628	.4875	.056		13P
.975	.043	1.95	.0161	2.925	-.015		13P
3.9	-.0445	4.875	-.066	5.85	-.0805		13P
6.825	-.087	7.8	-.0839	8.775	-.0717		13P
9.75	-.0512						13P
13.							12P
0.	.0784	.195	.099	.39	.1235		12P
.78	.1513	1.56	.1998	2.34	.2276		12P
3.12	.2373	3.9	.237	4.68	.2229		12P
5.46	.1876	6.24	.151	7.02	.1049		12P
7.8	.0432						12P
13.							13P
0.	.0784	.195	.077	.39	.068		13P
.78	.0663	1.56	.0498	2.34	.0316		13P
3.12	.0123	3.9	0.	4.68	-.0021		13P
5.46	-.0084	6.24	.001	7.02	.014		13P
7.8	.0432						13P
13.							12P
0.	.0912	.1463	.1093	.2925	.1242		12P

TITLE CAMBERED ARROW WING NAME DATE PAGE 2 OF 4

AD 3778 R1 6-8200

SEVEN FIELD, TEN DIGIT CRD FORMAT

1 10	11 20	21 30	31 40	41 50	51 60	61 69 70 71 72	DENT 80
.585	.1515	1.17	.192	1.755	.2175		12P
2.34	.2328	2.925	.236	3.51	.228		12P
4.095	.2103	4.68	.1856	5.265	.1515		12P
5.85	.1088						12P
13.							13P
0.	.0912	.1463	.0923	.2925	.0902		13P
.585	.0885	1.17	.08	1.755	.0705		13P
2.34	.0648	2.925	.060	3.51	.060		13P
4.095	.0633	4.68	.0736	5.265	.0885		13P
5.85	.1088						13P
13.							12P
0.	.104	.0975	.1199	.195	.1278		12P
.39	.149	.78	.1791	1.17	.2026		12P
1.56	.216	1.95	.2217	2.34	.2208		12P
2.73	.2138	3.12	.2007	3.51	.181		12P
3.9	.1568						12P
13.							13P
0.	.104	.0975	.1089	.195	.1058		13P
.39	.107	.78	.1041	1.17	.1046		13P
1.56	.104	1.95	.1047	2.34	.1088		13P
2.73	.1158	3.12	.1257	3.51	.139		13P
3.9	.1568						13P
13.							12P
0.	.115	.0488	.1218	.0975	.1271		12P
.195	.1385	.39	.1561	.585	.1709		12P
.78	.1832	.975	.1903	1.17	.1936		12P
1.365	.1949	1.56	.1929	1.755	.1873		12P
1.9	.1792						13P
PANEND							14P
AERODYNAMIC							1A
SAVE TAPE							2A
2.05	1.						3A
CARLSON	WING 2	CONSTANT CL					4A
1.	0.	1.	1.	1.			5A
0.	0.	0.					6A
CONSTANT CL							10A
.1							10AA
0.							11A
GIVEN WING	THICKNESS						14A
4.							15A
4.							15A
2.							15A
							16A
CARLSON	WING 2						4A
2.	0.	1.	1.	1.			5A
0.	0.	0.					6A
0.							7A
GIVEN WING	CAMBER						8A
GIVEN WING	THICKNESS						14A
2.							15A
4.							15A
							16A
CARLSON	WING 2	MIN DRAG					4A
3.	0.	1.	1.	1.			5A

TITLE CAMBERED ARROW WING NAME DATE PAGE 3 OF 4

AD 9770 01

SEVEN FIELD, TEN DIGIT CRD FORMAT

1 10	11 20	21 30	31 40	41 50	51 60	61	69 70	71	72	IDENT 80
0.	0.	0.								6A
0.	.1									13A
GIVEN WING	THICKNESS									14A
4.										15A
										16A
										BLANK
										BLANK
END OF DATA										17A

TITLE CAMBERED ARROW WING | NAME | DATE | PAGE 4 OF 4

Wing-body combination. — The card input format for a Boeing wing-body configuration is shown on the following pages. The configuration has a constant-chord swept wing, mounted below the axis of a cambered body of circular cross section. Section 6.4 describes the configuration and paneling scheme.

Along the X-axis, 24 body stations are specified. No body camber is specified in the definition card set. Eight meridian lines are requested. The θ array is specified so that a meridian line ($\bar{\theta}$ = 102.19 degrees) coincides with the wing plane. The wing planform is defined by four points and four control chords. Cards 16D and 17D contain the four chords which locate the wing 0.25 inch below the X-Y plane. Eleven equally spaced constant percent chord lines are specified on the wing. Card 3P locates the panel control points at 0.95 of the local streamwise panel chords through the panel centroids. Four transverse body panel edges aft of the wing trailing edge are located at body stations 25, 27, 29.5, and 32.415. There are no body panels aft of station 32.415.

The wing is divided into 100 panels. Wing buttock lines defining streamwise panel edges outboard of the wing-body intersection are specified on cards 10P. The nonstreamwise wing tip edge is specified on card 11P. Only one airfoil ordinate table is given since the wing has no twist or change in camber.

The input formats for two computer runs are shown. In the first run the save tape option is exercised on Card 2A. Two aerodynamic cases are specified. The first case shows the input card set required to calculate the nonlinear pressure coefficients over the wing and body at α = 0, 2, 3, 4, and 5 degrees. Body camber is specified on cards 6A at each of 50 source control stations. The x-locations of the source control stations are determined by first running the geometry definition and paneling sections of the program. (To do this, the PANEND card is immediately followed by the END OF DATA card, and all aerodynamic cards are omitted.) All force and moment coefficients are based on the half-wing area of 89.375 in.^{2}, as specified on card 6A.

The second case considered shows the input card set required to optimize the wing for minimum drag at a wing C_L of 0.1 degrees and Mach 1.8. Body camber is again specified. The END OF DATA card terminates the input. Discussion of results obtained for the Boeing wing-body configuration from a similar set of input cards is contained in section 6.4.

The second computer run, which uses the previously saved 'save tape,' consists of an analysis of the wing-body model with zero wing camber and at 6-degree angle of attack. A flow visualization of that case follows. All three flow visualization options are exercised.

A series of points defining a ring under the wing is specified in the POINTS option (Cards 5F-5FB). Velocity components are calculated at these points.

Four grids are defined in the GRIDS option (Cards 3F-3FC). One three-dimensional grid is positioned behind and under the wing near the body. Three one-dimensional line grids are positioned at a radius of one body length at various angles (θ = 0, 90, and 180 degrees). Velocity components, perturbation velocity components (POP = 1., Card 2F), and pressure coefficients are calculated at the points defined by these grids.

In the STREAMLINE option (Cards 4F-4FC), three streamlines are called for. Velocity components and pressure coefficients are also calculated along each streamline. The linear-pressure-coefficient formula is specified on Card 2F for all flow visualization options. The flow visualization is terminated by the VIZEND card, and the run is terminated by an END OF DATA card. Section 4.8 is a discussion of the results obtained for flow visualization around the Boeing wing-body configuration.

SEVEN FIELD, TEN DIGIT CRD FORMAT

1 10	11 20	21 30	31 40	41 50	51 60	61 69 70	71	72	IDENT 80
DEFINE									1D
BODY									2D
TR-805/EQUIVALENT/BODY									3D
24.	8.								4D
0.	25.	50.	75.	102.19	130.				5D
155.	180.								5D
0.	0.	0.	2.	0.					6D
1.5	0.	0.	2.	.270					6D
3.	0.	0.	2.	.4464					6D
4.5	0.	0.	2.	.5943					6D
6.	0.	0.	2.	.7234					6D
7.5	0.	0.	2.	.837					6D
9.	0.	0.	2.	.9364					6D
10.5	0.	0.	2.	1.0223					6D
12.	0.	0.	2.	1.0936					6D
13.5	0.	0.	2.	1.1479					6D
15.	0.	0.	2.	1.184					6D
15.1	0.	0.	0.						6D
17.5	0.	0.	0.						6D
20.	0.	0.	0.						6D
22.5	0.	0.	0.						6D
25.	0.	0.	0.						6D
27.5	0.	0.	0.						6D
29.9	0.	0.	0.						6D
31.	0.	0.	2.	1.174					6D
32.	0.	0.	2.	1.154					6D
33.	0.	0.	2.	1.124					6D
34.	0.	0.	2.	1.084					6D
35.	0.	0.	2.	1.034					6D
36.	0.	0.	2.	1.					6D
WING									10D
TR-805 WING	(TWP = -.25)								11D
2.	2.	4.	11.	1.	0.				12D
1.	1.	.001							13D
10.67	0.	40.27	10.774						14D
19.88	0.	43.518	8.603						15D
3.	0.	0.	0.	2.					16D
0.	-.25	9.21	-.25						17D
1.	0.	5.							16D
1.	70.	10.774	0.	2.					16D
0.	-.25	3.15	-.25						17D
3.	0.	10.774	8.603	2.					16D
0.	-.25	3.9068	-.25						17D
0.	10.	20.	30.	40.	50.				18D
60.	70.	80.	90.	100.					18D
WBX									19D
2.	.0001								20D
DEFEND									22D
PANEL									1P
50.	0.	1.	1.	.001					2P
.95	0.								3P
BODY PANEL									4P
4.	11.	.02							5P
25.	27.	29.5	32.415						6P

TITLE BOEING WING-BODY MODEL | NAME | DATE | PAGE 1 OF 3

SEVEN FIELD, TEN DIGIT CRD FORMAT

1 10	11 20	21 30	31 40	41 50	51 60	61 69	70 71	72	OPNT 80
1.	2.	3.	4.	5.	6.				7P
7.	8.	9.	10.	11.					7P
WING PANEL									8P
10.	1.	1.	.05						9P
1.7	2.62	3.54	4.46	5.38	6.3				10P
7.22	8.14	8.603							10P
0.	10.27	10.774	43.518	8.603					11P
15.									12P
0.	0.	.025	.0108	.05	.01556				12P
.1	.02155	.15	.02548	.2	.02832				12P
.3	.03215	.4	.0342	.5	.03385				12P
.6	.03112	.7	.02599	.8	.01915				12P
.9	.01084	.95	.00616	1.	0.				12P
15.									13P
0.	0.	.025	.00257	.05	.00325				13P
.1	.00428	.15	.0051	.2	.00581				13P
.3	.00701	.4	.00735	.5	.0065				13P
.6	.00469	.7	.00239	.8	.00068				13P
.9	0.	.95	0.	1.	0.				13P
PANEND									14P
AERODYNAMIC									1A
SAVE TAPE									2A
1.8	1.								3A
TR 805	GIVEN SHAPE								4A
2.	1.	1.	1.	1.					5A
89.375	0.	0.							6A
0.									7A
GIVEN BODY RADII									8A
TR-805 BODY CAMBER									9A
-.2	17	.152	.136	.123	1.111	1.10			9AA
.089	.078	.0675	.058	.048	.04	.032			9AA
-.025	.019	.013	.008	.004	.001	0.			9AA
0.	0.	0.	0.	0.	0.	0.			9AA
0.	0.	0.	0.	0.	0.	0.			9AA
0.	0.	0.	0.	0.	0.	0.			9AA
0.	0.	0.	0.	0.	0.	0.			9AA
0.									9AA
0.									11A
GIVEN WING CAMBER									12A
GIVEN WING THICKNESS									14A
2.									15A
2.									15A
									16A
TR 805	MIN DRAG								4A
3.	1.	0.	1.	1.					5A
89.375	0.	0.							6A
									7A
GIVEN BODY RADII									8A
TR 805 BODY CAMBER (ALPHA BODY									9A
0.	.025	.043	.056	.068	.079	.089			9AA
.099	.108	.1165	.125	.134	.142	.148			9AA
.156	.162	.167	.172	.175	.178	.180			9AA
.179	.1779	.1768	.1757	.1746	.1735	.1724			9AA
.1713	.1702	.1691	.168	.1679	.1668	.1657			9AA

TITLE BOEING WING BODY MODEL NAME DATE PAGE 2 OF 3

SEVEN FIELD, TEN DIGIT CRD FORMAT

1 10	11 20	21 30	31 40	41 50	51 60	61				IDENT 80
.1646	.1635	.1624	.1613	.1602	.1591	.158				9AA
.1569	.1558	.1547	.1536	.1525	.1514	.1503				9AA
.1492										9AA
0.	.159									13A
GIVEN WING	THICKNESS									14A
										16A
										BLANK
										BLANK
END OF DA	TA									17A

TITLE BOEING WING-BODY MODEL NAME DATE PAGE 3 OF 3

SEVEN FIELD, TEN DIGIT CRD FORMAT

1 10	11 20	21 30	31 40	41 50	51 60	61	69/70	71	72	IDENT 80
AERODYNAMIC										1A
USE TAPE										2A
1.8	1.									3A
TR 805 FLOW VISUALIZATION CASE										4A
2.	0.	0.	1.	1.						5A
89.375	0.	0.								6A
6.										7A
GIVEN BODY RADII										8A
GIVEN BODY CAMBER										9A
0.										11A
CONSTANT WING CAMBER										12A
0.										12AA
GIVEN WING THICKNESS										14A
										16A
										16A
FLOW VIZ										1F
0.	0.	1.								2F
POINTS										5F
9.										5FA
24.	4.	-1.								5FB
24.	4.	-.5								5FB
24.	4.3535	-.6465								5FB
24.	4.5	-1.								5FB
24.	4.3535	-1.3535								5FB
24.	4.	-1.5								5FB
24.	3.6465	-1.3535								5FB
24.	3.5	-1.								5FB
24.	3.6465	-.6465								5FB
GRIDS										3F
4.										3FA
30.	1.2	-1.2								3FB
.5	1.	.5	10.	3.	2.	2.				3FC
50.	0.	36.								3FB
2.	0.	0.	51.	0.	0.	2.				3FC
50.	36.	0.								3FB
2.	0.	0.	51.	0.	0.	2.				3FC
50.	0.	36.								3FB
2.	0.	0.	51.	0.	0.	2.				3FC
STREAMLINES										4F
5.	.01	1.								4FA
3.										4FB
28.	5.	.25	40.	20.	.1					4FC
28.	5.	-.5	40.	20.	.2					4FC
15.4	1.5	0.	30.	0.	.1					4FC
VIZEND										6F
END OF DATA										7F

TITLE BOEING WING-BODY MODEL | NAME | DATE | PAGE 1 OF 1

6. EXPERIMENTAL VERIFICATION

Four comparisons of experimental data with computed data are presented and discussed here. The first comparison, in section 6.1, is for a parabolic body. Section 6.2 discusses two arrow wings, one with camber and thickness and one with thickness only. Pressure distributions at three angles of attack are compared for each wing. Finally, two constant-chord wing-body configurations are considered in sections 6.3 and 6.4. One configuration has an unswept wing, and the second has wing leading edges swept behind the Mach cone. Body and wing pressure distributions are compared for both configurations.

6.1 Body Alone

Wind-tunnel pressure data for a body of revolution with a parabolic profile are published in reference 19. The fineness ratio of the body is 11. The pressure coefficients measured on the body at Mach 1.93 for zero incidence are shown in the lower half of figure 34, and are compared with pressure coefficients calculated by the three pressure-coefficient formulas in the program. The longitudinal pressure distributions for zero angle of attack calculated by the exact and nonlinear formulas agree closely with the wind-tunnel data.

The circumferential pressure distributions predicted by the exact formula for the lifting case ($\alpha = 5$ degrees) closely match the experimental data. There is some discrepancy near the top of the body ($\theta = 0$), part of which is probably due to boundary-layer growth and separation. The pressure distributions predicted by the linear and nonlinear formulas do not closely match the experimental data, but they show similar trends and C_p levels.

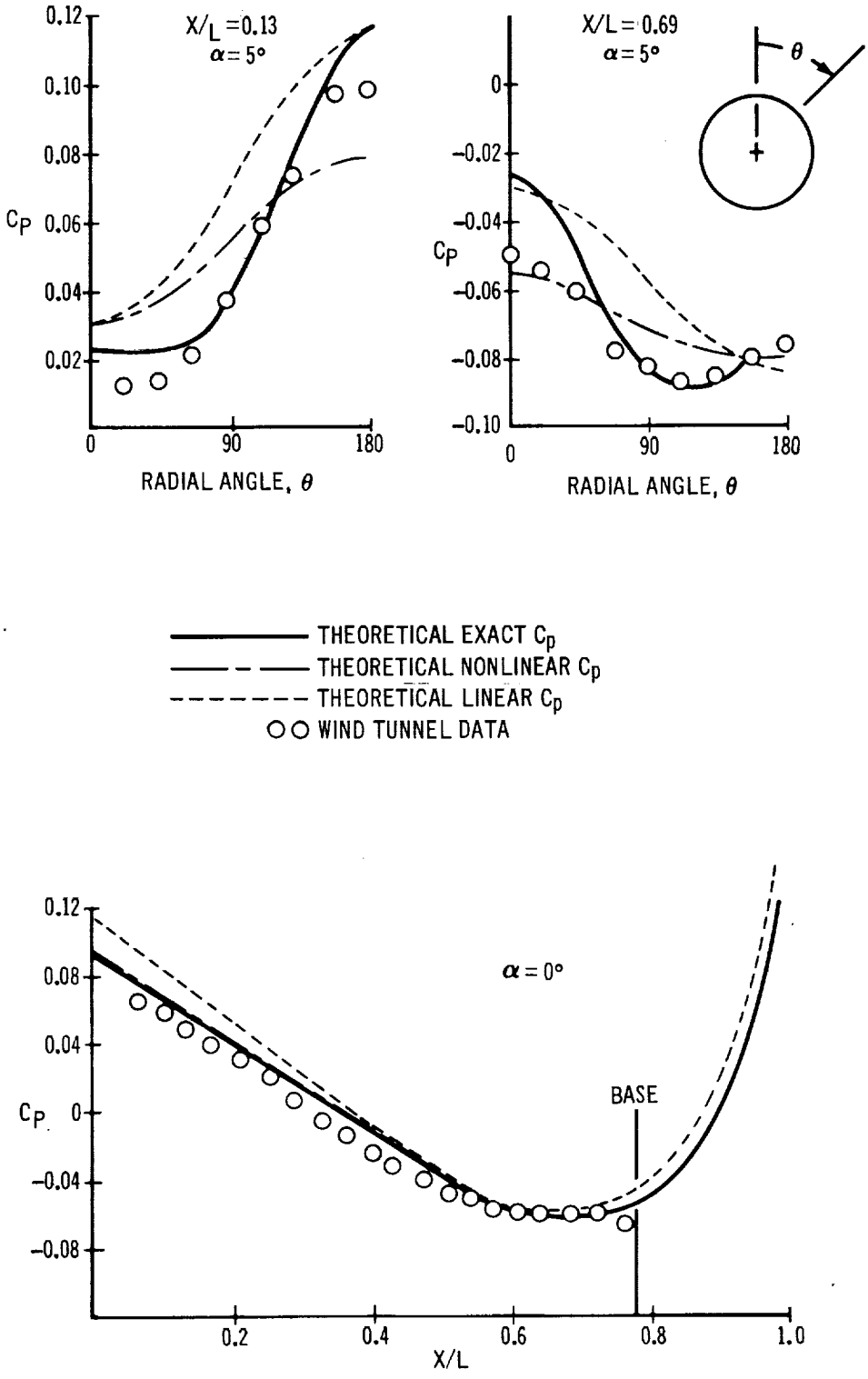

FIGURE 34 COMPARISON OF THEORETICAL AND EXPERIMENTAL PRESSURE DISTRIBUTIONS ON A PARABOLIC BODY OF REVOLUTION AT M = 1.93. FINENESS RATIO = 11.

6.2 Wing Alone

Two arrow wings of identical planform were analyzed. A complete tabulation of the experimental data for both wings is presented in reference 18. Both wings have a 3-percent biconvex symmetrical thickness distribution. Wing 1 (figure 36) has no camber or twist. Wing 2 (figure 37) is cambered and twisted to give theoretical minimum drag at a design C_L of 0.08 for a given leading edge pressure constraint. Comparison of experimental and theoretical data is made at Mach 2.05 and presented at five spanwise stations for three angles of attack. Figure 34 shows the planform and the 100-panel layout for both wings. The paneling was chosen so that the spanwise locations of the calculated pressures corresponded to the pressure taps on the test wings.

Agreement between the theoretical data and experimental data is good, except near the tip, for both wings at low and moderate angles of attack. At higher angles of attack the experimental pressure distributions show a distinct change in pattern and no longer agree with linear theory predictions. This is probably associated with an overexpansion of the flow on the upper surface, followed by the formation of a shock wave and vortex.

Satisfactory prediction of lift curves and drag polar shapes is illustrated by the Wing 2 comparison shown below:

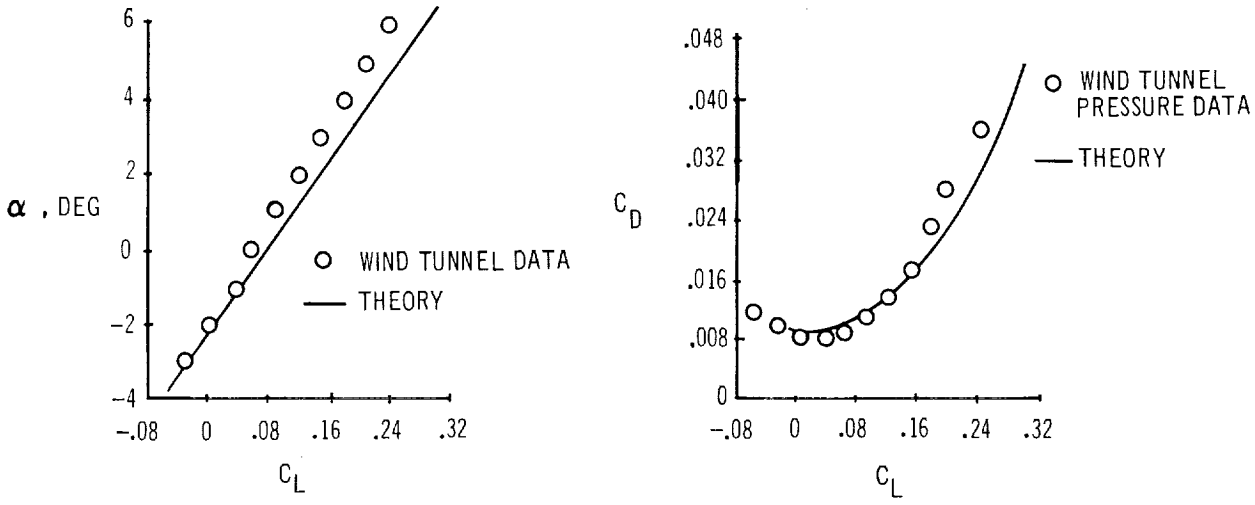

The pressure distributions predicted by the program also agree well with the linear theory calculations presented in reference 18.

PANEL LAYOUT USED FOR
PRESSURE DISTRIBUTION
COMPARISON

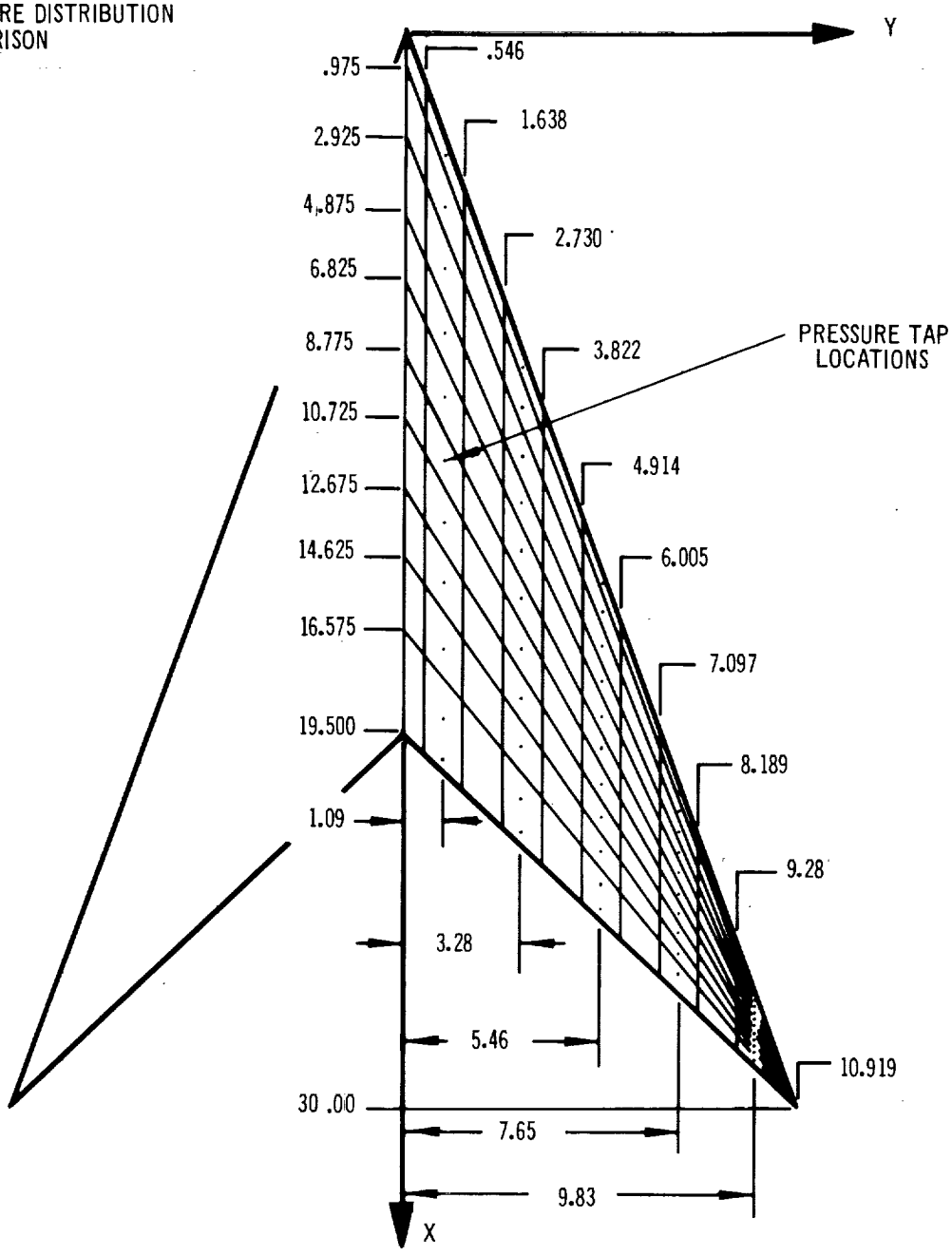

FIGURE 35 ARROW WING PLANFORM AND PANELING DESCRIPTION

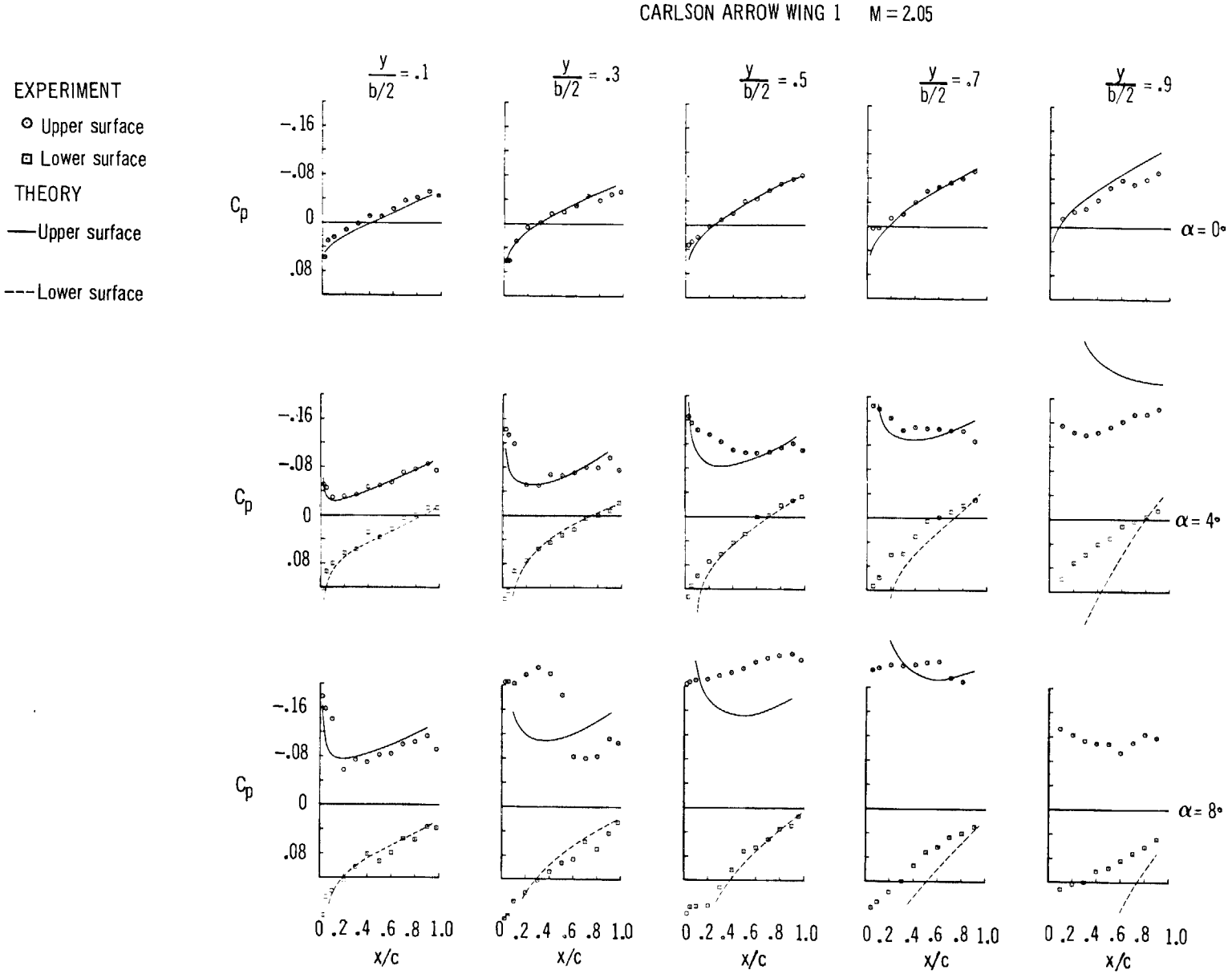

FIGURE 36 THEORETICAL AND EXPERIMENTAL PRESSURE DISTRIBUTIONS FOR AN UNCAMBERED ARROW WING

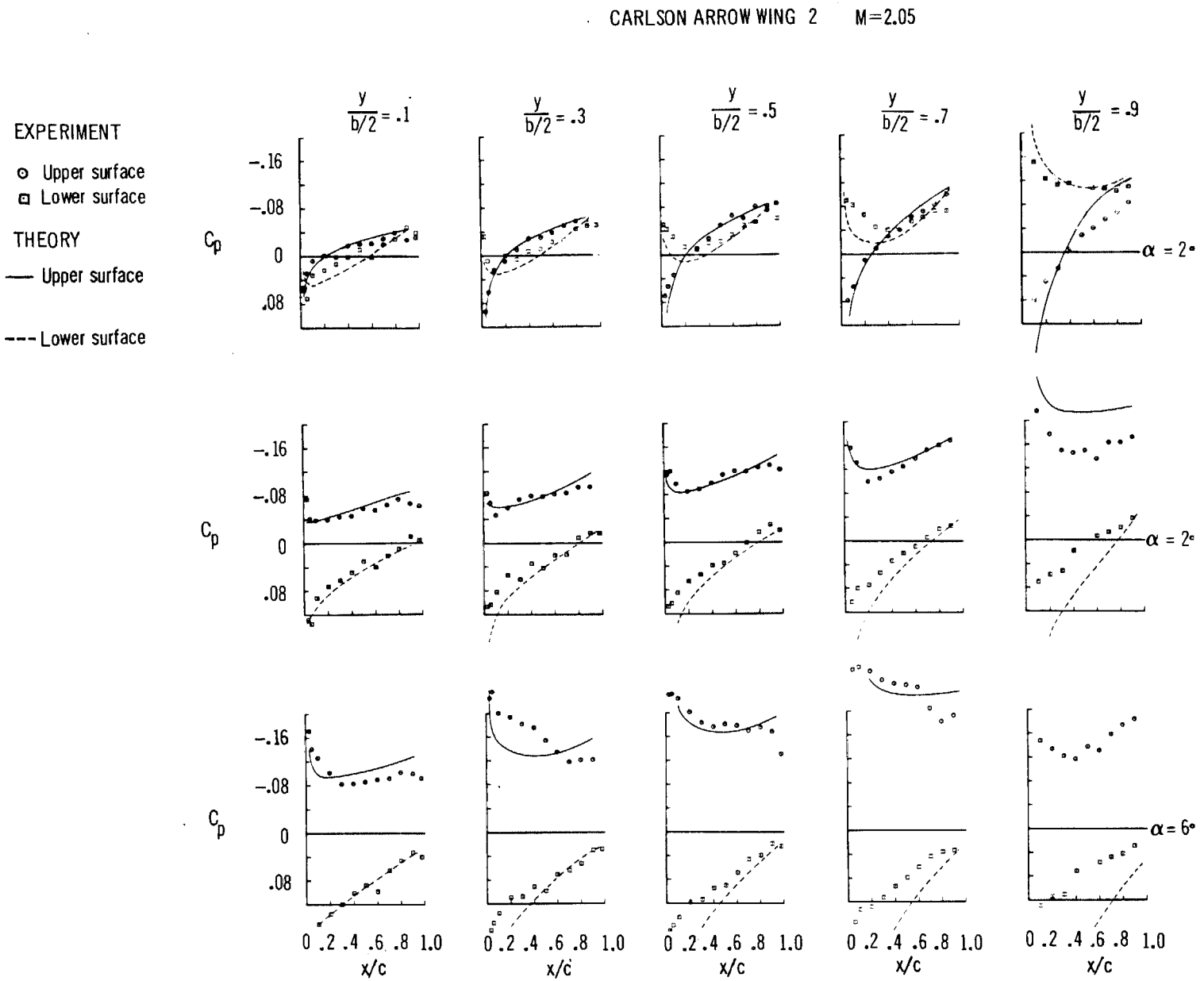

FIGURE 37 THEORETICAL AND EXPERIMENTAL PRESSURE DISTRIBUTIONS FOR A CAMBERED AND TWISTED ARROW WING

6.3 Nielsen Wing-Body

A classical experiment in wing-body interference was reported by Nielsen in reference 15. The configuration tested was a circular body of revolution with an ogival nose and an unswept, constant-chord wing with a 10-percent thick wedge-shaped airfoil. Model dimensions and configuration paneling are shown in figure 38. The model was equipped with apparatus to permit changing the wing incidence relative to the body axis. Data comparisons are made for the wing at incidence to the body, and for the wing and body at the same angle of attack. Only the incremental pressure coefficients above the values obtained for the wing and body at zero incidence are shown.

For this analysis, the wing is assumed to have no thickness. The half-wing planform is divided into one hundred equal-area panels as shown in figure 38. The half-body region aft of the wing leading edge is represented by six equal longitudinal strips of fourteen panels each. The calculated pressure distributions at Mach 1.48 are presented in figures 39 through 42 at five spanwise wing stations and for three body meridians. In figure 39, the calculated pressure distributions are compared with Nielsen's theoretical predictions and the experimental data for α_{wing} = 1.92 degrees; the body incidence is zero for this example. Both theoretical results for wing pressures agree well, except in the region enclosed by the Mach cone from the tip, y/r = 3.92, where the present theory tends to smooth out the pressure discontinuity. However, the program data does show acceptable agreement with the experimental data. The present theory for body pressures does not agree closely with Nielsen's predictions but does show excellent agreement with the wind-tunnel data.

Figures 41 and 42 show pressure data comparisons for the wing and body at the same angle of attack. The Mach number is 1.48 and the experimental data is for $\alpha_{wing} = \alpha_{body}$ = 2 degrees. Both theories again show agreement, except on the body, where the pressures calculated by the program show closer correlation to the experimental data.

The wind-tunnel test Reynolds number for both cases above is 1.5 million.

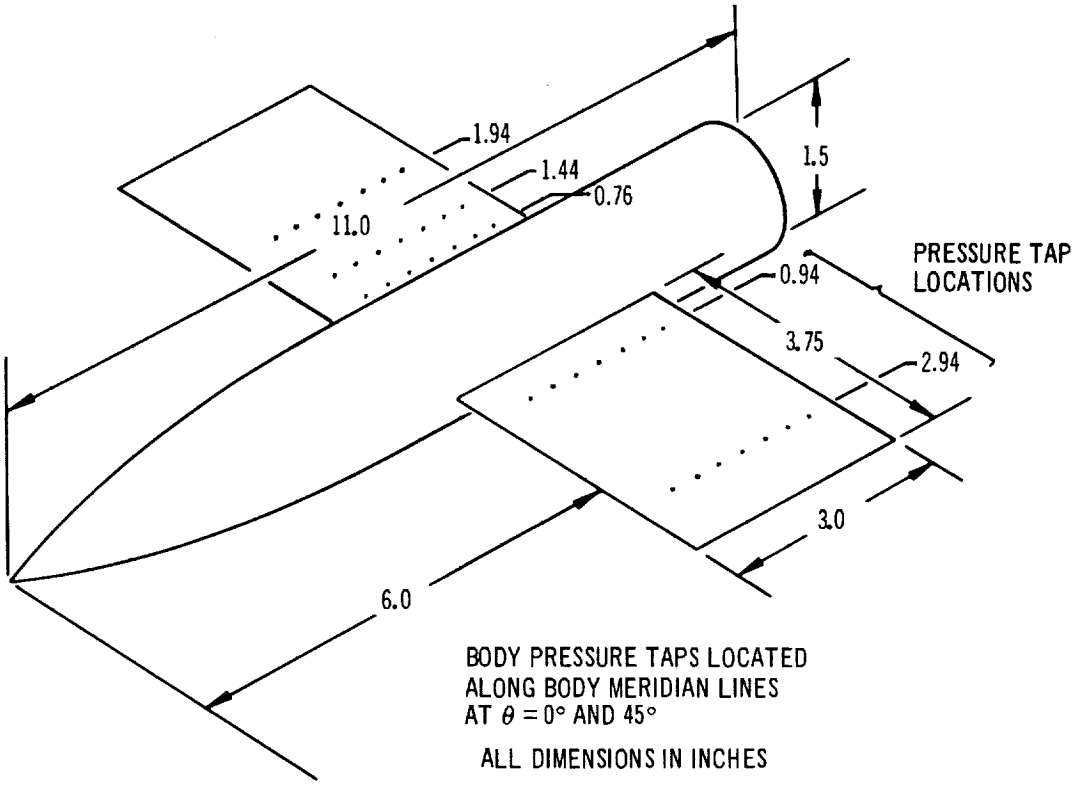

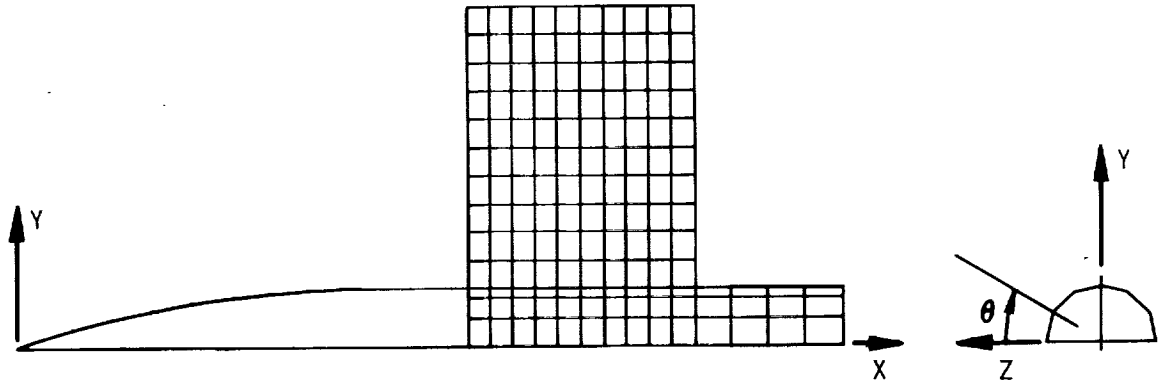

100 WING PANELS
84 BODY PANELS
$\theta = 0°, 30°, 60°, 90°, 120°, 150°, 180°$

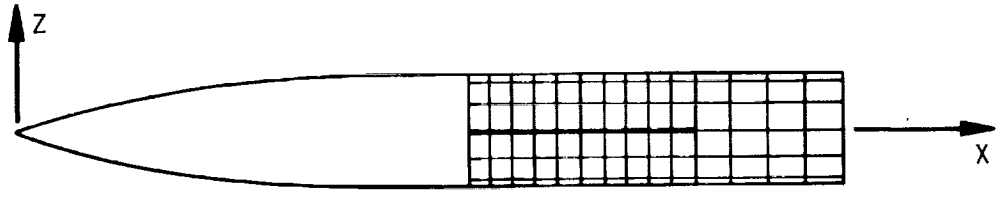

FIGURE 38 NIELSEN'S WING-BODY CONFIGURATION AND PANELING SCHEME

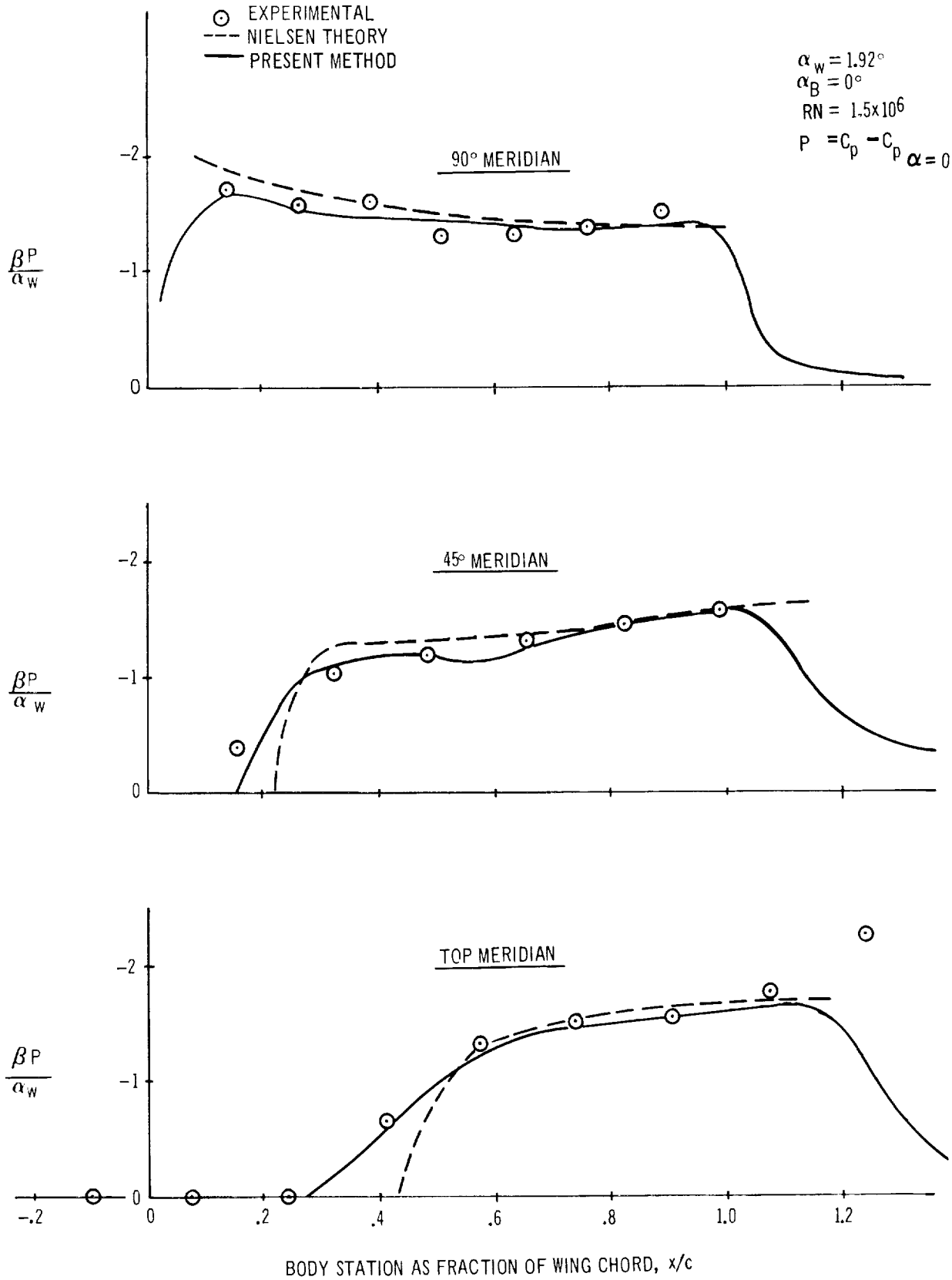

FIGURE 39 BODY PRESSURE DISTRIBUTION FOR NIELSEN WING–BODY COMBINATION WITH WING AT INCIDENCE

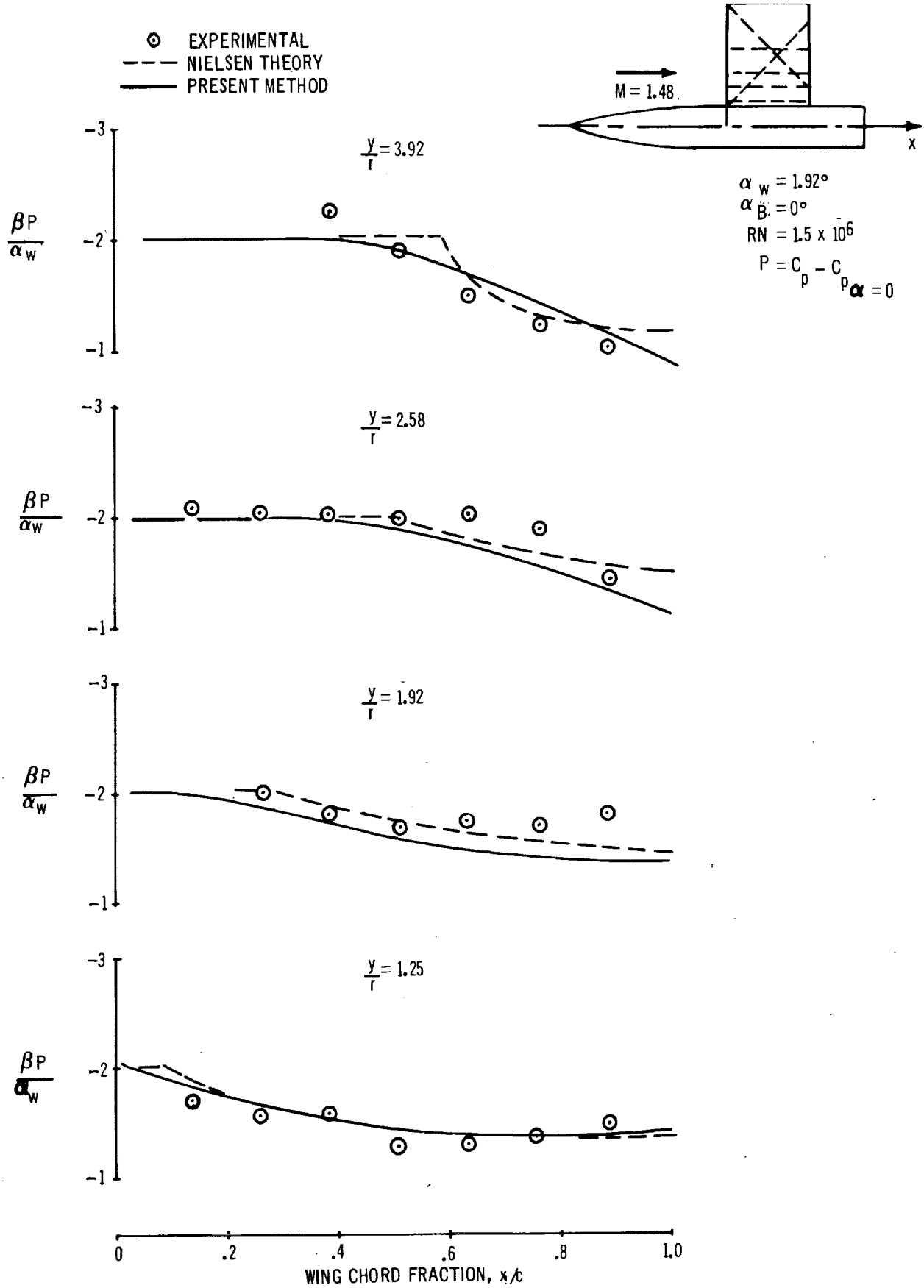

FIGURE 40 WING PRESSURE DISTRIBUTION FOR NIELSEN WING–BODY COMBINATION WITH WING AT INCIDENCE

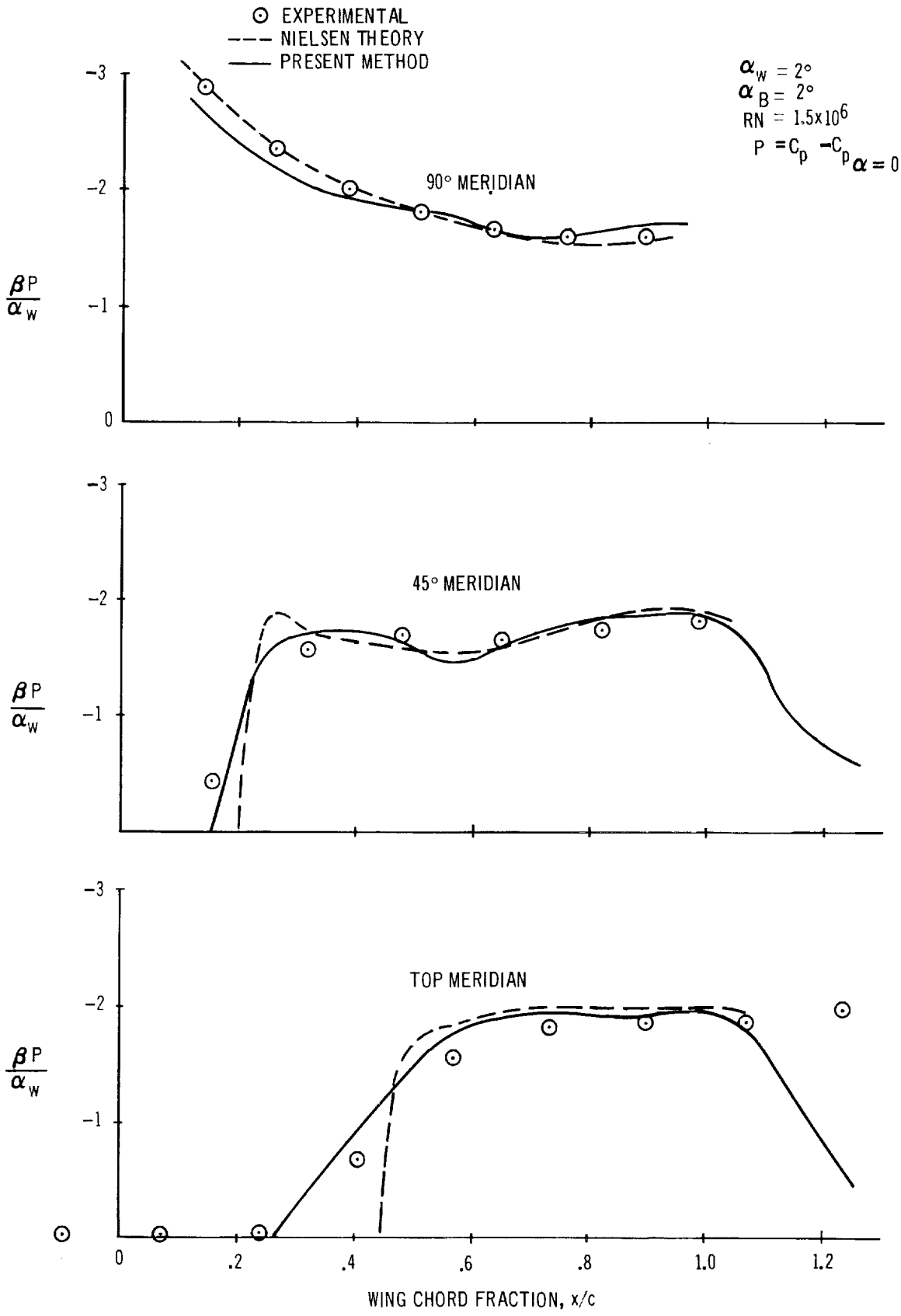

FIGURE 41 BODY PRESSURE DISTRIBUTION FOR NIELSEN WING–BODY COMBINATION WITH WING AND BODY AT INCIDENCE

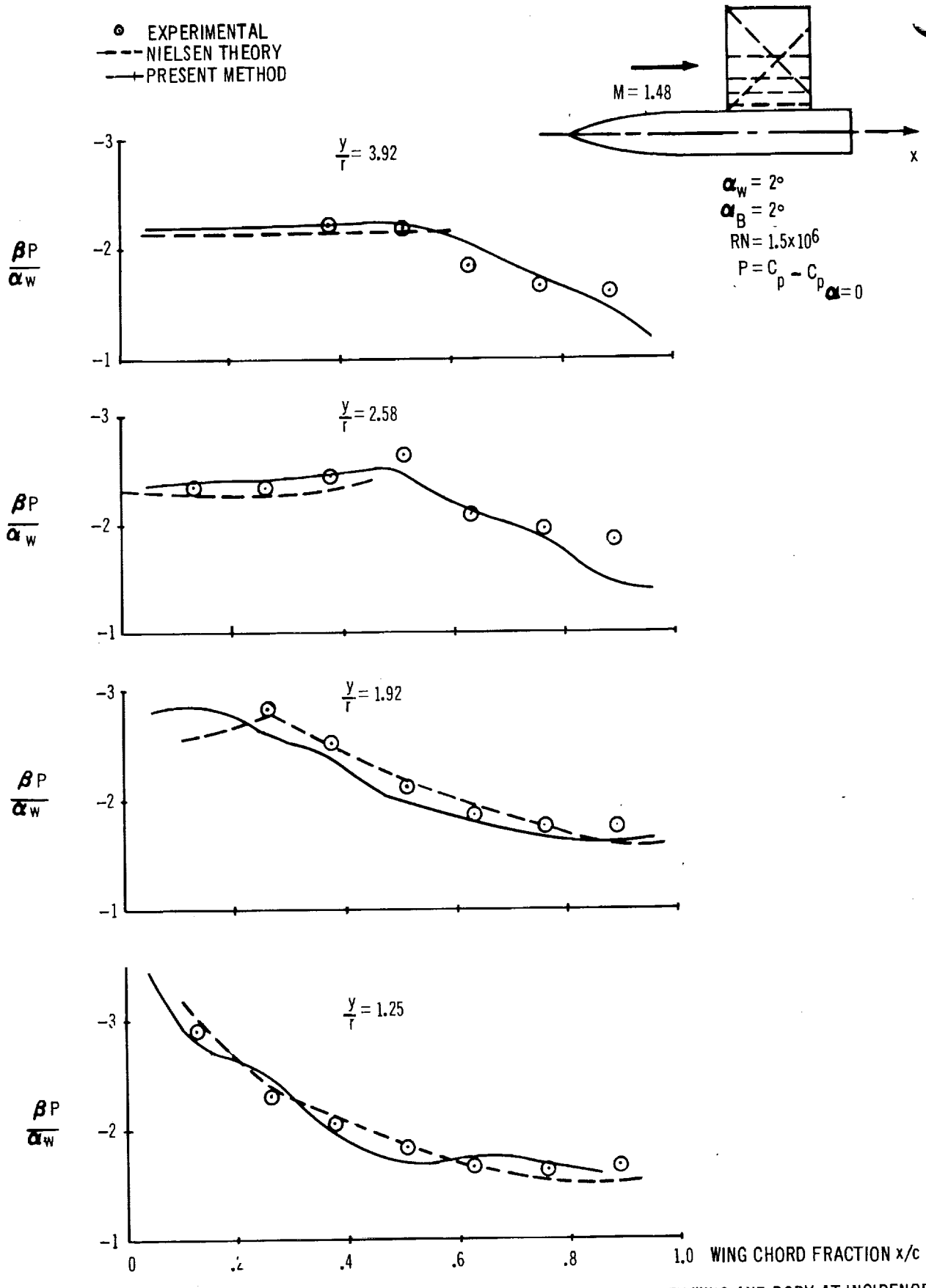

FIGURE 42 WING PRESSURE DISTRIBUTION FOR NIELSEN WING BODY COMBINATION WITH WING AND BODY AT INCIDENCE

6.4 Boeing Wing-Body

The wind-tunnel test model is a constant-chord, swept-wing configuration with a cambered cylindrical body (figure 43). Model dimensions and pressure tap locations are given in figure 44. The body has a drooped nose and a small amount of boat-tailing. Four streamwise rows of pressure taps are located on the upper and lower wing surfaces. The wing chord plane intersects the body side 0.25 inch below the body axis and has no incidence relative to the body. Five longitudinal rows of pressure taps are located on the body. The wing, with a 12-percent-thick airfoil oriented normal to the leading edge, is pretwisted to give a flat shape when aerodynamically loaded to a design C_L of 0.15 at Mach 1.8. Photographs in figure 45 show that the wing did achieve an untwisted shape at a 4-degree angle of attack. It is this untwisted wing with camber that is analyzed by the program.

The wing half-planform is represented by 100 panels spaced as shown in figure 46 on page 210 to obtain pressure coefficients at spanwise stations corresponding to wing pressure tap locations. The body aft of the wing leading edge is represented by 98 panels, 14 in each of 7 longitudinal strips.

Comparisons of wind tunnel and calculated wing and body pressure data are shown in figures 46 and 47. The Mach number is 1.8 and the comparison is for α = 4 degrees. Wing pressure predictions are good for the inboard stations. The experimental pressure distributions indicate the formation of a shock wave on the upper wing surface near the root trailing edge, which extends outboard and rearward across the span. Photographs of oil flow patterns taken during the wind-tunnel test verify the formation and location of the shock wave. The rapid recompression aft of the shock and subsequent flow separation are not well represented by the linear theory calculations.

Pressures calculated on the surface of the body, shown in figure 47, exhibit good agreement with wind-tunnel data. The body pressures due to thickness are calculated by the nonlinear pressure coefficient formula, equation (124). The wing pressures and pressures on the body due to the wing are predicted by the linear pressure coefficient formula, equation (125). The total body pressure

distribution shown includes body thickness and wing interference effects. The interference pressures due to the wing are added to the isolated body thickness pressures in the region influenced by the wing.

The program input format for this wing-body configuration, paneled as shown in figure 46, for nonlinear pressure calculations on wing and body, is presented on pages 188 through 191 of section 5.4. This same wing-body configuration, but with a different wing paneling scheme, was optimized for minimum drag at a wing C_L of 0.159. Discussion of the optimization follows in section 7.0. The program input format for this latter case is contained in Appendix C.

VIEW OF SUPERSONIC PRESSURE MODEL SHOWING PRESSURE LEADS FROM BODY

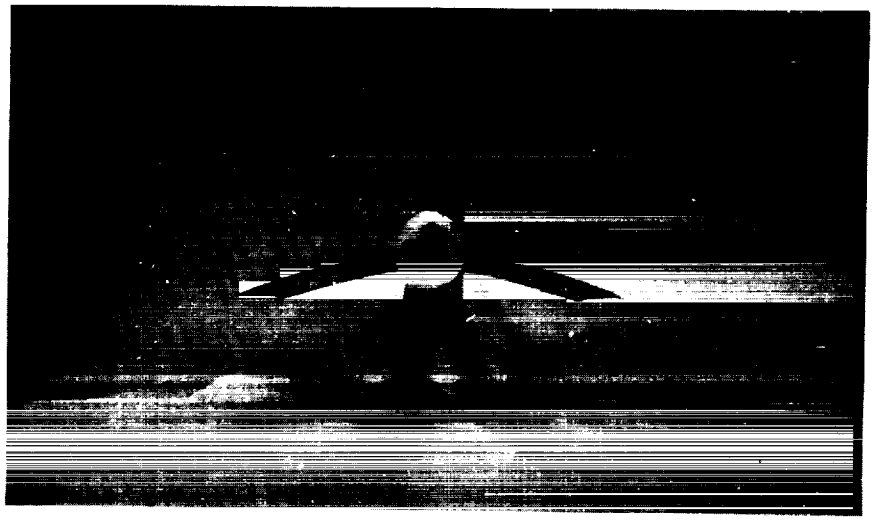

FRONT VIEW OF PRESHAPED WING

FIGURE 43 PHOTOS OF BOEING MODEL USED TO OBTAIN EXPERIMENTAL DATA

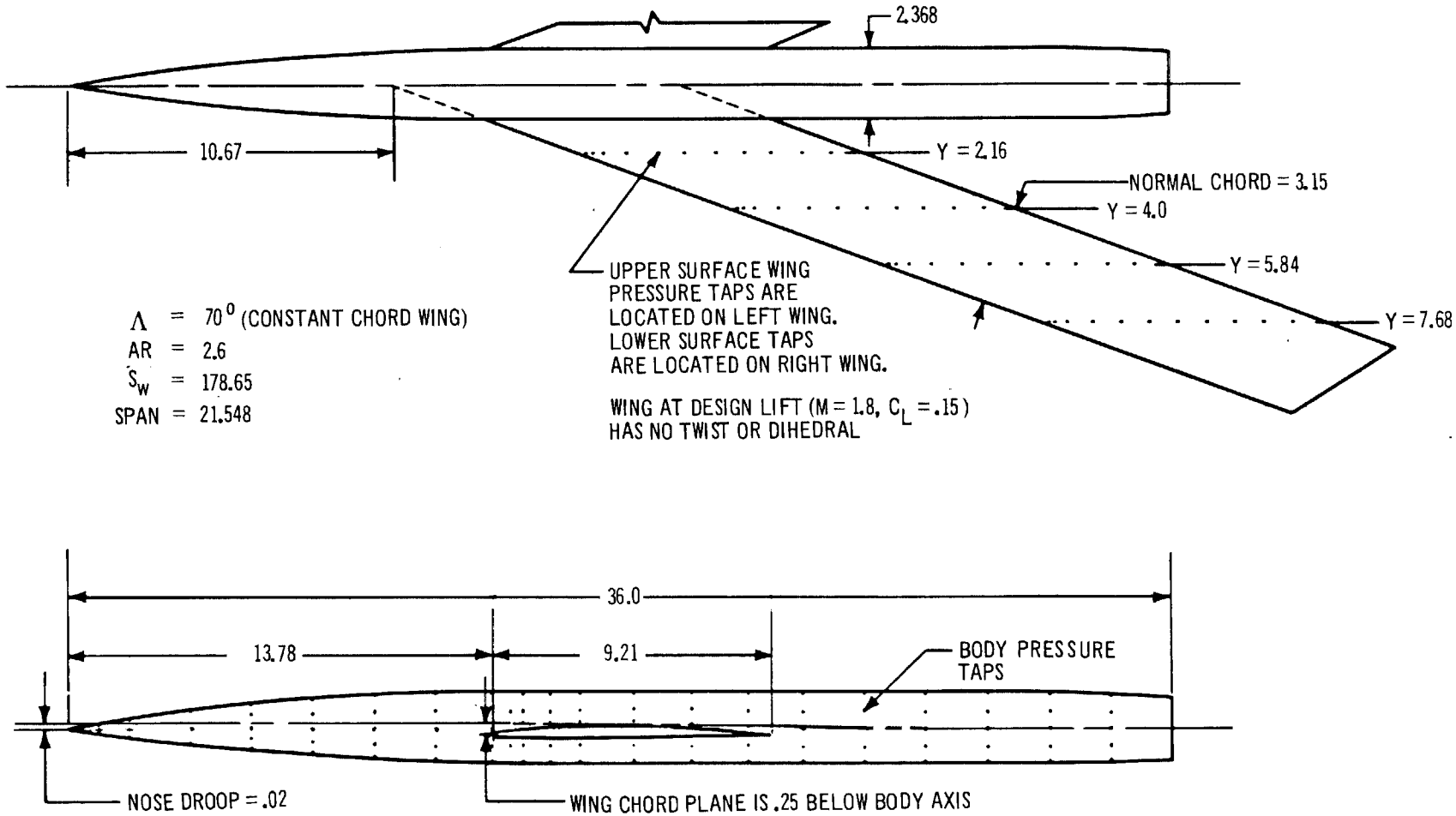

FIGURE 44 BOEING WING–BODY WIND–TUNNEL MODEL DESCRIPTION (ALL DIMENSIONS IN INCHES)

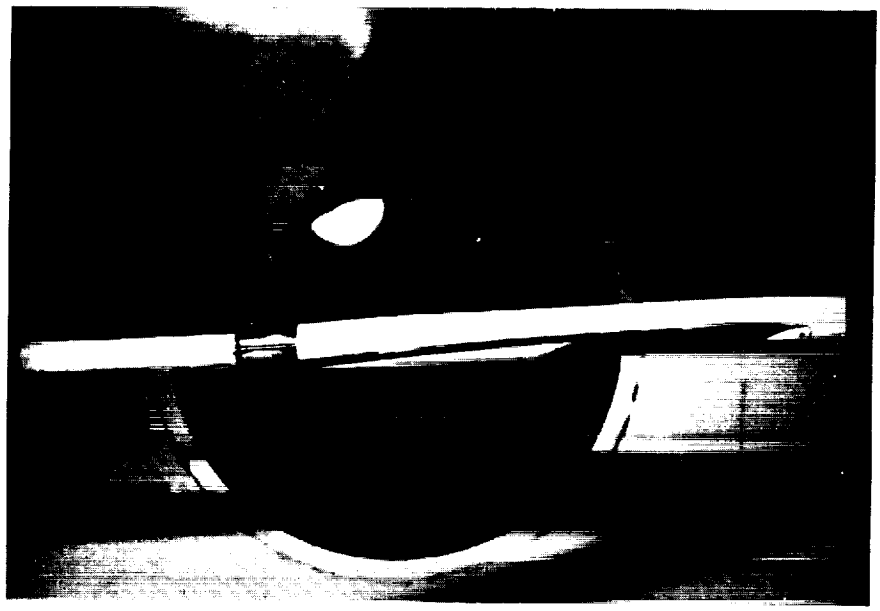

WIND–OFF CONDITION WITH THE TEST SECTION STING PITCHED TO 4° ANGLE OF ATTACK. THE BUILT–IN DOWNWARD DEFLECTION OF THE WING IS READILY APPARENT.

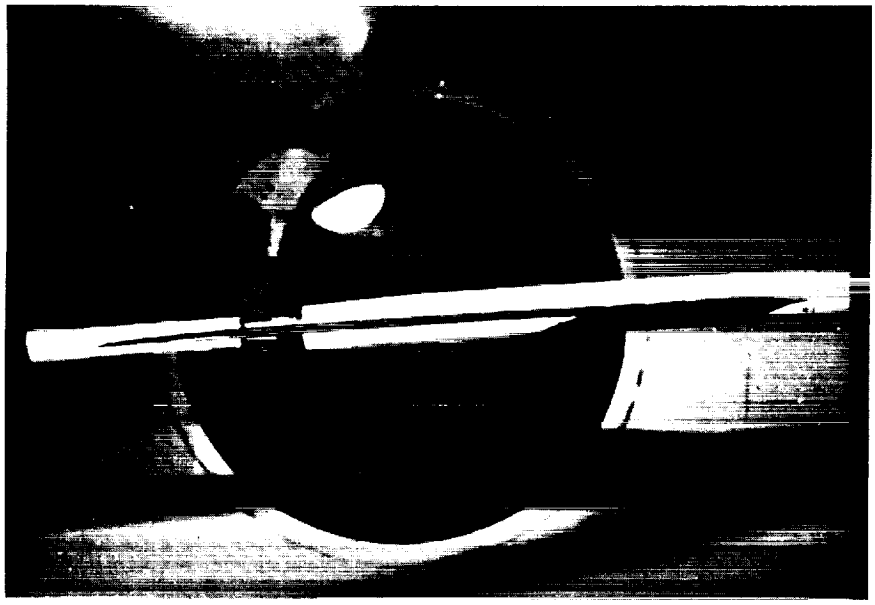

WIND–ON CONDITION FOR $\alpha = 4°$ and M = 1.8. THE WING IS AT DESIGN C_L AND HAS DEFLECTED INTO A FLAT SHAPE UNDER THE AERODYNAMIC LOAD.

FIGURE 45 COMPARISON OF WING SHAPE WITH AND WITHOUT AIRLOAD

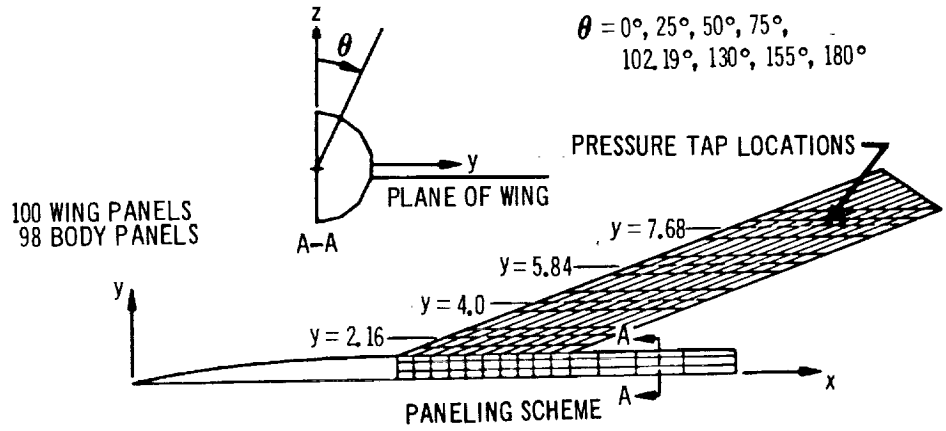

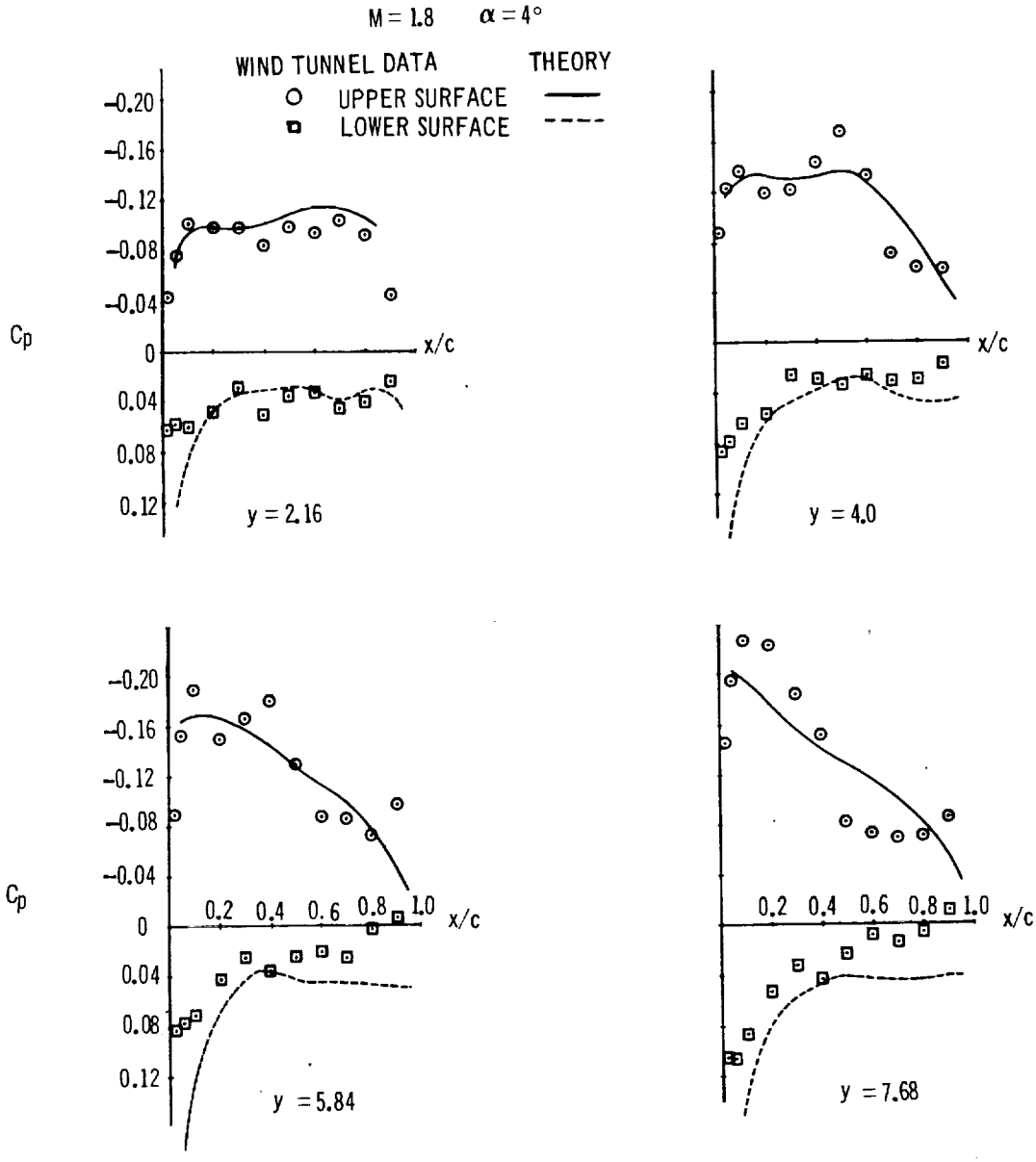

FIGURE 46 WING PRESSURE DISTRIBUTION FOR BOEING WING BODY MODEL

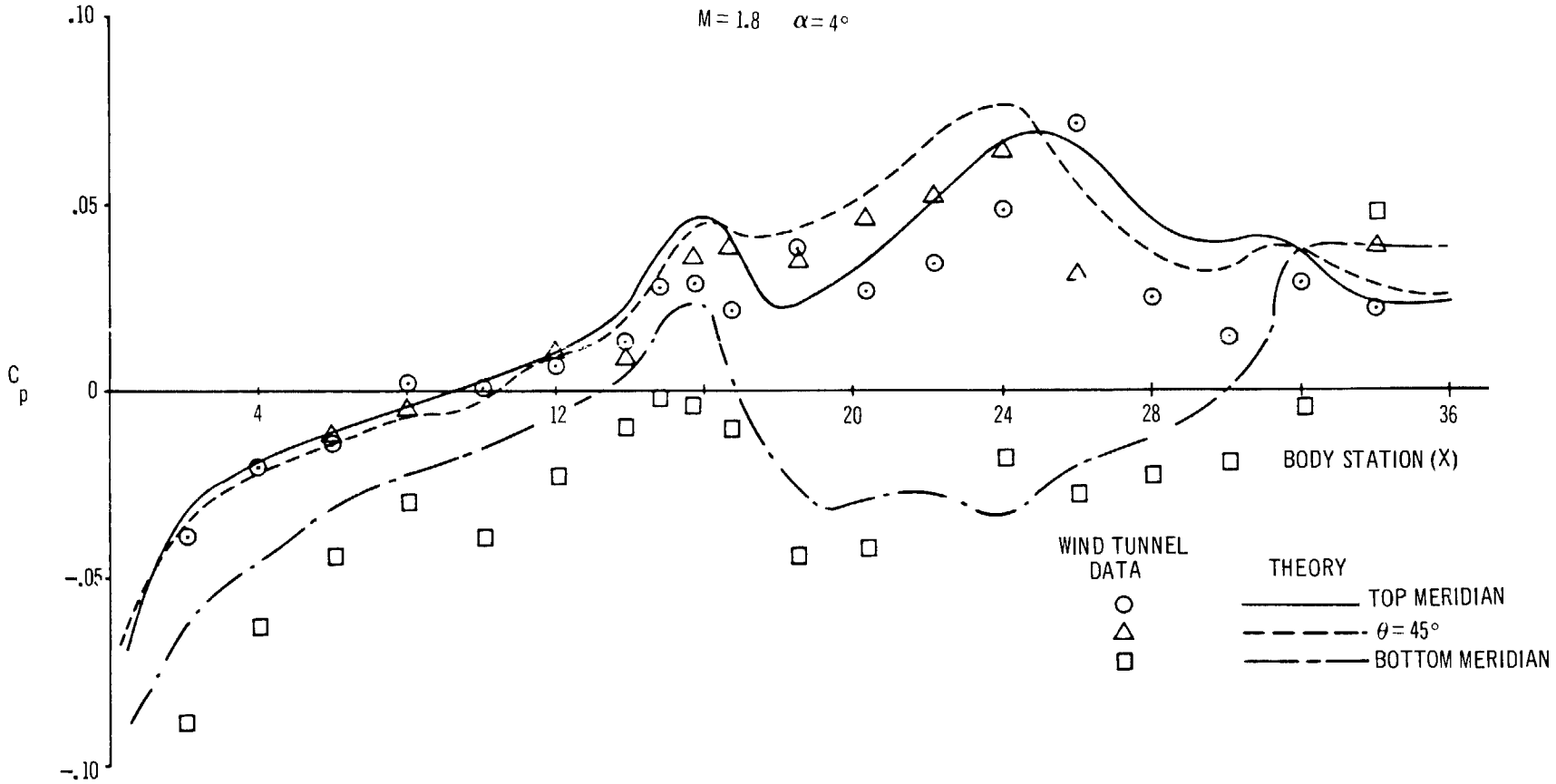

FIGURE 47 BODY PRESSURE DISTRIBUTION FOR BOEING WING–BODY MODEL

7. THEORETICAL OPTIMIZATION

The wing camber surface of the Boeing wing-body configuration, as described in the previous section, was optimized for minimum drag with constrained lift. Some graphical comparisons with the untwisted case are shown in figure 48, and a complete input-output tabulation is presented in Appendix C. The paneling chosen for this case was uniformly spaced both spanwise and chordwise on the wing. This paneling scheme differed slightly from that used in the example presented in section 6.4; in which the panels were chosen to coincide with the pressure tap locations. Both paneling schemes are illustrated on figure 49, page 216. Uniform panel spacing tends to minimize any undesirable oscillations in the wing geometry or pressure distributions, in wing optimization calculations.

At the wind-tunnel model design angle of attack of 4 degrees and Mach 1.8, the wing lift coefficient (based on the exposed wing) was 0.159. The optimized wing lift coefficient was constrained to the same value, and the body was kept at the same angle of attack. No constraint was placed on the center of pressure. The optimized wing camber surface reduced the wing drag by 19 percent (from 0.00936 to 0.00761) and the total configuration drag by 23 percent (from 0.01101 to 0.00849). A greater load was carried by the wing root, improving the spanwise lift distribution. The additional body load increased the total lift and reduced the negative pitching moment.

The additional load on the body due to the wing is shown by the top and bottom meridian pressure distributions in figure 48. Changes in the body interference pressures are larger toward the wing-body junction leading edge, where the major change occurred in the wing root pressure distribution. The chordwise pressure distributions on the wing show the effect of the optimized camber surface. Wing thickness effects are unchanged. In general the maximum camber location was moved more toward the trailing edge. Viscous limitations on the pressure gradients at the trailing edge would probably make some of the camber revision impractical.

Although the details of the optimized wing geometry are not shown in figure 48, the tabular panel slope data are given in Appendix C. The optimization shows an increase in wing incidence at the root and a decrease in the incidence of the next-to-last spanwise station near the highly loaded wing tip. Additional fine paneling in each of these areas could give more detail of the optimum geometry.

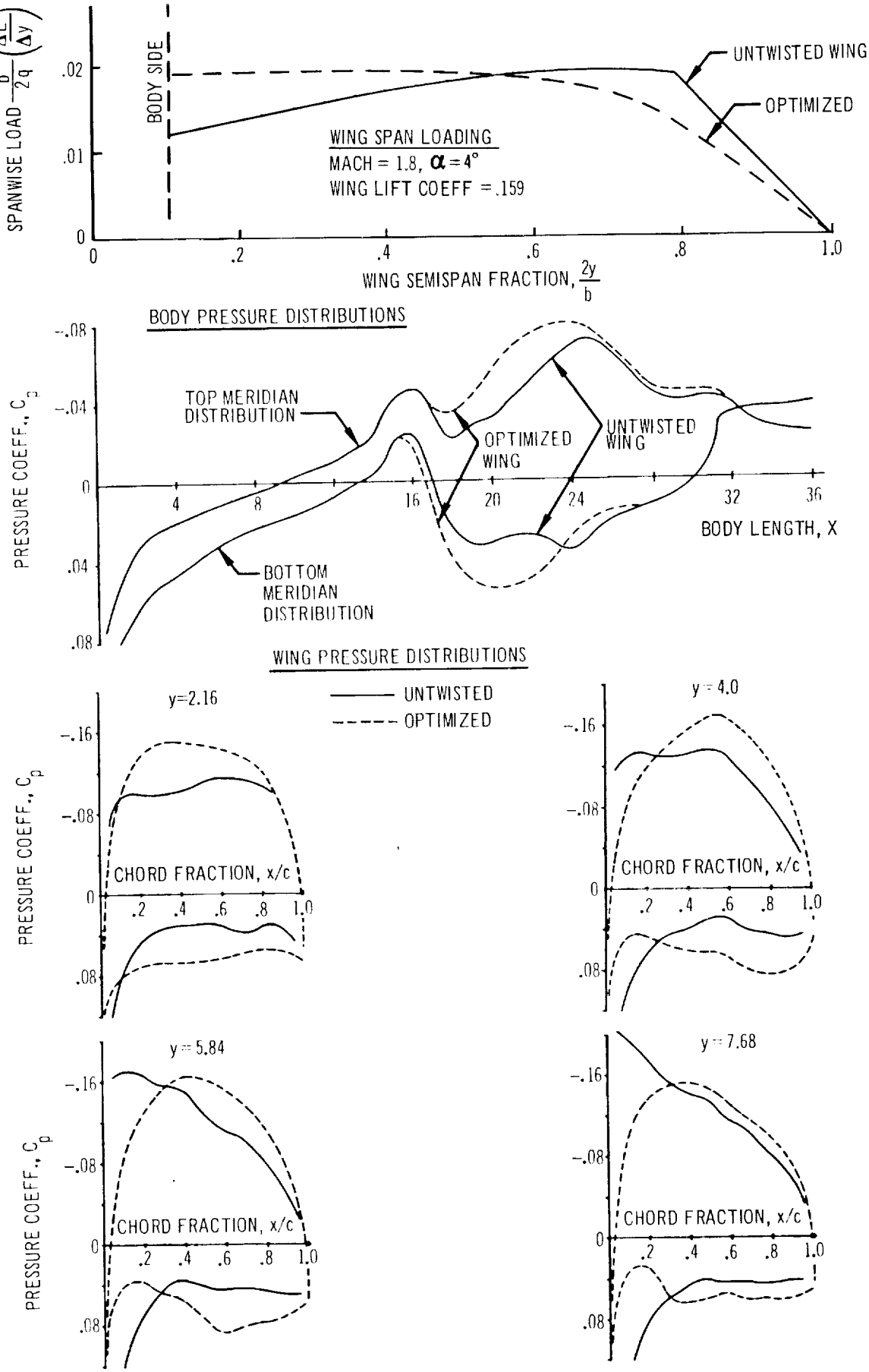

FIGURE 48 COMPARISON OF UNTWISTED AND OPTIMIZED DISTRIBUTIONS

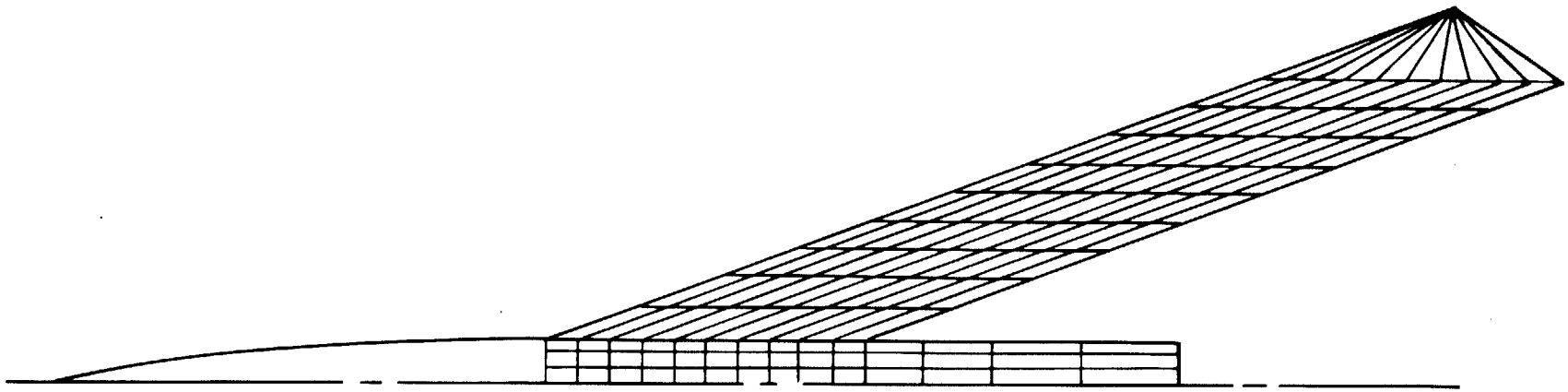

REVISED PANELING WITH CONSTANT WIDTH PANELS;
OPTIMIZATION SATISFACTORY EXCEPT AT TIP.

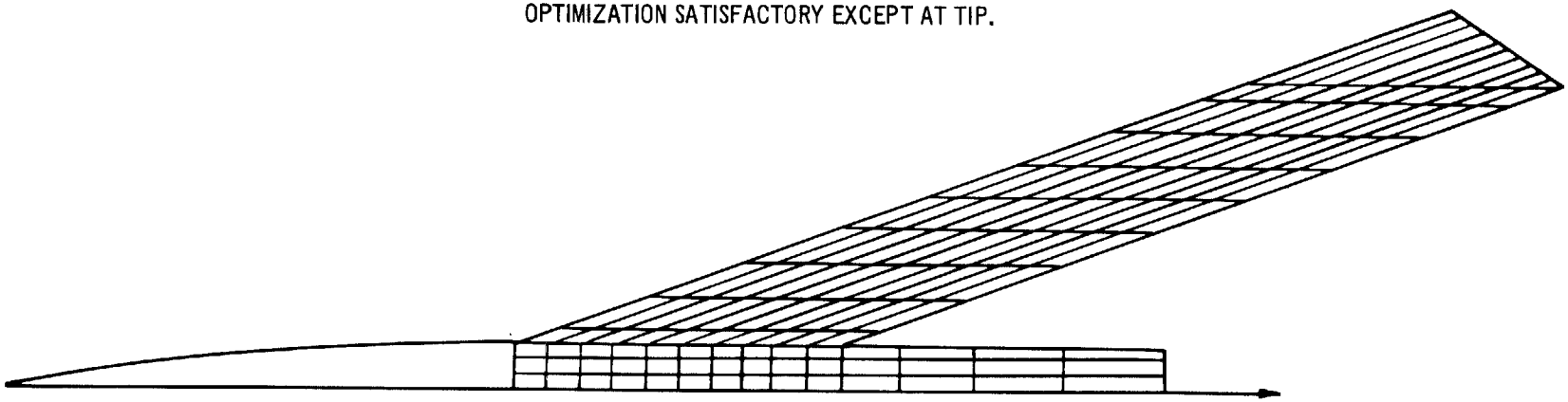

ORIGINAL PANEL WITH UNEVEN WIDTH PANELS; UNSATISFACTORY OPTIMIZATION
(PANEL WIDTHS CHOSEN TO MATCH MODEL PRESSURE TAP LOCATIONS)

FIGURE 49 COMPARISON OF PANELING SCHEMES TESTED FOR WING OPTIMIZATION

8. CONCLUSIONS

A digital computer program for calculating wing-body interference problems in supersonic flow has been developed. The program is based on the method of aerodynamic influence coefficients. A special effort has been made to reduce the number of geometric description inputs, and has significantly increased the practical value of the program.

A wide variety of aerodynamic problems involving wings, bodies, or wing-body combinations can be solved. The program may be used to determine the pressures, forces, and moments on given configurations; or to determine the wing camber surface corresponding to a given aerodynamic loading. In particular, the wing camber surface required to minimize the drag under given constraints of lift, or lift and pitching moment, may be calculated. The program may also be used to determine pressure-distributions, flow directions, and streamlines in the field around given configurations. The results of the program have been compared with other theories and experiments, and show good agreement in all cases.

The Boeing Company
Commercial Airplane Division
Renton, Washington
August 25, 1967

9. APPENDIXES

9.1 Appendix A - Preliminary Results of Integration

In the solution of certain problems concerning the linearized theory of supersonic aerodynamics, several integrals of standard form occur repeatedly; their evaluation can be carried out by elementary methods. Here is given a brief outline of the integration procedure and a summary of the results.

$$J_1 = \int \frac{d\,v}{(v^2 + e^2)\sqrt{a^2\,v^2 + 2b\,v + c}} ,$$

$$J_2 = \int \frac{v\,d\,v}{(v^2 + e^2)\sqrt{a^2\,v^2 + 2b\,v + c}} . \qquad \text{(A1)}$$

Let the following substitution be made:

$$v = \sqrt{\frac{b^2 - a\,c}{a^2}}\,\frac{u^2 + 1}{u^2 - 1} - \frac{b}{a} . \qquad \text{(A2)}$$

then

$$J_1 = -\frac{2a^2}{\sqrt{a}} \int \frac{(u^2 - 1)\,d\,u}{(b^2 - a\,c)(u^2 + 1)^2 - 2b\sqrt{b^2 - a\,c}\,(u^4 - 1) + b^2(u^2 - 1)^2 + e^2\,a^2(u^2 - 1)^2}$$

$$= \frac{\sqrt{a}}{e\,i}\,\frac{1}{\sqrt{a^2\,e^2 + 2a\,b\,e\,i - a\,c}}\,\tan^{-1}\sqrt{\frac{\sqrt{b^2 - a\,c} - b + a\,e\,i}{\sqrt{b^2 - a\,c} + b - a\,e\,i}}\,u$$

$$-\frac{\sqrt{a}}{e\,i}\,\frac{1}{\sqrt{a^2\,e^2 - 2a\,b\,e\,i - a\,c}}\,\tan^{-1}\sqrt{\frac{\sqrt{b^2 - a\,c} - b - a\,e\,i}{\sqrt{b^2 - a\,c} + b + a\,e\,i}}\,u . \qquad \text{(A3)}$$

The above results can be simplified by the following consideration:

let $$\tan^{-1}\sqrt{\frac{\sqrt{b^2 - a\,c} - b + a\,e\,i}{\sqrt{b^2 - a\,c} + b - a\,e\,i}}\,u = \alpha + i\,\beta , \qquad \text{(A4)}$$

and $$\sqrt{a\,e^2 + 2b\,ei - c} = \gamma + i\,\delta \tag{A5}$$

then $\gamma^2 - \delta^2 = a\,e^2 - c$ and $\gamma\,\delta = b\,e$, and γ satisfies the equation:

$$\gamma^4 - (a\,e^2 - c)\,\gamma^2 - b^2\,e^2 = 0. \tag{A6}$$

Furthermore,

$$J_1 = \frac{\sqrt{a}}{ei}\,\frac{\alpha + i\,\beta}{\sqrt{a}\,(\gamma + i\,\delta)} - \frac{\sqrt{a}}{ei}\,\frac{\alpha - i\,\beta}{\sqrt{a}\,(\gamma - i\,\delta)}$$

$$= -\frac{b\,\gamma}{\gamma^4 + b^2\,e^2}\,2\alpha + \frac{1}{e}\,\frac{\gamma^3}{\gamma^2 + b^2\,e^2}\,2\beta\,. \tag{A7}$$

On the other hand, since $\tan(\alpha + i\,\beta) = \sqrt{\dfrac{\sqrt{b^2 - ac} - b + aei}{\sqrt{b^2 - ac} + b - aei}}$, there follows

$$\frac{\tan 2\alpha + i \tanh 2\beta}{1 - i \tan 2\alpha \tanh 2\beta} = \frac{\sqrt{a\,v^2 + 2b\,v + c}\,(\gamma + i\,\delta)}{b\,v + c - i\,(b + a\,v)\,e}\,. \tag{A8}$$

Equating the real and the imaginary parts of the above equation, we get

$$(b\,v + c)\tan 2\alpha + (b + a\,v)\,e \tanh 2\beta = \sqrt{a\,v^2 + 2b\,v + c}\,(\gamma + \delta \tan 2\alpha \tanh 2\beta)$$

$$(b\,v + c)\tanh 2\beta - (b + a\,v)e \tan 2\alpha = \sqrt{a\,v^2 + 2b\,v + c}\,(\delta - \gamma \tan 2\alpha \tanh 2\beta) \tag{A9}$$

which gives the following solution for α and β:

$$\alpha = \frac{1}{2}\tan^{-1}\frac{\gamma^2 - b\,v}{\gamma\sqrt{a\,v^2 + 2b\,v + c}}\,; \qquad \alpha = \frac{1}{2}\tan^{-1}\frac{\gamma\sqrt{a\,v^2 + 2b\,v + c}}{b\,v - \gamma^2}$$

$$\beta = \frac{1}{2}\tanh^{-1}\frac{v\,\gamma + e\,\delta}{e\sqrt{a\,v^2 + 2b\,v + c}}\,; \qquad \beta = \frac{1}{2}\tanh^{-1}\frac{e\sqrt{a\,v^2 + 2b\,v + c}}{v\,\gamma + e\,\delta} \tag{A10}$$

The above results for α and β can now be substituted for the expression for J_1, and, omitting the integration constant, we have

$$\int \frac{dv}{(v^2 + e^2)\sqrt{a\,v^2 + 2b\,v + c}} = \frac{b\,\gamma}{\gamma^4 + b^2 e^2}\tan^{-1}\frac{b\,v - \gamma^2}{\gamma\sqrt{a\,v^2 + 2b\,v + c}}$$

$$+ \frac{1}{e} \frac{\gamma^3}{\gamma^4 + b^2 e^2} \tanh^{-1} \frac{e\sqrt{a\,v^2 + 2b\,v + c}}{v\,\gamma + e\,\delta}$$

$$\text{or} \quad = \frac{b\,\gamma}{\gamma^4 + b^2 e^2} \tan^{-1} \frac{\gamma\sqrt{a\,v^2 + 2b\,v + c}}{\gamma^2 - b\,v}$$

$$+ \frac{1}{e} \frac{\gamma^3}{\gamma^4 + b^2 e^2} \tanh^{-1} \frac{v\,\gamma + e\,\delta}{e\sqrt{a\,v^2 + 2b\,v + c}} \qquad \text{(A11)}$$

where γ is a non-zero root of the equation: $\gamma^4 - (a\,e^2 - c)\,\gamma^2 - b^2 e^2 = 0$ and $\gamma\,\delta = b\,e$. For $e = 0$ then taking $\gamma = \sqrt{-c}$ we obtain

$$\int \frac{d\,v}{v^2\sqrt{a\,v^2 + 2b\,v + c}} = -\frac{b}{c\sqrt{-c}} \tan^{-1} \frac{b\,v + c}{\sqrt{-c}\sqrt{a\,v^2 + 2b\,v + c}} - \frac{\sqrt{a\,v^2 + 2b\,v + c}}{c\,v}$$

$$\text{or} \quad = -\frac{b}{c\sqrt{-c}} \tan^{-1} \frac{\sqrt{-c}\sqrt{a\,v^2 + 2b\,v + c}}{-(b\,v + c)} - \frac{\sqrt{a\,v^2 + 2b\,v + c}}{c\,v} \qquad \text{(A12)}$$

In a like manner, the integral for J_2 can be evaluated:

$$\int \frac{v\,d\,v}{(v^2 + e^2)\sqrt{a\,v^2 + 2b\,v + c}} = \frac{\gamma^3}{\gamma^4 + b^2 e^2} \tan^{-1} \frac{b\,v - \gamma^2}{\gamma\sqrt{a\,v^2 + 2b\,v + c}}$$

$$- \frac{b\,e\,\gamma}{\gamma^4 + b^2 e^2} \tanh^{-1} \frac{e\sqrt{a\,v^2 + 2b\,v + c}}{v\,\gamma + e\,\delta}$$

$$\text{or} \quad = \frac{\gamma^3}{\gamma^4 + b^2 e^2} \tan^{-1} \frac{\gamma\sqrt{a\,v^2 + 2b\,v + c}}{\gamma^2 - b\,v}$$

$$- \frac{b\,e\,\gamma}{\gamma^4 + b^2 e^2} \tanh^{-1} \frac{v\,\gamma + e\,\delta}{e\sqrt{a\,v^2 + 2b\,v + c}} \qquad \text{(A13)}$$

where γ and δ are defined as before.

9.2 Appendix B - Velocity Functions

Equations (74) and (75) in the text give expressions for the three velocity components, u', v', w', at a point (x', y', z'), induced by a surface distribution of singularities located in the plane $z' = ax'$, and bounded by the x', y' plane and the plane $y' = mx'$. The primed coordinate system has its origin at the apex of this triangular region, with the x' axis parallel to the free stream.

Three velocity functions, P, S, and D, are defined by equation (75) in terms of the variables a', b', ξ', y', and z', where

$$a' = \beta\, a = \beta \tan \alpha$$

$$b' = \frac{1}{\beta\, m} = \frac{\tan \Lambda}{\beta}$$

$$\xi' = x'/\beta$$

and x', y', and z' are given in equation (73).

At points for which $\xi' > \sqrt{y'^2 + z'^2}$, the functions P, S, and D may in turn be expressed most simply in terms of seven auxiliary functions, F1 through F7, as given in equation (40). These functions are rewritten below in terms of the primed variables.

$$F1 = \frac{z' - a'\xi'}{\left|z' - a'\xi'\right|} \cos^{-1} \frac{y'(b'y' - \xi') - a'(a'b'y' - z') + b'(z' - a'\xi')^2}{\sqrt{\left[(z' - a'\xi')^2 + (1 - a'^2)y'^2\right]\left[(b'y' - \xi')^2 + b'^2(z' - a'\xi')^2 - (a'b'y' - z')^2\right]}} \qquad \text{(B1)}$$

For $z' = a'\xi'$

$F1 = \pi$ for $0 < y' < \xi'/b'$

$= \pi/2$ for $y' = 0,\ \xi'/b'$

$= 0$ for $y' < 0,\ y' > \xi'/b'$

$$F2 = \frac{1}{\sqrt{b'^2(1 - a'^2) - 1}} \cosh^{-1} \frac{b'\xi' - y' - a'b'z'}{\sqrt{(b'y' - \xi')^2 + b'^2(z' - a'\xi')^2 - (a'b'y' - z')^2}} \qquad \text{(B2)}$$

for $b' > 1/\sqrt{1 - a'^2}$

$$= \frac{\sqrt{\xi'^2 - y'^2 - z'^2}}{\xi' - y} \qquad \text{for} \quad b' = 1/\sqrt{1 - a'^2}$$

$$= \frac{1}{\sqrt{1 - b'^2(1 - a'^2)}} \cos^{-1} \frac{b'\xi' - y' - a'b'z'}{\sqrt{(b'y' - \xi')^2 + b'^2(z' - a'\xi')^2 - (a'b'y' - z')^2}}$$

$$\text{for} \quad b' < 1/\sqrt{1 - a'^2} \, .$$

$$F3 = \frac{z' - a'b'y'}{|z' - a'b'y'|} \cos^{-1} \frac{-\xi'(y' + a'b'z') + b'(y'^2 + z'^2)}{\sqrt{(y'^2 + z'^2)\,(b'y' - \xi')^2 + b'^2(z' - a'\xi')^2 - (a'b'y' - z')^2}} \qquad \text{(B3)}$$

For $z' = a'b'y'$

$F3 = \pi \quad$ for $\quad 0 < y' < \xi'/b'$

$= \pi/2 \quad$ for $\quad y' = 0, \quad y' = \xi'/b'$

$= 0 \quad$ for $\quad y' < 0, \quad y' > \xi'/b'$

For $z' = y' = 0$

$$F3 = F1 = -\cos^{-1} \frac{a'b'}{\sqrt{1 + a'^2 b'^2}}$$

$$F4 = F3 - (1 + a'^2 b'^2)\, F1 \qquad \text{for} \quad y' < 0 \qquad \text{(B4)}$$

$$= -a'^2 b'^2 \, F3 \qquad \text{for} \quad y' = 0$$

$$= F3 - (1 + a'^2 b'^2)\,(F1 + 2\pi) \qquad \text{for} \quad y' > 0, \quad \text{and} \quad a'b'y' < z' < a'\xi'$$

$$= -(1 + a'^2 b'^2)\,(F1 + \pi) \qquad \text{for} \quad y' > 0, \quad \text{and} \quad a'b'y' = z' < a'\xi'$$

$$F5 = \cosh^{-1} \frac{\xi'}{\sqrt{y'^2 + z'^2}} \qquad \text{(B5)}$$

$$F6 = \sqrt{1 - a'^2} \cosh^{-1} \frac{\xi' - a'z'}{\sqrt{(z' - a'\xi')^2 + (1 - a'^2)\, y'^2}} \qquad \text{(B6)}$$

$$F7 = F5 - (1 + a'^2 b'^2)\, F6 \qquad \text{(B7)}$$

For surface distributions of vorticity (constant pressure surfaces), the velocity functions may now be expressed in terms of these seven auxiliary functions, as follows, provided $\xi' > \sqrt{y'^2 + z'^2}$ and $a' > 0$:

$$P = -\frac{F1}{\pi} \tag{B8}$$

$$S = \frac{a'b'\left[b'^2(1 - a'^2) - 1\right] F2 + b' F3 + F7/a'}{\pi(1 + a'^2 b'^2)}$$

$$D = -\frac{\left[b'^2(1 - a'^2) - 1\right] F2 - b' F5 + F4/a'}{\pi(1 + a'^2 b'^2)}$$

If $a' = 0$, the same expressions apply, except

$$F4/a' \longrightarrow \frac{y'}{y'^2 + z'^2}\sqrt{\xi'^2 - (y'^2 + z'^2)}$$

$$F7/a' \longrightarrow \frac{z'}{y'^2 + z'^2}\sqrt{\xi'^2 - (y'^2 + z'^2)}$$

If $a' < 0$, the velocity functions are the same as for $a' > 0$, except that a' is replaced by $-a'$, z' is replaced by $-z'$, and D by $-D$. In addition, $P = -P$ if $z = a'\xi'$, for $a' < 0$.

For $\xi' \leq \sqrt{y'^2 + z'^2}$, the functions P, S, and D are zero except within the envelope of the Mach cones from the leading edge for the supersonic leading-edge case (that is, $b' < 1/\sqrt{1 - a'^2}$).

In this case, for $\xi' = \dfrac{b'(y' + a'b'z') + |z' - a'b'y'|\sqrt{1 - b'^2(1 - a'^2)}}{1 + a'^2 b'^2}$

(B9)

$$P = \pm 1/2$$

$$S = \pm \frac{b'}{2(1 + a'^2 b'^2)}\left(1 \mp a'\sqrt{1 - b'^2(1 - a'^2)}\right)$$

$$D = \frac{1}{2(1 + a'^2 b'^2)}\left(\pm a'b' + \sqrt{1 - b'^2(1 - a'^2)}\right)$$

for $y' \geq \dfrac{b'\xi'}{1 + a'^2 b'^2}\left(1 \mp a'\sqrt{1 - b'^2(1 - a'^2)}\right)$ or $y' \leq \xi'/b'$

$$P = S = D = 0 \quad \text{for} \quad y' < \frac{b'\xi'}{1 + a'^2 b'^2}\left(1 \mp a'\sqrt{1 - b'^2(1 - a'^2)}\right)$$

$$\text{or} \quad y' > \xi'/b' \quad .$$

$$\text{For} \quad \xi' > \frac{b'(y' + a'b'z') + z' - a'b'y' \sqrt{1 - b'^2(1 - a'^2)}}{1 + a'^2 b'^2}$$

$$\text{and} \qquad \xi'/b' > y' > \frac{b' \xi'}{1 + a'^2 b'^2} \left(1 \mp a' \sqrt{1 - b'^2(1 - a'^2)} \right)$$

$$P = 1 \qquad \text{for } z' \geq a' \xi'$$

$$= -1 \qquad \text{for } z' < a' \xi' \qquad \text{(B10)}$$

$$\left.\begin{aligned} S &= \frac{b'}{1 + a'^2 b'^2} \left(1 - a' \sqrt{1 - b'^2(1 - a'^2)} \right) \\ D &= \frac{1}{1 + a'^2 b'^2} \left(a'b' + \sqrt{1 - b'^2(1 - a'^2)} \right) \end{aligned}\right\} \quad \text{for} \quad z' > a'b'y'$$

$$\left.\begin{aligned} S &= \frac{-b'}{1 + a'^2 b'^2} \left(1 + a' \sqrt{1 - b'^2(1 - a'^2)} \right) \\ D &= \frac{1}{1 + a'^2 b'^2} \left(-a'b' + \sqrt{1 - b'^2(1 - a'^2)} \right) \end{aligned}\right\} \quad \text{for} \quad z' < a'b'y'$$

$$\left.\begin{aligned} S &= \frac{-a'b'}{1 + a'^2 b'^2} \sqrt{1 - b'^2(1 - a'^2)} \\ D &= \frac{1}{1 + a'^2 b'^2} \sqrt{1 - b'^2(1 - a'^2)} \end{aligned}\right\} \quad \text{for} \quad z' = a'b'y'$$

The geometry of this case is illustrated in the sketch on the following page.

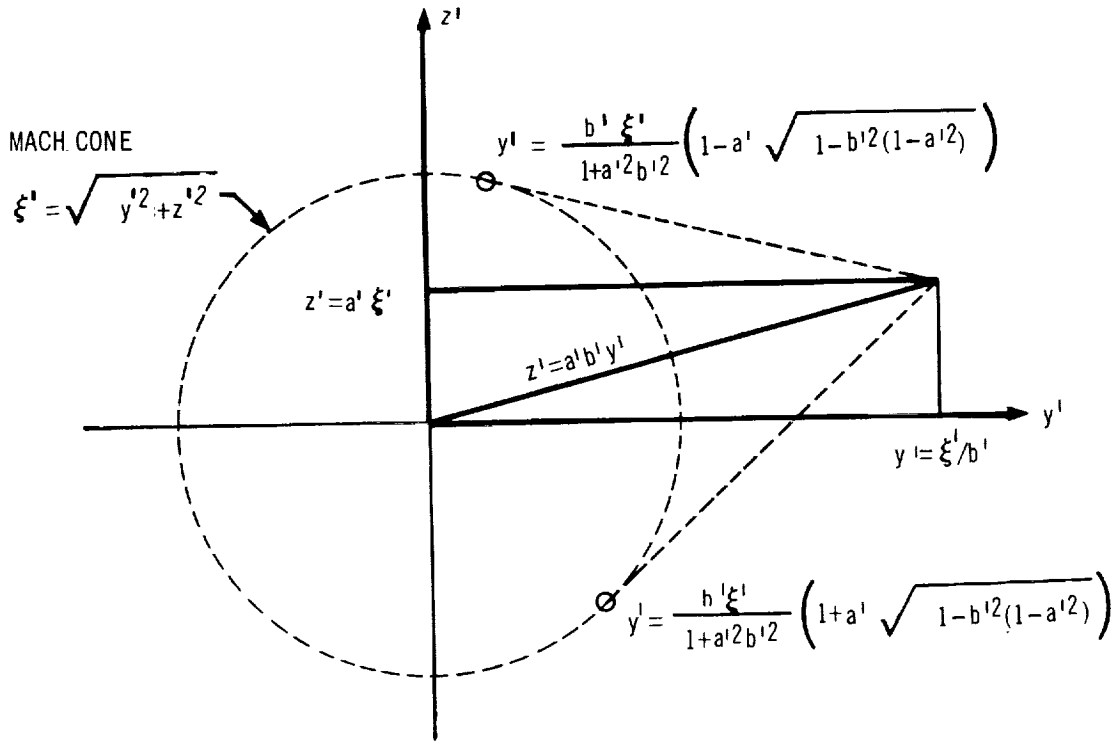

ENVELOPE OF MACH CONES FROM LEADING EDGE:

$$\xi' = \frac{b'(y' + a'b'z') + |z' - a'b'y'|\sqrt{1-b'^2(1-a'^2)}}{1 + a'^2b'^2}$$

For constant surface distributions of sources, the velocity components are required only for the case $a' = 0$. Then, for $\xi' > \sqrt{y'^2 + z'^2}$

$$P = -\frac{F2}{\beta\pi}$$

$$S = \frac{1}{\beta\pi}(b'F2 - F5) \qquad \text{(B11)}$$

$$D = \frac{F1}{\beta\pi}$$

For $\xi' \leq \sqrt{y'^2 + z'^2}$, the functions are all zero except within the envelope of the Mach cones from the leading edge of the supersonic leading-edge case, $b' < 1$.

In this case, for $\xi' = b'y' + |z'|\sqrt{1 - b'^2}$

$$\left.\begin{aligned} P &= \frac{-1}{2\beta\sqrt{1 - b'^2}} \\ S &= \frac{b'}{2\beta\sqrt{1 - b'^2}} \end{aligned}\right\} \quad \begin{matrix} y' \geq b'\xi' \\ y' \leq \xi'/b' \end{matrix} \qquad \text{(B12)}$$

$$D = \pm \frac{1}{2\beta}$$

$$P = S = D = 0 \quad \text{for} \quad y' < b'\xi' \quad \text{or} \quad y' > \xi'/b'$$

For $\xi' > b'y' + |z'|\sqrt{1 - b'^2}$

and $\xi'/b' > y' > b'\xi'$

$$P = \frac{-1}{\beta\sqrt{1 - b'^2}}$$

$$S = \frac{b'}{\beta\sqrt{1 - b'^2}} \qquad \text{(B13)}$$

$$D = \pm 1/\beta$$

where the upper sign corresponds to $z \geq 0$.

For linearly varying distributions of sources, the velocity components are given for $a' = 0$.

For $\xi' > \sqrt{y'^2 + z'^2}$

$$P = -\left[(\xi' - b'y')F2 + y'F5 - z'F1\right]/\pi c \qquad \text{(B14)}$$

$$S = \left[(\xi' - b'y')(b'F2 - F5) + \sqrt{\xi'^2 - (y'^2 + z'^2)} - b'zF1\right]/\pi c$$

$$D = \pm\left\{(\xi' - b'y')F1 + z'\left[(b'^2 - 1)F2 - b'F5\right]\right\}/\pi c$$

where c is the panel chord through the control point.

For $\xi' \leq \sqrt{y'^2 + z'^2}$, the functions are all zero except within the envelope of the Mach cones from a supersonic leading edge ($b' < 1$). In this region,

For $\xi' = b'y' + |z'|\sqrt{1 - b'^2}$

$$\left.\begin{aligned} P &= -\frac{(\xi' - b'y')}{2'c\sqrt{1 - b'^2}} \\ S &= \frac{b'(\xi' - b'y')}{2c\sqrt{1 - b'^2}} \\ D &= \pm\frac{(\xi' - b'y')}{2c} \end{aligned}\right\} \begin{aligned} y' &\geqslant b'\xi' \\ y' &\leqslant \xi'/b' \end{aligned} \qquad \text{(B15)}$$

For $\xi' > b'y' + |z'|\sqrt{1 - b'^2}$

and $\xi'/b' > y' > b'\xi'$

$$\begin{aligned} P &= -\frac{\xi' - b'y'}{c\sqrt{1 - b'^2}} \\ S &= \frac{b'(\xi' - b'y')}{c\sqrt{1 - b'^2}} \\ D &= \pm\frac{\xi' - b'y'}{c} \end{aligned} \qquad \text{(B16)}$$

9.3 Appendix C - Sample Wing-Body Case Printout

A sample printout is given here for the wing optimization of the Boeing wind-tunnel model described in section 6.4. A comparison between the planar and optimized wing cases is presented in section 7.0.

The uniform panel layout used for this example is shown in the upper sketch on figure 49.

MAY 20, 1967

PROGRAM FOR ANALYSIS AND DESIGN OF SUPERSONIC WING-BODY COMBINATIONS

DATA CARDS ARE LISTED BELOW

```
DEFINE                                                                  1D
BODY                                                                    2D
TR-805/EQUIVALENT/BODY                                                  3D
24.         8.                                                          4D
0.          25.         50.         75.         102.19      130.        5D
155.        180.                                                        5D
0.          0.          0.          2.          0.                      6D
1.5         0.          0.          2.          .270                    6D
3.          0.          0.          2.          .4464                   6D
4.5         0.          0.          2.          .5943                   6D
6.          0.          0.          2.          .7234                   6D
7.5         0.          0.          2.          .837                    6D
9.          0.          0.          2.          .9364                   6D
10.5        0.          0.          2.          1.0223                  6D
12.         0.          0.          2.          1.0936                  6D
13.5        0.          0.          2.          1.1479                  6D
15.         0.          0.          2.          1.184                   6D
15.1        0.          0.          0.                                  6D
17.5        0.          0.          0.                                  6D
20.         0.          0.          0.                                  6D
22.5        0.          0.          0.                                  6D
25.         0.          0.          0.                                  6D
27.5        0.          0.          0.                                  6D
29.9        0.          0.          0.                                  6D
31.         0.          0.          2.          1.174                   6D
32.         0.          0.          2.          1.154                   6D
33.         0.          0.          2.          1.124                   6D
34.         0.          0.          2.          1.084                   6D
35.         0.          0.          2.          1.034                   6D
36.         0.          0.          2.          1.                      6D
WING                                                                    10D
TR-805 WING(TWO=-.25)                                                   11D
2.          3.          4.          11.         1.
1.          1.          0.                                              13D
10.67       0.          40.27       10.774                              14D
19.88       0.          43.518      8.603       40.27       10.774
3.          0.          0.          0.          2.                      16D
0.          -.25        9.21        -.25                                17D
1.          0.          5.          0.          0.                      16D
3.                      8.603       8.603       2.
0.          -.25        9.21        -.25
3.                      10.774      10.774      2.
0.          -.25        0.          -.25
0.          10.         20.         30.         40.         50.         18D
60.         70.         80.         90.         100.                    18D
WBX                                                                     19D
2.          .0001                                                       20D
DEFEND                                                                  22D
PANEL                                                                   1P
50.         0.          1.          1.          .001                    2P
.95         0.                                                          3P
BODY PANEL                                                              4P
4.          11.         .02          01                                 5P
25.         27.         29.5        32.415                              6P
1.          2.          3.          4.          5.          6.          7P
```

```
7.          8.          9.          10.         11.                                   7P
WING PANEL                                                                            8P
10.         1.          1.          .05                                               9P
1.9846      2.8119      3.6392      4.4665      5.2938      6.1211
6.9484      7.7757      8.603
0.          40.27       10.774      40.270      10.774                                11P
15.                                                                                   12P
0.          0.          .025        .0108       .05         .01556                    12P
.1          .02155      .15         .02548      .2          .02832                    12P
.3          .03215      .4          .0342       .5          .03385                    12P
.6          .03112      .7          .02599      .8          .01915                    12P
.9          .01084      .95         .00616      1.          0.                        12P
15.                                                                                   13P
0.          0.          .025        -.00257     .05         -.00325                   13P
.1          -.00428     .15         -.0051      .2          -.00581                   13P
.3          -.00701     .4          -.00735     .5          -.0065                    13P
.6          -.00469     .7          -.00239     .8          -.00068                   13P
.9          0.          .95         0.          1.          0.                        13P
PANEND                                                                                14P
AERODYNAMIC                                                                           1A
SAVE TAPE
1.8         1.                                                                        2A
TR 805 MIN DRAG CLBAR=.159
3.          0.          0.          1.          1.                                    4A
89.375      0.          0.                                                            5A

GIVEN BODY RADII
TR-805 BODY CAMBER                                                                    6A
0.          .025        .043        .056        .068        .079        .089
.099        .108        .1165       .125        .134        .142        .148
.156        .162        .167        .172        .175        .178        .180
.179        .1779       .1768       .1757       .1746       .1735       .1724
.1713       .1702       .1691       .168        .1679       .1668       .1657
.1646       .1635       .1624       .1613       .1602       .1591       .158
.1569       .1559       .1547       .1536       .1525       .1514       .1503
.1492
0.          .159
GIVEN WING THICKNESS
                                                                                      11A

END OF DATA                                                                           11A

     A TOTAL OF   95  DATA CARDS WERE READ
```

MAY 20, 1967

BODY RADIUS AND Z-COORDINATE OF BODY CENTROID VERSUS X-PRIME

NO.	X-PRIME	RADIUS	Z-PRIME
1	0.0000	0.0000	0.0000
2	0.7243	0.1304	0.0000
3	1.4485	0.2607	0.0000
4	2.1728	0.3491	0.0000
5	2.8970	0.4343	0.0000
6	3.6213	0.5077	0.0000
7	4.3456	0.5791	0.0000
8	5.0698	0.6433	0.0000
9	5.7941	0.7057	0.0000
10	6.5184	0.7627	0.0000
11	7.2426	0.8175	0.0000
12	7.9669	0.8679	0.0000
13	8.6911	0.9159	0.0000
14	9.4154	0.9602	0.0000
15	10.1397	1.0017	0.0000
16	10.8639	1.0396	0.0000
17	11.5882	1.0740	0.0000
18	12.3124	1.1049	0.0000
19	13.0367	1.1311	0.0000
20	13.7610	1.1542	0.0000
21	14.5023	1.1720	0.0000
22	15.2436	1.1840	0.0000
23	15.9849	1.1840	0.0000
24	16.7262	1.1840	0.0000
25	17.4675	1.1840	0.0000
26	18.2088	1.1840	0.0000
27	18.9501	1.1840	0.0000
28	19.6914	1.1840	0.0000
29	20.4327	1.1840	0.0000
30	21.1740	1.1840	0.0000
31	21.9153	1.1840	0.0000
32	22.6566	1.1840	0.0000
33	23.3979	1.1840	0.0000
34	24.1392	1.1840	0.0000
35	24.8805	1.1840	0.0000
36	25.6218	1.1840	0.0000
37	26.3631	1.1840	0.0000
38	27.1044	1.1840	0.0000
39	27.8457	1.1840	0.0000
40	28.5870	1.1840	0.0000
41	29.3283	1.1840	0.0000
42	30.0696	1.1825	0.0000
43	30.8109	1.1757	0.0000
44	31.5522	1.1630	0.0000
45	32.2935	1.1452	0.0000
46	33.0348	1.1226	0.0000
47	33.7761	1.0930	0.0000
48	34.5174	1.0581	0.0000
49	35.2587	1.0252	0.0000
50	36.0000	1.0000	0.0000

BODY PANEL

4P

BODY PANEL ROUTINE

THERE ARE 15 TRANSVERSE VERTICAL PLANES THAT INTERSECT THE BODY
TO DEFINE PANEL LEADING AND TRAILING EDGES

X-INTERCEPTS

13.76097
14.75289
15.69159
16.61262
17.53366
18.45469
19.37572
20.29676
21.21779
22.13882
23.05986
25.00000
27.00000
29.50000
32.41500

BODY PANEL CORNER POINT COORDINATES
1 AND 2 INDICATE BODY-PANEL LEADING-EDGE POINTS, 3 AND 4 INDICATE TRAILING-EDGE POINTS

PANEL NO	PARTS	X 1	Y 1	Z 1	X 2	Y 2	Z 2	X 3	Y 3	Z 3	X 4	Y 4	Z 4
1	1	13.761	0.000	1.154	13.761	0.488	1.046	14.753	0.005	1.177	14.753	0.493	1.069
2	1	14.753	0.000	1.178	14.753	0.498	1.068	15.692	0.001	1.184	15.692	0.499	1.073
3	1	15.692	0.000	1.184	15.692	0.500	1.073	16.613	0.000	1.184	16.613	0.500	1.073
4	1	16.613	0.000	1.184	16.613	0.500	1.073	17.534	0.000	1.184	17.534	0.500	1.073
5	1	17.534	0.000	1.184	17.534	0.500	1.073	18.455	0.000	1.184	18.455	0.500	1.073
6	1	18.455	0.000	1.184	18.455	0.500	1.073	19.376	0.000	1.184	19.376	0.500	1.073
7	1	19.376	0.000	1.184	19.376	0.500	1.073	20.297	0.000	1.184	20.297	0.500	1.073
8	1	20.297	0.000	1.184	20.297	0.500	1.073	21.218	0.000	1.184	21.218	0.500	1.073
9	1	21.218	0.000	1.184	21.218	0.500	1.073	22.139	0.000	1.184	22.139	0.500	1.073
10	1	22.139	0.000	1.184	22.139	0.500	1.073	23.060	0.000	1.184	23.060	0.500	1.073
11	1	23.060	0.000	1.184	23.060	0.500	1.073	25.000	0.000	1.184	25.000	0.500	1.073
12	1	25.000	0.000	1.184	25.000	0.500	1.073	27.000	0.000	1.184	27.000	0.500	1.073
13	1	27.000	0.000	1.184	27.000	0.500	1.073	29.500	0.000	1.184	29.500	0.500	1.073
14	1	29.500	0.009	1.182	29.500	0.491	1.075	32.415	0.000	1.142	32.415	0.482	1.035
15	1	13.761	0.488	1.046	13.761	0.884	0.742	14.753	0.502	1.065	14.753	0.898	0.760
16	1	14.753	0.498	1.068	14.753	0.902	0.757	15.692	0.501	1.072	15.692	0.906	0.762
17	1	15.692	0.500	1.073	15.692	0.907	0.761	16.613	0.500	1.073	16.613	0.907	0.761
18	1	16.613	0.500	1.073	16.613	0.907	0.761	17.534	0.500	1.073	17.534	0.907	0.761
19	1	17.534	0.500	1.073	17.534	0.907	0.761	18.455	0.500	1.073	18.455	0.907	0.761
20	1	18.455	0.500	1.073	18.455	0.907	0.761	19.376	0.500	1.073	19.376	0.907	0.761
21	1	19.376	0.500	1.073	19.376	0.907	0.761	20.297	0.500	1.073	20.297	0.907	0.761
22	1	20.297	0.500	1.073	20.297	0.907	0.761	21.218	0.500	1.073	21.218	0.907	0.761
23	1	21.218	0.500	1.073	21.218	0.907	0.761	22.139	0.500	1.073	22.139	0.907	0.761
24	1	22.139	0.500	1.073	22.139	0.907	0.761	23.060	0.500	1.073	23.060	0.907	0.761
25	1	23.060	0.500	1.073	23.060	0.907	0.761	25.000	0.500	1.073	25.000	0.907	0.761
26	1	25.000	0.500	1.073	25.000	0.907	0.761	27.000	0.500	1.073	27.000	0.907	0.761
27	1	27.000	0.500	1.073	27.000	0.907	0.761	29.500	0.500	1.073	29.500	0.907	0.761
28	1	29.500	0.508	1.067	29.500	0.900	0.767	32.415	0.482	1.035	32.415	0.874	0.734
29	1	13.761	0.884	0.742	13.761	1.115	0.299	14.753	0.905	0.753	14.753	1.136	0.309
30	1	14.753	0.902	0.757	14.753	1.138	0.305	15.692	0.908	0.760	15.692	1.143	0.308
31	1	15.692	0.907	0.761	15.692	1.144	0.306	16.613	0.907	0.761	16.613	1.144	0.306
32	1	16.613	0.907	0.761	16.613	1.144	0.306	17.534	0.907	0.761	17.534	1.144	0.306
33	1	17.534	0.907	0.761	17.534	1.144	0.306	18.455	0.907	0.761	18.455	1.144	0.306
34	1	18.455	0.907	0.761	18.455	1.144	0.306	19.376	0.907	0.761	19.376	1.144	0.306
35	1	19.376	0.907	0.761	19.376	1.144	0.306	20.297	0.907	0.761	20.297	1.144	0.306
36	1	20.297	0.907	0.761	20.297	1.144	0.306	21.218	0.907	0.761	21.218	1.144	0.306
37	1	21.218	0.907	0.761	21.218	1.144	0.306	22.139	0.907	0.761	22.139	1.144	0.306
38	1	22.139	0.907	0.761	22.139	1.144	0.306	23.060	0.907	0.761	23.060	1.144	0.306
39	1	23.060	0.907	0.761	23.060	1.144	0.306	25.000	0.907	0.761	25.000	1.144	0.306
40	1	25.000	0.907	0.761	25.000	1.144	0.306	27.000	0.907	0.761	27.000	1.144	0.306
41	1	27.000	0.907	0.761	27.000	1.144	0.306	29.500	0.907	0.761	29.500	1.144	0.306
42	1	29.500	0.911	0.753	29.500	1.139	0.315	32.415	0.874	0.734	32.415	1.103	0.295
43	1	13.761	1.115	0.299	13.761	1.125	-0.250	14.753	1.138	0.299	14.753	1.151	-0.250
44	1	14.753	1.138	0.305	14.753	1.151	-0.250	15.692	1.144	0.305	15.692	1.157	-0.250
45	1	15.692	1.144	0.306	15.692	1.157	-0.250	16.613	1.144	0.306	16.613	1.157	-0.250
46	1	16.613	1.144	0.306	16.613	1.157	-0.250	17.534	1.144	0.306	17.534	1.157	-0.250
47	1	17.534	1.144	0.306	17.534	1.157	-0.250	18.455	1.144	0.306	18.455	1.157	-0.250
48	1	18.455	1.144	0.306	18.455	1.157	-0.250	19.376	1.144	0.306	19.376	1.157	-0.250
49	1	19.376	1.144	0.306	19.376	1.157	-0.250	20.297	1.144	0.306	20.297	1.157	-0.250
50	1	20.297	1.144	0.306	20.297	1.157	-0.250	21.218	1.144	0.306	21.218	1.157	-0.250
51	1	21.218	1.144	0.306	21.218	1.157	-0.250	22.139	1.144	0.306	22.139	1.157	-0.250
52	1	22.139	1.144	0.306	22.139	1.157	-0.250	23.060	1.144	0.306	23.060	1.157	-0.250
53	1	23.060	1.144	0.306	23.060	1.157	-0.250	25.000	1.144	0.306	25.000	1.157	-0.250
54	1	25.000	1.144	0.306	25.000	1.157	-0.250	27.000	1.144	0.306	27.000	1.157	-0.250

55	1	27.000	1.144	0.306	27.000	1.157	-0.250	29.500	1.144	0.306	29.500	1.157	-0.250
56	1	29.500	1.144	0.296	29.500	1.157	-0.240	32.415	1.103	0.295	32.415	1.116	-0.241
57	1	13.761	1.125	-0.250	13.761	0.884	-0.742	14.753	1.146	-0.260	14.753	0.905	-0.752
58	1	14.753	1.151	-0.250	14.753	0.902	-0.757	15.692	1.156	-0.253	15.692	0.908	-0.760
59	1	15.692	1.157	-0.250	15.692	0.907	-0.761	16.613	1.157	-0.250	16.613	0.907	-0.761
60	1	16.613	1.157	-0.250	16.613	0.907	-0.761	17.534	1.157	-0.250	17.534	0.907	-0.761
61	1	17.534	1.157	-0.250	17.534	0.907	-0.761	18.455	1.157	-0.250	18.455	0.907	-0.761
62	1	18.455	1.157	-0.250	18.455	0.907	-0.761	19.376	1.157	-0.250	19.376	0.907	-0.761
63	1	19.376	1.157	-0.250	19.376	0.907	-0.761	20.297	1.157	-0.250	20.297	0.907	-0.761
64	1	20.297	1.157	-0.250	20.297	0.907	-0.761	21.218	1.157	-0.250	21.218	0.907	-0.761
65	1	21.218	1.157	-0.250	21.218	0.907	-0.761	22.139	1.157	-0.250	22.139	0.907	-0.761
66	1	22.139	1.157	-0.250	22.139	0.907	-0.761	23.060	1.157	-0.250	23.060	0.907	-0.761
67	1	23.060	1.157	-0.250	23.060	0.907	-0.761	25.000	1.157	-0.250	25.000	0.907	-0.761
68	1	25.000	1.157	-0.250	25.000	0.907	-0.761	27.000	1.157	-0.250	27.000	0.907	-0.761
69	1	27.000	1.157	-0.250	27.000	0.907	-0.761	29.500	1.157	-0.250	29.500	0.907	-0.761
70	1	29.500	1.153	-0.259	29.500	0.911	-0.752	32.415	1.116	-0.241	32.415	0.874	-0.734
71	1	13.761	0.884	-0.742	13.761	0.488	-1.046	14.753	0.898	-0.760	14.753	0.502	-1.065
72	1	14.753	0.902	-0.757	14.753	0.498	-1.068	15.692	0.906	-0.762	15.692	0.501	-1.072
73	1	15.692	0.907	-0.761	15.692	0.500	-1.073	16.613	0.907	-0.761	16.613	0.500	-1.073
74	1	16.613	0.907	-0.761	16.613	0.500	-1.073	17.534	0.907	-0.761	17.534	0.500	-1.073
75	1	17.534	0.907	-0.761	17.534	0.500	-1.073	18.455	0.907	-0.761	18.455	0.500	-1.073
76	1	18.455	0.907	-0.761	18.455	0.500	-1.073	19.376	0.907	-0.761	19.376	0.500	-1.073
77	1	19.376	0.907	-0.761	19.376	0.500	-1.073	20.297	0.907	-0.761	20.297	0.500	-1.073
78	1	20.297	0.907	-0.761	20.297	0.500	-1.073	21.218	0.907	-0.761	21.218	0.500	-1.073
79	1	21.218	0.907	-0.761	21.218	0.500	-1.073	22.139	0.907	-0.761	22.139	0.500	-1.073
80	1	22.139	0.907	-0.761	22.139	0.500	-1.073	23.060	0.907	-0.761	23.060	0.500	-1.073
81	1	23.060	0.907	-0.761	23.060	0.500	-1.073	25.000	0.907	-0.761	25.000	0.500	-1.073
82	1	25.000	0.907	-0.761	25.000	0.500	-1.073	27.000	0.907	-0.761	27.000	0.500	-1.073
83	1	27.000	0.907	-0.761	27.000	0.500	-1.073	29.500	0.907	-0.761	29.500	0.500	-1.073
84	1	29.500	0.900	-0.767	29.500	0.508	-1.067	32.415	0.874	-0.734	32.415	0.482	-1.035
85	1	13.761	0.488	-1.046	13.761	0.000	-1.154	14.753	0.493	-1.069	14.753	0.005	-1.177
86	1	14.753	0.498	-1.068	14.753	0.000	-1.178	15.692	0.499	-1.073	15.692	0.001	-1.184
87	1	15.692	0.500	-1.073	15.692	0.000	-1.184	16.613	0.500	-1.073	16.613	0.000	-1.184
88	1	16.613	0.500	-1.073	16.613	0.000	-1.184	17.534	0.500	-1.073	17.534	0.000	-1.184
89	1	17.534	0.500	-1.073	17.534	0.000	-1.184	18.455	0.500	-1.073	18.455	0.000	-1.184
90	1	18.455	0.500	-1.073	18.455	0.000	-1.184	19.376	0.500	-1.073	19.376	0.000	-1.184
91	1	19.376	0.500	-1.073	19.376	0.000	-1.184	20.297	0.500	-1.073	20.297	0.000	-1.184
92	1	20.297	0.500	-1.073	20.297	0.000	-1.184	21.218	0.500	-1.073	21.218	0.000	-1.184
93	1	21.218	0.500	-1.073	21.218	0.000	-1.184	22.139	0.500	-1.073	22.139	0.000	-1.184
94	1	22.139	0.500	-1.073	22.139	0.000	-1.184	23.060	0.500	-1.073	23.060	0.000	-1.184
95	1	23.060	0.500	-1.073	23.060	0.000	-1.184	25.000	0.500	-1.073	25.000	0.000	-1.184
96	1	25.000	0.500	-1.073	25.000	0.000	-1.184	27.000	0.500	-1.073	27.000	0.000	-1.184
97	1	27.000	0.500	-1.073	27.000	0.000	-1.184	29.500	0.500	-1.073	29.500	0.000	-1.184
98	1	29.500	0.491	-1.075	29.500	0.009	-1.182	32.415	0.482	-1.035	32.415	0.000	-1.142

BODY PANEL CENTROID AND CONTROL POINT COORDINATES

PANEL	X_C	Y_C	Z_C	X_{CP}	Y_{CP}	Z_{CP}	AREA	THETA-INCLIN	ALPHA-INCID
1	14.259	0.246	1.112	14.703	0.249	1.122	0.501	-0.21817	0.02349
2	15.223	0.250	1.126	15.645	0.250	1.128	0.480	-0.21817	0.00619
3	16.152	0.250	1.129	16.567	0.250	1.129	0.472	-0.21817	0.00000
4	17.073	0.250	1.129	17.488	0.250	1.129	0.472	-0.21817	0.00000
5	17.994	0.250	1.129	18.409	0.250	1.129	0.472	-0.21817	0.00000
6	18.915	0.250	1.129	19.330	0.250	1.129	0.472	-0.21817	0.00000
7	19.836	0.250	1.129	20.251	0.250	1.129	0.472	-0.21817	0.00000
8	20.757	0.250	1.129	21.172	0.250	1.129	0.472	-0.21817	0.00000
9	21.678	0.250	1.129	22.093	0.250	1.129	0.472	-0.21817	0.00000
10	22.599	0.250	1.129	23.014	0.250	1.129	0.472	-0.21817	0.00000
11	24.030	0.250	1.129	24.903	0.250	1.129	0.994	-0.21817	0.00000
12	26.000	0.250	1.129	26.900	0.250	1.129	1.025	-0.21817	0.00000
13	28.250	0.250	1.129	29.375	0.250	1.129	1.281	-0.21817	0.00000
14	30.949	0.246	1.108	32.269	0.242	1.090	1.467	-0.21817	-0.01422
15	14.259	0.693	0.902	14.703	0.699	0.912	0.501	-0.65450	0.02349
16	15.223	0.702	0.915	15.645	0.704	0.917	0.480	-0.65450	0.00619
17	16.152	0.704	0.917	16.567	0.704	0.917	0.472	-0.65450	0.00000
18	17.073	0.704	0.917	17.488	0.704	0.917	0.472	-0.65450	0.00000
19	17.994	0.704	0.917	18.409	0.704	0.917	0.472	-0.65450	0.00000
20	18.915	0.704	0.917	19.330	0.704	0.917	0.472	-0.65450	0.00000
21	19.836	0.704	0.917	20.251	0.704	0.917	0.472	-0.65450	0.00000
22	20.757	0.704	0.917	21.172	0.704	0.917	0.472	-0.65450	0.00000
23	21.678	0.704	0.917	22.093	0.704	0.917	0.472	-0.65450	0.00000
24	22.599	0.704	0.917	23.014	0.704	0.917	0.472	-0.65450	0.00000
25	24.030	0.704	0.917	24.903	0.704	0.917	0.994	-0.65450	0.00000
26	26.000	0.704	0.917	26.900	0.704	0.917	1.025	-0.65450	0.00000
27	28.250	0.704	0.917	29.375	0.704	0.917	1.281	-0.65450	0.00000
28	30.949	0.691	0.901	32.269	0.680	0.886	1.467	-0.65450	-0.01422
29	14.259	1.010	0.526	14.703	1.019	0.531	0.501	-1.09083	0.02349
30	15.223	1.023	0.532	15.645	1.025	0.534	0.480	-1.09083	0.00619
31	16.152	1.025	0.534	16.567	1.025	0.534	0.472	-1.09083	0.00000
32	17.073	1.025	0.534	17.488	1.025	0.534	0.472	-1.09083	0.00000
33	17.994	1.025	0.534	18.409	1.025	0.534	0.472	-1.09083	0.00000
34	18.915	1.025	0.534	19.330	1.025	0.534	0.472	-1.09083	0.00000
35	19.836	1.025	0.534	20.251	1.025	0.534	0.472	-1.09083	0.00000
36	20.757	1.025	0.534	21.172	1.025	0.534	0.472	-1.09083	0.00000
37	21.678	1.025	0.534	22.093	1.025	0.534	0.472	-1.09083	0.00000
38	22.599	1.025	0.534	23.014	1.025	0.534	0.472	-1.09083	0.00000
39	24.030	1.025	0.534	24.903	1.025	0.534	0.994	-1.09083	0.00000
40	26.000	1.025	0.534	26.900	1.025	0.534	1.025	-1.09083	0.00000
41	28.250	1.025	0.534	29.375	1.025	0.534	1.281	-1.09083	0.00000
42	30.949	1.007	0.524	32.269	0.990	0.516	1.467	-1.09083	-0.01422
43	14.259	1.132	0.026	14.703	1.143	0.026	0.548	-1.54979	0.02338
44	15.222	1.147	0.028	15.645	1.150	0.028	0.522	-1.54686	0.00616
45	16.152	1.150	0.028	16.567	1.150	0.028	0.513	-1.54628	0.00000
46	17.073	1.150	0.028	17.488	1.150	0.028	0.513	-1.54628	0.00000
47	17.994	1.150	0.028	18.409	1.150	0.028	0.513	-1.54628	0.00000
48	18.915	1.150	0.028	19.330	1.150	0.028	0.513	-1.54628	0.00000
49	19.836	1.150	0.028	20.251	1.150	0.028	0.513	-1.54628	0.00000
50	20.757	1.150	0.028	21.172	1.150	0.028	0.513	-1.54628	0.00000
51	21.678	1.150	0.028	22.093	1.150	0.028	0.513	-1.54628	0.00000
52	22.599	1.150	0.028	23.014	1.150	0.028	0.513	-1.54628	0.00000
53	24.030	1.150	0.028	24.903	1.150	0.028	1.080	-1.54628	0.00000
54	26.000	1.150	0.028	26.900	1.150	0.028	1.113	-1.54627	0.00000
55	28.250	1.150	0.028	29.375	1.150	0.028	1.392	-1.54627	0.00000

56	30.949	1.130	0.028	32.269	1.111	0.027	1.594	-1.54627	-0.01415
57	14.259	1.016	-0.500	14.703	1.025	-0.504	0.552	-2.02624	0.02336
58	15.223	1.029	-0.505	15.645	1.032	-0.506	0.532	-2.02624	0.00615
59	16.152	1.032	-0.506	16.567	1.032	-0.506	0.524	-2.02624	0.00000
60	17.073	1.032	-0.506	17.488	1.032	-0.506	0.524	-2.02624	0.00000
61	17.994	1.032	-0.506	18.409	1.032	-0.506	0.524	-2.02624	0.00000
62	18.915	1.032	-0.506	19.330	1.032	-0.506	0.524	-2.02624	0.00000
63	19.836	1.032	-0.506	20.251	1.032	-0.506	0.524	-2.02624	0.00000
64	20.757	1.032	-0.506	21.172	1.032	-0.506	0.524	-2.02624	0.00000
65	21.678	1.032	-0.506	22.093	1.032	-0.506	0.524	-2.02624	0.00000
66	22.599	1.032	-0.506	23.014	1.032	-0.506	0.524	-2.02624	0.00000
67	24.030	1.032	-0.506	24.903	1.032	-0.506	1.104	-2.02624	0.00000
68	26.000	1.032	-0.506	26.900	1.032	-0.506	1.138	-2.02624	0.00000
69	28.250	1.032	-0.506	29.375	1.032	-0.506	1.423	-2.02624	0.00000
70	30.949	1.014	-0.497	32.269	0.997	-0.488	1.629	-2.02624	-0.01413
71	14.259	0.693	-0.903	14.703	0.699	-0.912	0.501	-2.48709	0.02349
72	15.223	0.702	-0.915	15.645	0.704	-0.917	0.480	-2.48709	0.00619
73	16.152	0.704	-0.917	16.567	0.704	-0.917	0.472	-2.48709	0.00000
74	17.073	0.704	-0.917	17.488	0.704	-0.917	0.472	-2.48709	0.00000
75	17.994	0.704	-0.917	18.409	0.704	-0.917	0.472	-2.48709	0.00000
76	18.915	0.704	-0.917	19.330	0.704	-0.917	0.472	-2.48709	0.00000
77	19.836	0.704	-0.917	20.251	0.704	-0.917	0.472	-2.48709	0.00000
78	20.757	0.704	-0.917	21.172	0.704	-0.917	0.472	-2.48709	0.00000
79	21.678	0.704	-0.917	22.093	0.704	-0.917	0.472	-2.48709	0.00000
80	22.599	0.704	-0.917	23.014	0.704	-0.917	0.472	-2.48709	0.00000
81	24.030	0.704	-0.917	24.903	0.704	-0.917	0.994	-2.48709	0.00000
82	26.000	0.704	-0.917	26.900	0.704	-0.917	1.025	-2.48709	0.00000
83	28.250	0.704	-0.917	29.375	0.704	-0.917	1.281	-2.48709	0.00000
84	30.949	0.691	-0.901	32.269	0.680	-0.886	1.467	-2.48709	-0.01422
85	14.259	0.246	-1.112	14.703	0.249	-1.122	0.501	-2.92343	0.02349
86	15.223	0.250	-1.126	15.645	0.250	-1.128	0.480	-2.92343	0.00619
87	16.152	0.250	-1.129	16.567	0.250	-1.129	0.472	-2.92343	0.00000
88	17.073	0.250	-1.129	17.488	0.250	-1.129	0.472	-2.92343	0.00000
89	17.994	0.250	-1.129	18.409	0.250	-1.129	0.472	-2.92343	0.00000
90	18.915	0.250	-1.129	19.330	0.250	-1.129	0.472	-2.92343	0.00000
91	19.836	0.250	-1.129	20.251	0.250	-1.129	0.472	-2.92343	0.00000
92	20.757	0.250	-1.129	21.172	0.250	-1.129	0.472	-2.92343	0.00000
93	21.678	0.250	-1.129	22.093	0.250	-1.129	0.472	-2.92343	0.00000
94	22.599	0.250	-1.129	23.014	0.250	-1.129	0.472	-2.92343	0.00000
95	24.030	0.250	-1.129	24.903	0.250	-1.129	0.994	-2.92343	0.00000
96	26.000	0.250	-1.129	26.900	0.250	-1.129	1.025	-2.92343	0.00000
97	28.250	0.250	-1.129	29.375	0.250	-1.129	1.281	-2.92343	0.00000
98	30.949	0.246	-1.108	32.269	0.242	-1.090	1.467	-2.92343	-0.01422

WING PANEL

BP

WING PANEL ROUTINE

THERE ARE 10 VERTICAL PLANES THAT INTERSECT THE WING TO DEFINE PANEL SIDE EDGES

LEADING-EDGE
Y-INTERCEPT

1.98460
2.81190
3.63920
4.46650
5.29380
6.12110
6.94840
7.77570
8.60300

OUTBOARD CUTTING PLANE
LEADING-EDGE

X-INTERCEPT	Y-INTERCEPT	SLOPE
40.27000	10.77400	0.00000

ZERO-SLOPE INDICATES STREAMWISE CUTTING PLANE

UNDRFLOW AT 25422 IN MQ

UNDRFLOW AT 25422 IN MQ

UNDRFLOW AT 25422 IN MQ

AIRFOIL COORDINATES ARE USED DIRECTLY BY PROGRAM

WING PANEL CORNER POINT COORDINATES
1 AND 2 INDICATE WING PANEL LEADING-EDGE POINTS, 3 AND 4 INDICATE TRAILING-EDGE POINTS

PANEL NO	PARTS	X 1	Y 1	Z 1	X 2	Y 2	Z 2	X 3	Y 3	Z 3	X 4	Y 4	Z 4
1	1	13.832	1.151	-0.250	16.122	1.985	-0.250	14.753	1.151	-0.250	17.043	1.985	-0.250
2	1	14.771	1.157	-0.250	17.043	1.985	-0.250	15.692	1.157	-0.250	17.965	1.985	-0.250
3	1	15.692	1.157	-0.250	17.965	1.985	-0.250	16.613	1.157	-0.250	18.886	1.985	-0.250
4	1	16.613	1.157	-0.250	18.886	1.985	-0.250	17.534	1.157	-0.250	19.807	1.985	-0.250
5	1	17.534	1.157	-0.250	19.807	1.985	-0.250	18.455	1.157	-0.250	20.728	1.985	-0.250
6	1	18.455	1.157	-0.250	20.728	1.985	-0.250	19.376	1.157	-0.250	21.649	1.985	-0.250
7	1	19.376	1.157	-0.250	21.649	1.985	-0.250	20.297	1.157	-0.250	22.570	1.985	-0.250
8	1	20.297	1.157	-0.250	22.570	1.985	-0.250	21.218	1.157	-0.250	23.491	1.985	-0.250
9	1	21.218	1.157	-0.250	23.491	1.985	-0.250	22.139	1.157	-0.250	24.412	1.985	-0.250
10	1	22.139	1.157	-0.250	24.412	1.985	-0.250	23.060	1.157	-0.250	25.333	1.985	-0.250
11	1	16.122	1.985	-0.250	18.395	2.812	-0.250	17.043	1.985	-0.250	19.316	2.812	-0.250
12	1	17.043	1.985	-0.250	19.316	2.812	-0.250	17.965	1.985	-0.250	20.237	2.812	-0.250
13	1	17.965	1.985	-0.250	20.237	2.812	-0.250	18.886	1.985	-0.250	21.159	2.812	-0.250
14	1	18.886	1.985	-0.250	21.159	2.812	-0.250	19.807	1.985	-0.250	22.080	2.812	-0.250
15	1	19.807	1.985	-0.250	22.080	2.812	-0.250	20.728	1.985	-0.250	23.001	2.812	-0.250
16	1	20.728	1.985	-0.250	23.001	2.812	-0.250	21.649	1.985	-0.250	23.922	2.812	-0.250
17	1	21.649	1.985	-0.250	23.922	2.812	-0.250	22.570	1.985	-0.250	24.843	2.812	-0.250
18	1	22.570	1.985	-0.250	24.843	2.812	-0.250	23.491	1.985	-0.250	25.764	2.812	-0.250
19	1	23.491	1.985	-0.250	25.764	2.812	-0.250	24.412	1.985	-0.250	26.685	2.812	-0.250
20	1	24.412	1.985	-0.250	26.685	2.812	-0.250	25.333	1.985	-0.250	27.606	2.812	-0.250
21	1	19.395	2.812	-0.250	20.668	3.639	-0.250	19.316	2.812	-0.250	21.589	3.639	-0.250
22	1	19.316	2.812	-0.250	21.589	3.639	-0.250	20.237	2.812	-0.250	22.510	3.639	-0.250
23	1	20.237	2.812	-0.250	22.510	3.639	-0.250	21.159	2.812	-0.250	23.431	3.639	-0.250
24	1	21.159	2.812	-0.250	23.431	3.639	-0.250	22.080	2.812	-0.250	24.353	3.639	-0.250
25	1	22.080	2.812	-0.250	24.353	3.639	-0.250	23.001	2.812	-0.250	25.274	3.639	-0.250
26	1	23.001	2.812	-0.250	25.274	3.639	-0.250	23.922	2.812	-0.250	26.195	3.639	-0.250
27	1	23.922	2.812	-0.250	26.195	3.639	-0.250	24.843	2.812	-0.250	27.116	3.639	-0.250
28	1	24.843	2.812	-0.250	27.116	3.639	-0.250	25.764	2.812	-0.250	28.037	3.639	-0.250
29	1	25.764	2.812	-0.250	28.037	3.639	-0.250	26.685	2.812	-0.250	28.958	3.639	-0.250
30	1	26.685	2.812	-0.250	28.958	3.639	-0.250	27.606	2.812	-0.250	29.879	3.639	-0.250
31	1	20.668	3.639	-0.250	22.941	4.466	-0.250	21.589	3.639	-0.250	23.862	4.466	-0.250
32	1	21.589	3.639	-0.250	23.862	4.466	-0.250	22.510	3.639	-0.250	24.783	4.466	-0.250
33	1	22.510	3.639	-0.250	24.783	4.466	-0.250	23.431	3.639	-0.250	25.704	4.466	-0.250
34	1	23.431	3.639	-0.250	25.704	4.466	-0.250	24.353	3.639	-0.250	26.626	4.466	-0.250
35	1	24.353	3.639	-0.250	26.626	4.466	-0.250	25.274	3.639	-0.250	27.547	4.466	-0.250
36	1	25.274	3.639	-0.250	27.547	4.466	-0.250	26.195	3.639	-0.250	28.468	4.466	-0.250
37	1	26.195	3.639	-0.250	28.468	4.466	-0.250	27.116	3.639	-0.250	29.389	4.466	-0.250
38	1	27.116	3.639	-0.250	29.389	4.466	-0.250	28.037	3.639	-0.250	30.310	4.466	-0.250
39	1	28.037	3.639	-0.250	30.310	4.466	-0.250	28.958	3.639	-0.250	31.231	4.466	-0.250
40	1	28.958	3.639	-0.250	31.231	4.466	-0.250	29.879	3.639	-0.250	32.152	4.466	-0.250
41	1	22.941	4.466	-0.250	25.214	5.294	-0.250	23.862	4.466	-0.250	26.135	5.294	-0.250
42	1	23.862	4.466	-0.250	26.135	5.294	-0.250	24.783	4.466	-0.250	27.056	5.294	-0.250
43	1	24.783	4.466	-0.250	27.056	5.294	-0.250	25.704	4.466	-0.250	27.977	5.294	-0.250
44	1	25.704	4.466	-0.250	27.977	5.294	-0.250	26.626	4.466	-0.250	28.899	5.294	-0.250
45	1	26.626	4.466	-0.250	28.899	5.294	-0.250	27.547	4.466	-0.250	29.820	5.294	-0.250
46	1	27.547	4.466	-0.250	29.820	5.294	-0.250	28.468	4.466	-0.250	30.741	5.294	-0.250
47	1	28.468	4.466	-0.250	30.741	5.294	-0.250	29.389	4.466	-0.250	31.662	5.294	-0.250
48	1	29.389	4.466	-0.250	31.662	5.294	-0.250	30.310	4.466	-0.250	32.583	5.294	-0.250
49	1	30.310	4.466	-0.250	32.583	5.294	-0.250	31.231	4.466	-0.250	33.504	5.294	-0.250
50	1	31.231	4.466	-0.250	33.504	5.294	-0.250	32.152	4.466	-0.250	34.425	5.294	-0.250
51	1	25.214	5.294	-0.250	27.487	6.121	-0.250	26.135	5.294	-0.250	28.408	6.121	-0.250
52	1	26.135	5.294	-0.250	28.408	6.121	-0.250	27.056	5.294	-0.250	29.329	6.121	-0.250
53	1	27.056	5.294	-0.250	29.329	6.121	-0.250	27.977	5.294	-0.250	30.250	6.121	-0.250
54	1	27.977	5.294	-0.250	30.250	6.121	-0.250	28.899	5.294	-0.250	31.172	6.121	-0.250

55	1	28.899	5.294	-0.250	31.172	6.121	-0.250	29.820	5.294	-0.250	32.093	6.121	-0.250
56	1	29.820	5.294	-0.250	32.093	6.121	-0.250	30.741	5.294	-0.250	33.014	6.121	-0.250
57	1	30.741	5.294	-0.250	33.014	6.121	-0.250	31.662	5.294	-0.250	33.935	6.121	-0.250
58	1	31.662	5.294	-0.250	33.935	6.121	-0.250	32.583	5.294	-0.250	34.856	6.121	-0.250
59	1	32.583	5.294	-0.250	34.856	6.121	-0.250	33.504	5.294	-0.250	35.777	6.121	-0.250
60	1	33.504	5.294	-0.250	35.777	6.121	-0.250	34.425	5.294	-0.250	36.699	6.121	-0.250
61	1	27.487	6.121	-0.250	29.760	6.948	-0.250	28.408	6.121	-0.250	30.681	6.948	-0.250
62	1	28.408	6.121	-0.250	30.681	6.948	-0.250	29.329	6.121	-0.250	31.602	6.948	-0.250
63	1	29.329	6.121	-0.250	31.602	6.948	-0.250	30.250	6.121	-0.250	32.523	6.948	-0.250
64	1	30.250	6.121	-0.250	32.523	6.948	-0.250	31.172	6.121	-0.250	33.445	6.948	-0.250
65	1	31.172	6.121	-0.250	33.445	6.948	-0.250	32.093	6.121	-0.250	34.366	6.948	-0.250
66	1	32.093	6.121	-0.250	34.366	6.948	-0.250	33.014	6.121	-0.250	35.287	6.948	-0.250
67	1	33.014	6.121	-0.250	35.287	6.948	-0.250	33.935	6.121	-0.250	36.208	6.948	-0.250
68	1	33.935	6.121	-0.250	36.208	6.948	-0.250	34.856	6.121	-0.250	37.129	6.948	-0.250
69	1	34.856	6.121	-0.250	37.129	6.948	-0.250	35.777	6.121	-0.250	38.051	6.948	-0.250
70	1	35.777	6.121	-0.250	38.051	6.948	-0.250	36.699	6.121	-0.250	38.972	6.948	-0.250
71	1	29.760	6.948	-0.250	32.033	7.776	-0.250	30.681	6.948	-0.250	32.954	7.776	-0.250
72	1	30.681	6.948	-0.250	32.954	7.776	-0.250	31.602	6.948	-0.250	33.875	7.776	-0.250
73	1	31.602	6.948	-0.250	33.875	7.776	-0.250	32.523	6.948	-0.250	34.796	7.776	-0.250
74	1	32.523	6.948	-0.250	34.796	7.776	-0.250	33.445	6.948	-0.250	35.718	7.776	-0.250
75	1	33.445	6.948	-0.250	35.718	7.776	-0.250	34.366	6.948	-0.250	36.639	7.776	-0.250
76	1	34.366	6.948	-0.250	36.639	7.776	-0.250	35.287	6.948	-0.250	37.560	7.776	-0.250
77	1	35.287	6.948	-0.250	37.560	7.776	-0.250	36.208	6.948	-0.250	38.481	7.776	-0.250
78	1	36.208	6.948	-0.250	38.481	7.776	-0.250	37.129	6.948	-0.250	39.402	7.776	-0.250
79	1	37.129	6.948	-0.250	39.402	7.776	-0.250	38.051	6.948	-0.250	40.324	7.776	-0.250
80	1	38.051	6.948	-0.250	40.324	7.776	-0.250	38.972	6.948	-0.250	41.245	7.776	-0.250
81	1	32.033	7.776	-0.250	34.305	8.603	-0.250	32.954	7.776	-0.250	35.227	8.603	-0.250
82	1	32.954	7.776	-0.250	35.227	8.603	-0.250	33.875	7.776	-0.250	36.148	8.603	-0.250
83	1	33.875	7.776	-0.250	36.148	8.603	-0.250	34.796	7.776	-0.250	37.069	8.603	-0.250
84	1	34.796	7.776	-0.250	37.069	8.603	-0.250	35.718	7.776	-0.250	37.990	8.603	-0.250
85	1	35.718	7.776	-0.250	37.990	8.603	-0.250	36.639	7.776	-0.250	38.912	8.603	-0.250
86	1	36.639	7.776	-0.250	38.912	8.603	-0.250	37.560	7.776	-0.250	39.833	8.603	-0.250
87	1	37.560	7.776	-0.250	39.833	8.603	-0.250	38.481	7.776	-0.250	40.754	8.603	-0.250
88	1	38.481	7.776	-0.250	40.754	8.603	-0.250	39.402	7.776	-0.250	41.675	8.603	-0.250
89	1	39.402	7.776	-0.250	41.675	8.603	-0.250	40.324	7.776	-0.250	42.597	8.603	-0.250
90	1	40.324	7.776	-0.250	42.597	8.603	-0.250	41.245	7.776	-0.250	43.518	8.603	-0.250
91	1	34.305	8.603	-0.250	40.270	10.774	-0.250	35.227	8.603	-0.250	40.270	10.774	-0.250
92	1	35.227	8.603	-0.250	40.270	10.774	-0.250	36.148	8.603	-0.250	40.270	10.774	-0.250
93	1	36.148	8.603	-0.250	40.270	10.774	-0.250	37.069	8.603	-0.250	40.270	10.774	-0.250
94	1	37.069	8.603	-0.250	40.270	10.774	-0.250	37.990	8.603	-0.250	40.270	10.774	-0.250
95	1	37.990	8.603	-0.250	40.270	10.774	-0.250	38.912	8.603	-0.250	40.270	10.774	-0.250
96	1	38.912	8.603	-0.250	40.270	10.774	-0.250	39.833	8.603	-0.250	40.270	10.774	-0.250
97	1	39.833	8.603	-0.250	40.270	10.774	-0.250	40.754	8.603	-0.250	40.270	10.774	-0.250
98	1	40.754	8.603	-0.250	40.270	10.774	-0.250	41.675	8.603	-0.250	40.270	10.774	-0.250
99	1	41.675	8.603	-0.250	40.270	10.774	-0.250	42.597	8.603	-0.250	40.270	10.774	-0.250
100	1	42.597	8.603	-0.250	40.270	10.774	-0.250	43.518	8.603	-0.250	40.270	10.774	-0.250

WING PANEL CENTROID AND CONTROL POINT COORDINATES

PANEL	X C	Y C	Z C	X CP	Y CP	Z CP	AREA	Z THICK	ALPHA-THICK	Z CAMBER	ALPHA-CAMBER
1	15.418	1.561	-0.250	15.834	1.561	-0.250	0.780	-0.13106	0.06738	-0.17193	0.04620
2	16.363	1.569	-0.250	16.778	1.569	-0.250	0.765	-0.09283	0.03510	-0.14713	0.01662
3	17.289	1.571	-0.250	17.703	1.571	-0.250	0.762	-0.06967	0.01634	-0.13461	0.01069
4	18.210	1.571	-0.250	18.624	1.571	-0.250	0.762	-0.05866	0.00011	-0.12665	0.00483
5	19.131	1.571	-0.250	19.545	1.571	-0.250	0.762	-0.06419	-0.01523	-0.12404	-0.00126
6	20.052	1.571	-0.250	20.466	1.571	-0.250	0.762	-0.08510	-0.02923	-0.12792	-0.00781
7	20.973	1.571	-0.250	21.387	1.571	-0.250	0.762	-0.11931	-0.03690	-0.14046	-0.01879
8	21.894	1.571	-0.250	22.308	1.571	-0.250	0.762	-0.15869	-0.04413	-0.16352	-0.02996
9	22.815	1.571	-0.250	23.229	1.571	-0.250	0.762	-0.20009	-0.05137	-0.19806	-0.04320
10	23.736	1.571	-0.250	24.150	1.571	-0.250	0.762	-0.25001	-0.05876	-0.24687	-0.06070
11	17.719	2.398	-0.250	18.134	2.398	-0.250	0.762	-0.13105	0.06738	-0.17192	0.04620
12	18.640	2.398	-0.250	19.055	2.398	-0.250	0.762	-0.09283	0.03510	-0.14713	0.01662
13	19.562	2.398	-0.250	19.976	2.398	-0.250	0.762	-0.06966	0.01634	-0.13461	0.01069
14	20.483	2.398	-0.250	20.897	2.398	-0.250	0.762	-0.05866	0.00011	-0.12665	0.00483
15	21.404	2.398	-0.250	21.818	2.398	-0.250	0.762	-0.06418	-0.01523	-0.12403	-0.00126
16	22.325	2.398	-0.250	22.739	2.398	-0.250	0.762	-0.08509	-0.02923	-0.12792	-0.00781
17	23.246	2.398	-0.250	23.660	2.398	-0.250	0.762	-0.11931	-0.03690	-0.14046	-0.01879
18	24.167	2.398	-0.250	24.581	2.398	-0.250	0.762	-0.15868	-0.04413	-0.16351	-0.02996
19	25.088	2.398	-0.250	25.502	2.398	-0.250	0.762	-0.20009	-0.05137	-0.19806	-0.04320
20	26.009	2.398	-0.250	26.423	2.398	-0.250	0.762	-0.25001	-0.05876	-0.24687	-0.06070
21	19.992	3.226	-0.250	20.407	3.226	-0.250	0.762	-0.13105	0.06738	-0.17192	0.04620
22	20.913	3.226	-0.250	21.328	3.226	-0.250	0.762	-0.09282	0.03510	-0.14713	0.01662
23	21.834	3.226	-0.250	22.249	3.226	-0.250	0.762	-0.06966	0.01634	-0.13460	0.01069
24	22.756	3.226	-0.250	23.170	3.226	-0.250	0.762	-0.05865	0.00011	-0.12664	0.00483
25	23.677	3.226	-0.250	24.091	3.226	-0.250	0.762	-0.06418	-0.01523	-0.12403	-0.00126
26	24.598	3.226	-0.250	25.012	3.226	-0.250	0.762	-0.08509	-0.02923	-0.12792	-0.00781
27	25.519	3.226	-0.250	25.933	3.226	-0.250	0.762	-0.11931	-0.03690	-0.14046	-0.01879
28	26.440	3.226	-0.250	26.854	3.226	-0.250	0.762	-0.15868	-0.04413	-0.16351	-0.02996
29	27.361	3.226	-0.250	27.776	3.226	-0.250	0.762	-0.20009	-0.05137	-0.19806	-0.04320
30	28.282	3.226	-0.250	28.697	3.226	-0.250	0.762	-0.25001	-0.05876	-0.24687	-0.06070
31	22.265	4.053	-0.250	22.680	4.053	-0.250	0.762	-0.13105	0.06738	-0.17192	0.04620
32	23.186	4.053	-0.250	23.601	4.053	-0.250	0.762	-0.09282	0.03510	-0.14712	0.01662
33	24.107	4.053	-0.250	24.522	4.053	-0.250	0.762	-0.06965	0.01634	-0.13460	0.01069
34	25.029	4.053	-0.250	25.443	4.053	-0.250	0.762	-0.05865	0.00011	-0.12664	0.00483
35	25.950	4.053	-0.250	26.364	4.053	-0.250	0.762	-0.06417	-0.01523	-0.12403	-0.00126
36	26.871	4.053	-0.250	27.285	4.053	-0.250	0.762	-0.08508	-0.02923	-0.12791	-0.00781
37	27.792	4.053	-0.250	28.206	4.053	-0.250	0.762	-0.11930	-0.03690	-0.14045	-0.01879
38	28.713	4.053	-0.250	29.128	4.053	-0.250	0.762	-0.15868	-0.04413	-0.16351	-0.02996
39	29.634	4.053	-0.250	30.049	4.053	-0.250	0.762	-0.20008	-0.05137	-0.19805	-0.04320
40	30.555	4.053	-0.250	30.970	4.053	-0.250	0.762	-0.25001	-0.05876	-0.24687	-0.06070
41	24.538	4.880	-0.250	24.953	4.880	-0.250	0.762	-0.13104	0.06738	-0.17192	0.04620
42	25.459	4.880	-0.250	25.874	4.880	-0.250	0.762	-0.09282	0.03510	-0.14712	0.01662
43	26.380	4.880	-0.250	26.795	4.880	-0.250	0.762	-0.06965	0.01634	-0.13460	0.01069
44	27.302	4.880	-0.250	27.716	4.880	-0.250	0.762	-0.05864	0.00011	-0.12664	0.00483
45	28.223	4.880	-0.250	28.637	4.880	-0.250	0.762	-0.06417	-0.01523	-0.12402	-0.00126
46	29.144	4.880	-0.250	29.558	4.880	-0.250	0.762	-0.08508	-0.02923	-0.12791	-0.00781
47	30.065	4.880	-0.250	30.479	4.880	-0.250	0.762	-0.11930	-0.03690	-0.14045	-0.01879
48	30.986	4.880	-0.250	31.401	4.880	-0.250	0.762	-0.15868	-0.04413	-0.16351	-0.02996
49	31.907	4.880	-0.250	32.322	4.880	-0.250	0.762	-0.20008	-0.05137	-0.19805	-0.04320
50	32.828	4.880	-0.250	33.243	4.880	-0.250	0.762	-0.25001	-0.05876	-0.24687	-0.06070
51	26.811	5.707	-0.250	27.226	5.707	-0.250	0.762	-0.13104	0.06738	-0.17192	0.04620
52	27.732	5.707	-0.250	28.147	5.707	-0.250	0.762	-0.09281	0.03510	-0.14712	0.01662
53	28.653	5.707	-0.250	29.068	5.707	-0.250	0.762	-0.06964	0.01634	-0.13459	0.01069
54	29.574	5.707	-0.250	29.989	5.707	-0.250	0.762	-0.05864	0.00011	-0.12663	0.00483
55	30.496	5.707	-0.250	30.910	5.707	-0.250	0.762	-0.06416	-0.01523	-0.12402	-0.00126

56	31.417	5.707	-0.250	31.831	5.707	-0.250	0.762	-0.08507	-0.02923	-0.12791	-0.00781
57	32.338	5.707	-0.250	32.752	5.707	-0.250	0.762	-0.11930	-0.03690	-0.14045	-0.01879
58	33.259	5.707	-0.250	33.674	5.707	-0.250	0.762	-0.15868	-0.04413	-0.16351	-0.02996
59	34.180	5.707	-0.250	34.595	5.707	-0.250	0.762	-0.20008	-0.05137	-0.19805	-0.04320
60	35.101	5.707	-0.250	35.516	5.707	-0.250	0.762	-0.25001	-0.05876	-0.24687	-0.06070
61	29.084	6.535	-0.250	29.498	6.535	-0.250	0.762	-0.13104	0.06738	-0.17191	0.04620
62	30.005	6.535	-0.250	30.420	6.535	-0.250	0.762	-0.09281	0.03510	-0.14712	0.01662
63	30.926	6.535	-0.250	31.341	6.535	-0.250	0.762	-0.06964	0.01634	-0.13459	0.01069
64	31.847	6.535	-0.250	32.262	6.535	-0.250	0.762	-0.05863	0.00011	-0.12663	0.00483
65	32.769	6.535	-0.250	33.183	6.535	-0.250	0.762	-0.06416	-0.01523	-0.12402	-0.00126
66	33.690	6.535	-0.250	34.104	6.535	-0.250	0.762	-0.08507	-0.02923	-0.12790	-0.00781
67	34.611	6.535	-0.250	35.026	6.535	-0.250	0.762	-0.11929	-0.03690	-0.14045	-0.01879
68	35.532	6.535	-0.250	35.947	6.535	-0.250	0.762	-0.15867	-0.04413	-0.16350	-0.02996
69	36.453	6.535	-0.250	36.868	6.535	-0.250	0.762	-0.20008	-0.05137	-0.19805	-0.04320
70	37.375	6.535	-0.250	37.789	6.535	-0.250	0.762	-0.25001	-0.05876	-0.24687	-0.06070
71	31.357	7.362	-0.250	31.771	7.362	-0.250	0.762	-0.13103	0.06738	-0.17191	0.04620
72	32.278	7.362	-0.250	32.693	7.362	-0.250	0.762	-0.09280	0.03510	-0.14711	0.01662
73	33.199	7.362	-0.250	33.614	7.362	-0.250	0.762	-0.06964	0.01634	-0.13459	0.01069
74	34.120	7.362	-0.250	34.535	7.362	-0.250	0.762	-0.05863	0.00011	-0.12663	0.00483
75	35.042	7.362	-0.250	35.456	7.362	-0.250	0.762	-0.06415	-0.01523	-0.12401	-0.00126
76	35.963	7.362	-0.250	36.377	7.362	-0.250	0.762	-0.08507	-0.02923	-0.12790	-0.00781
77	36.884	7.362	-0.250	37.299	7.362	-0.250	0.762	-0.11929	-0.03690	-0.14044	-0.01879
78	37.805	7.362	-0.250	38.220	7.362	-0.250	0.762	-0.15867	-0.04413	-0.16350	-0.02996
79	38.726	7.362	-0.250	39.141	7.362	-0.250	0.762	-0.20008	-0.05137	-0.19805	-0.04320
80	39.648	7.362	-0.250	40.062	7.362	-0.250	0.762	-0.25001	-0.05876	-0.24686	-0.06070
81	33.630	8.189	-0.250	34.044	8.189	-0.250	0.762	-0.13103	0.06738	-0.17191	0.04620
82	34.551	8.189	-0.250	34.965	8.189	-0.250	0.762	-0.09280	0.03510	-0.14711	0.01662
83	35.472	8.189	-0.250	35.887	8.189	-0.250	0.762	-0.06963	0.01634	-0.13458	0.01069
84	36.393	8.189	-0.250	36.808	8.189	-0.250	0.762	-0.05862	0.00011	-0.12662	0.00483
85	37.315	8.189	-0.250	37.729	8.189	-0.250	0.762	-0.06415	-0.01523	-0.12401	-0.00126
86	38.236	8.189	-0.250	38.650	8.189	-0.250	0.762	-0.08506	-0.02923	-0.12790	-0.00781
87	39.157	8.189	-0.250	39.572	8.189	-0.250	0.762	-0.11929	-0.03690	-0.14044	-0.01879
88	40.078	8.189	-0.250	40.493	8.189	-0.250	0.762	-0.15867	-0.04413	-0.16350	-0.02996
89	41.000	8.189	-0.250	41.414	8.189	-0.250	0.762	-0.20008	-0.05137	-0.19805	-0.04320
90	41.921	8.189	-0.250	42.335	8.189	-0.250	0.762	-0.25001	-0.05876	-0.24686	-0.06070
91	36.601	9.327	-0.250	36.877	9.327	-0.250	1.000	-0.17069	0.06738	-0.19794	0.04620
92	37.215	9.327	-0.250	37.491	9.327	-0.250	1.000	-0.14520	0.03510	-0.18141	0.01662
93	37.829	9.327	-0.250	38.105	9.327	-0.250	1.000	-0.12976	0.01634	-0.17306	0.01069
94	38.443	9.327	-0.250	38.720	9.327	-0.250	1.000	-0.12242	0.00011	-0.16775	0.00483
95	39.057	9.327	-0.250	39.334	9.327	-0.250	1.000	-0.12610	-0.01523	-0.16601	-0.00126
96	39.672	9.327	-0.250	39.948	9.327	-0.250	1.000	-0.14004	-0.02923	-0.16860	-0.00781
97	40.286	9.327	-0.250	40.562	9.327	-0.250	1.000	-0.16286	-0.03690	-0.17696	-0.01879
98	40.900	9.327	-0.250	41.176	9.327	-0.250	1.000	-0.18911	-0.04413	-0.19253	-0.02996
99	41.514	9.327	-0.250	41.790	9.327	-0.250	1.000	-0.21672	-0.05137	-0.21537	-0.04320
100	42.128	9.327	-0.250	42.405	9.327	-0.250	1.000	-0.25001	-0.05876	-0.24791	-0.06070

PANEND

14P

AERODYNAMIC 1A TIME 01.599 052067

SAVE TAPE

TP 805 MIN DRAG CLBAR=.159 JUN 15, 1967

DESCRIPTION OF CASE REQUESTED

SYMMETRICAL CONFIGURATION - PANELS LOCATED ON BOTH SIDES OF X-Z PLANE(SYM = 1.)

CASE = 3. OPTIMIZE WING SHAPE

CPCALC = 0. LINEAR CP

POLAR = 0. POLARS NOT REQUESTED

THICK = 1. WING THICKNESS PRESSURES TO BE ADDED

VOUT = 1. VELOCITY COMPONENTS TO BE PRINTED

MACH NUMBER = 1.8000

POINT ABOUT WHICH THE MOMENTS ARE TO BE COMPUTED
X-COORDINATE = 0.0000
Z-COORDINATE = 0.0000

REFERENCE CHORD LENGTH = 1.0000

WING REFERENCE AREA = 89.3750

WING SEMI-SPAN = 1.0000

GIVEN BODY RADII

TR-805 BODY CAMBER 6A

HEIGHT OF WING PLANE ABOVE BODY AXIS = -0.2500

INCLINATION OF BODY AXIS WITH RESPECT TO DEFINING AXIS = 0.0000 DEG.

ANGLE OF ATTACK WITH RESPECT TO BODY AXIS = -0.0000 DEG.

WING OPTIMIZED FOR CL BAR = 0.1590

GIVEN WING THICKNESS

BODY GEOMETRY

X-STATION	CAMBER	RADIUS	FIRST DERIVATIVE	SECOND DERIVATIVE
0.0000	0.0000	0.0000	0.1800	-0.0199
0.7243	0.0250	0.1304	0.1872	0.0398
1.4485	0.0430	0.2607	0.1512	-0.1393
2.1728	0.0560	0.3491	0.1142	0.0372
2.8970	0.0680	0.4343	0.1110	-0.0461
3.6213	0.0790	0.5077	0.0987	0.0121
4.3456	0.0890	0.5791	0.0941	-0.0247
5.0698	0.0990	0.6433	0.0869	0.0048
5.7941	0.1080	0.7057	0.0826	-0.0168
6.5184	0.1165	0.7627	0.0769	0.0013
7.2426	0.1250	0.8175	0.0728	-0.0126
7.9669	0.1340	0.8679	0.0678	-0.0015
8.6911	0.1420	0.9159	0.0638	-0.0094
9.4154	0.1480	0.9602	0.0591	-0.0037
10.1397	0.1560	1.0017	0.0550	-0.0075
10.8639	0.1620	1.0396	0.0498	-0.0067
11.5882	0.1670	1.0740	0.0454	-0.0056
12.3124	0.1720	1.1049	0.0392	-0.0113
13.0367	0.1750	1.1311	0.0342	-0.0027
13.7610	0.1780	1.1542	0.0281	-0.0142
14.5023	0.1800	1.1720	0.0213	-0.0039
15.2436	0.1790	1.1840	0.0073	-0.0340
15.9849	0.1779	1.1840	-0.0019	0.0091
16.7262	0.1768	1.1840	0.0005	-0.0024
17.4675	0.1757	1.1840	-0.0001	0.0007
18.2088	0.1746	1.1840	0.0000	-0.0002
18.9501	0.1735	1.1840	-0.0000	0.0000
19.6914	0.1724	1.1840	0.0000	-0.0000
20.4327	0.1713	1.1840	-0.0000	0.0000
21.1740	0.1702	1.1840	0.0000	-0.0000
21.9153	0.1691	1.1840	-0.0000	0.0000
22.6566	0.1680	1.1840	0.0000	-0.0000
23.3979	0.1679	1.1840	-0.0000	-0.0000
24.1392	0.1668	1.1840	0.0000	0.0000
24.8805	0.1657	1.1840	-0.0000	-0.0000
25.6218	0.1646	1.1840	0.0000	0.0000
26.3631	0.1635	1.1840	-0.0000	-0.0000
27.1044	0.1624	1.1840	0.0000	0.0000
27.8457	0.1613	1.1840	-0.0000	-0.0001
28.5870	0.1602	1.1840	0.0001	0.0004
29.3283	0.1591	1.1840	-0.0003	-0.0016
30.0696	0.1580	1.1825	-0.0050	-0.0109
30.8109	0.1569	1.1757	-0.0133	-0.0115
31.5522	0.1558	1.1630	-0.0208	-0.0090
32.2935	0.1547	1.1452	-0.0269	-0.0073
33.0348	0.1536	1.1226	-0.0350	-0.0146
33.7761	0.1525	1.0930	-0.0446	-0.0114
34.5174	0.1514	1.0581	-0.0475	0.0038
35.2587	0.1503	1.0252	-0.0398	0.0170

VELOCITY COMPONENTS ON BODY DUE TO BODY LINE SOURCES AND DOUBLETS

AXIAL(U)

THETA(DEG.) / X	0.0000	22.5000	45.0000	67.5000	90.0000	112.5000	135.0000	157.5000	180.0000
0.0000	-0.07284	-0.07207	-0.06985	-0.06654	-0.06263	-0.05873	-0.05541	-0.05320	-0.05242
0.7743	-0.07564	-0.07487	-0.07265	-0.06934	-0.06543	-0.06153	-0.05822	-0.05600	-0.05522
1.4485	-0.05419	-0.05374	-0.05248	-0.05059	-0.04836	-0.04613	-0.04424	-0.04297	-0.04253
2.1728	-0.02967	-0.02951	-0.02903	-0.02832	-0.02749	-0.02665	-0.02594	-0.02547	-0.02530
2.8970	-0.03196	-0.03175	-0.03116	-0.03028	-0.02925	-0.02821	-0.02733	-0.02674	-0.02654
3.6213	-0.02449	-0.02432	-0.02385	-0.02314	-0.02230	-0.02147	-0.02076	-0.02029	-0.02012
4.3456	-0.02323	-0.02309	-0.02270	-0.02211	-0.02142	-0.02073	-0.02014	-0.01975	-0.01961
5.0698	-0.01996	-0.01980	-0.01936	-0.01869	-0.01790	-0.01711	-0.01644	-0.01600	-0.01584
5.7941	-0.01791	-0.01780	-0.01751	-0.01706	-0.01653	-0.01601	-0.01556	-0.01527	-0.01516
6.5184	-0.01520	-0.01511	-0.01485	-0.01446	-0.01400	-0.01354	-0.01315	-0.01290	-0.01280
7.2426	-0.01399	-0.01389	-0.01358	-0.01313	-0.01260	-0.01207	-0.01161	-0.01131	-0.01121
7.9669	-0.01228	-0.01214	-0.01173	-0.01113	-0.01042	-0.00970	-0.00910	-0.00870	-0.00855
8.6911	-0.01002	-0.00995	-0.00974	-0.00943	-0.00906	-0.00869	-0.00838	-0.00817	-0.00810
9.4154	-0.00657	-0.00661	-0.00673	-0.00691	-0.00712	-0.00732	-0.00750	-0.00762	-0.00766
10.1397	-0.00721	-0.00710	-0.00676	-0.00627	-0.00568	-0.00509	-0.00460	-0.00426	-0.00415
10.8639	-0.00330	-0.00332	-0.00337	-0.00345	-0.00355	-0.00364	-0.00372	-0.00378	-0.00379
11.5882	-0.00122	-0.00127	-0.00143	-0.00167	-0.00196	-0.00224	-0.00248	-0.00264	-0.00269
12.3124	0.00101	0.00098	0.00090	0.00077	0.00063	0.00048	0.00035	0.00027	0.00024
13.0367	0.00416	0.00402	0.00363	0.00305	0.00236	0.00168	0.00109	0.00071	0.00057
13.7610	0.00593	0.00584	0.00558	0.00518	0.00472	0.00426	0.00386	0.00360	0.00351
14.5023	0.00895	0.00882	0.00845	0.00790	0.00726	0.00661	0.00606	0.00569	0.00557
15.2436	0.01780	0.01753	0.01674	0.01556	0.01417	0.01278	0.01160	0.01081	0.01053
15.9449	0.01979	0.01958	0.01899	0.01811	0.01707	0.01603	0.01515	0.01456	0.01435
16.7262	0.01434	0.01420	0.01379	0.01317	0.01244	0.01172	0.01110	0.01069	0.01054
17.4675	0.01213	0.01203	0.01177	0.01137	0.01091	0.01044	0.01005	0.00978	0.00969
18.2088	0.00978	0.00973	0.00957	0.00934	0.00907	0.00880	0.00857	0.00842	0.00837
18.9501	0.00814	0.00811	0.00804	0.00793	0.00780	0.00768	0.00757	0.00750	0.00747
19.6914	0.00680	0.00679	0.00677	0.00675	0.00672	0.00669	0.00666	0.00664	0.00664
20.4327	0.00577	0.00577	0.00579	0.00582	0.00585	0.00588	0.00590	0.00592	0.00593
21.1740	0.00495	0.00496	0.00500	0.00506	0.00512	0.00519	0.00524	0.00528	0.00529
21.9153	0.00431	0.00432	0.00437	0.00444	0.00452	0.00460	0.00467	0.00472	0.00473
22.6566	0.00380	0.00381	0.00386	0.00393	0.00402	0.00410	0.00417	0.00422	0.00424
23.3979	0.00255	0.00263	0.00286	0.00319	0.00359	0.00398	0.00432	0.00454	0.00462
24.1392	0.00326	0.00326	0.00325	0.00324	0.00322	0.00321	0.00320	0.00319	0.00318
24.8805	0.00292	0.00292	0.00291	0.00291	0.00291	0.00291	0.00290	0.00290	0.00290
25.6218	0.00266	0.00266	0.00265	0.00265	0.00264	0.00263	0.00262	0.00262	0.00261
26.3631	0.00242	0.00242	0.00241	0.00241	0.00240	0.00240	0.00239	0.00239	0.00239
27.1044	0.00220	0.00220	0.00220	0.00220	0.00219	0.00219	0.00219	0.00218	0.00218
27.8457	0.00204	0.00204	0.00204	0.00203	0.00203	0.00203	0.00203	0.00203	0.00203
28.5870	0.00180	0.00180	0.00180	0.00180	0.00180	0.00180	0.00180	0.00180	0.00180
29.3283	0.00193	0.00193	0.00193	0.00193	0.00194	0.00194	0.00194	0.00194	0.00194
30.0696	0.00463	0.00463	0.00463	0.00464	0.00464	0.00464	0.00464	0.00465	0.00465
30.8109	0.00907	0.00907	0.00907	0.00908	0.00909	0.00909	0.00910	0.00911	0.00911
31.5522	0.01222	0.01222	0.01223	0.01224	0.01226	0.01227	0.01228	0.01229	0.01229
32.2935	0.01385	0.01385	0.01386	0.01388	0.01390	0.01393	0.01395	0.01396	0.01396
33.0348	0.01649	0.01650	0.01652	0.01655	0.01658	0.01661	0.01664	0.01666	0.01666
33.7761	0.01944	0.01944	0.01947	0.01951	0.01955	0.01959	0.01963	0.01965	0.01966
34.5174	0.01724	0.01725	0.01728	0.01732	0.01738	0.01743	0.01748	0.01751	0.01752
35.2587	0.00899	0.00900	0.00904	0.00909	0.00915	0.00921	0.00926	0.00929	0.00931

RADIAL(VR)

THETA(DEG.)	0.0000	22.5000	45.0000	67.5000	90.0000	112.5000	135.0000	157.5000	180.0000
X									
0.0000	0.20133	0.19885	0.19178	0.18120	0.16873	0.15625	0.14567	0.13860	0.13612
0.7243	0.20756	0.20508	0.19801	0.18743	0.17496	0.16248	0.15190	0.14483	0.14235
1.4485	0.16784	0.16601	0.16082	0.15304	0.14387	0.13469	0.12692	0.12172	0.11989
2.1728	0.12875	0.12740	0.12357	0.11783	0.11105	0.10428	0.09854	0.09470	0.09335
2.8970	0.12399	0.12275	0.11922	0.11394	0.10772	0.10149	0.09621	0.09269	0.09145
3.6213	0.11143	0.11029	0.10704	0.10219	0.09646	0.09073	0.08587	0.08262	0.08148
4.3456	0.10573	0.10469	0.10173	0.09731	0.09209	0.08687	0.08245	0.07949	0.07845
5.0698	0.09900	0.09797	0.09501	0.09059	0.08538	0.08016	0.07574	0.07278	0.07175
5.7941	0.09353	0.09259	0.08992	0.08593	0.08122	0.07651	0.07251	0.06984	0.06891
6.5184	0.08751	0.08663	0.08410	0.08032	0.07587	0.07141	0.06763	0.06511	0.06422
7.2426	0.08356	0.08268	0.08016	0.07638	0.07193	0.06748	0.06370	0.06118	0.06030
7.9669	0.07935	0.07841	0.07575	0.07176	0.06705	0.06234	0.05835	0.05569	0.05475
8.6911	0.07423	0.07339	0.07101	0.06745	0.06324	0.05904	0.05548	0.05309	0.05226
9.4154	0.06697	0.06634	0.06453	0.06183	0.05865	0.05547	0.05277	0.05097	0.05034
10.1397	0.06565	0.06482	0.06244	0.05889	0.05469	0.05050	0.04694	0.04456	0.04373
10.8639	0.05796	0.05733	0.05553	0.05284	0.04966	0.04649	0.04380	0.04200	0.04137
11.5882	0.05221	0.05168	0.05018	0.04793	0.04527	0.04262	0.04037	0.03886	0.03834
12.3124	0.04619	0.04566	0.04416	0.04192	0.03927	0.03662	0.03438	0.03288	0.03235
13.0367	0.03848	0.03816	0.03725	0.03588	0.03427	0.03266	0.03130	0.03039	0.03007
13.7610	0.03238	0.03206	0.03116	0.02980	0.02820	0.02660	0.02525	0.02434	0.02403
14.5023	0.02422	0.02401	0.02342	0.02253	0.02149	0.02044	0.01955	0.01896	0.01875
15.2436	0.00605	0.00615	0.00644	0.00687	0.00738	0.00788	0.00831	0.00860	0.00870
15.9849	-0.00347	-0.00336	-0.00304	-0.00255	-0.00195	-0.00141	-0.00093	-0.00061	-0.00049
16.7262	-0.00095	-0.00084	-0.00052	-0.00004	0.00053	0.00110	0.00158	0.00190	0.00201
17.4675	-0.00163	-0.00151	-0.00119	-0.00071	-0.00014	0.00043	0.00091	0.00123	0.00134
18.2088	-0.00145	-0.00133	-0.00101	-0.00053	0.00004	0.00061	0.00109	0.00141	0.00152
18.9501	-0.00149	-0.00138	-0.00106	-0.00058	-0.00001	0.00056	0.00104	0.00136	0.00147
19.6914	-0.00148	-0.00137	-0.00105	-0.00057	0.00000	0.00057	0.00105	0.00137	0.00149
20.4327	-0.00148	-0.00137	-0.00105	-0.00057	-0.00000	0.00057	0.00105	0.00137	0.00148
21.1740	-0.00148	-0.00137	-0.00105	-0.00057	0.00000	0.00057	0.00105	0.00137	0.00148
21.9153	-0.00148	-0.00137	-0.00105	-0.00057	-0.00000	0.00057	0.00105	0.00137	0.00148
22.6566	-0.00148	-0.00137	-0.00105	-0.00057	-0.00000	0.00057	0.00105	0.00137	0.00148
23.3979	-0.00013	-0.00012	-0.00010	-0.00005	-0.00000	0.00005	0.00010	0.00012	0.00013
24.1392	-0.00148	-0.00137	-0.00105	-0.00057	-0.00000	0.00057	0.00105	0.00137	0.00148
24.8805	-0.00148	-0.00137	-0.00105	-0.00057	-0.00000	0.00057	0.00105	0.00137	0.00148
25.6218	-0.00148	-0.00137	-0.00105	-0.00057	0.00000	0.00057	0.00105	0.00137	0.00148
26.3631	-0.00149	-0.00137	-0.00105	-0.00057	-0.00000	0.00057	0.00105	0.00137	0.00148
27.1044	-0.00148	-0.00136	-0.00104	-0.00056	0.00001	0.00057	0.00106	0.00138	0.00149
27.8457	-0.00151	-0.00140	-0.00107	-0.00059	-0.00002	0.00054	0.00102	0.00135	0.00146
28.5870	-0.00139	-0.00128	-0.00096	-0.00048	0.00009	0.00066	0.00114	0.00146	0.00157
29.3283	-0.00182	-0.00171	-0.00139	-0.00091	-0.00034	0.00023	0.00071	0.00103	0.00114
30.0696	-0.00648	-0.00637	-0.00605	-0.00557	-0.00500	-0.00443	-0.00395	-0.00363	-0.00351
30.8109	-0.01488	-0.01477	-0.01445	-0.01396	-0.01340	-0.01283	-0.01235	-0.01203	-0.01191
31.5522	-0.02259	-0.02247	-0.02215	-0.02167	-0.02110	-0.02053	-0.02005	-0.01973	-0.01962
32.2935	-0.02872	-0.02861	-0.02829	-0.02781	-0.02724	-0.02667	-0.02619	-0.02587	-0.02576
33.0348	-0.03704	-0.03693	-0.03661	-0.03613	-0.03556	-0.03499	-0.03451	-0.03419	-0.03408
33.7761	-0.04698	-0.04687	-0.04655	-0.04607	-0.04550	-0.04493	-0.04445	-0.04413	-0.04402
34.5174	-0.04975	-0.04964	-0.04932	-0.04884	-0.04828	-0.04771	-0.04723	-0.04691	-0.04680
35.2587	-0.04159	-0.04148	-0.04116	-0.04068	-0.04012	-0.03955	-0.03907	-0.03875	-0.03864

TANGENTIAL(VT)

THETA(DEG.)	0.0000	22.5000	45.0000	67.5000	90.0000	112.5000	135.0000	157.5000	180.0000
X									
0.0000	0.00000	0.00923	0.01705	0.02228	0.02412	0.02228	0.01705	0.00923	0.00000
0.7243	0.00000	0.00923	0.01705	0.02228	0.02412	0.02228	0.01705	0.00923	0.00000

1.4485	0.00000	0.00793	0.01464	0.01913	0.02071	0.01913	0.01464	0.00793	0.00000
2.1728	0.00000	0.00698	0.01291	0.01686	0.01825	0.01686	0.01291	0.00698	0.00000
2.8970	0.00000	0.00571	0.01055	0.01378	0.01492	0.01378	0.01055	0.00571	0.00000
3.6213	0.00000	0.00547	0.01011	0.01321	0.01430	0.01321	0.01011	0.00547	0.00000
4.3456	0.00000	0.00504	0.00930	0.01216	0.01316	0.01216	0.00930	0.00504	0.00000
5.0698	0.00000	0.00484	0.00894	0.01167	0.01264	0.01167	0.00894	0.00484	0.00000
5.7941	0.00000	0.00468	0.00865	0.01130	0.01223	0.01130	0.00865	0.00468	0.00000
6.5184	0.00000	0.00443	0.00818	0.01068	0.01156	0.01068	0.00818	0.00443	0.00000
7.2426	0.00000	0.00427	0.00788	0.01030	0.01115	0.01030	0.00788	0.00427	0.00000
7.9669	0.00000	0.00427	0.00788	0.01030	0.01115	0.01030	0.00788	0.00427	0.00000
8.6911	0.00000	0.00428	0.00790	0.01032	0.01117	0.01032	0.00790	0.00428	0.00000
9.4154	0.00000	0.00397	0.00734	0.00959	0.01038	0.00959	0.00734	0.00397	0.00000
10.1397	0.00000	0.00370	0.00683	0.00892	0.00966	0.00892	0.00683	0.00370	0.00000
10.8639	0.00000	0.00373	0.00689	0.00900	0.00974	0.00900	0.00689	0.00373	0.00000
11.5882	0.00000	0.00331	0.00612	0.00800	0.00865	0.00800	0.00612	0.00331	0.00000
12.3124	0.00000	0.00301	0.00556	0.00727	0.00786	0.00727	0.00556	0.00301	0.00000
13.0367	0.00000	0.00266	0.00492	0.00643	0.00696	0.00643	0.00492	0.00266	0.00000
13.7610	0.00000	0.00216	0.00398	0.00520	0.00563	0.00520	0.00398	0.00216	0.00000
14.5023	0.00000	0.00180	0.00333	0.00434	0.00470	0.00434	0.00333	0.00180	0.00000
15.2436	0.00000	0.00116	0.00214	0.00280	0.00303	0.00280	0.00214	0.00116	0.00000
15.9849	0.00000	0.00032	0.00059	0.00077	0.00083	0.00077	0.00059	0.00032	0.00000
16.7262	-0.00000	-0.00020	-0.00038	-0.00049	-0.00053	-0.00049	-0.00038	-0.00020	-0.00000
17.4675	-0.00000	-0.00059	-0.00108	-0.00142	-0.00153	-0.00142	-0.00108	-0.00059	-0.00000
18.2088	-0.00000	-0.00081	-0.00150	-0.00196	-0.00212	-0.00196	-0.00150	-0.00081	-0.00000
18.9501	-0.00000	-0.00093	-0.00173	-0.00225	-0.00244	-0.00225	-0.00173	-0.00093	-0.00000
19.6914	-0.00000	-0.00098	-0.00181	-0.00237	-0.00256	-0.00237	-0.00181	-0.00098	-0.00000
20.4327	-0.00000	-0.00098	-0.00181	-0.00236	-0.00256	-0.00236	-0.00181	-0.00098	-0.00000
21.1740	-0.00000	-0.00095	-0.00175	-0.00229	-0.00247	-0.00229	-0.00175	-0.00095	-0.00000
21.9153	-0.00000	-0.00090	-0.00166	-0.00217	-0.00235	-0.00217	-0.00166	-0.00090	-0.00000
22.6566	-0.00000	-0.00085	-0.00157	-0.00205	-0.00221	-0.00205	-0.00157	-0.00085	-0.00000
23.3979	-0.00000	-0.00072	-0.00133	-0.00173	-0.00188	-0.00173	-0.00133	-0.00072	-0.00000
24.1392	-0.00000	-0.00054	-0.00100	-0.00131	-0.00142	-0.00131	-0.00100	-0.00054	-0.00000
24.8805	-0.00000	-0.00060	-0.00110	-0.00144	-0.00156	-0.00144	-0.00110	-0.00060	-0.00000
25.6218	-0.00000	-0.00058	-0.00108	-0.00140	-0.00152	-0.00140	-0.00108	-0.00058	-0.00000
26.3631	-0.00000	-0.00059	-0.00110	-0.00143	-0.00155	-0.00143	-0.00110	-0.00059	-0.00000
27.1044	-0.00000	-0.00059	-0.00110	-0.00143	-0.00155	-0.00143	-0.00110	-0.00059	-0.00000
27.8457	-0.00000	-0.00060	-0.00110	-0.00144	-0.00156	-0.00144	-0.00110	-0.00060	-0.00000
28.5870	-0.00000	-0.00060	-0.00110	-0.00144	-0.00156	-0.00144	-0.00110	-0.00060	-0.00000
29.3283	-0.00000	-0.00060	-0.00110	-0.00144	-0.00156	-0.00144	-0.00110	-0.00060	-0.00000
30.0696	-0.00000	-0.00060	-0.00110	-0.00144	-0.00156	-0.00144	-0.00110	-0.00060	-0.00000
30.8109	-0.00000	-0.00060	-0.00111	-0.00145	-0.00157	-0.00145	-0.00111	-0.00060	-0.00000
31.5522	-0.00000	-0.00061	-0.00112	-0.00146	-0.00158	-0.00146	-0.00112	-0.00061	-0.00000
32.2935	-0.00000	-0.00061	-0.00113	-0.00148	-0.00160	-0.00148	-0.00113	-0.00061	-0.00000
33.0348	-0.00000	-0.00062	-0.00114	-0.00149	-0.00161	-0.00149	-0.00114	-0.00062	-0.00000
33.7761	-0.00000	-0.00062	-0.00115	-0.00151	-0.00163	-0.00151	-0.00115	-0.00062	-0.00000
34.5174	-0.00000	-0.00063	-0.00116	-0.00152	-0.00164	-0.00152	-0.00116	-0.00063	-0.00000
35.2587	-0.00000	-0.00063	-0.00116	-0.00151	-0.00163	-0.00151	-0.00116	-0.00063	-0.00000

VELOCITY COMPONENTS ON WING PANELS DUE TO BODY PANEL PRESSURE SINGULARITIES

AXIAL(U)

SPANWISE STATION	1	2	3	4	5	6	7	8	9	10
CHORDWISE STATION										
1	-0.00335	-0.00025	0.00402	0.00294	0.00184	0.00049	-0.00049	-0.00018	-0.00179	-0.00120
2	0.00075	0.00637	0.00114	0.00135	-0.00008	-0.00070	-0.00036	-0.00165	-0.00127	-0.00251
3	0.00655	0.00760	0.00934	0.00023	-0.00105	-0.00085	-0.00198	-0.00128	-0.00270	-0.00136
4	0.01005	0.00618	0.00139	-0.00051	-0.00164	-0.00285	-0.00140	-0.00276	-0.00132	-0.00104
5	0.00920	0.00307	0.00061	-0.00031	-0.00402	-0.00140	-0.00321	-0.00146	-0.00014	-0.00005
6	0.00671	0.00192	-0.00100	-0.00050	-0.00153	-0.00456	-0.00163	-0.00003	-0.00054	-0.00036
7	0.00491	-0.00055	-0.00078	-0.00168	-0.00133	-0.00184	-0.00036	-0.00045	0.00047	0.00026
8	0.00078	-0.00036	-0.00299	-0.00138	-0.00214	-0.00028	-0.00048	0.00042	0.00026	0.00047
9	0.00064	-0.00340	-0.00012	-0.00246	-0.00011	-0.00054	0.00068	0.00025	0.00003	0.00012
10	-0.00430	-0.00297	0.00002	0.00048	-0.00067	0.00094	0.00023	0.00003	0.00002	0.00014

TRANSVERSE(V)

SPANWISE STATION	1	2	3	4	5	6	7	8	9	10
CHORDWISE STATION										
1	0.00765	0.00141	-0.00590	-0.00498	-0.00358	-0.00155	0.00005	-0.00024	0.00233	0.00162
2	0.00278	-0.00925	-0.00251	-0.00316	-0.00099	0.00013	-0.00013	0.00203	0.00165	0.00365
3	-0.00810	-0.01258	-0.01572	-0.00192	0.00030	0.00037	0.00236	0.00157	0.00390	0.00199
4	-0.01660	-0.01234	-0.00461	-0.00113	0.00116	0.00342	0.00162	0.00392	0.00196	0.00158
5	-0.02048	-0.00938	-0.00404	-0.00151	0.00475	0.00142	0.00446	0.00212	0.00021	0.00008
6	-0.02172	-0.00906	-0.00189	-0.00123	0.00125	0.00629	0.00229	0.00003	0.00084	0.00058
7	-0.02346	-0.00626	-0.00233	0.00082	0.00114	0.00249	0.00049	0.00069	-0.00069	-0.00034
8	-0.02108	-0.00699	0.00130	0.00063	0.00270	0.00028	0.00071	-0.00062	-0.00039	-0.00068
9	-0.02309	-0.00219	-0.00256	0.00269	-0.00013	0.00074	-0.00103	-0.00038	-0.00005	-0.00016
10	-0.01680	-0.00211	-0.00217	-0.00136	0.00079	-0.00146	-0.00037	-0.00007	-0.00004	-0.00020

VERTICAL(W)

SPANWISE STATION	1	2	3	4	5	6	7	8	9	10
CHORDWISE STATION										
1	0.01285	0.00765	0.00640	0.00514	0.00481	0.00455	0.00441	0.00428	0.00394	0.00362
2	0.03277	0.01306	0.00817	0.00668	0.00602	0.00550	0.00519	0.00466	0.00441	0.00372
3	0.05562	0.01792	0.01105	0.00852	0.00725	0.00648	0.00568	0.00520	0.00465	0.00394
4	0.08236	0.02278	0.01382	0.01025	0.00862	0.00712	0.00629	0.00552	0.00506	0.00412
5	0.10675	0.02908	0.01642	0.01216	0.00967	0.00789	0.00673	0.00596	0.00516	0.00417
6	0.13428	0.03452	0.01928	0.01376	0.01040	0.00851	0.00727	0.00622	0.00511	0.00411
7	0.15858	0.03993	0.02184	0.01471	0.01144	0.00916	0.00765	0.00613	0.00527	0.00421
8	0.18105	0.04502	0.02331	0.01618	0.01206	0.00967	0.00756	0.00629	0.00532	0.00421
9	0.20039	0.04783	0.02570	0.01699	0.01281	0.00963	0.00775	0.00641	0.00518	0.00422
10	0.21165	0.05183	0.02698	0.01822	0.01282	0.00991	0.00791	0.00627	0.00514	0.00426

VELOCITY COMPONENTS ON WING PANELS DUE TO BODY LINE SOURCES AND DOUBLETS

AXIAL(U)

SPANWISE STATION	1	2	3	4	5	6	7	8	9	10
CHORDWISE STATION										
1	0.01165	0.01114	0.00675	0.00497	0.00386	0.00300	0.00241	0.00197	0.00165	0.00135
2	0.01412	0.00779	0.00572	0.00432	0.00330	0.00262	0.00213	0.00177	0.00147	0.00126
3	0.00948	0.00684	0.00492	0.00368	0.00288	0.00231	0.00190	0.00157	0.00133	0.00118
4	0.00854	0.00575	0.00417	0.00320	0.00253	0.00206	0.00169	0.00142	0.00121	0.00111
5	0.00696	0.00485	0.00362	0.00280	0.00225	0.00183	0.00152	0.00129	0.00111	0.00105
6	0.00585	0.00418	0.00315	0.00248	0.00200	0.00164	0.00138	0.00118	0.00102	0.00100
7	0.00501	0.00362	0.00277	0.00221	0.00179	0.00149	0.00126	0.00108	0.00097	0.00093
8	0.00430	0.00317	0.00248	0.00196	0.00161	0.00135	0.00116	0.00101	0.00190	0.00090
9	0.00373	0.00284	0.00217	0.00176	0.00146	0.00124	0.00105	0.00178	0.00402	0.00117
10	0.00338	0.00244	0.00195	0.00160	0.00134	0.00111	0.00166	0.00396	0.00540	0.00219

TRANSVERSE(V)

SPANWISE STATION	1	2	3	4	5	6	7	8	9	10
CHORDWISE STATION										
1	0.00726	-0.00376	-0.00212	-0.00201	-0.00182	-0.00148	-0.00122	-0.00102	-0.00087	-0.00071
2	-0.00005	-0.00035	-0.00143	-0.00153	-0.00130	-0.00111	-0.00095	-0.00082	-0.00067	-0.00063
3	0.00407	-0.00019	-0.00091	-0.00097	-0.00093	-0.00083	-0.00073	-0.00061	-0.00053	-0.00054
4	0.00346	0.00048	-0.00034	-0.00059	-0.00062	-0.00060	-0.00052	-0.00047	-0.00041	-0.00047
5	0.00428	0.00103	0.00004	-0.00027	-0.00039	-0.00038	-0.00037	-0.00034	-0.00031	-0.00040
6	0.00474	0.00140	0.00037	-0.00003	-0.00018	-0.00022	-0.00024	-0.00023	-0.00022	-0.00035
7	0.00506	0.00173	0.00063	0.00018	0.00001	-0.00008	-0.00012	-0.00015	-0.00019	-0.00028
8	0.00539	0.00200	0.00081	0.00039	0.00015	0.00003	-0.00004	-0.00008	-0.00165	-0.00026
9	0.00568	0.00214	0.00107	0.00054	0.00028	0.00013	0.00007	-0.00129	-0.00497	-0.00069
10	0.00573	0.00248	0.00122	0.00067	0.00038	0.00026	-0.00091	-0.00471	-0.00728	-0.00227

VERTICAL(W)

SPANWISE STATION	1	2	3	4	5	6	7	8	9	10
CHORDWISE STATION										
1	-0.00268	0.00073	0.00071	0.00058	0.00044	0.00031	0.00021	0.00015	0.00009	0.00006
2	0.00009	0.00075	0.00073	0.00054	0.00037	0.00026	0.00018	0.00011	0.00007	0.00006
3	0.00030	0.00090	0.00068	0.00047	0.00031	0.00021	0.00014	0.00008	0.00007	0.00006
4	0.00087	0.00087	0.00059	0.00039	0.00026	0.00017	0.00009	0.00008	0.00006	0.00005
5	0.00094	0.00077	0.00050	0.00032	0.00021	0.00010	0.00009	0.00007	0.00006	0.00005
6	0.00088	0.00066	0.00041	0.00026	0.00012	0.00010	0.00008	0.00007	0.00006	0.00005
7	0.00075	0.00054	0.00033	0.00014	0.00012	0.00009	0.00008	0.00006	0.00005	0.00005
8	0.00058	0.00043	0.00017	0.00014	0.00011	0.00009	0.00007	0.00006	0.00010	0.00005
9	0.00041	0.00021	0.00016	0.00012	0.00010	0.00008	0.00007	0.00010	0.00020	0.00006
10	0.00008	0.00014	0.00014	0.00012	0.00010	0.00007	0.00010	0.00021	0.00026	0.00010

VELOCITY COMPONENTS ON WING PANELS DUE TO WING PANEL PRESSURE SINGULARITIES

AXIAL(U)

SPANWISE STATION	1	2	3	4	5	6	7	8	9	10
CHORDWISE STATION										
1	0.04017	0.03533	0.02755	0.02439	0.02385	0.02389	0.02417	0.02442	0.01049	0.05446
2	0.05735	0.04872	0.03995	0.03727	0.03711	0.03742	0.03792	0.03800	0.02205	0.08825
3	0.06279	0.05348	0.04706	0.04572	0.04619	0.04676	0.04728	0.04787	0.03257	0.09565
4	0.06200	0.05426	0.05158	0.05171	0.05275	0.05333	0.05419	0.05361	0.03709	0.04971
5	0.05819	0.05351	0.05431	0.05592	0.05715	0.05776	0.05830	0.05280	0.04181	0.04675
6	0.05314	0.05197	0.05578	0.05821	0.05937	0.05970	0.05742	0.04854	0.04691	0.04245
7	0.04690	0.04988	0.05556	0.05817	0.05905	0.05721	0.05260	0.04518	0.05031	0.03703
8	0.03916	0.04664	0.05275	0.05519	0.05422	0.05069	0.04612	0.04168	0.05176	0.03151
9	0.03024	0.03996	0.04609	0.04690	0.04436	0.04124	0.03727	0.03646	0.04844	0.02445
10	0.01818	0.02773	0.03161	0.03096	0.02880	0.02706	0.02408	0.02533	0.03748	0.02841

TRANSVERSE(V)

SPANWISE STATION	1	2	3	4	5	6	7	8	9	10
CHORDWISE STATION										
1	-0.11036	-0.09707	-0.07569	-0.06702	-0.06552	-0.06564	-0.06642	-0.06710	-0.02881	-0.14961
2	-0.15755	-0.13386	-0.10976	-0.10239	-0.10194	-0.10281	-0.10419	-0.10440	-0.06059	-0.22812
3	-0.17251	-0.14692	-0.12929	-0.12561	-0.12689	-0.12847	-0.12989	-0.13151	-0.08948	-0.24217
4	-0.17033	-0.14908	-0.14170	-0.14207	-0.14492	-0.14652	-0.14887	-0.14729	-0.10191	-0.17444
5	-0.15987	-0.14701	-0.14922	-0.15362	-0.15701	-0.15870	-0.16017	-0.14507	-0.11488	-0.17133
6	-0.14600	-0.14278	-0.15325	-0.15992	-0.16311	-0.16401	-0.15776	-0.13336	-0.12889	-0.16864
7	-0.12985	-0.13705	-0.15263	-0.15982	-0.16224	-0.15717	-0.14451	-0.12414	-0.13823	-0.16755
8	-0.10759	-0.12814	-0.14493	-0.15162	-0.14897	-0.13925	-0.12672	-0.11452	-0.14221	-0.16878
9	-0.08306	-0.10979	-0.12663	-0.12886	-0.12187	-0.11330	-0.10239	-0.10017	-0.13308	-0.17335
10	-0.04993	-0.07617	-0.08685	-0.08505	-0.07913	-0.07435	-0.06615	-0.06958	-0.10298	-0.16910

VERTICAL(W)

SPANWISE STATION	1	2	3	4	5	6	7	8	9	10
CHORDWISE STATION										
1	-0.04622	0.02481	0.05401	0.06246	0.06717	0.07296	0.07892	0.08441	0.11032	0.09366
2	-0.14086	-0.02190	0.02533	0.03784	0.04412	0.05102	0.05727	0.06422	0.11525	-0.00227
3	-0.22342	-0.06122	-0.00293	0.01271	0.02029	0.02803	0.03496	0.03526	0.11436	-0.05927
4	-0.29209	-0.09424	-0.03138	-0.01299	-0.00446	0.00429	0.00946	-0.00131	0.13023	-0.05149
5	-0.34751	-0.12311	-0.05935	-0.03964	-0.03020	-0.02173	-0.02094	-0.03150	0.14428	-0.05910
6	-0.39268	-0.14914	-0.08774	-0.06727	-0.05767	-0.05192	-0.04923	-0.05277	0.13260	-0.06371
7	-0.42810	-0.17448	-0.11675	-0.09640	-0.08909	-0.08111	-0.07405	-0.07277	0.10632	-0.06494
8	-0.45159	-0.20099	-0.14695	-0.12937	-0.12066	-0.10758	-0.10053	-0.09194	0.06586	-0.06525
9	-0.46501	-0.22607	-0.18084	-0.16365	-0.15046	-0.13502	-0.12841	-0.11428	0.01497	-0.06356
10	-0.46532	-0.25322	-0.21626	-0.19678	-0.18048	-0.16486	-0.15637	-0.13984	-0.05739	-0.07525

VELOCITY COMPONENTS ON WING PANELS DUE TO WING SOURCES

AXIAL(U)

SPANWISE STATION	1	2	3	4	5	6	7	8	9	10
CHORDWISE STATION										
1	-0.01440	-0.00890	-0.00478	-0.00453	0.00006	0.00447	0.00827	0.01187	0.01396	0.02115
2	-0.00055	0.00571	0.00660	0.01170	0.01665	0.02079	0.02464	0.02833	0.02461	0.03324
3	0.00248	0.00525	0.01117	0.01686	0.02146	0.02562	0.02955	0.02611	0.02751	0.03262
4	0.00111	0.00890	0.01577	0.02102	0.02559	0.02983	0.02670	0.02599	0.03168	0.03260
5	0.00358	0.01288	0.01916	0.02431	0.02894	0.02619	0.02523	0.02511	0.03137	0.03163
6	0.00683	0.01516	0.02120	0.02638	0.02410	0.02278	0.02257	0.02200	0.02799	0.03005
7	0.00794	0.01569	0.02170	0.02003	0.01817	0.01782	0.01753	0.01797	0.02221	0.02576
8	0.00975	0.01734	0.01654	0.01377	0.01324	0.01324	0.01153	0.01510	0.01631	0.01904
9	0.01198	0.01277	0.00819	0.00736	0.00726	0.00553	0.00486	0.00956	0.00830	0.01327
10	0.00776	-0.00238	-0.00373	-0.00400	-0.00576	-0.00654	-0.00698	-0.00204	-0.00606	0.00818

TRANSVERSE(V)

SPANWISE STATION	1	2	3	4	5	6	7	8	9	10
CHORDWISE STATION										
1	-0.00990	-0.00165	-0.00346	-0.00193	-0.00797	-0.01444	-0.02038	-0.02624	-0.02998	-0.03721
2	-0.03844	-0.03647	-0.03468	-0.04112	-0.04835	-0.05488	-0.06121	-0.06746	-0.06239	-0.07989
3	-0.03705	-0.03405	-0.04107	-0.04940	-0.05674	-0.06370	-0.07048	-0.06598	-0.06220	-0.08955
4	-0.02826	-0.03662	-0.04681	-0.05540	-0.06325	-0.07074	-0.06693	-0.06631	-0.05424	-0.09852
5	-0.02383	-0.03892	-0.04981	-0.05906	-0.06754	-0.06463	-0.06377	-0.06398	-0.04508	-0.10480
6	-0.01972	-0.03741	-0.04929	-0.05935	-0.05767	-0.05646	-0.05663	-0.05614	-0.03320	-0.10924
7	-0.01147	-0.03144	-0.04452	-0.04472	-0.04303	-0.04314	-0.04314	-0.03854	-0.01699	-0.11148
8	-0.00613	-0.02862	-0.03235	-0.02989	-0.02994	-0.03049	-0.02825	-0.02017	-0.00217	-0.11186
9	-0.00225	-0.01687	-0.01301	-0.01300	-0.01356	-0.01139	-0.01062	-0.00006	0.01456	-0.11281
10	0.01124	0.01859	0.01863	0.01804	0.02012	0.02100	0.02147	0.03342	0.04341	-0.11386

VERTICAL(W)

SPANWISE STATION	1	2	3	4	5	6	7	8	9	10
CHORDWISE STATION										
1	0.12128	0.12101	0.12101	0.12101	0.12101	0.12101	0.12101	0.12101	0.12101	0.12101
2	0.05126	0.05124	0.05124	0.05124	0.05124	0.05124	0.05124	0.05124	0.05124	0.05124
3	0.02572	0.02572	0.02572	0.02572	0.02572	0.02572	0.02572	0.02572	0.02572	0.02572
4	0.00823	0.00823	0.00823	0.00823	0.00823	0.00823	0.00823	0.00823	0.00823	0.00823
5	-0.00756	-0.00756	-0.00756	-0.00756	-0.00756	-0.00756	-0.00756	-0.00756	-0.00756	-0.00756
6	-0.02223	-0.02223	-0.02223	-0.02223	-0.02223	-0.02223	-0.02223	-0.02223	-0.02223	-0.02223
7	-0.03307	-0.03307	-0.03307	-0.03307	-0.03307	-0.03307	-0.03307	-0.03307	-0.03307	-0.03307
8	-0.04051	-0.04051	-0.04051	-0.04051	-0.04051	-0.04051	-0.04051	-0.04051	-0.04051	-0.04051
9	-0.04775	-0.04775	-0.04775	-0.04775	-0.04775	-0.04775	-0.04775	-0.04775	-0.04775	-0.04775
10	-0.05507	-0.05507	-0.05507	-0.05507	-0.05507	-0.05507	-0.05507	-0.05507	-0.05507	-0.05507

VELOCITY COMPONENTS ON BODY PANELS DUE TO BODY PANEL PRESSURE SINGULARITIES

AXIAL(U)

THETA(DEG.)	12.5000	37.5000	62.5000	88.7967	116.0950	142.5000	167.5000
ROW NO.							
1	-0.00002	-0.00008	-0.00030	-0.00215	-0.00598	-0.00064	-0.00019
2	0.00009	0.00012	0.00063	0.00712	-0.01910	-0.00142	-0.00042
3	0.00287	0.00175	0.00277	0.01917	-0.02314	-0.00925	0.00466
4	0.00502	0.00457	0.01230	0.02942	-0.02040	-0.00686	-0.00368
5	0.00199	0.00802	0.01681	0.03311	-0.01960	-0.01202	-0.01078
6	0.00292	0.00933	0.01910	0.03213	-0.02088	-0.01630	-0.01595
7	0.00652	0.01109	0.01884	0.02947	-0.02117	-0.01896	-0.01934
8	0.00995	0.01264	0.01792	0.02545	-0.02130	-0.02091	-0.02038
9	0.01157	0.01343	0.01690	0.02108	-0.02033	-0.02147	-0.02167
10	0.01255	0.01364	0.01572	0.01676	-0.01785	-0.02119	-0.02176
11	0.01261	0.01229	0.01075	0.00355	-0.01462	-0.01820	-0.02048
12	0.01349	0.01128	0.00605	-0.00124	-0.00833	-0.01136	-0.01255
13	0.00871	0.00752	0.00507	0.00099	-0.00376	-0.00724	-0.00924
14	0.00545	0.00463	0.00285	0.00029	-0.00244	-0.00422	-0.00502

TRANSVERSE(V)

THETA(DEG.)	12.5000	37.5000	62.5000	88.7967	116.0950	142.5000	167.5000
ROW NO.							
1	0.00002	0.00011	0.00029	0.00399	0.01233	0.00103	0.00022
2	0.00040	0.00062	-0.00176	-0.01845	0.04618	0.00068	0.00060
3	-0.00055	-0.00261	-0.00090	-0.07051	0.08618	0.00375	0.00052
4	0.00110	-0.00547	-0.01152	-0.13950	0.12455	0.00151	-0.00329
5	-0.00057	-0.00482	-0.02255	-0.20772	0.16665	0.00869	-0.00076
6	-0.00081	-0.00589	-0.03246	-0.27099	0.21123	0.01943	-0.00035
7	0.00115	-0.00451	-0.04416	-0.33027	0.25242	0.03065	0.00306
8	-0.00058	-0.00757	-0.05607	-0.38302	0.28990	0.04098	0.00546
9	-0.00011	-0.01027	-0.06876	-0.42788	0.32154	0.05049	0.00814
10	-0.00119	-0.01305	-0.07932	-0.46355	0.34771	0.05987	0.01061
11	-0.00303	-0.02108	-0.10317	-0.48277	0.39102	0.07701	0.01607
12	-0.00591	-0.03286	-0.11557	-0.48225	0.39618	0.08521	0.01901
13	-0.01095	-0.04490	-0.12745	-0.48613	0.40394	0.09207	0.02170
14	-0.01471	-0.05463	-0.13763	-0.47353	0.37638	0.09989	0.02523

VERTICAL(W)

THETA(DEG.)	12.5000	37.5000	62.5000	88.7967	116.0950	142.5000	167.5000
ROW NO.							
1	-0.00001	-0.00008	-0.00055	-0.00118	-0.00564	0.00079	0.00005
2	-0.00009	-0.00047	-0.00081	-0.00515	-0.02510	0.00552	0.00013
3	-0.00449	-0.00218	-0.00007	-0.00933	-0.05140	-0.00102	0.01480
4	-0.00933	-0.00446	-0.00340	-0.01722	-0.07501	-0.00452	0.01366
5	-0.00360	-0.00373	-0.00797	-0.02251	-0.10699	-0.01528	0.00830
6	0.00003	-0.00300	-0.01384	-0.03240	-0.13270	-0.02630	-0.00076
7	0.00115	-0.00630	-0.01911	-0.03638	-0.15780	-0.03832	-0.01138
8	0.00183	-0.00775	-0.02569	-0.04248	-0.18088	-0.05156	-0.02345
9	0.00127	-0.01066	-0.03018	-0.04777	-0.20275	-0.06496	-0.03579
10	-0.00006	-0.01414	-0.03734	-0.05248	-0.21873	-0.07719	-0.04787
11	-0.00524	-0.02159	-0.04651	-0.05499	-0.23750	-0.09569	-0.07120
12	-0.02341	-0.03763	-0.05524	-0.05741	-0.24608	-0.10830	-0.08085
13	-0.03701	-0.04689	-0.05826	-0.05622	-0.25029	-0.11775	-0.09202
14	-0.05120	-0.05766	-0.06570	-0.11854	-0.30376	-0.13160	-0.10675

VELOCITY COMPONENTS ON BODY PANELS DUE TO WING PANEL PRESSURE SINGULARITIES

AXIAL(U)

THETA(DEG.)	12.5000	37.5000	62.5000	88.7967	116.0950	142.5000	167.5000
ROW NO.							
1	-0.00000	-0.00000	-0.00000	0.00991	-0.00677	-0.00000	-0.00000
2	-0.00000	-0.00000	0.00641	0.01873	-0.01288	-0.00431	-0.00000
3	0.00209	0.00511	0.01213	0.02380	-0.01650	-0.00808	-0.00435
4	0.00742	0.01035	0.01670	0.02597	-0.01829	-0.01183	-0.00847
5	0.01201	0.01462	0.01958	0.02618	-0.01863	-0.01417	-0.01161
6	0.01528	0.01721	0.02092	0.02525	-0.01809	-0.01528	-0.01346
7	0.01696	0.01845	0.02119	0.02352	-0.01697	-0.01556	-0.01419
8	0.01749	0.01874	0.02065	0.02097	-0.01525	-0.01517	-0.01424
9	0.01740	0.01829	0.01917	0.01777	-0.01302	-0.01416	-0.01385
10	0.01672	0.01719	0.01723	0.01353	-0.01007	-0.01277	-0.01296
11	0.01369	0.01356	0.01040	0.00458	-0.00379	-0.00792	-0.00984
12	0.00877	0.00833	0.00678	0.00262	-0.00230	-0.00511	-0.00589
13	0.00643	0.00578	0.00425	0.00160	-0.00143	-0.00344	-0.00416
14	0.00435	0.00379	0.00267	0.00099	-0.00084	-0.00215	-0.00277

TRANSVERSE(V)

THETA(DEG.)	12.5000	37.5000	62.5000	88.7967	116.0950	142.5000	167.5000
ROW NO.							
1	0.00000	0.00000	0.00000	0.00827	-0.01214	0.00000	0.00000
2	0.00000	0.00000	0.00418	0.04388	-0.04867	-0.00611	0.00000
3	0.00197	0.00502	0.01452	0.09704	-0.09797	-0.01720	-0.00365
4	0.00322	0.01084	0.02880	0.15759	-0.15181	-0.02964	-0.00703
5	0.00497	0.01730	0.04443	0.21858	-0.20516	-0.04290	-0.01054
6	0.00683	0.02378	0.06031	0.27674	-0.25554	-0.05585	-0.01392
7	0.00857	0.03016	0.07593	0.33045	-0.30166	-0.06815	-0.01716
8	0.01035	0.03657	0.09091	0.37827	-0.34230	-0.07968	-0.02026
9	0.01212	0.04267	0.10438	0.41877	-0.37614	-0.08982	-0.02312
10	0.01358	0.04800	0.11632	0.45037	-0.40161	-0.09832	-0.02536
11	0.01616	0.05691	0.13337	0.47648	-0.41959	-0.10819	-0.02883
12	0.01805	0.06193	0.14199	0.48184	-0.42359	-0.11278	-0.02992
13	0.01918	0.06508	0.14589	0.48376	-0.42501	-0.11478	-0.03077
14	0.01999	0.06718	0.14850	0.47342	-0.39943	-0.11365	-0.03078

VERTICAL(W)

THETA(DEG.)	12.5000	37.5000	62.5000	88.7967	116.0950	142.5000	167.5000
ROW NO.							
1	0.00000	0.00000	0.00000	-0.01984	-0.00899	0.00000	0.00000
2	0.00000	0.00000	-0.01072	-0.04909	-0.01413	-0.00495	0.00000
3	-0.00259	-0.00750	-0.02250	-0.07292	-0.00997	-0.00791	-0.00322
4	-0.00811	-0.01449	-0.03280	-0.08939	0.00180	-0.00794	-0.00359
5	-0.01174	-0.01912	-0.03938	-0.09864	0.01928	-0.00397	-0.00071
6	-0.01286	-0.02067	-0.04238	-0.10237	0.03998	0.00307	0.00507
7	-0.01149	-0.01975	-0.04257	-0.10163	0.06237	0.01205	0.01281
8	-0.00843	-0.01711	-0.04047	-0.09675	0.08554	0.02222	0.02156
9	-0.00439	-0.01317	-0.03633	-0.08825	0.10842	0.03310	0.03079
10	0.00047	-0.00822	-0.03059	-0.07523	0.13084	0.04415	0.04027
11	0.01210	0.00450	-0.01106	-0.03691	0.16985	0.06752	0.05899
12	0.02592	0.02021	0.00668	-0.01237	0.19272	0.08497	0.07519
13	0.03748	0.03310	0.02219	0.00521	0.20964	0.09973	0.08857
14	0.05114	0.04871	0.04408	0.08737	0.27843	0.12090	0.10486

VELOCITY COMPONENTS ON BODY PANELS DUE TO WING SOURCES

AXIAL(U)

THETA(DEG.)	12.5000	37.5000	62.5000	88.7967	116.0950	142.5000	167.5000
ROW NO.							
1	-0.00000	-0.00000	-0.00000	-0.01746	-0.01483	-0.00000	-0.00000
2	-0.00000	-0.00000	-0.01181	-0.01010	-0.00962	-0.01002	-0.00000
3	-0.00625	-0.00872	-0.00864	-0.00561	-0.00578	-0.00773	-0.01313
4	-0.01331	-0.01218	-0.00975	-0.00643	-0.00803	-0.01140	-0.01228
5	-0.01091	-0.01024	-0.00846	-0.00500	-0.00560	-0.00845	-0.00946
6	-0.00818	-0.00731	-0.00524	-0.00167	-0.00228	-0.00529	-0.00652
7	-0.00529	-0.00424	-0.00194	0.00138	0.00079	-0.00206	-0.00341
8	-0.00221	-0.00106	0.00113	0.00388	0.00338	0.00102	-0.00019
9	0.00093	0.00191	0.00385	0.00637	0.00593	0.00380	0.00280
10	0.00364	0.00460	0.00647	0.00888	0.00845	0.00635	0.00531
11	0.00839	0.00937	0.00517	0.00283	0.00350	0.00597	0.00996
12	0.00375	0.00358	0.00314	0.00253	0.00244	0.00273	0.00289
13	0.00145	0.00132	0.00109	0.00088	0.00091	0.00108	0.00119
14	0.00066	0.00060	0.00050	0.00043	0.00044	0.00051	0.00056

TRANSVERSE(V)

THETA(DEG.)	12.5000	37.5000	62.5000	88.7967	116.0950	142.5000	167.5000
ROW NO.							
1	-0.00000	-0.00000	-0.00000	-0.01254	-0.01880	-0.00000	-0.00000
2	-0.00000	-0.00000	-0.00686	-0.02478	-0.02598	-0.01151	-0.00000
3	-0.00552	-0.00751	-0.01104	-0.02496	-0.02455	-0.01352	-0.00318
4	-0.00003	-0.00175	-0.00658	-0.01576	-0.01283	-0.00401	-0.00102
5	-0.00004	-0.00082	-0.00351	-0.00800	-0.00639	-0.00269	-0.00069
6	-0.00006	-0.00063	-0.00233	-0.00239	-0.00071	-0.00114	-0.00030
7	0.00004	-0.00016	-0.00072	0.00340	0.00499	0.00073	0.00020
8	0.00020	0.00049	0.00107	0.00848	0.00980	0.00254	0.00072
9	0.00036	0.00104	0.00267	0.01285	0.01394	0.00392	0.00103
10	0.00042	0.00147	0.00409	0.01681	0.01778	0.00526	0.00139
11	0.00080	0.00288	0.00416	0.00863	0.00687	0.00276	0.00228
12	-0.00007	0.00004	0.00089	0.00215	0.00175	0.00082	0.00020
13	0.00015	0.00056	0.00115	0.00163	0.00123	0.00075	0.00023
14	0.00013	0.00041	0.00072	0.00086	0.00058	0.00044	0.00015

VERTICAL(W)

THETA(DEG.)	12.5000	37.5000	62.5000	88.7967	116.0950	142.5000	167.5000
ROW NO.							
1	-0.00000	-0.00000	-0.00000	0.03411	-0.02338	-0.00000	-0.00000
2	-0.00000	-0.00000	0.02006	0.02711	-0.01888	-0.01357	-0.00000
3	0.00799	0.01358	0.01761	0.01797	-0.01283	-0.01175	-0.01298
4	0.01648	0.01616	0.01563	0.01123	-0.00866	-0.01219	-0.01259
5	0.01438	0.01391	0.01207	0.00463	-0.00395	-0.00906	-0.01024
6	0.01150	0.01044	0.00718	-0.00210	0.00081	-0.00559	-0.00754
7	0.00817	0.00650	0.00204	-0.00809	0.00509	-0.00193	-0.00450
8	0.00439	0.00223	-0.00283	-0.01259	0.00836	0.00159	-0.00122
9	0.00038	-0.00183	-0.00704	-0.01662	0.01132	0.00469	0.00190
10	-0.00326	-0.00559	-0.01098	-0.02050	0.01416	0.00757	0.00464
11	-0.00995	-0.01261	-0.00845	-0.00371	0.00291	0.00636	0.00988
12	-0.00519	-0.00492	-0.00393	-0.00118	0.00096	0.00280	0.00329
13	-0.00233	-0.00212	-0.00154	-0.00017	0.00014	0.00117	0.00149
14	-0.00114	-0.00100	-0.00064	0.00017	-0.00015	0.00049	0.00069

PRESSURES, FORCES, AND MOMENTS ON ISOLATED BODY

CD = 0.00087 CL = 0.00007 CM = -0.00412

BODY PRESSURE COEFFICIENTS(CP)

THETA(DEG.) X	0.0000	22.5000	45.0000	67.5000	90.0000	112.5000	135.0000	157.5000	180.0000
0.0000	0.14569	0.14413	0.13971	0.13308	0.12527	0.11745	0.11083	0.10640	0.10485
0.7243	0.15129	0.14974	0.14531	0.13868	0.13087	0.12306	0.11643	0.11200	0.11045
1.4485	0.10838	0.10749	0.10496	0.10118	0.09672	0.09226	0.08847	0.08595	0.08506
2.1728	0.05934	0.05901	0.05806	0.05665	0.05497	0.05330	0.05189	0.05094	0.05061
2.8970	0.06392	0.06351	0.06233	0.06057	0.05849	0.05642	0.05466	0.05348	0.05307
3.6213	0.04898	0.04864	0.04770	0.04628	0.04461	0.04294	0.04152	0.04057	0.04024
4.3456	0.04646	0.04618	0.04540	0.04423	0.04284	0.04146	0.04028	0.03950	0.03922
5.0698	0.03992	0.03960	0.03871	0.03738	0.03580	0.03422	0.03289	0.03200	0.03168
5.7941	0.03582	0.03561	0.03501	0.03412	0.03307	0.03202	0.03113	0.03053	0.03032
6.5184	0.03040	0.03022	0.02970	0.02892	0.02800	0.02709	0.02631	0.02579	0.02561
7.2426	0.02798	0.02777	0.02717	0.02626	0.02520	0.02413	0.02323	0.02263	0.02241
7.9669	0.02455	0.02427	0.02346	0.02226	0.02083	0.01941	0.01820	0.01739	0.01711
8.6911	0.02005	0.01990	0.01948	0.01886	0.01812	0.01739	0.01676	0.01635	0.01620
9.4154	0.01314	0.01322	0.01346	0.01381	0.01423	0.01465	0.01500	0.01524	0.01532
10.1397	0.01443	0.01419	0.01353	0.01253	0.01136	0.01019	0.00919	0.00853	0.00829
10.8639	0.00660	0.00664	0.00675	0.00691	0.00709	0.00728	0.00744	0.00755	0.00759
11.5882	0.00244	0.00255	0.00287	0.00335	0.00391	0.00447	0.00495	0.00527	0.00538
12.3124	-0.00203	-0.00197	-0.00180	-0.00155	-0.00125	-0.00095	-0.00070	-0.00053	-0.00047
13.0367	-0.00832	-0.00804	-0.00727	-0.00610	-0.00473	-0.00335	-0.00219	-0.00141	-0.00114
13.7610	-0.01187	-0.01168	-0.01116	-0.01037	-0.00944	-0.00851	-0.00773	-0.00720	-0.00702
14.5023	-0.01789	-0.01763	-0.01690	-0.01580	-0.01451	-0.01322	-0.01212	-0.01139	-0.01113
15.2436	-0.03560	-0.03505	-0.03347	-0.03112	-0.02833	-0.02555	-0.02319	-0.02162	-0.02106
15.9849	-0.03957	-0.03916	-0.03798	-0.03622	-0.03414	-0.03206	-0.03030	-0.02912	-0.02871
16.7262	-0.02869	-0.02840	-0.02757	-0.02634	-0.02488	-0.02343	-0.02220	-0.02137	-0.02108
17.4675	-0.02425	-0.02407	-0.02354	-0.02275	-0.02192	-0.02088	-0.02009	-0.01956	-0.01938
18.2088	-0.01956	-0.01945	-0.01915	-0.01869	-0.01815	-0.01761	-0.01715	-0.01684	-0.01674
18.9501	-0.01627	-0.01622	-0.01608	-0.01586	-0.01561	-0.01535	-0.01514	-0.01499	-0.01494
19.6914	-0.01359	-0.01358	-0.01355	-0.01349	-0.01343	-0.01337	-0.01332	-0.01329	-0.01327
20.4327	-0.01153	-0.01154	-0.01158	-0.01163	-0.01169	-0.01176	-0.01181	-0.01184	-0.01186
21.1740	-0.00990	-0.00993	-0.01000	-0.01011	-0.01025	-0.01038	-0.01049	-0.01056	-0.01059
21.9153	-0.00862	-0.00865	-0.00874	-0.00888	-0.00904	-0.00921	-0.00934	-0.00944	-0.00947
22.6566	-0.00759	-0.00762	-0.00772	-0.00786	-0.00803	-0.00820	-0.00834	-0.00844	-0.00847
23.3979	-0.00510	-0.00526	-0.00571	-0.00638	-0.00718	-0.00797	-0.00864	-0.00909	-0.00925
24.1392	-0.00652	-0.00652	-0.00650	-0.00647	-0.00645	-0.00642	-0.00639	-0.00637	-0.00637
24.8805	-0.00583	-0.00583	-0.00583	-0.00582	-0.00582	-0.00581	-0.00581	-0.00580	-0.00580
25.6218	-0.00532	-0.00532	-0.00531	-0.00529	-0.00528	-0.00526	-0.00524	-0.00523	-0.00523
26.3631	-0.00484	-0.00484	-0.00483	-0.00482	-0.00481	-0.00480	-0.00479	-0.00478	-0.00478
27.1044	-0.00441	-0.00441	-0.00440	-0.00440	-0.00439	-0.00438	-0.00437	-0.00437	-0.00436
27.8457	-0.00408	-0.00408	-0.00407	-0.00407	-0.00407	-0.00406	-0.00406	-0.00406	-0.00406
28.5870	-0.00360	-0.00360	-0.00360	-0.00360	-0.00360	-0.00360	-0.00360	-0.00360	-0.00360
29.3283	-0.00387	-0.00397	-0.00387	-0.00387	-0.00387	-0.00387	-0.00388	-0.00388	-0.00388
30.0696	-0.00926	-0.00926	-0.00927	-0.00927	-0.00928	-0.00928	-0.00929	-0.00929	-0.00929
30.8109	-0.01813	-0.01814	-0.01814	-0.01816	-0.01817	-0.01819	-0.01820	-0.01821	-0.01821
31.5522	-0.02444	-0.02444	-0.02446	-0.02448	-0.02451	-0.02454	-0.02457	-0.02458	-0.02459
32.2935	-0.02769	-0.02770	-0.02773	-0.02776	-0.02781	-0.02785	-0.02789	-0.02792	-0.02793
33.0348	-0.03299	-0.03300	-0.03304	-0.03309	-0.03315	-0.03322	-0.03327	-0.03331	-0.03332
33.7761	-0.03887	-0.03889	-0.03894	-0.03901	-0.03910	-0.03919	-0.03926	-0.03931	-0.03933
34.5174	-0.03447	-0.03449	-0.03456	-0.03465	-0.03476	-0.03487	-0.03496	-0.03502	-0.03504
35.2587	-0.01798	-0.01801	-0.01808	-0.01818	-0.01830	-0.01842	-0.01852	-0.01859	-0.01861

INCREMENTAL PRESSURES, FORCES, AND MOMENTS ON BODY PANELS DUE TO WING

CD = 0.00005 CL = 0.01760 CM = -0.39476

BODY PANEL PRESSURE COEFFICIENT(CP)

THETA(DEG.)	12.5000	37.5000	62.5000	88.7967	116.0950	142.5000	167.5000
ROW NO.							
1	0.00004	0.00015	0.00060	0.01939	0.05515	0.00128	0.00039
2	-0.00019	-0.00023	0.00955	-0.03150	0.08320	0.03150	0.00083
3	0.00259	0.00372	-0.01252	-0.07472	0.09084	0.05012	0.02565
4	0.00174	-0.00550	-0.03849	-0.09792	0.09343	0.06017	0.04884
5	-0.00618	-0.02480	-0.05586	-0.10858	0.08766	0.06929	0.06371
6	-0.02005	-0.03847	-0.06955	-0.11143	0.08251	0.07375	0.07187
7	-0.03639	-0.05061	-0.07616	-0.10874	0.07469	0.07316	0.07388
8	-0.05047	-0.06064	-0.07940	-0.10061	0.06634	0.07011	0.06962
9	-0.05981	-0.06724	-0.07985	-0.09042	0.05485	0.06366	0.06545
10	-0.06582	-0.07087	-0.07884	-0.07835	0.03893	0.05521	0.05883
11	-0.06940	-0.07044	-0.05265	-0.02192	0.02982	0.04031	0.04071
12	-0.05202	-0.04638	-0.03194	-0.00782	0.01637	0.02747	0.03110
13	-0.03316	-0.02924	-0.02081	-0.00693	0.00857	0.01920	0.02443
14	-0.02091	-0.01803	-0.01205	-0.00341	0.00567	0.01172	0.01446

BODY PANEL SLOPE(DR/DX)

THETA(DEG.)	12.5000	37.5000	62.5000	88.7967	116.0950	142.5000	167.5000
ROW NO.							
1	0.02348	0.02319	0.02266	0.02196	0.02122	0.02065	0.02036
2	0.00603	0.00629	0.00676	0.00738	0.00804	0.00854	0.00880
3	-0.00145	-0.00118	-0.00069	-0.00004	0.00065	0.00118	0.00145
4	-0.00145	-0.00118	-0.00069	-0.00004	0.00065	0.00118	0.00145
5	-0.00145	-0.00118	-0.00069	-0.00004	0.00065	0.00118	0.00145
6	-0.00145	-0.00118	-0.00069	-0.00004	0.00065	0.00118	0.00145
7	-0.00145	-0.00118	-0.00069	-0.00004	0.00065	0.00118	0.00145
8	-0.00145	-0.00118	-0.00069	-0.00004	0.00065	0.00118	0.00145
9	-0.00145	-0.00118	-0.00069	-0.00004	0.00065	0.00118	0.00145
10	-0.00081	-0.00066	-0.00039	-0.00002	0.00037	0.00066	0.00081
11	-0.00145	-0.00118	-0.00069	-0.00004	0.00065	0.00118	0.00145
12	-0.00145	-0.00118	-0.00069	-0.00004	0.00065	0.00118	0.00145
13	-0.00158	-0.00131	-0.00082	-0.00017	0.00052	0.00105	0.00132
14	-0.02519	-0.02492	-0.02442	-0.02377	-0.02309	-0.02256	-0.02229

PRESSURES, FORCES, AND MOMENTS ON WING PANELS IN PRESENCE OF BODY

CD = 0.00734 CL = 0.15900 CM = -4.74796

SPANWISE CD DISTRIBUTION(B/2Q * DD/DY)

SPANWISE STATION	1	2	3	4	5	6	7	8	9	10
	0.00387	0.00172	0.00112	0.00092	0.00075	0.00054	0.00038	0.00036	-0.00143	0.00032

SPANWISE CL DISTRIBUTION(B/2Q * DL/DY)

SPANWISE STATION	1	2	3	4	5	6	7	8	9	10
	0.01934	0.01902	0.01906	0.01915	0.01908	0.01876	0.01811	0.01706	0.01562	0.01371

UPPER SURFACE WING PANEL PRESSURE COEFFICIENTS(CP)

SPANWISE STATION	1	2	3	4	5	6	7	8	9	10
CHORDWISE STATION										
1	-0.06814	-0.07465	-0.06707	-0.05555	-0.05922	-0.06370	-0.06872	-0.07616	-0.04863	-0.15152
2	-0.14334	-0.13719	-0.10683	-0.10929	-0.11396	-0.12028	-0.12866	-0.13289	-0.09372	-0.24049
3	-0.16260	-0.14634	-0.14498	-0.13298	-0.13895	-0.14767	-0.15351	-0.14854	-0.11742	-0.25620
4	-0.16337	-0.15016	-0.14581	-0.15085	-0.15846	-0.16475	-0.16235	-0.15652	-0.13733	-0.16475
5	-0.15585	-0.14961	-0.15539	-0.16543	-0.16863	-0.16875	-0.16369	-0.15549	-0.14830	-0.15877
6	-0.14506	-0.14646	-0.15826	-0.17314	-0.16788	-0.15911	-0.15949	-0.14337	-0.15077	-0.14625
7	-0.12952	-0.13729	-0.15851	-0.15745	-0.15536	-0.14936	-0.14205	-0.12757	-0.14792	-0.12796
8	-0.10799	-0.13358	-0.13757	-0.13907	-0.13386	-0.12998	-0.11665	-0.11640	-0.14049	-0.10384
9	-0.09319	-0.10434	-0.11265	-0.10714	-0.10593	-0.09494	-0.08773	-0.09611	-0.12158	-0.07802
10	-0.05003	-0.04964	-0.05971	-0.05806	-0.04742	-0.04514	-0.03797	-0.05455	-0.07370	-0.07785

LOWER SURFACE WING PANEL PRESSURE COEFFICIENTS(CP)

SPANWISE STATION	1	2	3	4	5	6	7	8	9	10
CHORDWISE STATION										
1	0.09254	0.06668	0.04312	0.04202	0.03618	0.03187	0.02797	0.02152	-0.00668	0.06631
2	0.08605	0.05770	0.05297	0.03978	0.03447	0.02941	0.02303	0.01912	-0.00551	0.11252
3	0.08856	0.06758	0.04326	0.04990	0.04579	0.03937	0.03560	0.04293	0.01286	0.12641
4	0.08462	0.06689	0.06050	0.05600	0.05254	0.04858	0.05440	0.05793	0.01105	0.03409
5	0.07690	0.06542	0.06187	0.05824	0.05996	0.06230	0.06951	0.05572	0.01896	0.02823
6	0.06751	0.06141	0.06486	0.05968	0.06960	0.07967	0.07020	0.05079	0.03688	0.02353
7	0.05809	0.06225	0.06372	0.07523	0.08085	0.07947	0.06834	0.05317	0.05333	0.02017
8	0.04866	0.05298	0.07345	0.08167	0.08303	0.07276	0.06785	0.05033	0.06656	0.02219
9	0.02775	0.05551	0.07172	0.08048	0.07150	0.07003	0.06135	0.04973	0.07217	0.01978
10	0.02268	0.06127	0.06674	0.06576	0.06780	0.06312	0.05835	0.04675	0.07624	0.03580

WING PANEL PRESSURE DIFFERENCE(CL)

SPANWISE STATION	1	2	3	4	5	6	7	8	9	10

CHORDWISE STATION										
1	0.16067	0.14133	0.11020	0.09757	0.09540	0.09556	0.09670	0.09769	0.04194	0.21783
2	0.22938	0.19489	0.15980	0.14907	0.14842	0.14969	0.15169	0.15201	0.08821	0.35301
3	0.25117	0.21391	0.18824	0.18289	0.18474	0.18704	0.18911	0.19147	0.13028	0.38261
4	0.24799	0.21705	0.20631	0.20685	0.21099	0.21333	0.21675	0.21445	0.14838	0.19884
5	0.23276	0.21403	0.21726	0.22367	0.22859	0.23105	0.23320	0.21122	0.16726	0.18701
6	0.21257	0.20787	0.22312	0.23283	0.23748	0.23878	0.22969	0.19416	0.18766	0.16979
7	0.18761	0.19953	0.22222	0.23268	0.23621	0.22882	0.21039	0.18074	0.20125	0.14813
8	0.15665	0.18656	0.21101	0.22075	0.21689	0.20274	0.18450	0.16673	0.20705	0.12603
9	0.12094	0.15985	0.18437	0.18761	0.17743	0.16497	0.14908	0.14584	0.19375	0.09780
10	0.07270	0.11091	0.12645	0.12383	0.11522	0.10826	0.09632	0.10131	0.14994	0.11365

UPPER SURFACE WING PANEL SLOPE(DZ/DX)

SPANWISE STATION	1	2	3	4	5	6	7	8	9	10
CHORDWISE STATION										
1	0.03132	0.10057	0.12849	0.13556	0.13980	0.14519	0.15092	0.15622	0.18173	0.16472
2	-0.07290	0.02702	0.06932	0.08016	0.08561	0.09188	0.09774	0.10409	0.15483	0.03661
3	-0.15116	-0.02606	0.02515	0.03804	0.04419	0.05106	0.05712	0.05687	0.13541	-0.03893
4	-0.20874	-0.07047	-0.01685	-0.00223	0.00453	0.01169	0.01594	0.00440	0.13546	-0.04721
5	-0.25505	-0.10849	-0.05765	-0.04239	-0.03556	-0.02897	-0.02935	-0.04070	0.13426	-0.07011
6	-0.28676	-0.14320	-0.09728	-0.08249	-0.07640	-0.07254	-0.07111	-0.07572	0.10853	-0.08878
7	-0.30566	-0.17092	-0.13147	-0.11845	-0.11442	-0.10875	-0.10322	-0.10347	0.07475	-0.09757
8	-0.31408	-0.19967	-0.16759	-0.15718	-0.15263	-0.14195	-0.13703	-0.12972	0.02714	-0.10512
9	-0.31558	-0.22940	-0.20636	-0.19791	-0.18892	-0.17667	-0.17197	-0.15914	-0.03103	-0.11065
10	-0.31235	-0.26002	-0.24791	-0.23721	-0.22633	-0.21365	-0.20713	-0.19213	-0.11074	-0.12965

LOWER SURFACE WING PANEL SLOPE(DZ/DX)

SPANWISE STATION	1	2	3	4	5	6	7	8	9	10
CHORDWISE STATION										
1	-0.10343	-0.03418	-0.00626	0.00081	0.00505	0.01044	0.01617	0.02147	0.04698	0.02997
2	-0.14311	-0.04318	-0.00088	0.00995	0.01541	0.02167	0.02754	0.03389	0.08462	-0.03360
3	-0.18384	-0.05873	-0.00753	0.00536	0.01152	0.01838	0.02445	0.02420	0.10274	-0.07161
4	-0.20897	-0.07070	-0.01708	-0.00246	0.00430	0.01146	0.01572	0.00418	0.13524	-0.04743
5	-0.22459	-0.07803	-0.02719	-0.01192	-0.00510	0.00149	0.00111	-0.01024	0.16473	-0.03964
6	-0.22829	-0.08473	-0.03881	-0.02402	-0.01793	-0.01407	-0.01264	-0.01725	0.16700	-0.03031
7	-0.23187	-0.09712	-0.05768	-0.04466	-0.04063	-0.03496	-0.02943	-0.02968	0.14854	-0.02378
8	-0.22583	-0.11141	-0.07934	-0.06892	-0.06437	-0.05369	-0.04877	-0.04147	0.11540	-0.01686
9	-0.21283	-0.12665	-0.10361	-0.09517	-0.08618	-0.07393	-0.06922	-0.05639	0.07172	-0.00791
10	-0.19482	-0.14249	-0.13038	-0.11968	-0.10880	-0.09612	-0.08960	-0.07460	0.00679	-0.01212

WING CAMBER SLOPE(DZ/DX)

SPANWISE STATION	1	2	3	4	5	6	7	8	9	10
CHORDWISE STATION										
1	-0.03605	0.03320	0.06111	0.06818	0.07242	0.07781	0.08355	0.08884	0.11436	0.09734
2	-0.10801	-0.00808	0.03422	0.04506	0.05051	0.05678	0.06264	0.06899	0.11973	0.00151
3	-0.16750	-0.04240	0.00881	0.02170	0.02785	0.03472	0.04078	0.04053	0.11907	-0.05527
4	-0.20885	-0.07058	-0.01697	-0.00235	0.00442	0.01157	0.01583	0.00429	0.13535	-0.04732
5	-0.23982	-0.09326	-0.04242	-0.02716	-0.02033	-0.01374	-0.01412	-0.02547	0.14949	-0.05488
6	-0.25752	-0.11396	-0.06804	-0.05325	-0.04716	-0.04330	-0.04188	-0.04648	0.13776	-0.05955

7	-0.26876	-0.13402	-0.09457	-0.08156	-0.07753	-0.07185	-0.06632	-0.06657	0.11164	-0.06068
8	-0.26996	-0.15554	-0.12346	-0.11305	-0.10853	-0.09782	-0.09290	-0.08559	0.07127	-0.06099
9	-0.26421	-0.17802	-0.15499	-0.14654	-0.13755	-0.12530	-0.12059	-0.10777	0.02034	-0.05928
10	-0.25359	-0.20126	-0.18915	-0.17844	-0.16756	-0.15488	-0.14837	-0.13336	-0.05198	-0.07089

WING CHORD LENGTHS(C)

9.21046	9.21070	9.21094	9.21118	9.21142	9.21166	9.21190	9.21215	9.21239	6.14167

FORCES AND MOMENTS ON WING-BODY COMBINATION

CD = 0.00826 CL = 0.17666 CM = -5.14684

END OF DATA 11A

END OF DATA 11A TIME 20.821 061567

9.4 Appendix D - Sample Flow Visualization Case Printout

A sample printout is given here for the flow-field visualization about the Boeing wind-tunnel model described in section 6.4. A discussion of the results is given on pages 113 to 119 of this report. The panel layout used for this case is the same as used in the previous example, and is shown in the upper sketch on figure 49, page 216. Only those portions of the printout that illustrate the format and type of data are shown.

AUG 08, 1967

PROGRAM FOR ANALYSIS AND DESIGN OF SUPERSONIC WING-BODY COMBINATIONS

DATA CARDS ARE LISTED BELOW

```
AERODYNAMIC                                                          1A
USE TAPE                                                             2A
1.8       1.                                                         3A
TR 805 WING BODY                                                     4A
2.        0.        0.        1.        1.                         5A
89.375    0.        0.                                             6A
6.                                                                   7A
GIVEN BODY RADII                                    ---              8A
GIVEN BODY CAMBER                                                    9A
0.        0.                                                         11A
CONSTANT WING CAMBER                                                 12A
0.                                                                   12AA
GIVEN WING THICKNESS                                                 14A
                                                                     16A
                                                                     16A
FLOW VIZ                                                             1F
0.        0.        1.                                             2F
POINTS                                                               5F
9.                                                                   5FA
24.       4.        -1.                                            5FB
24.       4.        -.5                                            5FB
24.       4.3535    -.6465                                         5FB
24.       4.5       -1.                                            5FB
24.       4.3535    -1.3535                                        5FB
24.       4.        -1.5                                           5FB
24.       3.6465    -1.3535                                        5FB
24.       3.5       -1.                                            5FB
24.       3.6465    -.6465                                         5FB
GRIDS                                                                5F
4.                                                                   3FA
30.       1.2       -1.2                                           3FB
.5        1.        .5        10.       3.        2.        2.     3FC
50.       0.        36.                                            3FB
2.        0.        0.        51.       0.        0.        2.     3FC
50.       36.       0.                                             3FB
2.        0.        0.        51.       0.        0.        2.     3FC
50.       0.        -36.                                           3FB
2.        0.        0.        51.       0.        0.        2.     3FC
STREAMLINES                                                          4F
5.        .01       1.                                             4FA
3.                                                                   4FB
28.       5.        .25       40.       20.       .1             4FC
28.       5.        -.5       40.       20.       .2             4FC
15.4      1.5       0.        30.       0.        .1             4FC
VIZEND                                                               6F
END OF DATA                                                          7F
```

A TOTAL OF 46 DATA CARDS WERE READ

AERODYNAMIC 1A TIME 23.333 080867

USE TAPE 2A

TR 805 WING BODY AUG 08, 1967

DESCRIPTION OF CASE REQUESTED

SYMMETRICAL CONFIGURATION - PANELS LOCATED ON BOTH SIDES OF X-Z PLANE(SYM = 1.)

CASE = 2. CALCULATE CL, GIVEN SHAPE

CPCALC = 0. LINEAR CP

POLAR = 0. POLARS NOT REQUESTED

THICK = 1. WING THICKNESS PRESSURES TO BE ADDED

VOUT = 1. VELOCITY COMPONENTS TO BE PRINTED

MACH NUMBER = 1.8000

POINT ABOUT WHICH THE MOMENTS ARE TO BE COMPUTED
X-COORDINATE = 0.0000
Z-COORDINATE = 0.0000

REFERENCE CHORD LENGTH = 1.0000

WING REFERENCE AREA = 89.3750

WING SEMI-SPAN = 1.0000

GIVEN BODY RADII --- 8A

GIVEN BODY CAMBER 9A

HEIGHT OF WING PLANE ABOVE BODY AXIS = -0.2500

INCLINATION OF BODY AXIS WITH RESPECT TO DEFINING AXIS = 0.0000 DEG.

ANGLE OF ATTACK WITH RESPECT TO BODY AXIS = 6.0000 DEG.

CONSTANT WING CAMBER 12A

GIVEN WING THICKNESS 14A

BODY GEOMETRY

X-STATION	CAMBER	RADIUS	FIRST DERIVATIVE	SECOND DERIVATIVE
0.0000	0.0000	0.0000	0.1800	-0.0199
0.7243	0.0000	0.1304	0.1872	0.0398
1.4485	0.0000	0.2607	0.1512	-0.1393
2.1728	0.0000	0.3491	0.1142	0.0372
2.8970	0.0000	0.4343	0.1110	-0.0461
3.6213	0.0000	0.5077	0.0987	0.0121
4.3456	0.0000	0.5791	0.0941	-0.0247
5.0698	0.0000	0.6433	0.0869	0.0048
5.7941	0.0000	0.7057	0.0826	-0.0168
6.5184	0.0000	0.7627	0.0769	0.0013
7.2426	0.0000	0.8175	0.0728	-0.0126
7.9669	0.0000	0.8679	0.0678	-0.0015
8.6911	0.0000	0.9159	0.0638	-0.0094
9.4154	0.0000	0.9602	0.0591	-0.0037
10.1397	0.0000	1.0017	0.0550	-0.0075
10.8639	0.0000	1.0396	0.0498	-0.0067
11.5882	0.0000	1.0740	0.0454	-0.0056
12.3124	0.0000	1.1049	0.0392	-0.0113
13.0367	0.0000	1.1311	0.0342	-0.0027
13.7610	0.0000	1.1542	0.0281	-0.0142
14.5023	0.0000	1.1720	0.0213	-0.0039
15.2436	0.0000	1.1840	0.0073	-0.0340
15.9849	0.0000	1.1840	-0.0019	0.0091
16.7262	0.0000	1.1840	0.0005	-0.0024
17.4675	0.0000	1.1840	-0.0001	0.0007
18.2088	0.0000	1.1840	0.0000	-0.0002
18.9501	0.0000	1.1840	-0.0000	0.0000
19.6914	0.0000	1.1840	0.0000	-0.0000
20.4327	0.0000	1.1840	-0.0000	0.0000
21.1740	0.0000	1.1840	0.0000	-0.0000
21.9153	0.0000	1.1840	-0.0000	0.0000
22.6566	0.0000	1.1840	0.0000	-0.0000
23.3979	0.0000	1.1840	-0.0000	-0.0000
24.1392	0.0000	1.1840	0.0000	0.0000
24.8805	0.0000	1.1840	-0.0000	-0.0000
25.6218	0.0000	1.1840	0.0000	0.0000
26.3631	0.0000	1.1840	-0.0000	-0.0000
27.1044	0.0000	1.1840	0.0000	0.0000
27.8457	0.0000	1.1840	-0.0000	-0.0001
28.5870	0.0000	1.1840	0.0001	0.0004
29.3283	0.0000	1.1840	-0.0003	-0.0016
30.0696	0.0000	1.1825	-0.0050	-0.0109
30.8109	0.0000	1.1757	-0.0133	-0.0115
31.5522	0.0000	1.1630	-0.0208	-0.0090
32.2935	0.0000	1.1452	-0.0269	-0.0073
33.0348	0.0000	1.1226	-0.0350	-0.0146
33.7761	0.0000	1.0930	-0.0446	-0.0114
34.5174	0.0000	1.0581	-0.0475	0.0038
35.2587	0.0000	1.0252	-0.0398	0.0170

VELOCITY COMPONENTS ON BODY DUE TO BODY LINE SOURCES AND DOUBLETS

AXIAL(U)

THETA(DEG.)	0.0000	22.5000	45.0000	67.5000	90.0000	112.5000	135.0000	157.5000	180.0000
X									
0.0000	-0.03166	-0.03402	-0.04073	-0.05078	-0.06263	-0.07449	-0.08454	-0.09125	-0.09361
0.7243	-0.03446	-0.03682	-0.04353	-0.05358	-0.06543	-0.07729	-0.08734	-0.09405	-0.09641
1.4485	-0.01686	-0.01926	-0.02608	-0.03630	-0.04836	-0.06041	-0.07063	-0.07746	-0.07986
2.1728	-0.00369	-0.00550	-0.01066	-0.01838	-0.02749	-0.03659	-0.04431	-0.04947	-0.05128
2.8970	-0.00659	-0.00832	-0.01323	-0.02058	-0.02925	-0.03792	-0.04527	-0.05018	-0.05190
3.6213	-0.00198	-0.00352	-0.00793	-0.01453	-0.02230	-0.03008	-0.03668	-0.04105	-0.04263
4.3456	-0.00193	-0.00341	-0.00764	-0.01396	-0.02142	-0.02888	-0.03520	-0.03943	-0.04091
5.0698	0.00027	-0.00112	-0.00505	-0.01095	-0.01790	-0.02485	-0.03075	-0.03468	-0.03607
5.7941	0.00087	-0.00046	-0.00423	-0.00987	-0.01653	-0.02320	-0.02884	-0.03261	-0.03394
6.5184	0.00239	0.00114	-0.00241	-0.00773	-0.01400	-0.02027	-0.02559	-0.02914	-0.03039
7.2426	0.00305	0.00186	-0.00153	-0.00661	-0.01260	-0.01859	-0.02366	-0.02706	-0.02825
7.9669	0.00434	0.00322	0.00002	-0.00477	-0.01042	-0.01606	-0.02085	-0.02405	-0.02517
8.6911	0.00494	0.00387	0.00084	-0.00370	-0.00906	-0.01442	-0.01896	-0.02200	-0.02306
9.4154	0.00606	0.00505	0.00220	-0.00208	-0.00712	-0.01216	-0.01643	-0.01928	-0.02029
10.1397	0.00671	0.00576	0.00308	-0.00094	-0.00568	-0.01042	-0.01444	-0.01712	-0.01807
10.8639	0.00800	0.00713	0.00462	0.00087	-0.00355	-0.00797	-0.01172	-0.01422	-0.01510
11.5882	0.00871	0.00790	0.00559	0.00213	-0.00196	-0.00604	-0.00950	-0.01181	-0.01263
12.3124	0.01038	0.00964	0.00753	0.00436	0.00063	-0.00311	-0.00627	-0.00839	-0.00913
13.0367	0.01105	0.01039	0.00851	0.00569	0.00236	-0.00096	-0.00378	-0.00566	-0.00632
13.7610	0.01238	0.01180	0.01014	0.00765	0.00472	0.00179	-0.00070	-0.00236	-0.00294
14.5023	0.01363	0.01315	0.01177	0.00970	0.00726	0.00481	0.00275	0.00136	0.00088
15.2436	0.01910	0.01872	0.01765	0.01605	0.01417	0.01228	0.01068	0.00961	0.00924
15.9849	0.01971	0.01951	0.01894	0.01808	0.01707	0.01606	0.01520	0.01463	0.01443
16.7262	0.01345	0.01337	0.01315	0.01283	0.01244	0.01206	0.01173	0.01151	0.01144
17.4675	0.01081	0.01081	0.01084	0.01087	0.01091	0.01095	0.01098	0.01100	0.01101
18.2088	0.00830	0.00836	0.00853	0.00878	0.00907	0.00937	0.00962	0.00979	0.00985
18.9501	0.00667	0.00676	0.00700	0.00737	0.00780	0.00824	0.00861	0.00885	0.00894
19.6914	0.00544	0.00554	0.00582	0.00623	0.00672	0.00720	0.00762	0.00789	0.00799
20.4327	0.00459	0.00468	0.00495	0.00536	0.00585	0.00633	0.00674	0.00701	0.00711
21.1740	0.00396	0.00405	0.00430	0.00468	0.00512	0.00557	0.00594	0.00620	0.00629
21.9153	0.00350	0.00358	0.00380	0.00413	0.00452	0.00491	0.00524	0.00546	0.00554
22.6566	0.00316	0.00322	0.00341	0.00369	0.00402	0.00434	0.00462	0.00481	0.00487
23.3979	0.00289	0.00294	0.00309	0.00332	0.00359	0.00386	0.00408	0.00423	0.00429
24.1392	0.00267	0.00271	0.00283	0.00301	0.00322	0.00344	0.00362	0.00374	0.00378
24.8805	0.00248	0.00251	0.00260	0.00274	0.00291	0.00307	0.00322	0.00331	0.00334
25.6218	0.00231	0.00233	0.00240	0.00251	0.00264	0.00276	0.00287	0.00294	0.00297
26.3631	0.00215	0.00217	0.00223	0.00231	0.00240	0.00250	0.00258	0.00263	0.00265
27.1044	0.00201	0.00202	0.00206	0.00212	0.00219	0.00226	0.00232	0.00236	0.00238
27.8457	0.00189	0.00190	0.00193	0.00198	0.00203	0.00209	0.00213	0.00216	0.00217
28.5870	0.00169	0.00170	0.00172	0.00176	0.00180	0.00184	0.00187	0.00190	0.00190
29.3283	0.00186	0.00186	0.00188	0.00190	0.00194	0.00197	0.00199	0.00201	0.00202
30.0696	0.00441	0.00442	0.00447	0.00455	0.00464	0.00473	0.00480	0.00485	0.00487
30.8109	0.00816	0.00823	0.00843	0.00873	0.00909	0.00944	0.00974	0.00994	0.01001
31.5522	0.01013	0.01029	0.01075	0.01144	0.01226	0.01307	0.01376	0.01422	0.01438
32.2935	0.01030	0.01057	0.01136	0.01253	0.01390	0.01528	0.01645	0.01724	0.01751
33.0348	0.01130	0.01170	0.01285	0.01456	0.01658	0.01860	0.02031	0.02145	0.02185
33.7761	0.01218	0.01274	0.01434	0.01673	0.01955	0.02237	0.02476	0.02636	0.02692
34.5174	0.00788	0.00861	0.01067	0.01375	0.01738	0.02101	0.02409	0.02615	0.02687
35.2587	-0.00143	-0.00062	0.00167	0.00510	0.00915	0.01320	0.01663	0.01892	0.01973

RADIAL(VR)

THETA(DEG.)	0.0000	22.5000	45.0000	67.5000	90.0000	112.5000	135.0000	157.5000	180.0000
X									
0.0000	0.06980	0.07733	0.09878	0.13087	0.16873	0.20658	0.23867	0.26012	0.26765
0.7243	0.07603	0.08356	0.10501	0.13710	0.17496	0.21281	0.24490	0.26635	0.27388
1.4485	0.04391	0.05152	0.07319	0.10561	0.14387	0.18212	0.21455	0.23621	0.24382
2.1728	0.00905	0.01681	0.03893	0.07202	0.11105	0.15009	0.18318	0.20529	0.21305
2.8970	0.00551	0.01329	0.03545	0.06861	0.10772	0.14683	0.17999	0.20214	0.20992
3.6213	-0.00626	0.00156	0.02383	0.05715	0.09646	0.13576	0.16909	0.19135	0.19917
4.3456	-0.01079	-0.00296	0.01934	0.05272	0.09209	0.13146	0.16484	0.18714	0.19498
5.0698	-0.01777	-0.00991	0.01244	0.04590	0.08538	0.12485	0.15831	0.18066	0.18852
5.7941	-0.02206	-0.01420	0.00819	0.04169	0.08122	0.12074	0.15425	0.17664	0.18450
6.5184	-0.02759	-0.01972	0.00271	0.03628	0.07587	0.11546	0.14902	0.17145	0.17933
7.2426	-0.03165	-0.02377	-0.00131	0.03229	0.07193	0.11157	0.14517	0.16763	0.17551
7.9669	-0.03667	-0.02877	-0.00629	0.02736	0.06705	0.10674	0.14039	0.16287	0.17077
8.6911	-0.04058	-0.03268	-0.01017	0.02351	0.06324	0.10298	0.13666	0.15917	0.16707
9.4154	-0.04529	-0.03738	-0.01485	0.01887	0.05865	0.09843	0.13215	0.15468	0.16259
10.1397	-0.04935	-0.04143	-0.01888	0.01488	0.05469	0.09450	0.12826	0.15081	0.15873
10.8639	-0.05448	-0.04655	-0.02398	0.00981	0.04966	0.08952	0.12330	0.14588	0.15381
11.5882	-0.05896	-0.05103	-0.02843	0.00538	0.04527	0.08516	0.11898	0.14157	0.14951
12.3124	-0.06507	-0.05713	-0.03451	-0.00066	0.03927	0.07920	0.11305	0.13566	0.14361
13.0367	-0.07015	-0.06220	-0.03956	-0.00569	0.03427	0.07423	0.10811	0.13075	0.13870
13.7610	-0.07630	-0.06835	-0.04569	-0.01179	0.02820	0.06819	0.10210	0.12475	0.13271
14.5023	-0.08310	-0.07513	-0.05246	-0.01853	0.02149	0.06151	0.09544	0.11811	0.12607
15.2436	-0.09731	-0.08934	-0.06665	-0.03268	0.00738	0.04744	0.08140	0.10409	0.11206
15.9849	-0.10671	-0.09874	-0.07603	-0.04206	-0.00198	0.03809	0.07207	0.09477	0.10274
16.7262	-0.10419	-0.09622	-0.07352	-0.03955	0.00053	0.04060	0.07458	0.09728	0.10525
17.4675	-0.10486	-0.09689	-0.07419	-0.04022	-0.00014	0.03993	0.07391	0.09661	0.10458
18.2088	-0.10468	-0.09671	-0.07401	-0.04004	0.00004	0.04011	0.07409	0.09679	0.10476
18.9501	-0.10473	-0.09676	-0.07406	-0.04008	-0.00001	0.04006	0.07404	0.09674	0.10471
19.6914	-0.10472	-0.09675	-0.07405	-0.04007	0.00000	0.04008	0.07405	0.09675	0.10472
20.4327	-0.10472	-0.09675	-0.07405	-0.04008	-0.00000	0.04007	0.07405	0.09675	0.10472
21.1740	-0.10472	-0.09675	-0.07405	-0.04007	0.00000	0.04007	0.07405	0.09675	0.10472
21.9153	-0.10472	-0.09675	-0.07405	-0.04007	-0.00000	0.04007	0.07405	0.09675	0.10472
22.6566	-0.10472	-0.09675	-0.07405	-0.04007	-0.00000	0.04007	0.07405	0.09675	0.10472
23.3979	-0.10472	-0.09675	-0.07405	-0.04007	-0.00000	0.04007	0.07405	0.09675	0.10472
24.1392	-0.10472	-0.09675	-0.07405	-0.04007	-0.00000	0.04007	0.07405	0.09675	0.10472
24.8805	-0.10472	-0.09675	-0.07405	-0.04007	-0.00000	0.04007	0.07405	0.09675	0.10472
25.6218	-0.10472	-0.09675	-0.07405	-0.04007	0.00000	0.04007	0.07405	0.09675	0.10472
26.3631	-0.10472	-0.09675	-0.07405	-0.04008	-0.00000	0.04007	0.07405	0.09675	0.10472
27.1044	-0.10471	-0.09674	-0.07404	-0.04007	0.00001	0.04008	0.07405	0.09675	0.10473
27.8457	-0.10474	-0.09677	-0.07407	-0.04010	-0.00002	0.04005	0.07402	0.09672	0.10470
28.5870	-0.10463	-0.09666	-0.07396	-0.03998	0.00009	0.04017	0.07414	0.09684	0.10481
29.3283	-0.10506	-0.09709	-0.07439	-0.04041	-0.00034	0.03973	0.07371	0.09641	0.10438
30.0696	-0.10972	-0.10174	-0.07904	-0.04507	-0.00500	0.03508	0.06905	0.09175	0.09972
30.8109	-0.11810	-0.11013	-0.08743	-0.05347	-0.01340	0.02667	0.06064	0.08334	0.09131
31.5522	-0.12578	-0.11781	-0.09512	-0.06116	-0.02110	0.01895	0.05291	0.07560	0.08357
32.2935	-0.13186	-0.12390	-0.10122	-0.06728	-0.02724	0.01280	0.04674	0.06942	0.07738
33.0348	-0.14009	-0.13214	-0.10948	-0.07556	-0.03556	0.00444	0.03836	0.06102	0.06898
33.7761	-0.14989	-0.14194	-0.11931	-0.08545	-0.04550	-0.00555	0.02832	0.05094	0.05889
34.5174	-0.15255	-0.14461	-0.12201	-0.08819	-0.04828	-0.00838	0.02545	0.04805	0.05599
35.2587	-0.14441	-0.13647	-0.11387	-0.08003	-0.04012	-0.00020	0.03363	0.05624	0.06419

TANGENTIAL(VT)

THETA(DEG.)	0.0000	22.5000	45.0000	67.5000	90.0000	112.5000	135.0000	157.5000	180.0000
X									
0.0000	-0.00000	-0.02800	-0.05174	-0.06760	-0.07316	-0.06760	-0.05174	-0.02800	-0.00000
0.7243	-0.00000	-0.02800	-0.05174	-0.06760	-0.07316	-0.06760	-0.05174	-0.02800	-0.00000

1.4485	-0.00000	-0.02816	-0.05202	-0.06797	-0.07357	-0.06797	-0.05202	-0.02816	-0.00000
2.1728	-0.00000	-0.03396	-0.06275	-0.08198	-0.08874	-0.08198	-0.06275	-0.03396	-0.00000
2.8970	-0.00000	-0.03384	-0.06252	-0.08169	-0.08842	-0.08169	-0.06252	-0.03384	-0.00000
3.6213	-0.00000	-0.03527	-0.06518	-0.08516	-0.09218	-0.08516	-0.06518	-0.03527	-0.00000
4.3456	-0.00000	-0.03545	-0.06550	-0.08559	-0.09264	-0.08559	-0.06550	-0.03545	-0.00000
5.0698	-0.00000	-0.03615	-0.06680	-0.08728	-0.09447	-0.08728	-0.06680	-0.03615	-0.00000
5.7941	-0.00000	-0.03641	-0.06728	-0.08790	-0.09515	-0.08790	-0.06728	-0.03641	-0.00000
6.5184	-0.00000	-0.03690	-0.06818	-0.08909	-0.09643	-0.08909	-0.06818	-0.03690	-0.00000
7.2426	-0.00000	-0.03718	-0.06870	-0.08976	-0.09716	-0.08976	-0.06870	-0.03718	-0.00000
7.9669	-0.00000	-0.03758	-0.06944	-0.09073	-0.09820	-0.09073	-0.06944	-0.03758	-0.00000
8.6911	-0.00000	-0.03788	-0.06998	-0.09144	-0.09897	-0.09144	-0.06998	-0.03788	-0.00000
9.4154	-0.00000	-0.03822	-0.07063	-0.09228	-0.09988	-0.09228	-0.07063	-0.03822	-0.00000
10.1397	-0.00000	-0.03853	-0.07119	-0.09301	-0.10067	-0.09301	-0.07119	-0.03853	-0.00000
10.8639	-0.00000	-0.03886	-0.07180	-0.09382	-0.10155	-0.09382	-0.07180	-0.03886	-0.00000
11.5882	-0.00000	-0.03920	-0.07244	-0.09465	-0.10245	-0.09465	-0.07244	-0.03920	-0.00000
12.3124	-0.00000	-0.03956	-0.07309	-0.09550	-0.10337	-0.09550	-0.07309	-0.03956	-0.00000
13.0367	-0.00000	-0.03998	-0.07387	-0.09651	-0.10447	-0.09651	-0.07387	-0.03998	-0.00000
13.7610	-0.00000	-0.04034	-0.07454	-0.09739	-0.10542	-0.09739	-0.07454	-0.04034	-0.00000
14.5023	-0.00000	-0.04082	-0.07543	-0.09856	-0.10668	-0.09856	-0.07543	-0.04082	-0.00000
15.2436	-0.00000	-0.04136	-0.07643	-0.09986	-0.10809	-0.09986	-0.07643	-0.04136	-0.00000
15.9849	-0.00000	-0.04229	-0.07814	-0.10210	-0.11051	-0.10210	-0.07814	-0.04229	-0.00000
16.7262	-0.00000	-0.04270	-0.07891	-0.10310	-0.11159	-0.10310	-0.07891	-0.04270	-0.00000
17.4675	-0.00000	-0.04281	-0.07910	-0.10335	-0.11186	-0.10335	-0.07910	-0.04281	-0.00000
18.2088	-0.00000	-0.04269	-0.07889	-0.10307	-0.11156	-0.10307	-0.07889	-0.04269	-0.00000
18.9501	-0.00000	-0.04246	-0.07845	-0.10251	-0.11095	-0.10251	-0.07845	-0.04246	-0.00000
19.6914	-0.00000	-0.04217	-0.07791	-0.10180	-0.11019	-0.10180	-0.07791	-0.04217	-0.00000
20.4327	-0.00000	-0.04186	-0.07735	-0.10106	-0.10939	-0.10106	-0.07735	-0.04186	-0.00000
21.1740	-0.00000	-0.04157	-0.07681	-0.10036	-0.10862	-0.10036	-0.07681	-0.04157	-0.00000
21.9153	-0.00000	-0.04131	-0.07632	-0.09972	-0.10794	-0.09972	-0.07632	-0.04131	-0.00000
22.6566	-0.00000	-0.04108	-0.07591	-0.09918	-0.10735	-0.09918	-0.07591	-0.04108	-0.00000
23.3979	-0.00000	-0.04090	-0.07556	-0.09873	-0.10686	-0.09873	-0.07556	-0.04090	-0.00000
24.1392	-0.00000	-0.04075	-0.07529	-0.09837	-0.10647	-0.09837	-0.07529	-0.04075	-0.00000
24.8805	-0.00000	-0.04063	-0.07507	-0.09808	-0.10616	-0.09808	-0.07507	-0.04063	-0.00000
25.6218	-0.00000	-0.04054	-0.07490	-0.09786	-0.10592	-0.09786	-0.07490	-0.04054	-0.00000
26.3631	-0.00000	-0.04047	-0.07477	-0.09770	-0.10574	-0.09770	-0.07477	-0.04047	-0.00000
27.1044	-0.00000	-0.04041	-0.07468	-0.09757	-0.10561	-0.09757	-0.07468	-0.04041	-0.00000
27.8457	-0.00000	-0.04038	-0.07461	-0.09748	-0.10551	-0.09748	-0.07461	-0.04038	-0.00000
28.5870	-0.00000	-0.04035	-0.07455	-0.09741	-0.10543	-0.09741	-0.07455	-0.04035	-0.00000
29.3283	-0.00000	-0.04032	-0.07451	-0.09735	-0.10537	-0.09735	-0.07451	-0.04032	-0.00000
30.0696	-0.00000	-0.04040	-0.07464	-0.09753	-0.10556	-0.09753	-0.07464	-0.04040	-0.00000
30.8109	-0.00000	-0.04073	-0.07526	-0.09833	-0.10643	-0.09833	-0.07526	-0.04073	-0.00000
31.5522	-0.00000	-0.04125	-0.07623	-0.09960	-0.10780	-0.09960	-0.07623	-0.04125	-0.00000
32.2935	-0.00000	-0.04181	-0.07726	-0.10094	-0.10926	-0.10094	-0.07726	-0.04181	-0.00000
33.0348	-0.00000	-0.04234	-0.07823	-0.10222	-0.11064	-0.10222	-0.07823	-0.04234	-0.00000
33.7761	-0.00000	-0.04294	-0.07935	-0.10367	-0.11222	-0.10367	-0.07935	-0.04294	-0.00000
34.5174	-0.00000	-0.04341	-0.08020	-0.10479	-0.11342	-0.10479	-0.08020	-0.04341	-0.00000
35.2587	-0.00000	-0.04328	-0.07996	-0.10448	-0.11308	-0.10448	-0.07996	-0.04328	-0.00000

VELOCITY COMPONENTS ON WING PANELS DUE TO BODY PANEL PRESSURE SINGULARITIES

AXIAL(U)

SPANWISE STATION	1	2	3	4	5	6	7	8	9	10
CHORDWISE STATION										
1	-0.00162	0.00033	0.00319	0.00195	0.00179	0.00086	-0.00018	0.00012	-0.00147	-0.00103
2	0.00068	0.00436	-0.00288	0.00126	0.00064	-0.00021	0.00003	-0.00133	-0.00112	-0.00249
3	0.00668	0.00803	0.01687	0.00050	-0.00035	-0.00025	-0.00162	-0.00117	-0.00266	-0.00144
4	0.01016	0.00300	0.00032	-0.00016	-0.00074	-0.00242	-0.00129	-0.00277	-0.00135	-0.00108
5	0.00599	0.00136	0.00048	0.00014	-0.00340	-0.00137	-0.00320	-0.00152	-0.00022	-0.00010
6	0.00375	0.00145	-0.00081	-0.00025	-0.00154	-0.00455	-0.00167	-0.00010	-0.00057	-0.00043
7	0.00377	-0.00045	0.00004	-0.00183	-0.00132	-0.00190	-0.00049	-0.00051	0.00049	0.00029
8	0.00073	0.00037	-0.00257	-0.00141	-0.00223	-0.00043	-0.00056	0.00046	0.00030	0.00049
9	0.00132	-0.00295	-0.00115	-0.00266	-0.00029	-0.00063	0.00070	0.00031	0.00002	0.00018
10	-0.00389	-0.00248	-0.00159	0.00019	-0.00079	0.00097	0.00030	0.00001	0.00004	0.00019

TRANSVERSE(V)

SPANWISE STATION	1	2	3	4	5	6	7	8	9	10
CHORDWISE STATION										
1	0.00452	0.00007	-0.00488	-0.00352	-0.00343	-0.00199	-0.00031	-0.00064	0.00189	0.00139
2	0.00072	-0.00673	0.00337	-0.00292	-0.00189	-0.00047	-0.00063	0.00159	0.00144	0.00363
3	-0.01002	-0.01350	-0.02684	-0.00210	-0.00056	-0.00042	0.00188	0.00144	0.00385	0.00213
4	-0.01793	-0.00745	-0.00264	-0.00136	-0.00001	0.00287	0.00151	0.00395	0.00201	0.00164
5	-0.01586	-0.00620	-0.00337	-0.00189	0.00397	0.00145	0.00449	0.00223	0.00035	0.00019
6	-0.01600	-0.00743	-0.00166	-0.00135	0.00140	0.00633	0.00240	0.00016	0.00091	0.00069
7	-0.01924	-0.00529	-0.00306	0.00127	0.00123	0.00264	0.00072	0.00083	-0.00069	-0.00037
8	-0.01760	-0.00690	0.00113	0.00089	0.00294	0.00056	0.00087	-0.00066	-0.00042	-0.00070
9	-0.02023	-0.00169	-0.00059	0.00317	0.00023	0.00095	-0.00101	-0.00044	-0.00001	-0.00024
10	-0.01337	-0.00168	0.00062	-0.00076	0.00109	-0.00144	-0.00042	-0.00001	-0.00004	-0.00027

VERTICAL(W)

SPANWISE STATION	1	2	3	4	5	6	7	8	9	10
CHORDWISE STATION										
1	0.02600	0.01023	0.00683	0.00500	0.00497	0.00480	0.00443	0.00422	0.00386	0.00348
2	0.04572	0.01432	0.00763	0.00682	0.00627	0.00554	0.00511	0.00457	0.00424	0.00351
3	0.06508	0.01802	0.01118	0.00880	0.00727	0.00638	0.00556	0.00503	0.00437	0.00368
4	0.08566	0.02214	0.01399	0.01025	0.00844	0.00693	0.00609	0.00522	0.00472	0.00385
5	0.10355	0.02870	0.01633	0.01187	0.00936	0.00766	0.00639	0.00557	0.00487	0.00393
6	0.12660	0.03353	0.01868	0.01328	0.01007	0.00813	0.00680	0.00586	0.00487	0.00391
7	0.14709	0.03801	0.02102	0.01421	0.01096	0.00857	0.00718	0.00584	0.00500	0.00402
8	0.16568	0.04265	0.02247	0.01548	0.01130	0.00907	0.00720	0.00597	0.00502	0.00400
9	0.18273	0.04543	0.02449	0.01594	0.01201	0.00916	0.00737	0.00605	0.00488	0.00400
10	0.19324	0.04899	0.02524	0.01706	0.01215	0.00942	0.00747	0.00591	0.00484	0.00401

VELOCITY COMPONENTS ON WING PANELS DUE TO BODY LINE SOURCES AND DOUBLETS

AXIAL(U)

SPANWISE STATION	1	2	3	4	5	6	7	8	9	10
CHORDWISE STATION										
1	0.01160	0.01127	0.00687	0.00506	0.00392	0.00304	0.00243	0.00199	0.00165	0.00136
2	0.01424	0.00795	0.00583	0.00439	0.00335	0.00265	0.00214	0.00177	0.00148	0.00127
3	0.00970	0.00699	0.00502	0.00374	0.00291	0.00233	0.00190	0.00158	0.00134	0.00119
4	0.00877	0.00588	0.00425	0.00324	0.00255	0.00206	0.00170	0.00143	0.00122	0.00112
5	0.00718	0.00496	0.00368	0.00283	0.00226	0.00184	0.00153	0.00130	0.00111	0.00105
6	0.00604	0.00427	0.00320	0.00250	0.00201	0.00165	0.00139	0.00118	0.00102	0.00100
7	0.00516	0.00369	0.00280	0.00221	0.00180	0.00150	0.00126	0.00109	0.00097	0.00093
8	0.00442	0.00321	0.00247	0.00198	0.00162	0.00136	0.00116	0.00101	0.00191	0.00090
9	0.00382	0.00282	0.00220	0.00178	0.00147	0.00125	0.00106	0.00178	0.00403	0.00117
10	0.00333	0.00250	0.00197	0.00161	0.00135	0.00112	0.00167	0.00397	0.00543	0.00220

TRANSVERSE(V)

SPANWISE STATION	1	2	3	4	5	6	7	8	9	10
CHORDWISE STATION										
1	0.00943	-0.00701	-0.00546	-0.00487	-0.00423	-0.00351	-0.00296	-0.00253	-0.00219	-0.00185
2	0.00100	-0.00408	-0.00502	-0.00454	-0.00380	-0.00322	-0.00274	-0.00236	-0.00205	-0.00178
3	0.00407	-0.00436	-0.00473	-0.00412	-0.00352	-0.00300	-0.00257	-0.00223	-0.00195	-0.00172
4	0.00249	-0.00411	-0.00438	-0.00388	-0.00332	-0.00283	-0.00244	-0.00212	-0.00186	-0.00167
5	0.00235	-0.00396	-0.00421	-0.00370	-0.00316	-0.00271	-0.00234	-0.00204	-0.00179	-0.00162
6	0.00187	-0.00399	-0.00410	-0.00358	-0.00305	-0.00261	-0.00226	-0.00197	-0.00174	-0.00159
7	0.00128	-0.00404	-0.00404	-0.00350	-0.00298	-0.00255	-0.00220	-0.00193	-0.00175	-0.00153
8	0.00072	-0.00414	-0.00403	-0.00345	-0.00293	-0.00250	-0.00217	-0.00191	-0.00325	-0.00153
9	0.00014	-0.00428	-0.00405	-0.00344	-0.00290	-0.00248	-0.00213	-0.00317	-0.00662	-0.00198
10	-0.00045	-0.00445	-0.00410	-0.00344	-0.00290	-0.00242	-0.00316	-0.00665	-0.00900	-0.00358

VERTICAL(W)

SPANWISE STATION	1	2	3	4	5	6	7	8	9	10
CHORDWISE STATION										
1	0.06109	0.02978	0.01711	0.01098	0.00755	0.00546	0.00412	0.00321	0.00258	0.00199
2	0.06317	0.02928	0.01671	0.01066	0.00731	0.00530	0.00401	0.00314	0.00253	0.00197
3	0.06277	0.02888	0.01630	0.01035	0.00712	0.00518	0.00393	0.00309	0.00250	0.00195
4	0.06264	0.02835	0.01591	0.01011	0.00696	0.00508	0.00387	0.00305	0.00247	0.00194
5	0.06200	0.02783	0.01559	0.00991	0.00684	0.00501	0.00383	0.00302	0.00245	0.00192
6	0.06133	0.02739	0.01533	0.00976	0.00675	0.00495	0.00379	0.00300	0.00244	0.00191
7	0.06071	0.02703	0.01513	0.00964	0.00668	0.00491	0.00377	0.00298	0.00242	0.00190
8	0.06017	0.02675	0.01498	0.00956	0.00663	0.00488	0.00374	0.00297	0.00246	0.00190
9	0.05976	0.02654	0.01487	0.00950	0.00660	0.00486	0.00373	0.00300	0.00253	0.00190
10	0.05946	0.02640	0.01480	0.00946	0.00657	0.00484	0.00375	0.00309	0.00253	0.00194

VELOCITY COMPONENTS ON WING PANELS DUE TO WING PANEL PRESSURE SINGULARITIES

AXIAL(U)

SPANWISE STATION	1	2	3	4	5	6	7	8	9	10
CHORDWISE STATION										
1	0.08732	0.10456	0.11606	0.12644	0.13618	0.14457	0.15156	0.15736	0.16407	0.26144
2	0.05305	0.06110	0.06789	0.07433	0.07938	0.08339	0.08656	0.08917	0.09606	0.14600
3	0.04340	0.04878	0.05427	0.05829	0.06115	0.06323	0.06459	0.06645	0.08025	0.10417
4	0.03934	0.04306	0.04699	0.04930	0.05076	0.05134	0.05181	0.05411	0.06970	0.07089
5	0.03654	0.03994	0.04170	0.04271	0.04275	0.04248	0.04273	0.04651	0.05846	0.05362
6	0.03577	0.03666	0.03711	0.03667	0.03569	0.03518	0.03573	0.04122	0.04655	0.04124
7	0.03397	0.03334	0.03223	0.03049	0.02937	0.02891	0.02994	0.03709	0.03512	0.03063
8	0.03129	0.02890	0.02609	0.02425	0.02322	0.02304	0.02463	0.03113	0.02443	0.02002
9	0.02686	0.02207	0.01923	0.01770	0.01712	0.01701	0.01929	0.02306	0.01460	0.00915
10	0.01781	0.01315	0.01120	0.01059	0.01008	0.01026	0.01238	0.01301	0.00618	-0.00418

TRANSVERSE(V)

SPANWISE STATION	1	2	3	4	5	6	7	8	9	10
CHORDWISE STATION										
1	-0.23989	-0.28726	-0.31885	-0.34737	-0.37414	-0.39718	-0.41638	-0.43232	-0.45077	-0.71827
2	-0.14575	-0.16786	-0.18652	-0.20420	-0.21809	-0.22911	-0.23781	-0.24497	-0.26392	-0.45010
3	-0.11923	-0.13401	-0.14909	-0.16013	-0.16799	-0.17372	-0.17744	-0.18255	-0.22059	-0.37067
4	-0.10808	-0.11830	-0.12910	-0.13545	-0.13944	-0.14104	-0.14235	-0.14864	-0.19149	-0.32161
5	-0.10039	-0.10973	-0.11455	-0.11734	-0.11746	-0.11669	-0.11738	-0.12778	-0.16061	-0.30347
6	-0.09827	-0.10073	-0.10196	-0.10073	-0.09806	-0.09666	-0.09815	-0.11325	-0.12787	-0.29573
7	-0.09333	-0.09159	-0.08854	-0.08375	-0.08067	-0.07942	-0.08226	-0.10190	-0.09647	-0.29359
8	-0.08597	-0.07941	-0.07169	-0.06662	-0.06378	-0.06329	-0.06765	-0.08552	-0.06710	-0.25596
9	-0.07380	-0.06062	-0.05282	-0.04861	-0.04703	-0.04672	-0.05297	-0.06335	-0.04011	-0.30300
10	-0.04893	-0.03611	-0.03076	-0.02908	-0.02769	-0.02819	-0.03399	-0.03573	-0.01696	-0.31729

VERTICAL(W)

SPANWISE STATION	1	2	3	4	5	6	7	8	9	10
CHORDWISE STATION										
1	-0.19182	-0.14473	-0.12866	-0.12070	-0.11725	-0.11498	-0.11327	-0.11215	-0.11116	-0.11018
2	-0.21361	-0.14832	-0.12906	-0.12220	-0.11830	-0.11557	-0.11385	-0.11243	-0.11150	-0.11019
3	-0.23257	-0.15162	-0.13220	-0.12387	-0.11910	-0.11628	-0.11421	-0.11284	-0.11159	-0.11035
4	-0.25302	-0.15521	-0.13462	-0.12508	-0.12012	-0.11673	-0.11469	-0.11300	-0.11191	-0.11050
5	-0.27027	-0.16125	-0.13664	-0.12650	-0.12092	-0.11738	-0.11494	-0.11331	-0.11204	-0.11057
6	-0.29265	-0.16564	-0.13873	-0.12775	-0.12154	-0.11780	-0.11531	-0.11358	-0.11202	-0.11054
7	-0.31251	-0.16975	-0.14087	-0.12857	-0.12236	-0.11820	-0.11567	-0.11354	-0.11214	-0.11065
8	-0.33057	-0.17412	-0.14216	-0.12976	-0.12266	-0.11867	-0.11566	-0.11366	-0.11219	-0.11061
9	-0.34721	-0.17669	-0.14408	-0.13015	-0.12333	-0.11873	-0.11582	-0.11377	-0.11213	-0.11062
10	-0.35742	-0.18011	-0.14475	-0.13124	-0.12344	-0.11897	-0.11594	-0.11371	-0.11209	-0.11066

VELOCITY COMPONENTS ON WING PANELS DUE TO WING SOURCES

AXIAL(U)

SPANWISE STATION	1	2	3	4	5	6	7	8	9	10
CHORDWISE STATION										
1	-0.01440	-0.00890	-0.00478	-0.00453	0.00006	0.00447	0.00827	0.01187	0.01396	0.02115
2	-0.00055	0.00571	0.00660	0.01170	0.01665	0.02079	0.02464	0.02833	0.02461	0.03324
3	0.00248	0.00525	0.01117	0.01686	0.02146	0.02562	0.02955	0.02611	0.02751	0.03262
4	0.00111	0.00890	0.01577	0.02102	0.02559	0.02983	0.02670	0.02599	0.03168	0.03260
5	0.00358	0.01288	0.01916	0.02431	0.02894	0.02619	0.02523	0.02511	0.03137	0.03163
6	0.00683	0.01516	0.02120	0.02638	0.02410	0.02278	0.02257	0.02200	0.02799	0.03005
7	0.00794	0.01569	0.02170	0.02003	0.01817	0.01782	0.01753	0.01797	0.02221	0.02576
8	0.00975	0.01734	0.01654	0.01377	0.01324	0.01324	0.01153	0.01510	0.01631	0.01904
9	0.01198	0.01277	0.00819	0.00736	0.00726	0.00553	0.00486	0.00956	0.00830	0.01327
10	0.00776	-0.00238	-0.00373	-0.00400	-0.00576	-0.00654	-0.00698	-0.00204	-0.00606	0.00818

TRANSVERSE(V)

SPANWISE STATION	1	2	3	4	5	6	7	8	9	10
CHORDWISE STATION										
1	-0.00990	-0.00165	-0.00346	-0.00193	-0.00797	-0.01444	-0.02038	-0.02624	-0.02998	-0.03721
2	-0.03844	-0.03647	-0.03468	-0.04112	-0.04835	-0.05488	-0.06121	-0.06746	-0.06239	-0.07989
3	-0.03705	-0.03405	-0.04107	-0.04940	-0.05674	-0.06370	-0.07048	-0.06598	-0.06220	-0.08955
4	-0.02826	-0.03662	-0.04681	-0.05540	-0.06325	-0.07074	-0.06693	-0.06631	-0.05424	-0.09852
5	-0.02383	-0.03892	-0.04981	-0.05906	-0.06754	-0.06463	-0.06377	-0.06398	-0.04508	-0.10480
6	-0.01972	-0.03741	-0.04929	-0.05935	-0.05767	-0.05646	-0.05663	-0.05614	-0.03320	-0.10924
7	-0.01147	-0.03144	-0.04452	-0.04472	-0.04303	-0.04314	-0.04314	-0.03854	-0.01699	-0.11148
8	-0.00613	-0.02862	-0.03235	-0.02989	-0.02994	-0.03049	-0.02825	-0.02017	-0.00217	-0.11186
9	-0.00225	-0.01687	-0.01301	-0.01300	-0.01356	-0.01139	-0.01062	-0.00006	0.01456	-0.11281
10	0.01124	0.01859	0.01863	0.01804	0.02012	0.02100	0.02147	0.03342	0.04341	-0.11386

VERTICAL(W)

SPANWISE STATION	1	2	3	4	5	6	7	8	9	10
CHORDWISE STATION										
1	0.12128	0.12101	0.12101	0.12101	0.12101	0.12101	0.12101	0.12101	0.12101	0.12101
2	0.05126	0.05124	0.05124	0.05124	0.05124	0.05124	0.05124	0.05124	0.05124	0.05124
3	0.02572	0.02572	0.02572	0.02572	0.02572	0.02572	0.02572	0.02572	0.02572	0.02572
4	0.00823	0.00823	0.00823	0.00823	0.00823	0.00823	0.00823	0.00823	0.00823	0.00823
5	-0.00756	-0.00756	-0.00756	-0.00756	-0.00756	-0.00756	-0.00756	-0.00756	-0.00756	-0.00756
6	-0.02223	-0.02223	-0.02223	-0.02223	-0.02223	-0.02223	-0.02223	-0.02223	-0.02223	-0.02223
7	-0.03307	-0.03307	-0.03307	-0.03307	-0.03307	-0.03307	-0.03307	-0.03307	-0.03307	-0.03307
8	-0.04051	-0.04051	-0.04051	-0.04051	-0.04051	-0.04051	-0.04051	-0.04051	-0.04051	-0.04051
9	-0.04775	-0.04775	-0.04775	-0.04775	-0.04775	-0.04775	-0.04775	-0.04775	-0.04775	-0.04775
10	-0.05507	-0.05507	-0.05507	-0.05507	-0.05507	-0.05507	-0.05507	-0.05507	-0.05507	-0.05507

VELOCITY COMPONENTS ON BODY PANELS DUE TO BODY PANEL PRESSURE SINGULARITIES

AXIAL(U)

THETA(DEG.)	12.5000	37.5000	62.5000	88.7967	116.0950	142.5000	167.5000
ROW NO.							
1	0.00000	0.00001	0.00003	0.00157	-0.00919	-0.00091	-0.00028
2	0.00002	0.00056	0.00188	0.01869	-0.02887	-0.00287	-0.00078
3	0.00191	0.00112	0.00864	0.01959	-0.02301	-0.01412	0.00458
4	0.00373	0.00749	0.01312	0.02432	-0.01624	-0.00639	-0.00849
5	0.00523	0.01032	0.01549	0.02487	-0.01378	-0.01207	-0.01398
6	0.00696	0.01067	0.01737	0.02352	-0.01513	-0.01649	-0.01586
7	0.00877	0.01164	0.01605	0.02275	-0.01654	-0.01731	-0.01767
8	0.01063	0.01159	0.01500	0.01999	-0.01666	-0.01814	-0.01809
9	0.01071	0.01195	0.01474	0.01773	-0.01679	-0.01854	-0.01922
10	0.01056	0.01213	0.01421	0.01525	-0.01567	-0.01862	-0.01935
11	0.01035	0.01055	0.00945	0.00297	-0.01311	-0.01619	-0.01871
12	0.01334	0.01075	0.00494	-0.00197	-0.00752	-0.01062	-0.01215
13	0.00813	0.00693	0.00446	0.00076	-0.00331	-0.00647	-0.00830
14	0.00461	0.00385	0.00233	0.00020	-0.00187	-0.00345	-0.00420

TRANSVERSE(V)

THETA(DEG.)	12.5000	37.5000	62.5000	88.7967	116.0950	142.5000	167.5000
ROW NO.							
1	-0.00000	-0.00001	-0.00003	-0.00521	0.01925	0.00148	0.00031
2	-0.00009	0.00008	-0.00118	-0.05481	0.07330	0.00122	0.00056
3	0.00044	-0.00210	-0.00471	-0.10807	0.11521	0.00488	0.00131
4	0.00331	-0.00296	-0.01780	-0.16279	0.14329	0.00404	-0.00525
5	-0.00174	-0.00432	-0.02897	-0.21270	0.17291	0.01354	-0.00131
6	-0.00240	-0.00904	-0.03908	-0.25731	0.20434	0.02431	0.00161
7	-0.00029	-0.00843	-0.04989	-0.30072	0.23366	0.03397	0.00426
8	-0.00153	-0.01098	-0.05969	-0.34145	0.26137	0.04130	0.00616
9	-0.00110	-0.01406	-0.07121	-0.37870	0.28729	0.04935	0.00878
10	-0.00234	-0.01697	-0.08082	-0.41038	0.31072	0.05880	0.01132
11	-0.00348	-0.02339	-0.10177	-0.42632	0.34123	0.07418	0.01615
12	-0.00473	-0.03467	-0.11093	-0.42296	0.35369	0.08204	0.01914
13	-0.01162	-0.04556	-0.12061	-0.42403	0.35963	0.08715	0.02117
14	-0.01477	-0.05331	-0.12793	-0.41451	0.33443	0.09281	0.02409

VERTICAL(W)

THETA(DEG.)	12.5000	37.5000	62.5000	88.7967	116.0950	142.5000	167.5000
ROW NO.							
1	0.00000	0.00001	0.00006	-0.00213	-0.01003	0.00113	0.00007
2	0.00002	-0.00006	0.00125	-0.00855	-0.04184	0.00623	0.00012
3	-0.00219	0.00171	-0.00367	-0.01227	-0.06819	-0.00686	0.01779
4	-0.00479	-0.00548	-0.00755	-0.01936	-0.08609	-0.01059	0.01144
5	-0.00354	-0.00732	-0.01313	-0.02283	-0.11022	-0.02062	0.00304
6	-0.00345	-0.00699	-0.01917	-0.03152	-0.12748	-0.03102	-0.00627
7	-0.00326	-0.01152	-0.02348	-0.03383	-0.14559	-0.04199	-0.01653
8	-0.00336	-0.01297	-0.02918	-0.03847	-0.16383	-0.05429	-0.02787
9	-0.00385	-0.01515	-0.03303	-0.04296	-0.18209	-0.06643	-0.03913
10	-0.00470	-0.01825	-0.03925	-0.04693	-0.19559	-0.07714	-0.05016
11	-0.00935	-0.02579	-0.04836	-0.04945	-0.21321	-0.09522	-0.07308
12	-0.02873	-0.04211	-0.05572	-0.05151	-0.21987	-0.10650	-0.08339
13	-0.04257	-0.05078	-0.05825	-0.05078	-0.22382	-0.11472	-0.09328
14	-0.05510	-0.06010	-0.06551	-0.10674	-0.27143	-0.12654	-0.10579

VELOCITY COMPONENTS ON BODY PANELS DUE TO WING PANEL PRESSURE SINGULARITIES

AXIAL(U)

THETA(DEG.)	12.5000	37.5000	62.5000	88.7967	116.0950	142.5000	167.5000
ROW NO.							
1	0.00000	0.00000	0.00000	0.02154	-0.01471	0.00000	0.00000
2	0.00000	0.00000	0.01393	0.02308	-0.01590	-0.00937	0.00000
3	0.00454	0.01110	0.01518	0.02052	-0.01437	-0.01009	-0.00946
4	0.01258	0.01354	0.01606	0.01941	-0.01385	-0.01222	-0.01087
5	0.01335	0.01452	0.01760	0.01905	-0.01381	-0.01248	-0.01105
6	0.01364	0.01566	0.01750	0.01843	-0.01340	-0.01270	-0.01150
7	0.01503	0.01566	0.01727	0.01776	-0.01294	-0.01259	-0.01205
8	0.01532	0.01609	0.01711	0.01697	-0.01241	-0.01267	-0.01210
9	0.01532	0.01608	0.01701	0.01554	-0.01148	-0.01249	-0.01198
10	0.01535	0.01601	0.01597	0.01257	-0.00943	-0.01188	-0.01191
11	0.01418	0.01368	0.00993	0.00407	-0.00350	-0.00777	-0.01012
12	0.00871	0.00769	0.00552	0.00211	-0.00184	-0.00441	-0.00560
13	0.00528	0.00477	0.00340	0.00125	-0.00112	-0.00275	-0.00344
14	0.00355	0.00308	0.00221	0.00082	-0.00069	-0.00176	-0.00223

TRANSVERSE(V)

THETA(DEG.)	12.5000	37.5000	62.5000	88.7967	116.0950	142.5000	167.5000
ROW NO.							
1	-0.00000	-0.00000	-0.00000	0.01798	-0.02638	-0.00000	-0.00000
2	-0.00000	-0.00000	0.00908	0.08085	-0.08420	-0.01327	-0.00000
3	0.00427	0.01092	0.02426	0.13477	-0.13002	-0.02688	-0.00794
4	0.00369	0.01478	0.03772	0.18068	-0.16866	-0.03529	-0.00885
5	0.00533	0.01932	0.05093	0.22301	-0.20511	-0.04562	-0.01128
6	0.00693	0.02601	0.06438	0.26230	-0.23910	-0.05609	-0.01438
7	0.00936	0.03194	0.07701	0.30003	-0.27176	-0.06567	-0.01677
8	0.01064	0.03700	0.08876	0.33579	-0.30245	-0.07429	-0.01921
9	0.01220	0.04244	0.10065	0.36870	-0.33054	-0.08305	-0.02155
10	0.01396	0.04794	0.11116	0.39634	-0.35328	-0.09084	-0.02409
11	0.01618	0.05561	0.12538	0.41924	-0.36915	-0.09909	-0.02697
12	0.01743	0.05845	0.12986	0.42185	-0.37102	-0.10161	-0.02736
13	0.01805	0.06060	0.13251	0.42305	-0.37197	-0.10303	-0.02786
14	0.01852	0.06170	0.13402	0.41394	-0.34083	-0.10142	-0.02778

VERTICAL(W)

THETA(DEG.)	12.5000	37.5000	62.5000	88.7967	116.0950	142.5000	167.5000
ROW NO.							
1	-0.00000	-0.00000	-0.00000	-0.04313	-0.01954	-0.00000	-0.00000
2	-0.00000	-0.00000	-0.02331	-0.07136	-0.01458	-0.01075	-0.00000
3	-0.00562	-0.01629	-0.03031	-0.07704	0.00066	-0.00865	-0.00699
4	-0.01324	-0.01841	-0.03371	-0.07878	0.01676	-0.00428	-0.00220
5	-0.01162	-0.01748	-0.03440	-0.07607	0.03537	0.00300	0.00425
6	-0.00905	-0.01608	-0.03214	-0.07253	0.05426	0.01135	0.01091
7	-0.00692	-0.01290	-0.02928	-0.06870	0.07291	0.02016	0.01830
8	-0.00320	-0.00961	-0.02588	-0.06384	0.09159	0.02934	0.02636
9	0.00093	-0.00559	-0.02162	-0.05656	0.11093	0.03889	0.03463
10	0.00529	-0.00105	-0.01589	-0.04552	0.13085	0.04902	0.04299
11	0.01630	0.01148	0.00347	-0.01032	0.16733	0.07186	0.06131
12	0.03157	0.02874	0.02157	0.01030	0.18712	0.08932	0.07833
13	0.04344	0.04094	0.03474	0.02463	0.20099	0.10194	0.09036
14	0.05538	0.05435	0.05307	0.09444	0.25970	0.11978	0.10431

VELOCITY COMPONENTS ON BODY PANELS DUE TO WING SOURCES

AXIAL(U)

THETA(DEG.)	12.5000	37.5000	62.5000	88.7967	116.0950	142.5000	167.5000
ROW NO.							
1	-0.00000	-0.00000	-0.00000	-0.01746	-0.01483	-0.00000	-0.00000
2	-0.00000	-0.00000	-0.01181	-0.01010	-0.00962	-0.01002	-0.00000
3	-0.00625	-0.00872	-0.00864	-0.00561	-0.00578	-0.00773	-0.01313
4	-0.01331	-0.01218	-0.00975	-0.00643	-0.00803	-0.01140	-0.01228
5	-0.01091	-0.01024	-0.00846	-0.00500	-0.00560	-0.00845	-0.00946
6	-0.00818	-0.00731	-0.00524	-0.00167	-0.00228	-0.00529	-0.00652
7	-0.00529	-0.00424	-0.00194	0.00138	0.00079	-0.00206	-0.00341
8	-0.00221	-0.00106	0.00113	0.00388	0.00338	0.00102	-0.00019
9	0.00093	0.00191	0.00385	0.00637	0.00593	0.00380	0.00280
10	0.00364	0.00460	0.00647	0.00888	0.00845	0.00635	0.00531
11	0.00839	0.00937	0.00517	0.00283	0.00350	0.00597	0.00956
12	0.00375	0.00358	0.00314	0.00253	0.00244	0.00273	0.00289
13	0.00145	0.00132	0.00109	0.00088	0.00091	0.00108	0.00119
14	0.00066	0.00060	0.00050	0.00043	0.00044	0.00051	0.00056

TRANSVERSE(V)

THETA(DEG.)	12.5000	37.5000	62.5000	88.7967	116.0950	142.5000	167.5000
ROW NO.							
1	-0.00000	-0.00000	-0.00000	-0.01254	-0.01880	-0.00000	-0.00000
2	-0.00000	-0.00000	-0.00686	-0.02478	-0.02598	-0.01151	-0.00000
3	-0.00552	-0.00751	-0.01104	-0.02496	-0.02455	-0.01352	-0.00318
4	-0.00003	-0.00175	-0.00658	-0.01576	-0.01283	-0.00401	-0.00102
5	-0.00004	-0.00082	-0.00351	-0.00800	-0.00639	-0.00269	-0.00069
6	-0.00006	-0.00063	-0.00233	-0.00239	-0.00071	-0.00114	-0.00030
7	0.00004	-0.00016	-0.00072	0.00340	0.00499	0.00073	0.00020
8	0.00020	0.00049	0.00107	0.00848	0.00980	0.00254	0.00072
9	0.00036	0.00104	0.00267	0.01285	0.01394	0.00392	0.00103
10	0.00042	0.00147	0.00409	0.01681	0.01778	0.00526	0.00139
11	0.00080	0.00288	0.00416	0.00863	0.00687	0.00276	0.00228
12	-0.00007	0.00004	0.00089	0.00215	0.00175	0.00082	0.00020
13	0.00015	0.00056	0.00115	0.00163	0.00123	0.00075	0.00023
14	0.00013	0.00041	0.00072	0.00086	0.00058	0.00044	0.00015

VERTICAL(W)

THETA(DEG.)	12.5000	37.5000	62.5000	88.7967	116.0950	142.5000	167.5000
ROW NO.							
1	-0.00000	-0.00000	-0.00000	0.03411	-0.02338	-0.00000	-0.00000
2	-0.00000	-0.00000	0.02006	0.02711	-0.01888	-0.01357	-0.00000
3	0.00799	0.01358	0.01761	0.01797	-0.01283	-0.01175	-0.01298
4	0.01648	0.01616	0.01563	0.01123	-0.00866	-0.01719	-0.01259
5	0.01438	0.01391	0.01207	0.00463	-0.00395	-0.00906	-0.01024
6	0.01150	0.01044	0.00718	-0.00210	0.00081	-0.00559	-0.00754
7	0.00817	0.00650	0.00204	-0.00809	0.00509	-0.00193	-0.00450
8	0.00439	0.00223	-0.00283	-0.01259	0.00836	0.00159	-0.00122
9	0.00038	-0.00183	-0.00704	-0.01662	0.01132	0.00469	0.00190
10	-0.00326	-0.00559	-0.01098	-0.02050	0.01416	0.00757	0.00464
11	-0.00895	-0.01261	-0.00845	-0.00371	0.00291	0.00636	0.00988
12	-0.00519	-0.00492	-0.00393	-0.00118	0.00096	0.00280	0.00329
13	-0.00233	-0.00212	-0.00154	-0.00017	0.00014	0.00117	0.00149
14	-0.00114	-0.00100	-0.00064	0.00017	-0.00015	0.00049	0.00069

PRESSURES, FORCES, AND MOMENTS ON ISOLATED BODY

CD = 0.00130 CL = 0.00399 CM = 0.00291

BODY PRESSURE COEFFICIENTS(CP)

THETA(DEG.) / X	0.0000	22.5000	45.0000	67.5000	90.0000	112.5000	135.0000	157.5000	180.0000
0.0000	0.06332	0.06803	0.08146	0.10156	0.12527	0.14897	0.16907	0.18250	0.18722
0.7243	0.06892	0.07363	0.08706	0.10716	0.13087	0.15458	0.17468	0.18810	0.19282
1.4485	0.03372	0.03851	0.05217	0.07261	0.09672	0.12083	0.14127	0.15492	0.15972
2.1728	0.00738	0.01100	0.02132	0.03676	0.05497	0.07319	0.08863	0.09894	0.10257
2.8970	0.01318	0.01663	0.02645	0.04115	0.05849	0.07583	0.09054	0.10036	0.10381
3.6213	0.00395	0.00705	0.01586	0.02905	0.04461	0.06017	0.07336	0.08217	0.08527
4.3456	0.00386	0.00683	0.01528	0.02792	0.04284	0.05776	0.07041	0.07886	0.08182
5.0698	-0.00053	0.00223	0.01011	0.02190	0.03580	0.04970	0.06149	0.06937	0.07213
5.7941	-0.00174	0.00091	0.00846	0.01975	0.03307	0.04639	0.05768	0.06523	0.06788
6.5184	-0.00478	-0.00228	0.00482	0.01546	0.02800	0.04055	0.05118	0.05829	0.06078
7.2426	-0.00610	-0.00372	0.00307	0.01322	0.02520	0.03717	0.04733	0.05411	0.05649
7.9669	-0.00869	-0.00644	-0.00004	0.00953	0.02083	0.03213	0.04170	0.04810	0.05035
8.6911	-0.00988	-0.00775	-0.00168	0.00741	0.01812	0.02884	0.03792	0.04359	0.04612
9.4154	-0.01211	-0.01011	-0.00440	0.00415	0.01423	0.02431	0.03286	0.03857	0.04057
10.1397	-0.01341	-0.01153	-0.00616	0.00188	0.01136	0.02084	0.02888	0.03425	0.03613
10.8639	-0.01601	-0.01425	-0.00924	-0.00175	0.00709	0.01594	0.02343	0.02844	0.03020
11.5882	-0.01743	-0.01581	-0.01118	-0.00426	0.00391	0.01208	0.01900	0.02363	0.02525
12.3124	-0.02077	-0.01928	-0.01505	-0.00872	-0.00125	0.00622	0.01255	0.01678	0.01827
13.0367	-0.02210	-0.02078	-0.01701	-0.01138	-0.00473	0.00192	0.00756	0.01132	0.01265
13.7610	-0.02476	-0.02360	-0.02028	-0.01530	-0.00944	-0.00358	0.00139	0.00471	0.00588
14.5023	-0.02727	-0.02630	-0.02353	-0.01939	-0.01451	-0.00963	-0.00549	-0.00273	-0.00175
15.2436	-0.03820	-0.03744	-0.03531	-0.03211	-0.02833	-0.02456	-0.02136	-0.01922	-0.01847
15.9849	-0.03942	-0.03902	-0.03787	-0.03616	-0.03414	-0.03212	-0.03041	-0.02926	-0.02886
16.7262	-0.02689	-0.02674	-0.02631	-0.02565	-0.02488	-0.02412	-0.02346	-0.02303	-0.02288
17.4675	-0.02161	-0.02163	-0.02167	-0.02174	-0.02182	-0.02189	-0.02196	-0.02200	-0.02202
18.2088	-0.01660	-0.01672	-0.01705	-0.01756	-0.01815	-0.01874	-0.01925	-0.01958	-0.01970
18.9501	-0.01334	-0.01351	-0.01400	-0.01474	-0.01561	-0.01648	-0.01721	-0.01771	-0.01788
19.6914	-0.01089	-0.01108	-0.01163	-0.01246	-0.01343	-0.01441	-0.01523	-0.01578	-0.01598
20.4327	-0.00917	-0.00936	-0.00991	-0.01073	-0.01169	-0.01266	-0.01348	-0.01402	-0.01422
21.1740	-0.00792	-0.00810	-0.00860	-0.00936	-0.01025	-0.01113	-0.01189	-0.01239	-0.01257
21.9153	-0.00701	-0.00716	-0.00760	-0.00826	-0.00904	-0.00982	-0.01048	-0.01092	-0.01108
22.6566	-0.00632	-0.00645	-0.00682	-0.00738	-0.00803	-0.00869	-0.00924	-0.00962	-0.00975
23.3979	-0.00578	-0.00588	-0.00619	-0.00664	-0.00718	-0.00771	-0.00816	-0.00847	-0.00857
24.1392	-0.00533	-0.00542	-0.00566	-0.00602	-0.00645	-0.00687	-0.00723	-0.00747	-0.00756
24.8805	-0.00495	-0.00502	-0.00521	-0.00549	-0.00582	-0.00615	-0.00643	-0.00662	-0.00668
25.6218	-0.00462	-0.00467	-0.00481	-0.00502	-0.00528	-0.00553	-0.00574	-0.00589	-0.00594
26.3631	-0.00431	-0.00435	-0.00446	-0.00462	-0.00481	-0.00500	-0.00516	-0.00527	-0.00531
27.1044	-0.00402	-0.00404	-0.00412	-0.00424	-0.00439	-0.00453	-0.00465	-0.00473	-0.00476
27.8457	-0.00379	-0.00381	-0.00387	-0.00396	-0.00407	-0.00417	-0.00426	-0.00432	-0.00434
28.5870	-0.00339	-0.00340	-0.00345	-0.00352	-0.00360	-0.00368	-0.00375	-0.00379	-0.00381
29.3283	-0.00371	-0.00372	-0.00376	-0.00381	-0.00387	-0.00393	-0.00399	-0.00402	-0.00403
30.0696	-0.00881	-0.00885	-0.00895	-0.00910	-0.00928	-0.00946	-0.00961	-0.00971	-0.00974
30.8109	-0.01632	-0.01646	-0.01687	-0.01747	-0.01817	-0.01888	-0.01948	-0.01988	-0.02002
31.5522	-0.02026	-0.02059	-0.02151	-0.02289	-0.02451	-0.02614	-0.02752	-0.02844	-0.02876
32.2935	-0.02060	-0.02115	-0.02271	-0.02505	-0.02781	-0.03057	-0.03291	-0.03447	-0.03502
33.0348	-0.02260	-0.02341	-0.02569	-0.02912	-0.03315	-0.03719	-0.04062	-0.04290	-0.04371
33.7761	-0.02435	-0.02548	-0.02867	-0.03346	-0.03910	-0.04474	-0.04953	-0.05272	-0.05385
34.5174	-0.01577	-0.01721	-0.02133	-0.02749	-0.03476	-0.04203	-0.04819	-0.05230	-0.05375
35.2587	0.00286	0.00124	-0.00334	-0.01020	-0.01830	-0.02639	-0.03326	-0.03784	-0.03945

INCREMENTAL PRESSURES, FORCES, AND MOMENTS ON BODY PANELS DUE TO WING

CD = 0.00177 CL = 0.01667 CM = -0.36813

BODY PANEL PRESSURE COEFFICIENT(CP)

THETA(DEG.)	12.5000	37.5000	62.5000	88.7967	116.0950	142.5000	167.5000
ROW NO.							
1	-0.00000	-0.00002	-0.00006	-0.01130	0.07745	0.00183	0.00055
2	-0.00004	-0.00112	-0.00800	-0.06334	0.10880	0.04453	0.00156
3	-0.00039	-0.00699	-0.03037	-0.06901	0.08632	0.06386	0.03601
4	-0.00599	-0.01771	-0.03885	-0.07459	0.07625	0.06003	0.06327
5	-0.01533	-0.02922	-0.04925	-0.07783	0.06639	0.06600	0.06898
6	-0.02483	-0.03804	-0.05924	-0.08058	0.06163	0.06895	0.06776
7	-0.03703	-0.04612	-0.06275	-0.08378	0.05739	0.06391	0.06625
8	-0.04748	-0.05323	-0.06649	-0.08168	0.05137	0.05957	0.06076
9	-0.05391	-0.05987	-0.07120	-0.07928	0.04468	0.05445	0.05680
10	-0.05911	-0.06550	-0.07329	-0.07342	0.03328	0.04829	0.05191
11	-0.06585	-0.06719	-0.04911	-0.01974	0.02623	0.03596	0.03773
12	-0.05160	-0.04405	-0.02720	-0.00533	0.01384	0.02459	0.02972
13	-0.02972	-0.02603	-0.01790	-0.00577	0.00704	0.01627	0.02109
14	-0.01763	-0.01510	-0.01010	-0.00291	0.00424	0.00940	0.01174

BODY PANEL SLOPE(DR/DX)

THETA(DEG.)	12.5000	37.5000	62.5000	88.7967	116.0950	142.5000	167.5000
ROW NO.							
1	-0.08032	-0.06116	-0.02643	0.01972	0.06798	0.10500	0.12416
2	-0.09482	-0.07566	-0.04094	0.00491	0.05348	0.09050	0.10965
3	-0.10224	-0.08308	-0.04835	-0.00257	0.04606	0.08308	0.10224
4	-0.10224	-0.08308	-0.04835	-0.00257	0.04606	0.08308	0.10224
5	-0.10224	-0.08308	-0.04835	-0.00257	0.04606	0.08308	0.10224
6	-0.10224	-0.08308	-0.04835	-0.00257	0.04606	0.08308	0.10224
7	-0.10224	-0.08308	-0.04835	-0.00257	0.04606	0.08308	0.10224
8	-0.10224	-0.08308	-0.04835	-0.00257	0.04606	0.08308	0.10224
9	-0.10224	-0.08308	-0.04835	-0.00257	0.04606	0.08308	0.10224
10	-0.10224	-0.08308	-0.04835	-0.00257	0.04606	0.08308	0.10224
11	-0.10224	-0.08308	-0.04835	-0.00257	0.04606	0.08308	0.10224
12	-0.10224	-0.08308	-0.04835	-0.00257	0.04606	0.08308	0.10224
13	-0.10237	-0.08321	-0.04849	-0.00270	0.04593	0.08295	0.10211
14	-0.12598	-0.10682	-0.07209	-0.02631	0.02232	0.05934	0.07850

PRESSURES, FORCES, AND MOMENTS ON WING PANELS IN PRESENCE OF BODY

CD = 0.01949 CL = 0.18361 CM = -5.42608

SPANWISE CD DISTRIBUTION(B/2Q * DD/DY)

SPANWISE STATION	1	2	3	4	5	6	7	8	9	10
	0.00186	0.00192	0.00201	0.00208	0.00212	0.00215	0.00222	0.00242	0.00260	0.00213

SPANWISE CL DISTRIBUTION(B/2Q * DL/DY)

SPANWISE STATION	1	2	3	4	5	6	7	8	9	10
	0.01680	0.01779	0.01867	0.01941	0.02002	0.02059	0.02141	0.02305	0.02455	0.02015

UPPER SURFACE WING PANEL PRESSURE COEFFICIENTS(CP)

SPANWISE STATION	1	2	3	4	5	6	7	8	9	10
CHORDWISE STATION										
1	-0.16579	-0.21452	-0.24268	-0.25782	-0.28390	-0.30588	-0.32415	-0.34268	-0.35644	-0.56583
2	-0.13484	-0.15824	-0.15489	-0.18337	-0.20003	-0.21325	-0.22674	-0.23586	-0.24208	-0.35603
3	-0.12453	-0.13811	-0.17466	-0.15877	-0.17035	-0.18187	-0.18886	-0.18594	-0.21256	-0.27307
4	-0.11876	-0.12168	-0.13465	-0.14681	-0.15633	-0.16163	-0.15786	-0.15751	-0.20251	-0.20705
5	-0.10660	-0.11828	-0.13002	-0.13998	-0.14111	-0.13828	-0.13257	-0.14280	-0.18144	-0.17239
6	-0.10478	-0.11510	-0.12141	-0.13059	-0.12053	-0.11014	-0.11602	-0.12862	-0.14999	-0.14371
7	-0.10168	-0.10454	-0.11355	-0.10181	-0.09604	-0.09265	-0.09650	-0.11126	-0.11757	-0.11524
8	-0.09239	-0.09964	-0.08509	-0.07717	-0.07169	-0.07441	-0.07352	-0.09540	-0.08590	-0.08092
9	-0.08799	-0.06942	-0.05694	-0.04836	-0.05112	-0.04631	-0.05180	-0.06944	-0.05352	-0.04756
10	-0.05000	-0.02157	-0.01570	-0.01678	-0.00975	-0.01161	-0.01471	-0.02991	-0.01117	-0.01279

LOWER SURFACE WING PANEL PRESSURE COEFFICIENTS(CP)

SPANWISE STATION	1	2	3	4	5	6	7	8	9	10
CHORDWISE STATION										
1	0.18348	0.20371	0.22155	0.24793	0.26083	0.27240	0.28208	0.28676	0.29986	0.47593
2	0.07736	0.08616	0.11668	0.11394	0.11750	0.12032	0.11950	0.12080	0.14217	0.22797
3	0.04907	0.05701	0.04242	0.07438	0.07425	0.07106	0.06950	0.07984	0.10821	0.14360
4	0.03860	0.05056	0.05332	0.05040	0.04670	0.04373	0.04940	0.05892	0.07631	0.07650
5	0.03956	0.04148	0.03677	0.03087	0.02991	0.03162	0.03834	0.04325	0.05240	0.04208
6	0.03831	0.03155	0.02705	0.01607	0.02224	0.03060	0.02689	0.03628	0.03620	0.02124
7	0.03421	0.02881	0.01538	0.02014	0.02143	0.02299	0.02328	0.03711	0.02290	0.00730
8	0.03278	0.01598	0.01929	0.01984	0.02118	0.01774	0.02499	0.02913	0.01181	-0.00084
9	0.01947	0.01885	0.01997	0.02243	0.01737	0.02173	0.02534	0.02280	0.00449	-0.01095
10	0.02125	0.03102	0.02910	0.02558	0.03058	0.02944	0.03480	0.02213	0.01354	-0.02950

WING PANEL PRESSURE DIFFERENCE(CL)

SPANWISE STATION	1	2	3	4	5	6	7	8	9	10

CHORDWISE STATION										
1	0.34927	0.41823	0.46423	0.50575	0.54473	0.57828	0.60622	0.62944	0.65630	1.04576
2	0.21220	0.24440	0.27157	0.29731	0.31753	0.33357	0.34624	0.35667	0.38426	0.58400
3	0.17360	0.19512	0.21708	0.23315	0.24459	0.25293	0.25835	0.26579	0.32118	0.41667
4	0.15736	0.17224	0.18797	0.19721	0.20303	0.20536	0.20726	0.21642	0.27881	0.28354
5	0.14616	0.15976	0.16679	0.17084	0.17102	0.16990	0.17090	0.18605	0.23384	0.21447
6	0.14309	0.14666	0.14846	0.14666	0.14277	0.14074	0.14292	0.16490	0.18619	0.16495
7	0.13589	0.13335	0.12892	0.12195	0.11746	0.11564	0.11978	0.14837	0.14047	0.12253
8	0.12517	0.11562	0.10438	0.09701	0.09287	0.09216	0.09851	0.12452	0.09771	0.08009
9	0.10746	0.08827	0.07691	0.07079	0.06849	0.06804	0.07714	0.09224	0.05842	0.03661
10	0.07125	0.05259	0.04480	0.04235	0.04033	0.04105	0.04951	0.05205	0.02472	-0.01672

UPPER SURFACE WING PANEL SLOPE(DZ/DX)

SPANWISE STATION	1	2	3	4	5	6	7	8	9	10
CHORDWISE STATION										
1	-0.03734	-0.03734	-0.03734	-0.03734	-0.03734	-0.03734	-0.03734	-0.03734	-0.03734	-0.03734
2	-0.06962	-0.06962	-0.06962	-0.06962	-0.06962	-0.06962	-0.06962	-0.06962	-0.06962	-0.06962
3	-0.08838	-0.08838	-0.08838	-0.08838	-0.08838	-0.08838	-0.08838	-0.08838	-0.08838	-0.08838
4	-0.10461	-0.10461	-0.10461	-0.10461	-0.10461	-0.10461	-0.10461	-0.10461	-0.10461	-0.10461
5	-0.11995	-0.11995	-0.11995	-0.11995	-0.11995	-0.11995	-0.11995	-0.11995	-0.11995	-0.11995
6	-0.13395	-0.13395	-0.13395	-0.13395	-0.13395	-0.13395	-0.13395	-0.13395	-0.13395	-0.13395
7	-0.14162	-0.14162	-0.14162	-0.14162	-0.14162	-0.14162	-0.14162	-0.14162	-0.14162	-0.14162
8	-0.14885	-0.14885	-0.14885	-0.14885	-0.14885	-0.14885	-0.14885	-0.14885	-0.14885	-0.14885
9	-0.15609	-0.15609	-0.15609	-0.15609	-0.15609	-0.15609	-0.15609	-0.15609	-0.15609	-0.15609
10	-0.16348	-0.16348	-0.16348	-0.16348	-0.16348	-0.16348	-0.16348	-0.16348	-0.16348	-0.16348

LOWER SURFACE WING PANEL SLOPE(DZ/DX)

SPANWISE STATION	1	2	3	4	5	6	7	8	9	10
CHORDWISE STATION										
1	-0.17210	-0.17210	-0.17210	-0.17210	-0.17210	-0.17210	-0.17210	-0.17210	-0.17210	-0.17210
2	-0.13982	-0.13982	-0.13982	-0.13982	-0.13982	-0.13982	-0.13982	-0.13982	-0.13982	-0.13982
3	-0.12106	-0.12106	-0.12106	-0.12106	-0.12106	-0.12106	-0.12106	-0.12106	-0.12106	-0.12106
4	-0.10483	-0.10483	-0.10483	-0.10483	-0.10483	-0.10483	-0.10483	-0.10483	-0.10483	-0.10483
5	-0.08949	-0.08949	-0.08949	-0.08949	-0.08949	-0.08949	-0.08949	-0.08949	-0.08949	-0.08949
6	-0.07548	-0.07548	-0.07548	-0.07548	-0.07548	-0.07548	-0.07548	-0.07548	-0.07548	-0.07548
7	-0.06782	-0.06782	-0.06782	-0.06782	-0.06782	-0.06782	-0.06782	-0.06782	-0.06782	-0.06782
8	-0.06059	-0.06059	-0.06059	-0.06059	-0.06059	-0.06059	-0.06059	-0.06059	-0.06059	-0.06059
9	-0.05335	-0.05335	-0.05335	-0.05335	-0.05335	-0.05335	-0.05335	-0.05335	-0.05335	-0.05335
10	-0.04596	-0.04596	-0.04596	-0.04596	-0.04596	-0.04596	-0.04596	-0.04596	-0.04596	-0.04596

WING CAMBER SLOPE(DZ/DX)

SPANWISE STATION	1	2	3	4	5	6	7	8	9	10
CHORDWISE STATION										
1	-0.10472	-0.10472	-0.10472	-0.10472	-0.10472	-0.10472	-0.10472	-0.10472	-0.10472	-0.10472
2	-0.10472	-0.10472	-0.10472	-0.10472	-0.10472	-0.10472	-0.10472	-0.10472	-0.10472	-0.10472
3	-0.10472	-0.10472	-0.10472	-0.10472	-0.10472	-0.10472	-0.10472	-0.10472	-0.10472	-0.10472
4	-0.10472	-0.10472	-0.10472	-0.10472	-0.10472	-0.10472	-0.10472	-0.10472	-0.10472	-0.10472
5	-0.10472	-0.10472	-0.10472	-0.10472	-0.10472	-0.10472	-0.10472	-0.10472	-0.10472	-0.10472
6	-0.10472	-0.10472	-0.10472	-0.10472	-0.10472	-0.10472	-0.10472	-0.10472	-0.10472	-0.10472
7	-0.10472	-0.10472	-0.10472	-0.10472	-0.10472	-0.10472	-0.10472	-0.10472	-0.10472	-0.10472
8	-0.10472	-0.10472	-0.10472	-0.10472	-0.10472	-0.10472	-0.10472	-0.10472	-0.10472	-0.10472
9	-0.10472	-0.10472	-0.10472	-0.10472	-0.10472	-0.10472	-0.10472	-0.10472	-0.10472	-0.10472
10	-0.10472	-0.10472	-0.10472	-0.10472	-0.10472	-0.10472	-0.10472	-0.10472	-0.10472	-0.10472

WING CHORD LENGTHS(C)

9.21046	9.21070	9.21094	9.21118	9.21142	9.21166	9.21190	9.21215	9.21239	6.14167

FORCES ANC MOMENTS ON WING-BODY COMBINATION

CD = 0.02256 CL = 0.20427 CM = -5.79131

FLOW VIZ IF

VELOCITY COMPONENTS DUE TC WING PANEL PRESSURE SINGULARITIES *ARE* CALCULATED IN THE FIELD

FOR THIS FLOW VISUALIZATION PRESSURE COEFFICIENTS
WILL BE CALCULATED USING--------A LINEAR CP FORMULA

POINTS

X	Y	Z	UP	VP	WP	U	V	W	CP
24.000000	4.000000	-1.000000	-0.035626	0.083641	-0.067841	0.958896	0.083641	0.036687	0.071253
24.000000	4.000000	-0.500000	-0.037989	0.095841	-0.102854	0.956533	0.095841	0.001675	0.075978
24.000000	4.353500	-0.646500	-0.054127	0.135089	-0.073926	0.940394	0.135089	0.030602	0.108255
24.000000	4.500000	-1.000000	-0.044122	0.110457	-0.039143	0.950400	0.110457	0.065385	0.088243
24.000000	4.353500	-1.353500	-0.036710	0.084660	-0.042606	0.957812	0.084660	0.061922	0.073420
24.000000	4.000000	-1.500000	-0.032834	0.070346	-0.052916	0.961688	0.070346	0.051612	0.065668
24.000000	3.646500	-1.353500	-0.029664	0.061164	-0.062843	0.964858	0.061164	0.041686	0.059328
24.000000	3.500000	-1.000000	-0.026597	0.055984	-0.072542	0.967925	0.055984	0.031986	0.053194
24.000000	3.646500	-0.646500	-0.028592	0.060013	-0.087351	0.965930	0.060013	0.017177	0.057184

GRIDS

COMPUTE** 4**GRIDS

OPTION REQUESTED---RECTANGULAR GRID

X-Z CUT, FOR THIS CUT Y= 1.20000

X	Y	Z	U	V	W	CP
30.000000	1.200000	-1.200000	0.9899668	0.0338168	0.0704108	0.0091102
30.500000	1.200000	-1.200000	0.9917703	0.0332524	0.0739117	0.0055031
31.000000	1.200000	-1.200000	0.9952464	0.0305906	0.0792592	-0.0014491
31.500000	1.200000	-1.200000	0.9996132	0.0255415	0.0851683	-0.0101826
32.000000	1.200000	-1.200000	1.0010858	0.0234452	0.0884505	-0.0131279
32.500000	1.200000	-1.200000	1.0027476	0.0211703	0.0920858	-0.0164515
33.000000	1.200000	-1.200000	1.0041351	0.0189602	0.0953730	-0.0192265
33.500000	1.200000	-1.200000	1.0084280	0.0130533	0.1015207	-0.0278122
34.000000	1.200000	-1.200000	1.0106221	0.0086157	0.1054965	-0.0322004
34.500000	1.200000	-1.200000	1.0120738	0.0047569	0.1088115	-0.0351039
30.000000	1.200000	-0.700000	0.9943630	0.0476981	0.1039270	0.0003179
30.500000	1.200000	-0.700000	0.9972555	0.0447768	0.1089371	-0.0054673
31.000000	1.200000	-0.700000	1.0011633	0.0390014	0.1135523	-0.0132829
31.500000	1.200000	-0.700000	1.0029871	0.0357785	0.1170331	-0.0169305
32.000000	1.200000	-0.700000	1.0047936	0.0323835	0.1206735	-0.0205435
32.500000	1.200000	-0.700000	1.0061961	0.0292708	0.1239940	-0.0233484
33.000000	1.200000	-0.700000	1.0094400	0.0233545	0.1283378	-0.0298363
33.500000	1.200000	-0.700000	1.0119922	0.0170708	0.1310087	-0.0349407
34.000000	1.200000	-0.700000	1.0135186	0.0119647	0.1333637	-0.0379935
34.500000	1.200000	-0.700000	1.0143696	0.0072765	0.1350083	-0.0396954

X-Z CUT, FOR THIS CUT Y= 0.000000

X	Y	Z	U	V	W	CP
50.000000	0.000000	-36.000000	0.9945219	0.0000000	0.1045285	-0.0000000
52.000000	0.000000	-36.000000	0.9945219	0.0000000	0.1045285	-0.0000000
54.000000	0.000000	-36.000000	0.9918172	0.0000000	0.1004773	0.0054094
56.000000	0.000000	-36.000000	0.9894597	0.0000000	0.0967958	0.0101243
58.000000	0.000000	-36.000000	0.9900376	0.0000000	0.0975222	0.0089687
60.000000	0.000000	-36.000000	0.9906894	0.0000000	0.0983827	0.0076650
62.000000	0.000000	-36.000000	0.9917537	0.0000000	0.0998836	0.0055364
64.000000	0.000000	-36.000000	0.9929589	0.0000000	0.1016262	0.0031261
66.000000	0.000000	-36.000000	0.9945595	0.0000000	0.1040015	-0.0000752
68.000000	0.000000	-36.000000	0.9872165	-0.0000000	0.0929860	0.0146107
70.000000	0.000000	-36.000000	0.9857952	-0.0000000	0.0906324	0.0174533
72.000000	0.000000	-36.000000	0.9860376	-0.0000000	0.0907592	0.0169685
74.000000	0.000000	-36.000000	0.9860979	-0.0000000	0.0906217	0.0168479
76.000000	0.000000	-36.000000	0.9882600	-0.0000000	0.0936611	0.0125238
78.000000	0.000000	-36.000000	0.9889623	-0.0000000	0.0945617	0.0111192
80.000000	0.000000	-36.000000	0.9902288	-0.0000000	0.0963357	0.0085862
82.000000	0.000000	-36.000000	0.9908648	-0.0000000	0.0971795	0.0073142
84.000000	0.000000	-36.000000	0.9936806	-0.0000000	0.1013505	0.0016826
86.000000	0.000000	-36.000000	0.9958968	-0.0000000	0.1046963	-0.0027498
88.000000	0.000000	-36.000000	0.9868218	0.0000000	0.0910749	0.0154001
90.000000	0.000000	-36.000000	0.9849899	0.0000000	0.0883658	0.0190639
92.000000	0.000000	-36.000000	0.9898543	0.0000000	0.0953142	0.0093352
94.000000	0.000000	-36.000000	0.9967822	0.0000000	0.1053693	-0.0045206
96.000000	0.000000	-36.000000	1.0055096	0.0000000	0.1180327	-0.0219755
98.000000	0.000000	-36.000000	0.9924414	0.0000000	0.0991497	0.0041610
100.000000	0.000000	-36.000000	0.9935522	0.0000000	0.1006177	0.0019394

102.000000	0.000000	-36.000000	0.9938063	0.0000000	0.1009284	0.0014312
104.000000	0.000000	-36.000000	0.9938109	0.0000000	0.1008784	0.0014220
106.000000	0.000000	-36.000000	0.9937830	0.0000000	0.1007942	0.0014779
108.000000	0.000000	-36.000000	0.9937623	0.0000000	0.1007198	0.0015192
110.000000	0.000000	-36.000000	0.9937425	0.0000000	0.1006552	0.0015587
112.000000	0.000000	-36.000000	0.9937361	0.0000000	0.1006013	0.0015717
114.000000	0.000000	-36.000000	0.9937287	0.0000000	0.1005600	0.0015863
116.000000	0.000000	-36.000000	0.9937224	0.0000000	0.1005251	0.0015989
118.000000	0.000000	-36.000000	0.9937331	0.0000000	0.1004975	0.0015775
120.000000	0.000000	-36.000000	0.9937376	0.0000000	0.1004718	0.0015687
122.000000	0.000000	-36.000000	0.9937451	0.0000000	0.1004518	0.0015536
124.000000	0.000000	-36.000000	0.9937481	0.0000000	0.1004345	0.0015475
126.000000	0.000000	-36.000000	0.9937547	0.0000000	0.1004190	0.0015343
128.000000	0.000000	-36.000000	0.9937664	0.0000000	0.1004074	0.0015110
130.000000	0.000000	-36.000000	0.9937759	0.0000000	0.1003968	0.0014920
132.000000	0.000000	-36.000000	0.9937852	0.0000000	0.1003866	0.0014734
134.000000	0.000000	-36.000000	0.9937904	0.0000000	0.1003795	0.0014630
136.000000	0.000000	-36.000000	0.9938037	0.0000000	0.1003709	0.0014365
138.000000	0.000000	-36.000000	0.9938063	0.0000000	0.1003664	0.0014311
140.000000	0.000000	-36.000000	0.9938256	0.0000000	0.1003597	0.0013926
142.000000	0.000000	-36.000000	0.9938306	0.0000000	0.1003561	0.0013826
144.000000	0.000000	-36.000000	0.9938453	0.0000000	0.1003532	0.0013533
146.000000	0.000000	-36.000000	0.9938508	0.0000000	0.1003464	0.0013421
148.000000	0.000000	-36.000000	0.9938598	0.0000000	0.1003445	0.0013241
150.000000	0.000000	-36.000000	0.9938663	0.0000000	0.1003407	0.0013112

VELOCITY COMPONENTS AND PRESSURE COEFFICIENTS DUE TO WING SOURCES

			PERTURBATION COMPONENTS			
X	Y	Z	U	V	W	CP
50.000000	0.000000	-36.000000	-0.0000000	-0.0000000	-0.0000000	0.0000000
52.000000	0.000000	-36.000000	-0.0000000	-0.0000000	-0.0000000	0.0000000
54.000000	0.000000	-36.000000	-0.0000000	-0.0000000	-0.0000000	0.0000000
56.000000	0.000000	-36.000000	-0.0000000	-0.0000000	-0.0000000	0.0000000
58.000000	0.000000	-36.000000	-0.0000000	-0.0000000	-0.0000000	0.0000000
60.000000	0.000000	-36.000000	-0.0000000	-0.0000000	-0.0000000	0.0000000
62.000000	0.000000	-36.000000	-0.0000000	-0.0000000	-0.0000000	0.0000000
64.000000	0.000000	-36.000000	-0.0000000	-0.0000000	-0.0000000	0.0000000
66.000000	0.000000	-36.000000	-0.0000000	-0.0000000	-0.0000000	0.0000000
68.000000	0.000000	-36.000000	-0.0043796	-0.0000000	-0.0065808	0.0087593
70.000000	0.000000	-36.000000	-0.0034716	-0.0000000	-0.0053295	0.0069432
72.000000	0.000000	-36.000000	-0.0017007	-0.0000000	-0.0027447	0.0034015
74.000000	0.000000	-36.000000	0.0004381	-0.0000000	0.0004439	-0.0008761
76.000000	0.000000	-36.000000	0.0024402	-0.0000000	0.0034841	-0.0048804
78.000000	0.000000	-36.000000	0.0011195	-0.0000000	0.0015651	-0.0022389
80.000000	0.000000	-36.000000	0.0006614	-0.0000000	0.0009071	-0.0013228
82.000000	0.000000	-36.000000	0.0004644	-0.0000000	0.0006280	-0.0009288
84.000000	0.000000	-36.000000	0.0003515	-0.0000000	0.0004714	-0.0007031
86.000000	0.000000	-36.000000	0.0002798	-0.0000000	0.0003763	-0.0005597
88.000000	0.000000	-36.000000	0.0002287	-0.0000000	0.0003065	-0.0004574
90.000000	0.000000	-36.000000	0.0010102	-0.0000000	0.0014519	-0.0020205
92.000000	0.000000	-36.000000	0.0028410	-0.0000000	0.0041645	-0.0056820
94.000000	0.000000	-36.000000	0.0018283	-0.0000000	0.0027644	-0.0036565
96.000000	0.000000	-36.000000	-0.0025533	-0.0000000	-0.0035393	0.0051066
98.000000	0.000000	-36.000000	-0.0096415	-0.0000000	-0.0139832	0.0192830

100.000000	0.000000	-36.000000	-0.0052882	-0.0000000	-0.0079038	0.0105763
102.000000	0.000000	-36.000000	-0.0037836	-0.0000000	-0.0058319	0.0075673
104.000000	0.000000	-36.000000	-0.0030700	-0.0000000	-0.0048886	0.0061400
106.000000	0.000000	-36.000000	-0.0026370	-0.0000000	-0.0043287	0.0052739
108.000000	0.000000	-36.000000	-0.0023328	-0.0000000	-0.0039509	0.0046657
110.000000	0.000000	-36.000000	-0.0021122	-0.0000000	-0.0036802	0.0042244
112.000000	0.000000	-36.000000	-0.0019333	-0.0000000	-0.0034760	0.0038665
114.000000	0.000000	-36.000000	-0.0017935	-0.0000000	-0.0033132	0.0035871
116.000000	0.000000	-36.000000	-0.0016814	-0.0000000	-0.0031826	0.0033628
118.000000	0.000000	-36.000000	-0.0015727	-0.0000000	-0.0030739	0.0031454
120.000000	0.000000	-36.000000	-0.0014866	-0.0000000	-0.0029843	0.0029732
122.000000	0.000000	-36.000000	-0.0014101	-0.0000000	-0.0029074	0.0028202
124.000000	0.000000	-36.000000	-0.0013480	-0.0000000	-0.0028412	0.0026959
126.000000	0.000000	-36.000000	-0.0012902	-0.0000000	-0.0027847	0.0025804
128.000000	0.000000	-36.000000	-0.0012340	-0.0000000	-0.0027330	0.0024679
130.000000	0.000000	-36.000000	-0.0011857	-0.0000000	-0.0026885	0.0023714
132.000000	0.000000	-36.000000	-0.0011418	-0.0000000	-0.0026494	0.0022837
134.000000	0.000000	-36.000000	-0.0011063	-0.0000000	-0.0026127	0.0022126
136.000000	0.000000	-36.000000	-0.0010656	-0.0000000	-0.0025821	0.0021311
138.000000	0.000000	-36.000000	-0.0010391	-0.0000000	-0.0025520	0.0020781
140.000000	0.000000	-36.000000	-0.0009975	-0.0000000	-0.0025266	0.0019951
142.000000	0.000000	-36.000000	-0.0009729	-0.0000000	-0.0025018	0.0019459
144.000000	0.000000	-36.000000	-0.0009404	-0.0000000	-0.0024789	0.0018807
146.000000	0.000000	-36.000000	-0.0009185	-0.0000000	-0.0024611	0.0018370
148.000000	0.000000	-36.000000	-0.0008949	-0.0000000	-0.0024410	0.0017899
150.000000	0.000000	-36.000000	-0.0008746	-0.0000000	-0.0024246	0.0017492

VELOCITY COMPONENTS AND PRESSURE COEFFICIENTS DUE TO WING PANEL PRESSURE SINGULARITIES

			PERTURBATION COMPONENTS			
X	Y	Z	U	V	W	CP
50.000000	0.000000	-36.000000	0.0000000	-0.0000000	-0.0000000	-0.0000000
52.000000	0.000000	-36.000000	0.0000000	-0.0000000	-0.0000000	-0.0000000
54.000000	0.000000	-36.000000	0.0000000	-0.0000000	-0.0000000	-0.0000000
56.000000	0.000000	-36.000000	0.0000000	-0.0000000	-0.0000000	-0.0000000
58.000000	0.000000	-36.000000	0.0000000	-0.0000000	-0.0000000	-0.0000000
60.000000	0.000000	-36.000000	0.0000000	-0.0000000	-0.0000000	-0.0000000
62.000000	0.000000	-36.000000	0.0000000	-0.0000000	-0.0000000	-0.0000000
64.000000	0.000000	-36.000000	0.0000000	-0.0000000	-0.0000000	-0.0000000
66.000000	0.000000	-36.000000	0.0000000	-0.0000000	-0.0000000	-0.0000000
68.000000	0.000000	-36.000000	-0.0045827	-0.0000000	-0.0068814	0.0091655
70.000000	0.000000	-36.000000	-0.0064104	-0.0000000	-0.0097605	0.0128207
72.000000	0.000000	-36.000000	-0.0073106	-0.0000000	-0.0112952	0.0146211
74.000000	0.000000	-36.000000	-0.0084367	-0.0000000	-0.0131945	0.0168733
76.000000	0.000000	-36.000000	-0.0084920	-0.0000000	-0.0135055	0.0169840
78.000000	0.000000	-36.000000	-0.0065850	-0.0000000	-0.0108480	0.0131701
80.000000	0.000000	-36.000000	-0.0057292	-0.0000000	-0.0097198	0.0114584
82.000000	0.000000	-36.000000	-0.0050734	-0.0000000	-0.0088732	0.0101468
84.000000	0.000000	-36.000000	-0.0045653	-0.0000000	-0.0082363	0.0091306
86.000000	0.000000	-36.000000	-0.0044012	-0.0000000	-0.0080972	0.0088024
88.000000	0.000000	-36.000000	-0.0046732	-0.0000000	-0.0085935	0.0093464
90.000000	0.000000	-36.000000	-0.0102006	-0.0000000	-0.0167720	0.0204012
92.000000	0.000000	-36.000000	-0.0075220	-0.0000000	-0.0130605	0.0150440
94.000000	0.000000	-36.000000	0.0003190	-0.0000000	-0.0017535	-0.0006380
96.000000	0.000000	-36.000000	0.0133954	-0.0000000	0.0171633	-0.0267909
98.000000	0.000000	-36.000000	0.0074062	0.0000000	0.0087093	-0.0148124

100.000000	0.000000	-36.000000	0.0041647	0.0000000	0.0040968	-0.0083295
102.000000	0.000000	-36.000000	0.0029193	0.0000000	0.0023411	-0.0058387
104.000000	0.000000	-36.000000	0.0022173	0.0000000	0.0013559	-0.0044345
106.000000	0.000000	-36.000000	0.0017636	0.0000000	0.0007211	-0.0035272
108.000000	0.000000	-36.000000	0.0014464	0.0000000	0.0002779	-0.0028929
110.000000	0.000000	-36.000000	0.0012129	0.0000000	-0.0000484	-0.0024258
112.000000	0.000000	-36.000000	0.0010344	0.0000000	-0.0002979	-0.0020689
114.000000	0.000000	-36.000000	0.0008941	-0.0000000	-0.0004943	-0.0017882
116.000000	0.000000	-36.000000	0.0007813	-0.0000000	-0.0006525	-0.0015626
118.000000	0.000000	-36.000000	0.0006890	-0.0000000	-0.0007823	-0.0013780
120.000000	0.000000	-36.000000	0.0006124	-0.0000000	-0.0008905	-0.0012247
122.000000	0.000000	-36.000000	0.0005479	-0.0000000	-0.0009818	-0.0010958
124.000000	0.000000	-36.000000	0.0004931	-0.0000000	-0.0010597	-0.0009862
126.000000	0.000000	-36.000000	0.0004461	-0.0000000	-0.0011270	-0.0008922
128.000000	0.000000	-36.000000	0.0004054	-0.0000000	-0.0011853	-0.0008108
130.000000	0.000000	-36.000000	0.0003700	-0.0000000	-0.0012365	-0.0007399
132.000000	0.000000	-36.000000	0.0003389	-0.0000000	-0.0012817	-0.0006778
134.000000	0.000000	-36.000000	0.0003115	-0.0000000	-0.0013217	-0.0006229
136.000000	0.000000	-36.000000	0.0002871	-0.0000000	-0.0013574	-0.0005743
138.000000	0.000000	-36.000000	0.0002655	-0.0000000	-0.0013894	-0.0005309
140.000000	0.000000	-36.000000	0.0002461	-0.0000000	-0.0014183	-0.0004922
142.000000	0.000000	-36.000000	0.0002287	-0.0000000	-0.0014444	-0.0004574
144.000000	0.000000	-36.000000	0.0002130	-0.0000000	-0.0014681	-0.0004259
146.000000	0.000000	-36.000000	0.0001988	-0.0000000	-0.0014897	-0.0003976
148.000000	0.000000	-36.000000	0.0001859	-0.0000000	-0.0015094	-0.0003717
150.000000	0.000000	-36.000000	0.0001741	-0.0000000	-0.0015275	-0.0003483

VELOCITY COMPONENTS AND [illegible] COEFFICIENTS DUE TO BODY PANEL PRESSURE SINGULARITIES

			PERTURBATION COMPONENTS			
X	Y	Z	U	V	W	CP
50.000000	0.000000	-36.000000	0.0000000	-0.0000000	0.0000000	-0.0000000
52.000000	0.000000	-36.000000	0.0000000	-0.0000000	0.0000000	-0.0000000
54.000000	0.000000	-36.000000	0.0000000	-0.0000000	0.0000000	-0.0000000
56.000000	0.000000	-36.000000	0.0000000	-0.0000000	0.0000000	-0.0000000
58.000000	0.000000	-36.000000	0.0000000	-0.0000000	0.0000000	-0.0000000
60.000000	0.000000	-36.000000	0.0000000	-0.0000000	0.0000000	-0.0000000
62.000000	0.000000	-36.000000	0.0000000	-0.0000000	0.0000000	-0.0000000
64.000000	0.000000	-36.000000	0.0000000	-0.0000000	0.0000000	-0.0000000
66.000000	0.000000	-36.000000	-0.0001032	-0.0000000	-0.0001545	0.0002064
68.000000	0.000000	-36.000000	-0.0015649	-0.0000000	-0.0023660	0.0031338
70.000000	0.000000	-36.000000	-0.0013694	-0.0000000	-0.0021233	0.0027387
72.000000	0.000000	-36.000000	-0.0012970	-0.0000000	-0.0020571	0.0025941
74.000000	0.000000	-36.000000	-0.0017421	-0.0000000	-0.0027676	0.0034842
76.000000	0.000000	-36.000000	-0.0011736	-0.0000000	-0.0018563	0.0023471
78.000000	0.000000	-36.000000	-0.0008299	-0.0000000	-0.0014799	0.0016598
80.000000	0.000000	-36.000000	0.0001831	-0.0000000	0.0000179	-0.0003662
82.000000	0.000000	-36.000000	0.0000443	-0.0000000	-0.0001907	-0.0000886
84.000000	0.000000	-36.000000	0.0002731	-0.0000000	0.0001628	-0.0005461
86.000000	0.000000	-36.000000	0.0005364	-0.0000000	0.0005713	-0.0010728
88.000000	0.000000	-36.000000	0.0010044	-0.0000000	0.0021814	-0.0020049
90.000000	0.000000	-36.000000	0.0004194	-0.0000000	0.0004230	-0.0008388
92.000000	0.000000	-36.000000	0.0002900	-0.0000000	0.0002352	-0.0005800
94.000000	0.000000	-36.000000	0.0002206	-0.0000000	0.0001360	-0.0004411
96.000000	0.000000	-36.000000	0.0001758	-0.0000000	0.0000723	-0.0003517
98.000000	0.000000	-36.000000	0.0001444	-0.0000000	0.0000278	-0.0002889

100.000000	0.000000	-36.000000	0.0001212	-0.0000000	-0.0000046	-0.0002425
102.000000	0.000000	-36.000000	0.0001034	-0.0000000	-0.0000298	-0.0002068
104.000000	0.000000	-36.000000	0.0000894	-0.0000000	-0.0000496	-0.0001787
106.000000	0.000000	-36.000000	0.0000780	-0.0000000	-0.0000658	-0.0001561
108.000000	0.000000	-36.000000	0.0000688	-0.0000000	-0.0000788	-0.0001376
110.000000	0.000000	-36.000000	0.0000611	-0.0000000	-0.0000896	-0.0001222
112.000000	0.000000	-36.000000	0.0000546	-0.0000000	-0.0000988	-0.0001092
114.000000	0.000000	-36.000000	0.0000491	-0.0000000	-0.0001066	-0.0000982
116.000000	0.000000	-36.000000	0.0000444	-0.0000000	-0.0001133	-0.0000888
118.000000	0.000000	-36.000000	0.0000403	-0.0000000	-0.0001191	-0.0000806
120.000000	0.000000	-36.000000	0.0000367	-0.0000000	-0.0001246	-0.0000735
122.000000	0.000000	-36.000000	0.0000336	-0.0000000	-0.0001290	-0.0000672
124.000000	0.000000	-36.000000	0.0000309	-0.0000000	-0.0001330	-0.0000618
126.000000	0.000000	-36.000000	0.0000284	-0.0000000	-0.0001368	-0.0000569
128.000000	0.000000	-36.000000	0.0000263	-0.0000000	-0.0001397	-0.0000526
130.000000	0.000000	-36.000000	0.0000243	-0.0000000	-0.0001426	-0.0000487
132.000000	0.000000	-36.000000	0.0000226	-0.0000000	-0.0001454	-0.0000452
134.000000	0.000000	-36.000000	0.0000210	-0.0000000	-0.0001477	-0.0000421
136.000000	0.000000	-36.000000	0.0000196	-0.0000000	-0.0001498	-0.0000393
138.000000	0.000000	-36.000000	0.0000184	-0.0000000	-0.0001516	-0.0000367
140.000000	0.000000	-36.000000	0.0000172	-0.0000000	-0.0001533	-0.0000344
142.000000	0.000000	-36.000000	0.0000161	-0.0000000	-0.0001549	-0.0000323
144.000000	0.000000	-36.000000	0.0000152	-0.0000000	-0.0001563	-0.0000303
146.000000	0.000000	-36.000000	0.0000143	-0.0000000	-0.0001578	-0.0000285
148.000000	0.000000	-36.000000	0.0000134	-0.0000000	-0.0001591	-0.0000269
150.000000	0.000000	-36.000000	0.0000127	-0.0000000	-0.0001603	-0.0000254

VELOCITY COMPONENTS AND PRESSURE COEFFICIENTS DUE TO BODY LINE SOURCES AND DOUBLETS

			PERTURBATION COMPONENTS			
X	Y	Z	U	V	W	CP
50.000000	0.000000	-36.000000	0.0000000	0.0000000	-0.0000000	-0.0000000
52.000000	0.000000	-36.000000	0.0000000	0.0000000	-0.0000000	-0.0000000
54.000000	0.000000	-36.000000	-0.0027047	0.0000000	-0.0040511	0.0054094
56.000000	0.000000	-36.000000	-0.0050622	0.0000000	-0.0077327	0.0101243
58.000000	0.000000	-36.000000	-0.0044843	0.0000000	-0.0070062	0.0089687
60.000000	0.000000	-36.000000	-0.0038325	0.0000000	-0.0061458	0.0076650
62.000000	0.000000	-36.000000	-0.0027682	0.0000000	-0.0046446	0.0055364
64.000000	0.000000	-36.000000	-0.0015630	0.0000000	-0.0029022	0.0031261
66.000000	0.000000	-36.000000	0.0001408	0.0000000	-0.0003725	-0.0002817
68.000000	0.000000	-36.000000	0.0032239	-0.0000000	0.0042858	-0.0064478
70.000000	0.000000	-36.000000	0.0025247	-0.0000000	0.0033173	-0.0050493
72.000000	0.000000	-36.000000	0.0018241	-0.0000000	0.0023277	-0.0036482
74.000000	0.000000	-36.000000	0.0013168	-0.0000000	0.0016114	-0.0026335
76.000000	0.000000	-36.000000	0.0009635	-0.0000000	0.0011134	-0.0019269
78.000000	0.000000	-36.000000	0.0007359	-0.0000000	0.0007960	-0.0014717
80.000000	0.000000	-36.000000	0.0005945	-0.0000000	0.0006021	-0.0011890
82.000000	0.000000	-36.000000	0.0009076	-0.0000000	0.0010870	-0.0018152
84.000000	0.000000	-36.000000	0.0030994	-0.0000000	0.0044241	-0.0061988
86.000000	0.000000	-36.000000	0.0049598	-0.0000000	0.0073174	-0.0099196
88.000000	0.000000	-36.000000	-0.0048600	0.0000000	-0.0073478	0.0097200
90.000000	0.000000	-36.000000	-0.0007610	0.0000000	-0.0012646	0.0015221
92.000000	0.000000	-36.000000	-0.0002767	0.0000000	-0.0005534	0.0005533
94.000000	0.000000	-36.000000	-0.0001075	0.0000000	-0.0003061	0.0002150
96.000000	0.000000	-36.000000	-0.0000303	0.0000000	-0.0001921	0.0000605
98.000000	0.000000	-36.000000	0.0000104	0.0000000	-0.0001328	-0.0000208

100.000000	0.000000	-36.000000	0.0000325	0.0000000	-0.0000992	-0.0000651
102.000000	0.000000	-36.000000	0.0000453	0.0000000	-0.0000795	-0.0000906
104.000000	0.000000	-36.000000	0.0000524	0.0000000	-0.0000678	-0.0001047
106.000000	0.000000	-36.000000	0.0000564	0.0000000	-0.0000608	-0.0001128
108.000000	0.000000	-36.000000	0.0000580	0.0000000	-0.0000569	-0.0001160
110.000000	0.000000	-36.000000	0.0000589	0.0000000	-0.0000551	-0.0001177
112.000000	0.000000	-36.000000	0.0000584	0.0000000	-0.0000544	-0.0001168
114.000000	0.000000	-36.000000	0.0000572	0.0000000	-0.0000543	-0.0001144
116.000000	0.000000	-36.000000	0.0000562	0.0000000	-0.0000549	-0.0001124
118.000000	0.000000	-36.000000	0.0000547	0.0000000	-0.0000557	-0.0001093
120.000000	0.000000	-36.000000	0.0000532	0.0000000	-0.0000572	-0.0001063
122.000000	0.000000	-36.000000	0.0000518	0.0000000	-0.0000585	-0.0001036
124.000000	0.000000	-36.000000	0.0000502	0.0000000	-0.0000600	-0.0001005
126.000000	0.000000	-36.000000	0.0000485	0.0000000	-0.0000611	-0.0000971
128.000000	0.000000	-36.000000	0.0000468	0.0000000	-0.0000630	-0.0000936
130.000000	0.000000	-36.000000	0.0000454	0.0000000	-0.0000640	-0.0000908
132.000000	0.000000	-36.000000	0.0000436	0.0000000	-0.0000654	-0.0000873
134.000000	0.000000	-36.000000	0.0000423	0.0000000	-0.0000669	-0.0000846
136.000000	0.000000	-36.000000	0.0000406	0.0000000	-0.0000681	-0.0000811
138.000000	0.000000	-36.000000	0.0000397	0.0000000	-0.0000690	-0.0000794
140.000000	0.000000	-36.000000	0.0000380	0.0000000	-0.0000705	-0.0000760
142.000000	0.000000	-36.000000	0.0000369	0.0000000	-0.0000713	-0.0000737
144.000000	0.000000	-36.000000	0.0000356	0.0000000	-0.0000720	-0.0000712
146.000000	0.000000	-36.000000	0.0000344	0.0000000	-0.0000735	-0.0000688
148.000000	0.000000	-36.000000	0.0000336	0.0000000	-0.0000745	-0.0000671
150.000000	0.000000	-36.000000	0.0000322	0.0000000	-0.0000754	-0.0000644

STREAMLINES

INITIAL POINT X= 28.00000 Y= 5.00000 Z= 0.25000

INITIAL STEPSIZE= 0.10000

ACTUAL POINTS DETERMINED BY INTEGRATOR

X	Y	Z	U	V	W	CP
19.719375	5.254200	-0.850826	0.995034	0.006823	0.110100	-0.001023
20.116930	5.249246	-0.806946	0.986889	0.018857	0.108812	0.015266
20.514372	5.269423	-0.763038	0.979787	0.030035	0.108627	0.029470
20.911711	5.282135	-0.718714	0.979211	0.031767	0.110292	0.030622
21.309011	5.291940	-0.673626	0.979314	0.032633	0.113467	0.030415
21.706090	5.304834	-0.627065	0.981881	0.029813	0.116609	0.025282
22.103052	5.316099	-0.579219	0.983740	0.028117	0.120457	0.021563
22.499806	5.327873	-0.529754	0.982744	0.030777	0.124931	0.023557
22.896242	5.341235	-0.478151	0.981644	0.033761	0.130543	0.025756
23.292368	5.354256	-0.424212	0.983259	0.032820	0.137725	0.022527
23.687965	5.368713	-0.366845	0.980426	0.038616	0.147516	0.028191
24.082750	5.385085	-0.304648	0.979753	0.041023	0.161532	0.029537
24.476556	5.402209	-0.236388	0.982257	0.037558	0.182267	0.024529
24.868612	5.419263	-0.158577	0.984128	0.029938	0.214884	0.020787
25.257733	5.417026	-0.066293	1.008395	-0.031953	0.255421	-0.027746
25.644658	5.384511	0.029016	1.048595	-0.140246	0.235557	-0.108146
26.032763	5.321678	0.102060	1.069636	-0.189655	0.164838	-0.150228
26.227812	5.286965	0.129413	1.070556	-0.190801	0.136495	-0.152067
26.423434	5.252197	0.152249	1.071348	-0.189522	0.114428	-0.153653
26.619506	5.217798	0.171534	1.071178	-0.186042	0.096982	-0.153311
26.815956	5.184100	0.187994	1.069850	-0.180732	0.083075	-0.150657
27.012742	5.151373	0.202267	1.067122	-0.173958	0.072250	-0.145200
27.209805	5.119574	0.214705	1.066235	-0.169700	0.062688	-0.143476
27.407085	5.088537	0.225518	1.065356	-0.165497	0.054339	-0.141669
27.505798	5.073301	0.230375	1.064772	-0.163203	0.050533	-0.140499
27.604560	5.058277	0.234900	1.063958	-0.160591	0.047026	-0.138873
27.703370	5.043485	0.239111	1.063326	-0.158262	0.043656	-0.137608
27.802201	5.028749	0.243011	1.063598	-0.157337	0.040458	-0.138152
27.901074	5.014221	0.246632	1.063051	-0.155189	0.037433	-0.137059
28.000000	5.000000	0.250000	1.061827	-0.152238	0.034690	-0.134609
28.098949	4.985880	0.253101	1.061621	-0.150702	0.031871	-0.134197
28.197928	4.971909	0.255946	1.061256	-0.148916	0.029166	-0.133468
28.296938	4.958114	0.258547	1.060695	-0.146835	0.026592	-0.132346
28.395978	4.944499	0.260916	1.060132	-0.144749	0.024146	-0.131220
28.495054	4.931105	0.263064	1.058726	-0.141395	0.021831	-0.128408
28.594166	4.917950	0.265002	1.058808	-0.140280	0.019548	-0.128572
28.792643	4.893565	0.268371	1.052399	-0.128206	0.016127	-0.115753
28.991234	4.870024	0.271085	1.049252	-0.120911	0.012648	-0.109461
29.189980	4.847770	0.273195	1.046051	-0.113600	0.009625	-0.103058
29.388870	4.826788	0.274753	1.043393	-0.106960	0.006728	-0.097742
29.587885	4.806995	0.275782	1.040727	-0.100260	0.004113	-0.092410
29.787020	4.788425	0.276340	1.038372	-0.093645	0.001758	-0.087701
30.185615	4.754953	0.276282	1.033588	-0.080735	-0.001860	-0.078133
30.584775	4.729198	0.275163	1.026018	-0.063631	-0.004125	-0.062993
30.984132	4.706637	0.273256	1.022695	-0.052919	-0.005449	-0.056346
31.383698	4.688282	0.271103	1.017988	-0.039962	-0.005262	-0.046933

31.783450	4.674244	0.269363	1.017341	-0.033125	-0.003246	-0.045638
32.183309	4.664251	0.268913	1.008546	-0.014434	0.001327	-0.028048
32.583302	4.661258	0.270645	1.003968	-0.003081	0.007856	-0.018892
32.983270	4.661645	0.275345	1.000847	0.004571	0.015733	-0.012649
33.383183	4.664354	0.283176	0.999529	0.008314	0.023241	-0.010015
33.783028	4.667536	0.293802	1.001200	0.006552	0.029692	-0.013357
34.182805	4.670442	0.306819	0.999280	0.009644	0.035306	-0.009517
34.582499	4.674595	0.321901	0.998899	0.010067	0.039964	-0.008754
34.982127	4.678605	0.338687	0.999227	0.009433	0.043810	-0.009410
35.381698	4.682024	0.356864	0.999969	0.008086	0.047060	-0.010894
35.781216	4.685128	0.376237	1.000004	0.007772	0.049864	-0.010964
36.180688	4.687771	0.396605	1.001872	0.004684	0.052087	-0.014701
36.580125	4.689193	0.417779	1.002766	0.003052	0.054205	-0.016488
36.979520	4.690146	0.439752	1.003563	0.001678	0.056144	-0.018081
37.378875	4.690594	0.462446	1.004159	0.000659	0.057926	-0.019275
37.778193	4.690690	0.485807	1.004597	-0.000178	0.059572	-0.020150
38.177474	4.690479	0.509758	1.004982	-0.000856	0.060903	-0.020921
38.975957	4.688711	0.558968	1.006748	-0.003551	0.063012	-0.024452
39.774337	4.685409	0.609759	1.006855	-0.003959	0.065168	-0.024665
40.572598	4.683946	0.662427	1.004760	0.001789	0.067463	-0.020475
41.370510	4.684174	0.718423	0.991789	0.028514	0.073785	0.005466

INITIAL POINT X= 28.00000 Y= 5.00000 Z= -0.50000

INITIAL STEPSIZE= 0.20000

ACTUAL POINTS DETERMINED BY INTEGRATOR

X	Y	Z	U	V	W	CP
19.690964	4.012190	-1.013294	0.972486	0.051450	0.108229	0.044072
20.087851	4.034232	-0.968644	0.971605	0.055906	0.110652	0.045833
20.484533	4.057610	-0.922828	0.970861	0.060843	0.113485	0.047322
20.880826	4.085266	-0.876113	0.965559	0.073387	0.114844	0.057926
21.276679	4.117567	-0.828673	0.962686	0.083696	0.116279	0.063673
21.672101	4.154201	-0.780647	0.958366	0.097513	0.116193	0.072311
22.066692	4.199647	-0.733504	0.947682	0.121420	0.111106	0.093680
22.460306	4.254823	-0.688640	0.940477	0.141171	0.103570	0.108090
22.853377	4.316519	-0.647514	0.936429	0.155498	0.091726	0.116187
23.245694	4.385909	-0.612010	0.929759	0.171193	0.076564	0.129525
23.637966	4.458730	-0.583431	0.928560	0.172648	0.058637	0.131923
24.030825	4.530943	-0.562431	0.928839	0.168165	0.040704	0.131366
24.424453	4.600680	-0.548553	0.931303	0.159864	0.026282	0.126437
24.819114	4.665126	-0.539442	0.937620	0.146052	0.017441	0.113804
25.214664	4.724278	-0.533364	0.942123	0.135030	0.011778	0.104797
25.610919	4.778734	-0.529196	0.946864	0.123879	0.008664	0.095316
26.007906	4.827583	-0.525775	0.953111	0.110374	0.007954	0.082821
26.405524	4.871027	-0.522431	0.956811	0.099068	0.008415	0.075421
26.803550	4.910499	-0.518633	0.960503	0.088453	0.010185	0.068038
27.002745	4.928288	-0.516390	0.962753	0.083105	0.011534	0.063538
27.202042	4.944840	-0.513839	0.965184	0.077268	0.013152	0.058675
27.401425	4.960275	-0.510947	0.966971	0.072432	0.014879	0.055102
27.600876	4.974720	-0.507695	0.968758	0.067677	0.016706	0.051528
27.800411	4.987839	-0.504035	0.971740	0.061429	0.018761	0.045564
28.000000	5.000000	-0.500000	0.973376	0.057068	0.020486	0.042291
28.199646	5.011041	-0.495587	0.976154	0.050970	0.022608	0.036736
28.399343	5.020922	-0.490741	0.978256	0.045934	0.024848	0.032532
28.599073	5.029840	-0.485438	0.980159	0.041531	0.027209	0.028725

28.798828	5.037877	-C.479663	0.981934	0.037437	0.029487	C.025176
28.998577	5.045773	-C.473512	0.977706	0.042270	0.030625	0.033631
29.198291	5.054286	-0.467060	0.979456	0.038096	0.032948	C.030132
29.398031	5.061751	-C.460094	0.979574	0.036515	0.035293	0.029896
29.597758	5.069058	-0.452650	0.979909	0.034980	0.037772	0.029226
29.797480	5.076003	-0.444711	0.980598	0.033090	0.040106	C.027847
29.997196	5.082580	-C.436331	0.981023	0.031656	0.042155	0.026998
30.196903	5.088874	-0.427545	0.981501	0.030138	0.044214	0.026041
30.596282	5.100554	-C.408565	0.982672	0.027255	0.049212	0.023699
30.995579	5.111851	-C.387750	0.979735	0.031158	0.052524	0.029573
31.394796	5.123367	-0.365555	0.982031	0.026533	0.057289	0.024981
31.793914	5.133719	-C.341097	0.983140	0.025771	0.063662	C.022763
32.192882	5.144093	-C.314319	0.984030	0.025144	0.067371	0.020985
32.591689	5.154193	-C.285216	0.986280	0.025040	0.078827	0.016484
32.990562	5.153139	-C.266962	0.981953	0.038683	0.079636	C.025137
33.389498	5.161486	-C.248868	1.003327	-0.017025	-0.016981	-0.017610
33.789008	5.162602	-C.248878	0.994116	0.007593	-0.018688	0.000813
34.188526	5.177441	-0.249931	0.971941	0.067724	0.037622	C.045161
34.587073	5.205940	-C.227265	0.986873	0.041641	0.059939	0.015297
34.986118	5.218228	-0.202432	0.989271	0.045989	0.063342	0.010501
35.384806	5.240066	-0.178931	0.991266	0.052693	0.058286	0.006512
35.783646	5.261317	-C.157139	0.992731	0.051654	0.049333	0.003583
36.182732	5.280890	-C.138510	0.994528	0.045077	0.044214	-C.000012
36.582013	5.297404	-0.121133	0.996070	0.037731	0.043014	-0.003097
36.981400	5.311112	-0.103764	0.997601	0.030956	0.043969	-0.006157
37.380837	5.322312	-C.085764	0.998993	0.025231	0.046146	-C.008943
37.780282	5.331456	-0.066795	1.000109	0.020758	0.048821	-0.011175
38.179707	5.339006	-0.046744	1.000949	0.017185	0.051636	-C.012854
38.978448	5.350478	-0.003402	1.002331	0.011825	0.056937	-0.015619
39.777017	5.358386	0.043759	1.005486	0.008892	0.061729	-C.021928
40.575368	5.365146	0.094633	1.007906	0.008745	0.066430	-C.026768
41.373487	5.373147	0.148848	1.006589	0.012100	0.070253	-0.024134

INITIAL POINT X= 15.40000 Y= 1.50000 Z= 0.00000

INITIAL STEPSIZE= 0.10000

ACTUAL POINTS DETERMINED BY INTEGRATOR

X	Y	Z	U	V	W	CP
-0.031842	0.793774	-1.611701	0.994522	0.000000	0.104528	-0.000000
0.315966	0.793774	-1.569890	0.994522	0.000000	0.104528	-0.000000
0.713775	0.793774	-1.528078	0.994522	0.000000	0.104528	-C.000000
1.111584	0.793774	-1.486267	0.994522	0.000000	0.104528	-0.000000
1.509393	0.793774	-1.444456	0.994522	0.000000	0.104528	-0.000000
1.907242	0.794103	-1.403130	0.994522	0.000000	0.104528	-C.000000
2.304898	0.792956	-1.359581	0.994522	0.000000	0.104528	-0.000000
2.703275	0.797269	-1.324250	0.971408	0.019216	0.073478	0.046227
3.102203	0.807397	-1.296927	0.963549	0.028816	0.060987	C.061546
3.501244	0.820438	-1.272491	0.964663	0.032139	0.060000	0.059717
3.900153	0.832939	-1.245795	0.972173	0.029998	0.067534	0.044697
4.298999	0.845894	-1.218295	0.971412	0.034266	0.065235	C.046221
4.697877	0.861755	-1.192961	0.968631	0.040926	0.060482	C.051783
5.096687	0.878566	-1.167119	0.972633	0.041738	0.064320	0.043778
5.495418	0.896454	-1.140781	0.972573	0.046036	0.063746	0.043899
5.894082	0.916574	-1.115058	0.971859	0.051240	0.062708	C.045326
6.292640	0.938032	-1.088779	0.973916	0.053833	0.065307	0.041213

6.691076	0.960758	-1.061758	0.974470	0.057761	0.066675	0.040104
7.089376	0.995380	-1.034317	0.974636	0.062105	0.068062	0.039773
7.487519	1.011213	-1.005868	0.976088	0.064999	0.071331	0.036869
7.885490	1.033406	-0.976120	0.977052	0.068150	0.074583	0.034939
8.283270	1.066859	-0.945145	0.977593	0.071547	0.077884	0.033859
8.680845	1.096459	-0.912594	0.978884	0.073791	0.082409	0.031276
9.078207	1.126730	-0.878149	0.980137	0.075638	0.087349	0.028769
9.475338	1.157102	-0.841807	0.980892	0.077619	0.092243	0.027260
9.872230	1.189633	-0.803391	0.982067	0.078591	0.097878	0.024910
10.268882	1.221169	-0.762645	0.983474	0.078661	0.104017	0.022095
10.665286	1.252554	-0.719520	0.984527	0.078527	0.110113	0.019991
11.061438	1.284291	-0.673983	0.985677	0.077596	0.116446	0.017690
11.457348	1.315105	-0.625901	0.987248	0.075364	0.123146	0.014548
11.853020	1.344415	-0.575262	0.988608	0.072633	0.129684	0.011828
12.248459	1.373060	-0.522158	0.989749	0.069443	0.135968	0.009545
12.643678	1.399678	-0.466643	0.991413	0.064750	0.142297	0.006218
13.038700	1.424635	-0.408775	0.993209	0.059063	0.148347	0.002625
13.236142	1.435945	-0.379018	0.993876	0.056267	0.151111	0.001292
13.433538	1.446874	-0.348752	0.994457	0.053422	0.153721	0.000125
13.630892	1.457187	-0.318008	0.995003	0.050465	0.156183	-0.000963
13.828208	1.466850	-0.286816	0.995711	0.047113	0.158553	-0.002377
14.025450	1.476121	-0.255062	0.996499	0.043457	0.160774	-0.003954
14.222699	1.484341	-0.223043	0.997338	0.039596	0.162853	-0.005633
14.419781	1.492996	-0.190208	0.977409	0.066873	0.174018	0.034225
14.615672	1.507295	-0.152531	0.972728	0.067173	0.200936	0.043588
14.713318	1.513281	-0.131812	0.978206	0.050872	0.211748	0.032632
14.810940	1.517231	-0.110504	0.986633	0.028281	0.215638	0.015777
14.908664	1.518863	-0.089362	0.995719	0.005276	0.212170	-0.002395
15.006562	1.518361	-0.068984	1.004069	-0.014554	0.203578	-0.019095
15.104653	1.516097	-0.049703	1.011463	-0.030569	0.192229	-0.033881
15.202950	1.512497	-0.031689	1.018183	-0.043359	0.179480	-0.047323
15.301425	1.507477	-0.015065	1.039076	-0.075544	0.165622	-0.088108
15.400000	1.500000	0.000000	1.041507	-0.079420	0.154618	-0.093970
15.498688	1.492607	0.014349	1.038666	-0.075960	0.146046	-0.088288
15.597514	1.485409	0.027826	1.038657	-0.075479	0.137447	-0.088271
15.696440	1.478226	0.040558	1.039309	-0.075425	0.130215	-0.089574
15.795445	1.471059	0.052662	1.039786	-0.074953	0.124140	-0.090528
15.894518	1.463944	0.064236	1.040169	-0.074378	0.118958	-0.091293
15.993647	1.456883	0.075350	1.040536	-0.073905	0.114405	-0.092028
16.192040	1.442787	0.096356	1.042818	-0.075765	0.106182	-0.096593
16.390566	1.428364	0.115832	1.043423	-0.075441	0.099030	-0.097803
16.589215	1.414225	0.134237	1.042038	-0.072994	0.094144	-0.095032
16.787975	1.400543	0.151766	1.040523	-0.070500	0.089324	-0.092003
16.986832	1.387107	0.169356	1.040573	-0.070785	0.084187	-0.092102
17.185770	1.373629	0.183903	1.039657	-0.069590	0.078228	-0.090270
17.384813	1.360364	0.198252	1.040293	-0.069350	0.071583	-0.091543
17.583930	1.346854	0.211276	1.042602	-0.072810	0.064603	-0.096161
17.783113	1.333149	0.223025	1.039129	-0.068148	0.058565	-0.089214
17.982406	1.320050	0.233536	1.040510	-0.071235	0.050339	-0.091976
18.181733	1.306217	0.242330	1.039690	-0.071565	0.041642	-0.090336
18.381087	1.291758	0.249183	1.045609	-0.083117	0.028809	-0.102175
18.580404	1.275854	0.253786	1.037655	-0.077074	0.021383	-0.086267
18.779840	1.261247	0.257122	1.035534	-0.079931	0.011790	-0.083024
18.979154	1.244785	0.258156	1.036886	-0.091292	-0.001339	-0.084727
19.178183	1.225249	0.256509	1.039633	-0.115172	-0.016360	-0.090223
19.376452	1.199421	0.252899	1.038299	-0.160660	-0.020111	-0.087554
19.572354	1.160284	0.253005	1.042383	-0.283874	0.036413	-0.095723

19.762551	1.112200	0.281932	1.000333	-0.285277	0.414229	-0.011622
19.946248	1.081963	0.349977	0.999132	0.040522	0.280998	-0.009220
20.121452	1.083894	0.325228	0.997408	0.010530	0.354232	-0.005773
20.311916	1.077836	0.382199	0.999022	0.035644	0.214293	-0.009001
20.508545	1.093472	0.416653	1.034508	0.031405	0.156062	-0.075972
20.706647	1.096543	0.443225	1.034192	0.014160	0.131355	-0.079341
20.905203	1.097764	0.467014	1.033814	0.000389	0.115461	-0.078584
21.104069	1.096951	0.488251	1.032429	-0.009243	0.105794	-0.075815
21.303086	1.094179	0.507820	1.033724	-0.020266	0.097285	-0.079404
21.502205	1.089403	0.525955	1.033460	-0.028458	0.091177	-0.077877
21.701379	1.083189	0.543006	1.033267	-0.036223	0.085973	-0.077489
21.900576	1.075351	0.559086	1.034460	-0.045551	0.080823	-0.079876
22.099773	1.065833	0.574247	1.033891	-0.052481	0.076773	-0.078737
22.298962	1.055015	0.588607	1.033847	-0.060375	0.072240	-0.078651
22.498121	1.042590	0.602063	1.033625	-0.068518	0.067294	-0.078206
22.697231	1.028556	0.614639	1.032943	-0.077338	0.063533	-0.076842
22.896241	1.012620	0.626482	1.033002	-0.088652	0.059309	-0.076560
23.095105	0.994479	0.637621	1.030648	-0.099125	0.056499	-0.072253
23.293743	0.973780	0.648219	1.031326	-0.118335	0.053779	-0.073609
23.491810	0.948252	0.658848	1.003032	-0.145979	0.056443	-0.017021
23.688744	0.915956	0.671763	1.002553	-0.183743	0.078135	-0.016062
23.883971	0.877773	0.692015	1.002442	-0.205531	0.137062	-0.015841
24.077924	0.841859	0.724588	1.001977	-0.154782	0.154490	-0.014910
24.272764	0.818863	0.763442	1.002005	-0.087693	0.179072	-0.014967
24.469686	0.804818	0.795679	1.001330	-0.060702	0.144778	-0.013616
24.667715	0.793577	0.821241	0.999531	-0.052036	0.120229	-0.010019
24.866221	0.783202	0.843251	0.998568	-0.054661	0.103343	-0.008053
25.064951	0.772022	0.862767	0.999252	-0.056372	0.094098	-0.009461
25.263836	0.760585	0.880416	1.023740	-0.060900	0.084087	-0.058436
25.462874	0.748389	0.895790	1.023866	-0.064265	0.074705	-0.058697
25.661980	0.735664	0.909738	1.021359	-0.066143	0.069485	-0.053675
25.861123	0.722389	0.922598	1.022139	-0.071078	0.061462	-0.055233
26.060283	0.707930	0.933827	1.023597	-0.077311	0.054190	-0.058131
26.259436	0.692403	0.943655	1.024566	-0.081901	0.046905	-0.060087
26.458604	0.676408	0.952394	1.020919	-0.081224	0.043901	-0.052794
26.657801	0.660499	0.960589	1.019498	-0.082945	0.039251	-0.049951
26.856989	0.643974	0.967737	1.019165	-0.086167	0.033853	-0.049287
27.056162	0.627105	0.974479	0.999941	-0.083508	0.036674	-0.010839
27.255327	0.610294	0.981589	0.999748	-0.087372	0.032235	-0.010453
27.454422	0.592221	0.987447	1.000569	-0.094037	0.026718	-0.012094
27.653427	0.572868	0.992180	1.000519	-0.100295	0.021073	-0.011994
27.852312	0.552117	0.995895	1.001019	-0.109402	0.016575	-0.012992
28.050984	0.529335	0.999067	1.001569	-0.120423	0.014272	-0.014095
28.249419	0.504682	1.002972	0.999704	-0.127032	0.024849	-0.010364
28.447730	0.479546	1.009283	0.997742	-0.123905	0.039235	-0.006440
28.646134	0.455906	1.018071	0.998495	-0.112357	0.046524	-0.007947
28.844816	0.434970	1.027371	0.998344	-0.097642	0.045782	-0.007644
29.043793	0.416714	1.036013	0.998178	-0.086569	0.040508	-0.007212
29.242976	0.400253	1.043435	0.997941	-0.079074	0.034130	-0.006837
29.442294	0.384971	1.049639	0.997682	-0.074378	0.028179	-0.004320
29.641704	0.370552	1.054890	0.999658	-0.069796	0.025137	-0.010272
29.841193	0.357016	1.059417	1.000349	-0.066335	0.019167	-0.011654
30.040744	0.344035	1.062745	0.999776	-0.063770	0.014967	-0.010508

FLOW VIZUALIZATION DONE LAST CARD READ=VIZEND

END OF DATA

7F

10. REFERENCES

1. Woodward, F. A.: A Method of Aerodynamic Influence Coefficients with Application to the Analysis and Design of Supersonic Wings. Boeing Document D6-8178, April 1962.
2. Middleton, Wilbur D.; and Carlson, Harry W.: Numerical Method of Estimating and Optimizing the Supersonic Aerodynamic Characteristics of Arbitrary Planform Wings. AIAA Journal of Aircraft, vol. 2, no. 4, July-August 1965.
3. Yoshihara, H.; Kainer, J.; and Strand, T.: On Optimum Thin Lifting Surfaces at Supersonic Speeds. Journal of the Aero/Space Sciences, vol. 25, no. 8, August 1958, pp. 473-479.
4. Grant, F. C.: The Proper Combination of Lift Loadings for Least Drag on a Supersonic Wing. NACA TR 1275, 1956.
5. Carlson, H. W.; and Middleton, W. D.: A Numerical Method for the Design of Camber Surfaces of Supersonic Wings with Arbitrary Planforms. NASA TN D-2341, June 1964.
6. LaRowe, E., and J. E. Love: Analysis and Design of Supersonic Wing-Body Combinations, Including Flow Properties in the Near Field. NASA CR-73107, August 1967.
   Part II—Digital Computer Program Description
7. Woodward, F. A., et al.: A Method of Optimizing Camber Surfaces for Wing-Body Combinations at Supersonic Speeds—Theory and Application. Boeing Document D6-10741, Part I, 1965.
8. Woodward, F. A.; and LaRowe, E.: A Modified Linear Theory and Its Application to Wings with Supersonic Edges. NASA CR-73108, Boeing Document D6-15045, August 1967.
9. Heaslet, M. A.; Lomax, L.; and Jones, A. L.: Volterra's Solution of the Wave Equation as Applied to Three-Dimensional Supersonic Airfoil Problems. NACA Report 889, April 1947.
10. Liepmann, H. W.; and Roshko, A.: Elements of Gas Dynamics. John Wiley and Sons, 1957.
11. Von Karman, T.; and Moore, N. B.: The Resistance of Slender Bodies Moving with Supersonic Velocities with Special Reference to Projectiles. Trans. ASME, vol. 54, pp. 303-310, 1932.

12. Van Dyke, Milton D.: First- and Second-Order Theory of Supersonic Flow Past Bodies of Revolution. Journal of the Aeronautical Sciences, vol. 18, no. 3, 1951.

13. Tucker, W. A.: A Method for the Design of Sweptback Wings Warped to Produce Specified Flight Characteristics at Supersonic Speeds. NACA TR 1226, 1955.

14. Cohen, Doris; and Friedman, M. D.: Theoretical Investigation of the Supersonic Lift and Drag of Thin, Sweptback Wings with Increased Sweep Near the Root. NACA TN 2959, 1953.

15. Snow, R. N.: Aerodynamics of Thin Quadrilateral Wings at Supersonic Speeds. Quart. Appl. Math., vol. 5, 1948.

16. Nielsen, Jack, N.: Quasi-Cylindrical Theory of Wing-Body Interference at Supersonic Speeds and Comparison with Experiment. NACA Rept. 1252, 1952.

17. Ting, Lu: Diffraction of Disturbances Around a Convex Right Corner with Applications in Acoustics and Wing-Body Interference. Journal of the Aeronautical Sciences, vol. 24, no. 11, November 1957.

18. Carlson, Harry W.: Pressure Distributions at Mach Number 2.05 on a Series of Highly-Swept Arrow Wings Employing Various Degrees of Twist and Camber. NASA TN D-1264, 1962.

19. Donovan, A. F.; and Lawrence, H. R., ed.: Aerodynamic Components of Aircraft at High Speeds. Vol. VII, High Speed Aerodynamics and Jet Propulsion. Princeton University Press, Princeton, New Jersey, 1954.